NASA SP-140

INTERSTELLAR GRAINS

RENSSELAER POLYTECHNIC INSTITUTE

Troy, New York

August 24-26, 1965

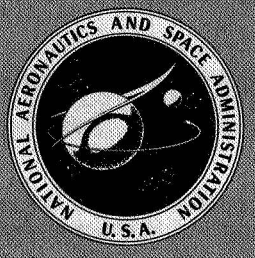

NATIONAL AERONAUTICS AND SPACE ADMINISTRATION

NASA SP-140

INTERSTELLAR GRAINS

Edited by
J. MAYO GREENBERG
and
T. P. ROARK

Proceedings of a conference held August 24-26, 1965, at Rensselaer Polytechnic Institute in Troy, New York

Scientific and Technical Information Division
OFFICE OF TECHNOLOGY UTILIZATION 1967
NATIONAL AERONAUTICS AND SPACE ADMINISTRATION
Washington, D.C.

For Sale by the Superintendent of Documents,
U.S. Government Printing Office, Washington, D.C. 20402
Price $1.25
Library of Congress Catalog Card Number 67–60065

Foreword

MANY THEORETICAL AND EXPERIMENTAL INVESTIGATIONS conducted during the past two decades have involved as offshoot research topics the understanding of the nature and characteristics of interstellar grains. The formation and interaction processes of interstellar grains are very complex, and the problem of chemical identification of these grains has puzzled astronomers for many years. Information on interstellar grains has been obtained from observations of space reddening, from studies concerning the dependence of interstellar grain extinction on wavelength, and from interstellar polarizations.

The importance of this information to the physics and astronomy programs of the National Aeronautics and Space Administration may be fairly obvious. Thus when the National Science Foundation, under the auspices of Commission 34 of the International Astronomical Union, announced its sponsorship of an international Colloquium on Interstellar Grains in a dual effort to consolidate existing information and to stimulate new research, NASA extended support to the colloquium through a grant (NGR 32–018–050) and by publication of these proceedings. Because of the many similarities of the scientific problems encountered in the study of aerosols and interstellar grains, the New York State Atmospheric Sciences Research Center also contributed to the support of the meeting.

The colloquium was held August 24–26, 1965, at Rensselaer Polytechnic Institute in Troy, New York. The members of the organizing committee were Alfred Behr, Göttingen University Observatory, Göttingen, Germany; Jan Borgman, Kapteyn Observatory, Roden, The Netherlands; Bertram Donn, NASA Goddard Space Flight Center, Greenbelt, Maryland; J. Mayo Greenberg, Rensselaer Polytechnic Institute, Troy, New York; H. C. van de Hulst, Leiden University, Leiden, The Netherlands; and Bengt Strömgren, Princeton, New Jersey. Engineers actively engaged in studying the problems of interstellar grains or related fields were invited to participate.

Among the topics discussed were granular extinction; polarization and its dependence on wavelength and spatial distribution; scattering properties of grains; physics and chemistry of the formation and growth of interstellar grains; and the interactions of grains with the interstellar medium.

The presentation of many of the papers was followed by a brief discussion period; the remarks are included in this compilation. Some of the papers presented here have been modified or enlarged in response to the suggestions and contributions made during these discussion periods.

Several of the papers have appeared previously in part or in slightly modified versions in various scientific journals. These papers are identified, and footnotes give information concerning previous publication. This publication is, however, the only collection under one cover of the information presented at the colloquium and is expected to serve as a useful reference volume on interstellar grains.

MAURICE DUBIN
Chief, Interplanetary Dust and Cometary Physics

Contents

Introduction

THE INTERSTELLAR GRAINS PROBLEM has been the subject of scientific investigation for over 40 years. At various times during these years concentrated efforts have been made to arrive at definitive solutions. A new wave of research work, both theoretical and observational, was in progress at the time of the International Astronomical Union meeting in 1964. It therefore seemed appropriate and timely to gather together the various people actively engaged in the interstellar grains problem and those with interests in related scientific subjects in order to focus attention on the key avenues of research. It was hoped that such a scientific confrontation would result in a higher level of understanding and would consequently stimulate and coordinate future work in this field.

An organizing committee was formed during the International Astronomical Union meeting to arrange for a conference on interstellar grains to be held at Rensselaer Polytechnic Institute the following year.

The facilities and cooperation provided by the host institution contributed greatly to the overall success of the meeting.

During the course of the meeting approximately thirty papers were given. Many of these presented entirely divergent points of view. There were significant differences on the observational interpretations as well as on theoretical interpretations. The discussions as they appear in this volume have gone through several editing processes primarily in the interest of clarity and succinctness. We believe that little if anything essential has been deleted and perhaps even a modicum of the flavor of the originals may have been retained.

The publication of the proceedings of the Colloquium on Interstellar Grains has been delayed for various reasons, and although some of the papers have already appeared elsewhere, several very interesting ones are not yet in print. Furthermore the discussions contain both opinions and information which are as pertinent now as they were when originally spoken. We believe that these two features are equally important and we suggest that the discussions, following each paper, be considered an integral part of that paper.

The principal issues discussed at the colloquium have been the subject of further observational and theoretical investigations. Among these are: (1) The question of uniformity (and value) of the ratio of total to

selective extinction; (2) Dielectric grains versus graphite or graphite core plus dielectric mantle grains; (3) Variations of the reddening law and of the wavelength dependence of polarization and their respective association with localized phenomena or with problems of galactic structure; (4) Formation of interstellar molecules, mainly OH and H_2; (5) The diffuse interstellar lines; and (6) The physics and chemistry of grain nucleation and growth. We believe that those who participated in the meeting were aided by having had the opportunity to discuss these problems with their co-workers. We hope that the information contained herein will serve as a refresher for those who participated and will be of value to new workers in this field, even though some of the problems have been carried considerably beyond the point at which they end here. I should like to express my thanks to Mrs. Martha Hanner for her assistance in the preparation of this volume.

J. MAYO GREENBERG
Rensselaer Polytechnic Institute
Troy, New York

Observed Interstellar Extinction in the Ultraviolet[1]

T. P. STECHER
NASA Goddard Space Flight Center
Greenbelt, Maryland

AN OBSERVATIONAL PROGRAM to measure stellar energy distributions in the ultraviolet between 3000 Å and 1200 Å has recently been completed. The instrumentation used was similar to that reported in reference 1. A necessary preliminary for discussion of this material is some knowledge of the extinction due to interstellar absorption. The trend of this extinction was first reported in 1964. (See ref. 2.) Additional observational material has since been obtained and is presented herein.

Five pairs of stars with similar Morgan-Keenan (MK) spectral classifications have been observed that are suitable for obtaining extinction: ζ Per and ρ Leo; ξ Per and ζ Pup; o Per and β Can Maj; σ Sco and π Sco; and δ Sco and τ Sco. The telemetry records were hand reduced by the author, each star was multiplied by the absolute calibration curve for the appropriate instrument, and the resulting flux curve was placed on a magnitude scale. Since interstellar extinction is obtained from the magnitude difference between two stars, the calibration factors completely cancel when both stars are observed by the same instrument. When the pair members are observed by different instruments, the consistency of the calibration from one instrument to another enters, but the absolute calibration does not. The instruments used for each reddening pair were calibrated at the same time, and comparison with stars observed by more than one instrument indicates that the error is negligible.

The extinction curve for each star pair has been normalized to a color excess $B-V=1$ by using colors reported in references 3 and 4. For various observational reasons, the extinction curves are not com-

[1] The contents of this paper were published previously in the Astrophys. J. (pub. by the Univ. of Chicago Press), vol. 142, 1965, p. 1683.

plete for any star pairs. Therefore, the mean values Δm and the standard deviation for the available points at each wavelength λ are plotted in figure 1. A point-by-point computer reduction of all the star data is in progress and is expected to yield more pairs and greater accuracy for the existing pairs.

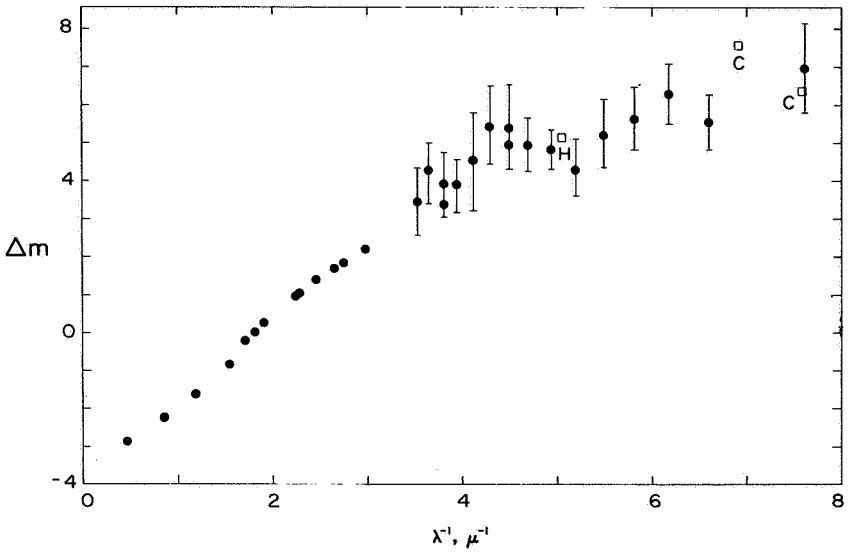

FIGURE 1.—Observed mean value for interstellar extinction. Solid circles: mean values for interstellar extinction and their mean errors for up to five pairs of stars as a function of inverse wavelength; solid circles without error bars: data from ref. 5; the square marked *H* is from ref. 6; the squares marked *C* are from ref. 7; all values are normalized with respect to $B-V=1$ and $V=0$.

In figure 1, the mean extinction points are plotted, along with the mean extinction curve of reference 5 with $V=0$ for reference. An additional point was obtained from reference 6, and two points were obtained from reference 7. The separation between scatter that is intrinsic to extinction and observational scatter is difficult at this time, but for some stars the peak at $\lambda^{-1}=4.4$ microns^{-1} appears to be considerably higher and drops off more rapidly before beginning to rise again. The results reported in reference 8 indicate that this variation is probably intrinsic. A possible explanation for the peak is suggested in the paper which follows.

REFERENCES

1. STECHER, T. P.; and MILLIGAN, J. E.: Stellar Spectrophotometry from above the Atmosphere. Astron. J., vol. 136, 1962, p. 1.

2. STECHER, T. P.: Ultraviolet Spectrophotometry of Early-Type Stars. Astrophys. J., vol. 69, 1964, p. 558.

3. JOHNSON, H. L.; and BORGMAN, J.: The Law of Interstellar Extinction. Bull. Astron. Inst. Netherlands, vol. 17, 1963, p. 115.

4. MACRAE, D.: Observatory Handbook. Roy. Astron. Soc., Canada, 1961, p. 70.

5. BOGGESS, A.; and BORGMAN, J.: Interstellar Extinction in the Middle Ultraviolet. Astrophys. J., vol. 140, 1964, p. 1633.

6. ALEXANDER, J. D.; BOWEN, P. J.; GROSS, M. J.; and HEDDLE, D. W. O.: Southern Hemisphere Observations of Ultra-violet Radiation from Celestial Objects I. Experimental Techniques and Rocket Payload Technology. Proc. Roy. Soc. (London), vol. A279, 1964, p. 510.

7. CHUBB, T. A.; and BYRAM, E. T.: Stellar Brightness Measurement at 1314 and 1427 Å: Observation of the OI Twilight Glow. Astrophys. J., vol. 138, 1963, p. 617.

8. JOHNSON, H. L.: Interstellar Extinction in the Galaxy. Astrophys. J., vol. 141, 1965, p. 923.

Graphite and Interstellar Extinction [1]

T. P. STECHER AND BERTRAM DONN
NASA Goddard Space Flight Center
Greenbelt, Maryland

THE THEORY THAT GRAPHITE PARTICLES could be responsible for interstellar extinction is presented in references 1 and 2, and this paper will present evidence that further supports this contention. The complex dielectric constant ($m = n(1 - ik)$) for graphite has been measured as a function of energy by the authors of reference 3, and the optical constants as function of wavelength λ have been obtained from this measurement. A large variation occurs in both n and k at wavelengths below 3000 Å.

The results reported in the preceding paper indicated the desirability of performing Mie scattering calculations on graphite. The measured values of the complex index of refraction corresponding to 17 wavelengths were used in the calculation for spherical particles. The IBM 7094 computer program for Mie scattering follows that of van de Hulst. (See ref. 4.) The Oort-van de Hulst size distribution (ref. 5), which may not be applicable to the type of particle discussed herein, has been used to obtain an integrated cross section for extinction. The steps were in terms of 0.8×10^{-6} cm for the particle radius with the 1/eth value of the frequency function being 5.6×10^{-6} cm. In figure 1, this curve is compared with the mean observed interstellar extinction of Boggess and Borgman (ref. 6) and the further observational results reported in the preceding paper. The maximum in the theoretical extinction curve at $\lambda^{-1} = 4.4$ microns^{-1} is the signature of graphite. This maximum rapidly increases as the relative size of the particle radius decreases. At the same time, the extinction for $\lambda^{-1} < 2$ decreases. A 50-percent increase in the relative radius of the particles appears sufficient to produce the variation in the ratio of selective to total extinction observed by the author of reference 7. A maximum in the observed interstellar extinction curve also occurs at $\lambda^{-1} = 4.4$ microns^{-1}. The

[1] The contents of this paper were published previously in the Astrophys. J. (pub. by the Univ. of Chicago Press), vol. 142, 1965, p. 1681.

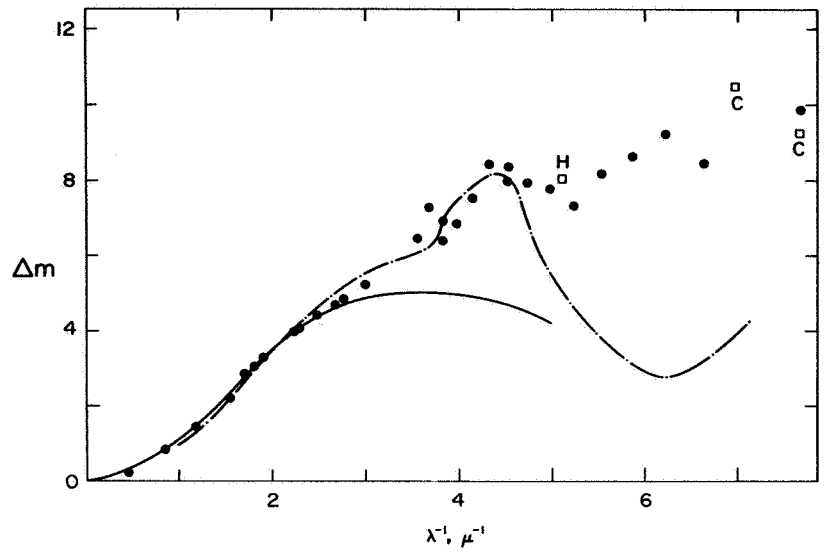

FIGURE 1.—Observed and theoretical interstellar extinction. Circles for $\lambda^{-1} > 3\ \mu^{-1}$: mean observed interstellar extinction reported in paper by Stecher in the present compilation; circles for $\lambda^{-1} \leq 3\ \mu^{-1}$: mean observed extinction of investigation of ref. 6; squares marked *H* and *C*: observed extinction obtained from other sources as reported in the paper by Stecher in the present compilation; dash-dot curve: theoretical interstellar extinction for graphite grains; solid curve: theoretical extinction by van de Hulst (ref. 5).

authors think that this coincidence provides a strong argument in favor of graphite. For the first time there is structure in the extinction curve and it can be accounted for by a particular substance. It is, of course, possible that some other material could have the same signature and also be abundant in interstellar space, but this seems improbable. The albedo for this particle-size distribution is somewhat larger than that reported in reference 8 and may be sufficiently high to account for reflection nebulae (ref. 9).

For shorter wavelengths, the calculated curve is inconsistent with the observations. It seems unlikely that a particle-size distribution could be found that would be satisfactory. The addition of a dielectric material either as a coating of the graphite or as separate small particles could easily bring up the curve. A promising "dielectric" which is already present is graphite itself. Graphite is strongly anisotropic. The calculations of the present investigation were made with optical constants measured for the electric vector in the basal planes. When the electric vector is perpendicular to the basal planes, the conductivity is at least 100 times smaller (ref. 8) and graphite then acts like a dielectric. Since graphite is presumed to be present in the form of flakes that are almost randomly oriented, a sizable proportion of the flakes will present this thin dielectric face to the radiation.

The fact that both the ratio of crystal axis and the "dielectric" index of refraction are uncertain precludes a quantitative calculation at this time. This conjecture could be observationally checked by polarization measurements at $\lambda^{-1}=6\ \mu^{-1}$. If graphite is assumed to be the sole cause of interstellar extinction, a reversal in the sign of polarization would be expected when the "dielectric" extinction exceeds that of the conducting plane.

In addition to the proposal of reference 2 for interstellar carbon grains, it has been pointed out (ref. 10) that graphite flakes may grow in space if countering effects can be neglected. The exponential whisker growth mechanism (ref. 11) was shown to apply. For a plate of 10^{-6} cm thickness, the length reaches 5×10^{-6} cm in 6×10^{8} years for $N_H=1/cm^3$ and in 6×10^{7} years for the number density of hydrogen atoms $N_H=10/cm^3$.

Grains such as these are intermediate in structure and mass between classical grains proposed by van de Hulst (ref. 5) and Platt particles (ref. 12).

The assumption that the grains are graphite indicates the possibility of obtaining considerable detailed information concerning the particle-size distribution in the interstellar clouds between the Earth and any particular star by means of rocket observations.

REFERENCES

1. CAYREL, P.; and SCHATZMAN, E.: Sur la Polarisation Interstellaire par des Particules de Graphite. Ann. Astrophys., vol. 17, 1954, p. 555.

2. HOYLE, F.; and WICKRAMASINGHE, N. C.: On Graphite Particles as Interstellar Grains. Roy. Astron. Soc., Monthly Notices, vol. 124, 1962, p. 417.

3. TAFT, E. A.; and PHILIPP, H. R.: Optical Properties of Graphite. Phys. Rev., vol. 138A, 1965, p. 197.

4. VAN DE HULST, H. C.: Light Scattering by Small Particles. John Wiley & Sons, Inc., 1957.

5. VAN DE HULST, H. C.: The Solid Particles in Interstellar Space. Rech. Astron. Obs. Utrecht, vol. 11, pt. 2, 1949.

6. BOGGESS, A., III; and BORGMAN, J.: Interstellar Extinction in the Middle Ultraviolet. Astrophys. J., vol, 140, 1964, p. 1636.

7. JOHNSON, H. L.: Interstellar Extinction in the Galaxy. Astrophys. J., vol. 141, 1965, p. 923.

8. WICKRAMASINGHE, N. C.: A Note on Interstellar Polarization by Graphite Flakes. Roy. Astron. Soc., Monthly Notices, vol. 125, 1962, p. 87.

9. VAN HOUTEN, C. J.: Surface Photometry of Extragalactic Nebulae. Bull. Astron. Inst. Netherlands, vol. 16, no. 509, 1961, p. 1.

10. DONN, B.: The Physics and Chemistry of Interstellar Grains. I. Crystal Growth in Space Astron. J., vol. 70, 1965, p. 320.

11. SEARS, G. W.: The Origin of Screw Dislocations—Role of Colloidal Particles. Acta Metallurgica, vol. 3, 1955, p. 306.

12. PLATT, J. R.: On the Optical Properties of Interstellar Dust. Astrophys. J., vol. 123, 1956, p. 486.

DISCUSSION

Greenberg: I would like to inquire about the two points in the extreme ultraviolet obtained by Chubb and Byram; can you explain how one obtains the extinction from their data?

Stecher: I looked up the $B-V$ colors for all the stars they had observed and plotted them in terms of magnitude. There are a couple of B stars way off from the highly reddened end, and there is a cluster of B stars presumably unreddened that have very little color excess in the $B-V$ region. I didn't attempt to put a probable error on it, as this was sort of a straight-line fit through the diagram and it was just indicative. As I mentioned, there was much scatter.

Nandy: You have used three O stars in the Perseus region and two O stars in the Scorpius region. H. L. Johnson has recently reported that the Scorpius stars show an extinction law similar to that in Cygnus, whereas the Perseus stars exhibit a different extinction law. Can you combine your observations if a difference exists in the extinction law?

Stecher: The observations that I have are weak enough so that between intrinsic variation and observational error I really don't want to say there is an intrinsic variation. The data indicate that this bump at $\lambda 2200$ Å is stronger in the Scorpius region. On the graphite interpretation this would mean more small particles.

Nandy: It is interesting that in the Perseus region the slope of the ultraviolet part relative to the blue is different from that in Cygnus.

Stecher: Yes, I am aware of that and I have no explanation.

Wickramasinghe: This slope difference could be due to a difference in the sizes of the particles. Smaller graphite particles mixed with larger ones would give the bump indicated.

Greenberg: You presented two curves, one of which gave a match, more or less, to some spot in the ultraviolet which is characteristic of graphite as reported in the literature. I qualify that by saying that it is not necessarily graphite, but suppose it is. That first one matched the extinction in the near ultraviolet and the visible very poorly. The next curve that you gave was presented with this mixture of particles where you got a relatively good fit from $\lambda^{-1}=0.80$ up to $\lambda^{-1}=3$. What I don't understand is how you combined these two calculations, the one which didn't fit anywhere, but which did fit, more or less, the bump in the ultraviolet, and the other which fit in the near ultraviolet down to the far infrared.

Stecher: I thought the first curve fit quite well.

Greenberg: As I recall, it deviated very drastically around $\lambda^{-1}=3$, and it deviated very significantly, I believe, around $\lambda^{-1}=1.5$ to 2. It wasn't drawn any farther down than that. The point I'm raising is what we mean by a fit. At $\lambda^{-1}=3$ this curve is considerably off from the

observations and just seems to cross somewhere. I can always make curves cross somewhere, but I don't see that it looks anything like the observed points.

Stecher: The graphite refractive indices were obtained from a very small graph in the Physical Review and the second curve was plotted from Taft and Phillips' original numbers. Therefore, there is a slight difference, especially in the infrared, a region in which I was not particularly interested. The difference between Boggess and Borgman's points and van de Hulst's curve is about 15 percent of the scaling of the size distribution. I don't think that a 15-percent difference in the scaling of the radii is important.

Greenberg: For the graphite? I don't understand. Your graphite curve does not fit in the near ultraviolet. It doesn't really fit anywhere; the slope is all wrong. I'm raising a point which I feel is very important: What do we mean by a fit? Now if one is matching signature—there is a signature of this hump at about $\lambda^{-1}=4.4$—that I think would be rather significant if there is an absorptive type of material which we can identify. I think this is important even if we don't match it anywhere else. However, I don't believe that there is a fit to an extinction curve.

Wickramasinghe: I don't see your objection. The fit in the visible and near ultraviolet is quite satisfactory to within the observational error. The hump itself is the signature I think; this is the most interesting and significant point. Dr. Stecher used an Oort-van de Hulst distribution of sizes, although I think there is no particular justification for using it with graphite particles. I have done it with several types of distributions, mainly with Gaussian dispersions centered at 0.05 μ with dispersion σ between 0.01 μ and 0.02 μ. One gets a very good fit in the visible as well as a hump centered at $\lambda^{-1}=2200$ Å. It is important to note that Dr. Stecher's observations show a pronounced quenching effect centered at about $\lambda^{-1}=0.22$ μ for stars located in different parts of the galaxy. This fact suggests strongly that one is observing a spectroscopic feature of the grains—independent of the size.

Stecher: Since I didn't have any really strong justification for using the Oort-van de Hulst distribution, the difference in the scaling of the radii of something on the order of 10 percent will run it through a mean curve which again is not really what one should fit. This is why I didn't attempt to fit it any closer. I think the general agreement is reasonably good.

Greenberg: If you change the size to bring that curve down to fit in the near ultraviolet, the curve will drop down farther on in the ultraviolet. You will still have the hump when you bring it down, and it will have the same qualitative features. The details of the extinction in the far ultraviolet are perhaps still not known.

Wickramasinghe: Yes, one should insist, I think, on a perfectly

271-992 O-67—2

good fit between the theory and the observations in the visible, while also reproducing the qualitative features of the ultraviolet observations at least.

Greenberg: Yes, we do know something about the visible, but how much we know about the far infrared is another point that can be raised.

Nandy: I have a definition of a good fit. By good fitting, I mean that the variance should be less than the standard error of the observations. Therefore, it is important to know the standard error of the observations. If the standard error is very large, fitting will be poor in any case.

Wickramasinghe: Yes, I think it is worth adding to this observation that the standard of error is in general greater in the ultraviolet than in the visible. And, if one draws bars denoting the rms error at each wavelength point, one should get a fit within the error bars for any tenable grain model.

Borgman: In answer to the remark of Dr. Wickramasinghe, I think that observational errors could not explain the deviation from the theoretical curve—these errors are so large that they certainly must mean that the theoretical curve or the physical variables used in the computations must be in error.

Some Observational Limitations of Extinction Measurements in the Rocket Ultraviolet

JAN BORGMAN
Kapteyn Observatory
Roden, The Netherlands

EVEN BEFORE ANY MEASUREMENT of stellar fluxes in the ultraviolet had been obtained, predictions were being made on the basis of stellar atmosphere models. At the moment, it seems that such computations (for example, see ref. 1) are in reasonable agreement with actual observations from rockets (ref. 2) in the spectral region down to about 2000 Å. At shorter wavelengths it is necessary to take into account the appreciable blanketing by spectral lines which unavoidably is present in the transmission bands of any wide-band photometric system, even in the case of early B stars, as has been shown in reference 3.

It must be anticipated that the reduction of extinction measurements in the UV from spaceborne instruments will follow the same procedure that has been used so far: stars with the same intrinsic energy distribution but with different amounts of reddening material in the line of sight are compared, the difference in energy distribution being attributed to the wavelength dependence of interstellar extinction.

In past investigations of interstellar extinction in the visible and near UV, assumptions about equal energy distribution have sometimes been challenged, even if the stars concerned had the same MK classification and their spectra at moderate dispersion showed no complicated structure or differences of any photometric significance. This situation would undoubtedly become more critical in the UV, particularly below 1500 Å where the spectra of O and B stars must be expected to be quite complicated. Hence, when deriving extinction data from wide-band measurements below 1500 Å, one faces a problem which looks somewhat like the equivalent situation in the infrared when extinction measurements have to be derived from M-type supergiants. For the moment, it is assumed that wide-band photometry, aimed at obtaining extinction data, should be restricted to the wavelength region $\lambda > 1500$ Å.

It is likely that significant measurements of the reddening law in the UV will be made from stabilized satellites rather than from rockets, as the stars to be investigated are faint and are to be found in densely populated regions of the sky. Hence the desirability is evident of predicting the encountered fluxes in order to compile a sensible and realistic observing program, which can be carried out by the experiment in terms of its dynamic range and available observing time.

To this end fluxes have been computed of reddened stars by using the relation

$$F(\lambda, V_o \ A_v) = F(\lambda, 0, 0) \times 10^{-0.4(V_o + c_\lambda A_V)}$$

where

$F(\lambda, 0, 0)$ is the intrinsic flux in photons/cm^2-A-sec at wavelength λ

V_o is the apparent visual magnitude if the absorption has been removed

A_V is the visual absorption

c_λ represents the extinction law, $c_\lambda = A_\lambda / A_V$

Typical flux values at four wavelengths for a B0 star of apparent visual magnitude $V=10$ and visual absorption $A_V=2$ (hence $V_0=8$) are given in table I. The adopted values of c_λ are also tabulated; they

TABLE I.—*Adopted Extinction Law and Flux Values for a B0 Star* [$V=10$, $A_V=2$, $V_o=8$]

λ, Å	c_λ	F, photons/cm^2-Å-sec
3300	1.70	0.09
2600	2.07	.07
2200	2.58	.04
1500	2.58	.08

are based on the data given in reference 4, except for the 1500-Å extinction which has been assumed to be the same as that at 2200 Å.

Suppose the star of table I is observed with an 8-inch telescope in 200-Å bands centered at the four wavelengths in the table, with an efficiency of 4 percent (resulting from an optical efficiency of 20 percent and a detector efficiency of 20 percent). It is found that the star would develop 100 primary photoelectrons in the 200-Å bandpass at 2200 Å in 1 second and correspondingly more in the other three wavelength regions. The counting of 10 000 events would take 100 seconds (100 percent collection efficiency and no dark current assumed). This reasonable time being assumed, stars are selected for an observing program, intended for a study of the extinction law. It is likely that one would want to observe stars which have already been studied in other wavelength regions from the ground. A sensible target could be the observa-

tion of the 1259 stars in the catalogue of reference 5. In that catalogue, 1193 stars have spectral types earlier than A1; for these stars, fluxes have been computed following the procedure described earlier. In addition, 975 stars appear to have fluxes at all four wavelengths in excess of 10^{-2} photons/cm^2-Å-sec and are considered to be observable in terms of photon statistics. A breakdown of the figures is given in table II.

TABLE II.—*Numbers of Several Star Spectral Types* [a]

Spectral type	Catalogue	Flux computed	Flux $> 10^{-2}$ photons/cm^2-Å-sec
O		200	164
B0–B1.5		637	533
B2–A0		356	278
Total	1259	1193	[b] 975

[a] Data obtained from reference 5.

[b] Of these 975 stars, $A_V < 1$ magnitude for 94; $1 \leq A_V < 2$ for 485; and $A_V \geq 2$ for 396.

The actual extinction information relative to extinction measurements in the visible and infrared must come from stars with a visual extinction of at least 1 magnitude, of which there are 881. If the one-third of the Milky Way not represented in Hiltner's catalogue (ref. 5) and the additional observation of some unreddened stars is accounted for, the total number of stars would be about 1500, the observing time ranging from a few seconds to approximately 7 minutes on the basis of the adopted instrumental specifications.

In the case of Orbiting Astronomical Observatory A1 (OAO–A1), not all these stars could be observed because the guidance system is not compatible with the small diaphragm required to isolate many of the stars in galactic clusters. However, outside of clusters, much information on the extinction law should be accessible to a moderately sized instrument with a field of view of a few minutes of arc.

REFERENCES

1. UNDERHILL, A. B.: A Program for Computing Early-Type Model Atmospheres and Testing the Flux Integral. Pub. Dominion Astrophys. Obs., vol. 11, 1962, p. 433.

2. STRÖMGREN, B.: Comparison of Observed and Theoretically Calculated Intensities in the Continuous Spectra of Main-Sequence B Stars. Rev. Mod. Phys., vol. 36, 1964, p. 532.

3. MIHALAS, D. M.; and MORTON, D. C.: A Model for a B1V Star with Line Blanketing. Astrophys. J., vol. 142, 1965, p. 253.

4. BOGGESS, A.; and BORGMAN, J.: Interstellar Extinction in the Middle Ultraviolet. Astrophys. J., vol. 140, 1964, p. 1636.

5. HILTNER, W. A.: Photoelectric, Polarization and Spectrographic Observations of O and B Stars. Astrophys. J. Suppl. Ser., vol. 2, 1956, p. 389.

DISCUSSION

Nandy: When we compare two stars to derive the extinction curve, we assume that their intrinsic energy distribution is the same for reddened and unreddened stars. The spectral behavior of the stars is often determined from spectrophotometric measurements in the visual wavelength region. Can we assume that stars which have the same spectral colors based on measurements in blue and visual wavelengths will have the same energy distribution in the far ultraviolet? Is the influence of metal abundances likely to be more important in the ultraviolet?

Borgman: Down to 2000 Å, for the stars that have been investigated, a reasonable agreement has been found between atmospheric radiation fields computed from stellar atmosphere models and the observations. Below 2000 Å I think the procedure is much more questionable. But any questions of this kind can be avoided by observing a sufficiently large number of stars and seeing how the scatter is around the reddening path in a color-color diagram. If it is small, then one feels reasonably certain that the simplest interpretation is valid.

Nandy: That is why it is dangerous to derive any conclusion from measurements of only a few stars in the ultraviolet. We have to observe many more stars.

Borgman: Yes, certainly anyone would agree with you; but having not so many data available, I do not consider it unreasonable to analyze the few stars that have been observed. In the case of Boggess' results we made these color-color plots and we were quite pleased that the scatter wasn't much larger than we had hoped for. We didn't publish the color-color plots, but anyone could make them up from the numbers that we published and see what they are worth. I agree with you that more observations are desirable; but many of these observations have to be made from satellites in order to increase the accuracy. These highly reddened objects are faint and require long integration times.

Wickramasinghe: Do you think the spectrophotometric method that Stecher and Milligan are using is any improvement on the use of filters in the ultraviolet?

Borgman: No, I am afraid that I often prefer reasonably wide-band filter measurements just because I think that the final analysis of any scanner observations is always such that one simply selects points from the scans. Therefore, rather than scanning through each point I prefer integrating the information.

Wickramasinghe: But the scanner method would reproduce narrow absorption peaks which you couldn't detect with a filter.

Borgman: And you think of absorption peaks in terms of interstellar absorption?

Comment: Yes, I think so.

Borgman: I see; well, I don't believe that they can be seen on the scans that have been obtained so far.

Spitzer: You mentioned the complications of blanketing in the wide-band measures down to 1500 Å. We now have preliminary sounding rocket data at Princeton on the absorption lines in two Scorpius stars (π Sco and δ Sco). The spectrograms have a resolution of about 1 Å, but they are not really suitable for spectrophotometry. They do suggest that down to 1500 Å the correction for line absorption due to blanketing may be quite small. Except for the two Si IV lines, and the corresponding C IV doublet, the other lines are relatively weak.

Borgman: I see; this is something which is rather promising because I thought that one should refrain from going beyond 1500 Å because of what Morton had said earlier, and in a sense it confirms what Byram and Chubb have found.

Hall: What would be the intensity of the galactic background of these wavelengths? Do you have any idea—compared with the stars?

Borgman: No one knows. This is, of course, a problem, and that is why I said "some" observational limitations in the title. A bright sky might mean that in an experiment like the OAO–A1 the diaphragm sizes are too large to measure the stars in Hiltner's catalogue.

Hall: Isn't the scattering by the optics at these very short wavelengths another problem?

Borgman: That can be reasonably investigated and cured in the lab. I think that the experimenters are confident that this won't be a limitation.

Hall: I didn't quite understand why there was so much flux at 1500 Å.

Borgman: That is just because I took the same extinction there as at 2200 Å, and the star simply gets brighter.

Hall: You mean it is brighter at $\lambda = 3300$ Å, dips down, and then comes back again?

Borgman: Yes, but that is simply a disguise, of course. It is the interstellar reddening that makes it fainter down to $\lambda = 2200$ Å and because I did choose not to increase the interstellar reddening beyond $\lambda = 2200$ Å, the star itself wins again and finally doubles the output.

Strömgren: As material grows in the coming years this analysis of the color-color diagram, I think, is going to be very important. Dr. Spitzer pointed out that if we don't go much beyond $\lambda = 2000$ Å the additional parameter (blanketing) should not be a serious one. It probably is well to look out for parameters that might cause scatter. The rotation parameter is important here. It is hoped that the model atmosphere work will be extended into the far UV as more data on the extinction in this region become available. It is a difficult extension to account for the rotation parameter as well.

Nandy: Work on rotating stars that has been done in Edinburgh by Guthrie shows that there is a difference in the intrinsic colors depending on whether the star is observed pole-on or equator-on.

Stecher: In reference to the application by Dr. Strömgren about gravity darkening, Collins has found more than one magnitude of difference for a very rapidly rotating star. If the additional Morgan classification for the early B stars is used, there is quite a spread in temperature between, for example, a B2 star and a B0 star. The temperature range is quite large and it may be more accurate to use classifications such as Dr. Strömgren's filters to determine whether or not the two stars are similar. This is always going to be a problem—are they really similar—especially when the excitation spectrum doesn't distinguish absolutely.

Strömgren: I think it is well to emphasize that, because as we go to this wide wavelength band we will probably need the results of quite extensive model atmosphere calculations in order to interpret these scatter diagrams. If you look in the wavelength regions that can be measured from the ground and then limit yourself to main sequence stars, you can subdivide according to beta index, but the evidence is that this does not affect the continuous curve much, even in the ultraviolet. The rotational effects imply two parameters: the angle and the speed of rotation, and I think it will become necessary, in order to analyze the data over a wide wavelength range, to go beyond what we can observe in the visual region for our calculations. However, this will be necessary only when we aim at quite a high standard of accuracy; I wouldn't say that it is very important at the present time.

Borgman: Whatever theoretical work will develop, data can be obtained almost without any theory on the stellar radiation field at all, simply by observing color indices and plotting them to see how the scatter looks. This sounds like a crude approach; but, on the other hand, there is little to hold against it. I would also like to add to what Dr. Stecher said a moment ago about the accuracy that one really needs in the temperature, that it is gratifying to remember that the temperature reddening looks a little bit like interstellar reddening. If it were the same you wouldn't notice it at all.

Greenberg: I must comment on temperature reddening looking like interstellar reddening. Over a limited spectral range it looks like λ^{-1}. I can't remember how far into the UV you can carry it and still say that the temperature reddening might look like the interstellar reddening.

Wickramasinghe: Certainly this would apply in the visible region, but I think the differences would be rather large in the ultraviolet.

Greenberg: It is my recollection that it would not apply in the ultraviolet.

Borgman: We shouldn't be too exacting about such a statement as I made. I think that the observations are still so crude that it holds.

Observations of Interstellar Reddening in Cygnus and Perseus[1]

K. NANDY
Royal Observatory
Edinburgh, Scotland

THE OBJECT OF THE EDINBURGH SPECTROPHOTOMETRIC SURVEY is to determine the interstellar extinction law as precisely as possible and to search for intrinsic variations in it. The observations have been extended to early type stars up to a limiting magnitude of $11^{m}.0$ in regions extending from $\ell^{II}=50°$ to $\ell^{II}=200°$. The 16/24/60-inch Schmidt telescope of the Royal Observatory has been used in conjunction with an objective prism and grating. Spectra extend from $\lambda=3300$ Å to $\lambda=9000$ Å with a dispersion of 1000 Å/mm at Hγ. Since few stars fainter than 9^{m} have been measured in earlier investigations, the present survey extends considerably the amount of information available.

In determining the extinction from a comparison of pairs of stars, one reddened and the other unreddened, one is faced by the problem of having to find two intrinsically similar stars in the same galactic region. Uncertainties in the assigned spectral types of stars give rise to systematic errors in the extinction curve. Such errors can be reduced by increasing the number of pairs of stars observed, and the study of interstellar extinction by earlier authors has been affected by the relatively small number of stars observed. The present paper describes the results for two regions in the direction of Cygnus ($\ell^{II}=80°$) and Perseus ($\ell^{II}=140°$).

METHODS OF OBSERVATION AND MEASUREMENT

The Edinburgh Schmidt telescope has a field diameter of about 4°. The performance of the telescope is described in reference 1. The objective prism of angle 1°.8, made of LF5 glass, has a high ultraviolet transmission. The spectra were broadened to 0.3 mm by varying the sidereal rate.

[1] The contents of this paper were published previously in the Pub. Roy. Obs. Edinburgh, vol. 3, 1964, p. 142, and vol. 5, 1965, p. 13.

In order to reduce overlapping of spectra, different emulsion-filter combinations were used to restrict the length of spectra and several have been found suitable. The plates were calibrated from the known magnitude differences between center and first-order side images of prism-crossed-by-grating spectra. For wavelength identification, hydrogen lines as well as features such as the sharp cutoff wavelength of the emulsions provided suitable reference points.

The tracings were taken with a Joyce Loebl microdensitometer which records density ($D=\log_{10} 1/T$). Absolute density values were converted to "Baker densities" by using the equation

$$\Delta=\log_{10}\frac{1-T}{T}$$

where this modified function of the transparency T is approximately linearly related to magnitude over a wide range of T. (See ref. 2.)

The monochromatic magnitude difference between a reddened and a comparison star of the same spectral type and luminosity class consists of two parts: (a) an intrinsic magnitude difference; and (b) a difference in the effect of interstellar extinction on these two stars.

If the reddened and the comparison stars are situated in the same galactic region, the extinction law and the energy distribution in the spectrum of the same type of star may be assumed to be the same. Monochromatic magnitude differences as functions of wavelength for any pair of two such stars should therefore represent effects of interstellar extinction.

The main sources of error are: (a) uncertainty in spectral classification; (b) difficulties in determining wavelengths at which observations are made; (c) graininess of plates; and (d) overlapping of spectra. Results of reference 3 show that the errors of the observed extinction curve arise primarily from uncertainties in spectral classification. An error of ± 1 subclass in spectral type may result in an error of ± 0.15 in the slope of the reddening curve in the ultraviolet relative to blue. Accuracy of spectral classification is therefore highly important; measuring the largest possible number of pairs of stars is useful.

EXTINCTION LAWS FOR CYGNUS AND PERSEUS

Observations

A region of 30 square degrees in Cygnus (centered on 20^h15^m, 38°) and 40 square degrees in Perseus (centered on 2^h12^m, 57°30′) has been investigated for which spectral types on the MK system exist.

As reported in references 3 and 4, 28 pairs of stars in Cygnus and 41 pairs of stars in Perseus have been measured. The extinction curves have been normalized so that the slope of the line fitted at $\lambda^{-1}=1.34\ \mu^{-1}$

and $\lambda^{-1}=2.28\ \mu^{-1}$ is unity, and the zero point is chosen such that the extinction $\Delta m_\lambda=1$ at $\lambda^{-1}=2.22\ \mu^{-1}$. Magnitude differences for a number of pairs of stars have been compared with photoelectric measures and the agreement is good. (See ref. 3.)

Extinction curves from O and B stars

Results of reference 5 have suggested that a higher ratio of $(U-B)$ color excesses to $(B-V)$ color excesses for O stars in Cygnus than found elsewhere is due to intrinsic ultraviolet deficiency in these stars. In this case the observed extinction effect for Cygnus stars should be a function of spectral type. In order to test this theory, the mean extinction curve derived from O stars has been compared with that derived from B stars. The difference is found to be within an observational error of ± 5 percent both in Cygnus and in Perseus and has, therefore, no significance.

Intrinsic rms dispersion

Comparing the observed rms dispersion with predicted standard errors of observation reveals that the intrinsic dispersion in the extinction curves in either direction is less than 3 percent.

Dependence on distance

In each region of Cygnus and Perseus, all the stars which have been studied by present and earlier authors have been divided into two groups of approximately equal number:

		Mean $m-M$	
Group	$m-M$	*Cygnus*	*Perseus*
I	<12.0	10.4	11.2
II	≥ 12.0	12.0	12.4

where m is the apparent magnitude and M is the absolute magnitude. For each group magnitude differences have been calculated for pairs of highly and moderately reddened stars belonging to the same group. A third group of extinction curves has been obtained by comparing moderately reddened stars with nearby slightly reddened stars.

Neither in Cygnus nor in Perseus do the mean extinction curves derived for each of three different groups differ from each other by more than 4 percent. It is therefore concluded that in the directions of Cygnus and Perseus the extinction law is independent of distance out to at least 2.5 kiloparsecs.

Weighted mean extinction curves

Since there are no significant differences in the extinction curves derived from different groups of stars, weighted mean extinction curves have been derived for the two regions, Cygnus and Perseus. The weight is equal to the difference in the color excesses of the pair of the stars compared.

For the Cygnus region, all available observational data have been combined to give a weighted mean extinction curve with a standard error of $\pm 0.008^m$. Spectrophotometric data of other observers for stars in the Perseus region are fewer than those for Cygnus stars. The mean extinction curve has therefore been obtained from the 41 pairs of stars studied by the author with a standard error of $\pm 0.01^m$.

A comparison between the results for Cygnus and Perseus is shown in figure 1. Least-square fitting of the observed points of figure 1 by orthogonal polynomials shows that the best fitting for each of two curves is either two straight lines intersecting at 4300 Å or polynomials of degree higher than three to give the variance σ^2 of the order of the standard error of the curve.

It is of interest that the curve for Cygnus stars in reference 6 appears to consist of two linear parts between 0.8 μ^{-1} and 3.0 μ^{-1}.

The ratio of the slope of the ultraviolet part of the curve to that of the blue-visible part is 0.64 for the Cygnus curve, in agreement with the result of reference 6, and 0.46 for the Perseus curve.

Observations and theory

The 30-percent difference in the slopes of the ultraviolet part of the reddening curves relative to the blue part appears to be in agreement

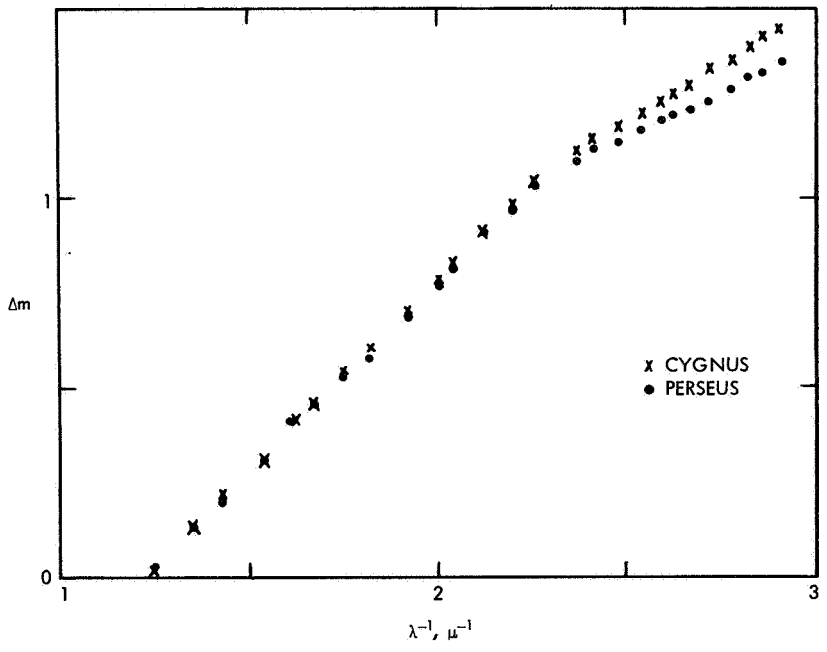

FIGURE 1.—Weighted mean extinction curve in directions of Cygnus and Perseus.

with the prediction of reference 7. A further requirement for the validity of the theory of reference 7 is that the ratio of the slope of the ultraviolet part to that of the blue-visible part should be dependent on the angle of viewing the spiral arm, or in other words, on the alinement properties of the particles and on the polarizability. (See ref. 8.) However, the dependence on galactic longitude has not been confirmed by the work reported in references 9 or 10.

The extinction of the Pleiades star HD 23512 offers a further test for the verification of the prediction of reference 8. This star is reddened by an amount of 0.35; polarizability is the same as the average value in Perseus and about four times that in Cygnus.

This Pleiades star, which has been studied at Edinburgh, is also discussed in reference 11. The slope of the ultraviolet part of the Pleiades extinction curve (fig. 2) relative to the blue-visible part is essentially the same as that found for the Cygnus curve; the small difference in the infrared may not be significant. The variation in the extinction law cannot be explained, therefore, by differences in alinement of the particles. An alternative possibility is that differences in composition of the particles may be responsible for the variation of the extinction law.

Figures 3 and 4 present comparisons of the observed extinction law

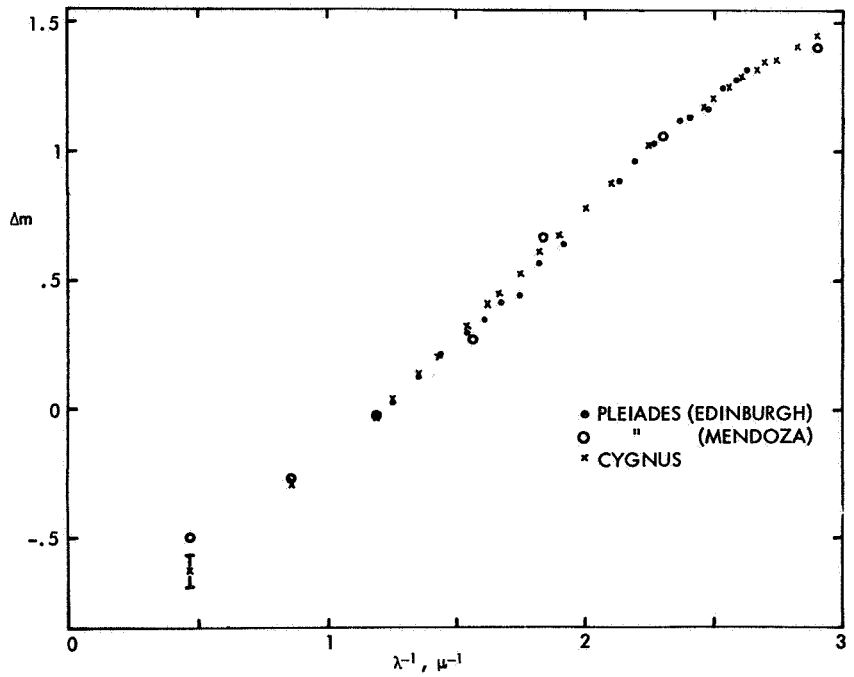

FIGURE 2.—Pleiades extinction curve. Vertical line denotes uncertainty of data point.

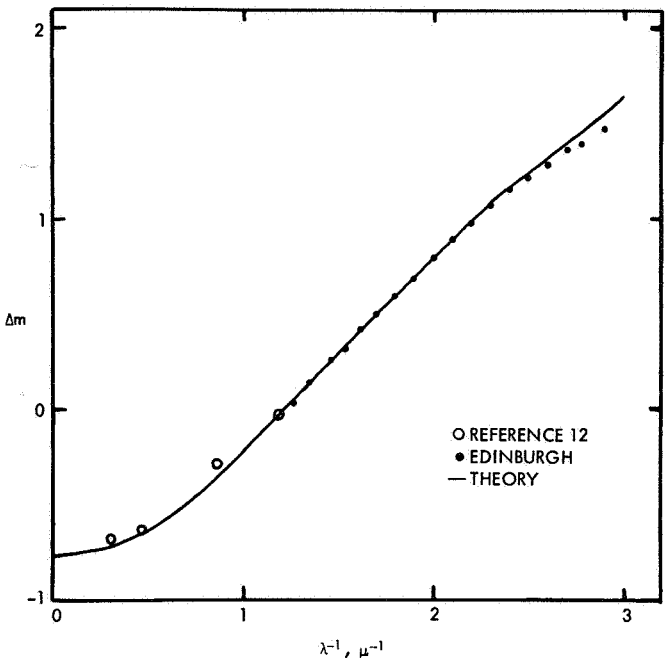

FIGURE 3.—Comparison of observed extinction law in Cygnus with theoretical extinction curve.

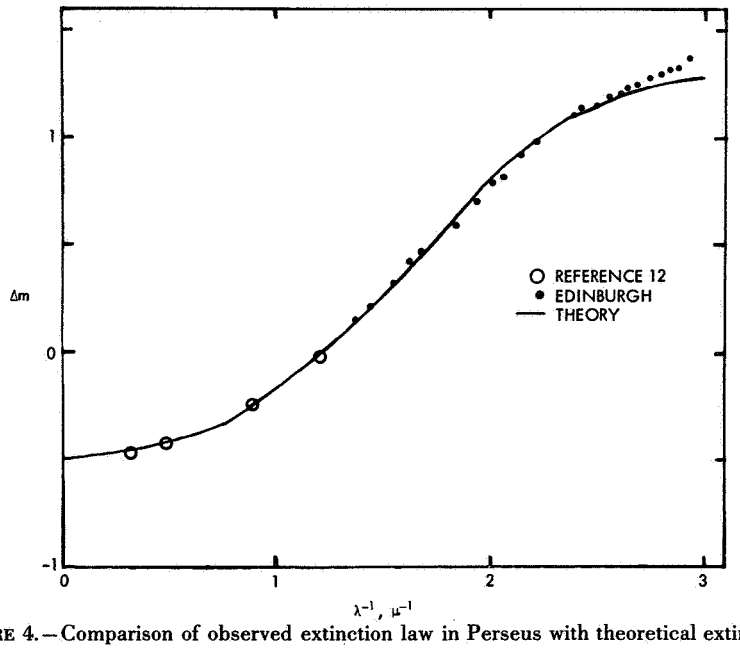

FIGURE 4.—Comparison of observed extinction law in Perseus with theoretical extinction curve.

in Cygnus and Perseus as obtained in the present investigation and as reported in reference 12 with the theoretical extinction curve. Graphite cores with radii less than 0.06 covered with ice mantles reproduce best the observed Cygnus curve (fig. 3), whereas a Gaussian distribution of pure graphite particles with dispersion of $\pm 0.01\ \mu$ centered at radius $a = 0.06\ \mu$ fits best the Perseus curve (fig. 4). (See ref. 13.) The wavelength 4300 Å is close to that at which the refractive index of graphite particles ceases to be constant. Over the wavelength region $0.8 < \lambda^{-1} < 2.3$, the extinction of graphite is close to the λ^{-1} law and thereafter deviates from the linearity depending on particle sizes. (See ref. 14.) It is difficult to explain the discontinuity in gradient in terms of any known absorption process; the fluctuations in mean particle size in the line of sight may be averaged out to simulate the observed two-straight-line effect for the mean reddening curve.

CONCLUSIONS

In the direction of both Cygnus and Perseus, the extinction is very uniform over a distance of at least 2.5 kpc in the line of sight, but the extinction law in Cygnus is significantly different from that in Perseus. The slope of the ultraviolet part of the curve relative to the blue part decreases in Perseus by about 30 percent as compared with that in the Cygnus region.

The difference between the Cygnus and Perseus laws can be explained if it is assumed that the extinction in Perseus is due to graphite grains and that in Cygnus, to graphite cores with ice mantles. Therefore, a difference in composition may exist between the Cygnus and the Perseus arms.

REFERENCES

1. GUTHRIE, B. N. G.; LAWRENCE, L. C.; NANDY, K.; PRATT, N. M.; and REDDISH, V. C.: Spectrophotometry and Multicolor Photometry at the Royal Observatory, Edinburgh. Communication Roy. Obs. Edinburgh, no. 27, 1965.

2. BAKER, E. A.: Spectrophotometric Measurements of Early-Type Stars I. Methods of Observation and Results for Oe 5 Stars. Pub. Roy. Obs. Edinburgh, vol. 1, 1949, p. 15.

3. NANDY, K.: Observations of Interstellar Reddening I. Results for Region in Cygnus. Pub. Roy. Obs. Edinburgh, vol. 3, no. 6, 1964, p. 142.

4. NANDY, K.: Observations of Interstellar Reddening II. Results for Region in Perseus. Pub. Roy. Obs. Edinburgh, vol. 5, no. 2, 1965, p. 13.

5. RODGERS, A. W.: Photoelectric Spectrophotometry of O-Type Stars. Roy. Astron. Soc., Monthly Notices, vol. 122, 1961, p. 413.

6. WHITFORD, A. E.: The Law of Interstellar Reddening. Astron. J., vol. 63, 1958, p. 201.

7. GREENBERG, J. M.; and MELTZER, A. S.: The Effect of Orientation of Non-Spherical Particles on Interstellar Extinction. Astrophys. J., vol. 132, 1960, p. 667.

8. WILSON, R.: The Relation Between Interstellar Extinction and Polarization. Roy. Astron. Soc., Monthly Notices, vol. 120, 1960, p. 51.

9. UNDERHILL, A. B.; and WALKER, G. H.: The Shape of the Interstellar Reddening Curve. Roy. Astron. Soc., Monthly Notices, 1965.

10. JOHNSON, H. L.: Interstellar Extinction in the Galaxy. Astrophys. J., vol. 141, 1965, p. 923.

11. MENDOZA, E. E., V: La Ley de Extincion Interestallar en las Pleyades. Tonantazintla y Tacubaya, vol. 4, no. 26, 1965.

12. JOHNSON, H. L.; and BORGMAN, J.: The Law of Interstellar Extinction. Bull. Astron. Inst. Netherlands, vol. 17, 1963, p. 115.

13. NANDY, K.; and WICKRAMASINGHE, N. C.: A Survey of Recent Interstellar Reddening Observations. Pub. Roy. Obs. Edinburgh, vol. 5, no. 3, 1965, p. 29.

14. WICKRAMASINGHE, N. C.; and GUILLAUME, C.: Interstellar Extinction by Graphite Grains. Nature, vol. 207, 1965, p. 366.

DISCUSSION

Field: In your diagram you included the slopes of the reddening law as functions of λ^{-1}. It makes a difference, doesn't it, how the normalization is carried out there?

Nandy: The shape of the reddening curve does not depend on how it is normalized. The normalization procedure which I have used is as follows: A smooth curve is drawn through the observed points, and the magnitude differences Δm_λ at $\lambda^{-1}=1.34\ \mu^{-1}$ and $\lambda^{-1}=2.28\ \mu^{-1}$ are read off this curve. The normalizing factor by which all observed magnitude differences are multiplied is the reciprocal of the slope of the line joining the two points (Δm_λ, $1.34\ \mu^{-1}$) and (Δm_λ, $2.28\ \mu^{-1}$). The zero point of Δm_λ is fixed so that $\Delta m_\lambda=1$ at $\lambda^{-1}=2.22\ \mu^{-1}$.

O'Dell: Other papers herein will show that there is some physical basis for thinking that the deviations you find might be due to very small-scale changes, primarily the presence of very high luminosity stars. In this case an even better requirement above this (taking all standard stars in the same region) would be to be sure that they are very close in space, because even in Perseus you are looking over a distance of several kpc and this could be integrating over regions which are generally of a 1-w density and a low mass cutoff region. This is something which I think may account for the differences observed and is something to watch out for.

Strömgren: In that connection, how many stars were measured in the Pleiades?

Nandy: Only one star.

Strömgren: Is this the star that has a high color excess measured by Mendoza?

Nandy: Yes, this is the star HD 23512 (Hertzsprung number 371).

Strömgren: The fact that the reddening is unusually high is of interest in connection with Dr. O'Dell's question.

Wampler: It is listed by Mendoza V as A0 V. I looked at a spectrum obtained by Helmut Apt and the calcium line appears too strong for A0. If the star is a fairly rapid rotator, some of the other metallic lines may be washed out. They do seem to be present and seem to be rather diffuse. I also looked at Dr. Herbige's plates and came to the same conclusion. Perhaps the spectral type is in fact closer to A2 than A0.

Nandy: It is spectroscopic binary?

Wampler: I don't know. It is not noted as a spectroscopic binary. Dr. Apt didn't think so at the time. He didn't have it in his list of binaries.

Nandy: This is the difficulty in deriving the reddening curve from one star.

Behr: I have two questions: what are the galactic coordinates of the two fields and what are the diameters or sizes of the fields?

Nandy: The galactic coordinates for Cygnus are $\ell^{II} \approx 70°$ and $b^{II} \approx 1°$ and for Perseus, $\ell^{II} \approx 140°$ and $b^{II} \approx -2°$.

Behr: That is exactly in the galactic plane and it is just in the region of high absorption. What is the area?

Nandy: The area is about 30 square degrees in each direction.

Behr: Do you think that these 30 stars are typical for the whole Cygnus arm?

Nandy: No, I do not say that. I am combining my results with Johnson and others. Excluding the Cepheus stars which show anomalous reddening, the majority of stars studied by Johnson and Borgman in the Cygnus arm exhibit the Cygnus reddening curve. The Scorpio-Ophiuchus stars also show Cygnus extinction.

Hall: Some years ago I tried to find out where the polarization in the Perseus direction was produced. There was no evidence of polarization beyond our own spiral arm. If I remember correctly, I tried this also with color excess and came to the conclusion that most of the absorption was in the Orion arm. Maybe I'm wrong on this. Have you tried this? In other words, you may be observing only the effects due to our arm when you observe Perseus.

Nandy: The space distribution of stars in the Perseus direction shows that the highly reddened stars are inside the Perseus arm, whereas the comparison stars are moderately reddened and are near the edge of the Perseus arm. Therefore, the extra extinction of the highly reddened stars, as compared with that of the moderately reddened stars, has probably been produced in the Perseus arm.

Donn: What was the graphite size distribution that you used?

Nandy: For Cygnus, graphite cores with radii less than 0.06 μ covered with ice mantles, whereas for Perseus, the Gaussian distribution of pure graphite particles with a dispersion of 0.01 μ centered at 0.06 μ fairly reproduces the observations.

Wickramasinghe: The precise values are not particularly significant here. It does seem that the Cygnus curve could be reproduced rather insensitively with respect to the core radius, as long as one had an equilibrium distribution of mantles.

Nandy: Yes, I have left this problem for you because you can discuss it much better.

271-992 O-67—3

The Shape of the Interstellar Reddening Curve[1]

ANNE B. UNDERHILL AND GORDON A. H. WALKER
Dominion Astrophysical Observatory
Victoria, British Columbia, Canada

WHEN THE OBSERVED SPECTRAL INTENSITY DISTRIBUTION of an early-type star has been freed from the distortions caused by absorption in the Earth's atmosphere and by instrumental sensitivity factors, it is a measure of the true spectral intensity distribution of the star and of the modifications to that distribution caused by the interstellar material between the Earth and the star. Thus, if one knew the true intensity distribution from the star, one could derive the shape of the interstellar reddening curve. In practice it is customary to compare the intensity distributions of pairs of stars of apparently the same spectral type, within the errors of classification, but which suffer different amounts of reddening, and to attribute the difference to interstellar reddening. In this way one can determine the shape of the interstellar reddening curve.

The results of reference 1 show that the monochromatic extinction, expressed in magnitudes, varies linearly with λ^{-1} from ultraviolet wavelengths to about 4500 Å, where the slope of the curve appears to change and there is a second linear section to about 20 000 Å. At still longer wavelengths, the extinction becomes independent of wavelength, more or less as suggested by theoretical studies of the extinction caused by small grains.

In recent years, model atmospheres in radiative equilibrium, which are believed to give a good representation of the parts of a stellar atmosphere in which the continuous spectrum is formed, have been obtained. This paper presents a comparison between the intensity distributions of some early B and late O type stars observed by the authors of references 2 and 3 and the intensity distributions from model atmospheres believed to represent O9 and B0 stars (refs. 4 and 5). Since the

[1] The contents of this paper were published previously in the Monthly Notices of the Roy. Astron. Soc., vol. 131, 1966, pp. 475–481.

models are constructed using a well-defined procedure and their continuous spectrum can be calculated in any desired detail, the differences between the observed and computed intensity distributions can be established with precision.

By studying heavily reddened and lightly reddened stars, one can separate the effects due to interstellar reddening from those due to departures of the continuous spectrum of the stars from the predicted spectrum of the models. In particular, it should be possible to confirm or deny the existence of the "knee" in the reddening curve near $\lambda = 4500$. This feature is difficult to account for with the present theories of the interaction between radiation and the interstellar grains. Some doubt exists about whether it is of interstellar origin or merely a reflection of differences of spectral type between the stars being compared. In addition, it would be reassuring to establish that the continuous spectrum of stars actually conforms to the predictions of the models. Since the predictions depend chiefly upon the variation of the adopted continuous absorption coefficients (H, He I, He II, and electron scattering) with wavelength, any serious departures from the predicted spectrum would necessitate a revision of the principles upon which the models have been constructed.

OBSERVED INTENSITY DISTRIBUTIONS

For the present purpose it is necessary only to study the relative intensity distribution in a stellar spectrum. The absolute intensity distributions given in reference 2 for ζ Ophiuchi, O9.5V, and ϵ Orionis, Bola, and those given in reference 3 for HD 154368 (O9.5Ia) and HD 167971 are used. (The spectral type listed for this star in reference 4 is O8f. However, spectrograms taken at the Dominion Astrophysical Observatory suggest a type near B0V in accord with classifications given in references 5 and 6.) Reference 3 gives data for ζ Ophiuchi which are in accord with those of reference 2. The observations of reference 2 extend from 3390 Å to 10 800 Å; those of reference 3, from 4000 Å to 6500 Å. The published data are converted into fluxes per angstrom relative to the flux at 5000 Å. Thus the intensity distribution in each star is represented by the function $F_\lambda(\lambda)/F_\lambda(5000\ \text{Å})$.

THEORETICAL INTENSITY DISTRIBUTIONS

The observed relative intensity distributions will be compared with those predicted from models computed in references 7 and 8. The computed continuous spectrum F_ν for five models is given in table I. The computations were performed using the Theoretical Spectrum Program. (See ref. 9.) Detailed data are given for the range from 2000 Å to 12 213 Å. The relative energy distributions $F_\lambda(\lambda)/F_\lambda(5000\ \text{Å})$ are listed in table II. These data are the standards with which the observed relative intensity

TABLE I.—*Emergent Spectrum* F_ν *of Five Models*

λ, Å [a]	F_ν, ergs/cm²-sec-$(\Delta\nu^\circ)$ [b]				
	Model 63	Model 89	Model 97	Model 64	Model 98
2000	2.5002×10^{-3}	3.3823×10^{-3}	4.5305×10^{-3}	5.1925×10^{-3}	6.7421×10^{-3}
2200	2.2804	3.0781	4.1129	4.7434	6.2218
2400	2.0869	2.7704	3.6991	4.2840	5.6005
2600	1.9231	2.5166	3.3341	3.8556	5.0725
2800	1.7869	2.3104	3.0351	3.4960	4.6123
3000	1.6578	2.1299	2.7698	3.1784	4.1835
3100	1.5950	2.0441	2.6517	3.0378	3.9941
3200	1.5395	1.9646	2.5437	2.9091	3.8202
3300	1.4849	1.8867	2.4331	2.7875	3.6509
3400	1.4294	1.8145	2.3251	2.6731	3.4931
3500	1.4044	1.7725	2.2615	2.5915	3.3663
3600	1.3526	1.7013	2.1668	2.4868	3.2273
3646V	1.3263	1.6658	2.1197	2.4348	3.1583
3646R	1.7716	2.1365	2.5775	2.8455	3.4428
3700	1.7710	2.1256	2.5547	2.8121	3.3885
3800	1.7049	2.0433	2.4538	2.7011	3.2539
3900	1.6431	1.9639	2.3558	2.5961	3.1269
4000	1.5821	1.8823	2.2586	2.4932	3.0074
4200	1.4647	1.7360	2.0824	2.2975	2.7897
4400	1.3600	1.6080	1.9270	2.1251	2.5894
4600	1.2673	1.4949	1.7892	1.9711	2.4037
4800	1.1842	1.3939	1.6665	1.8339	2.2374
5000	1.1104	1.3041	1.5557	1.7109	2.0861
5200	1.0439	1.2234	1.4573	1.6011	1.9508
5400	.9830	1.1506	1.3674	1.5022	1.8297
5600	.9280	1.0859	1.2862	1.4125	1.7203
5800	.8776	1.0240	1.2128	1.3311	1.6226
6000	.8291	.9653	1.1407	1.2567	1.5309
6500	.7251	.8407	.9874	1.0900	1.3321
7000	.6376	.7364	.8646	.9564	1.1677
7500	.5653	.6514	.7633	.8460	1.0301
8000	.5072	.5823	.6811	.7542	.9179
8206V	.4838	.5553	.6484	.7195	.8756
8206R	.5150	.5861	.6767	.7413	.8926
8700	.4635	.5263	.6078	.6672	.8019
9214	.4164	.4727	.5453	.5994	.7208
10503	.3275	.3700	.4254	.4695	.5649
12213	.2460	.2774	.3192	.3518	.4231

[a] V denotes immediately toward the violet, and R denotes immediately toward the red.

[b] ν° is frequency in $(\text{Å})^{-1}$

TABLE II.—*Relative Intensity Distributions* $F_\lambda(\lambda)/F_\lambda$ (5000 Å) *of Five Models*

λ (Å)	$F_\lambda(\lambda)/F_\lambda$(5000 Å) for —					λ^{-1}, μ^{-1}
	Model 63	Model 89	Model 97	Model 64	Model 98	
2000	14.106	16.213	18.20	18.969	20.200	5.000
2200	10.639	12.194	13.662	14.323	15.532	4.545
2400	8.160	9.225	10.328	10.875	11.804	4.167
2600	6.420	7.137	7.925	8.335	8.990	3.846
2800	5.133	5.653	6.224	6.517	7.053	3.571
3000	4.149	4.538	4.947	5.163	5.572	3.333
3100	3.739	4.077	4.434	4.619	4.983	3.226
3200	3.382	3.677	3.989	4.148	4.468	3.125
3300	3.068	3.321	3.589	3.739	4.016	3.030
3400	2.785	3.010	3.235	3.380	3.629	2.941
3500	2.583	2.775	2.969	3.094	3.296	2.857
3600	2.350	2.517	2.687	2.803	2.984	2.778
3646V	2.247	2.402	2.562	2.675	2.845	2.742
3646R	3.000	3.080	3.114	3.166	3.103	2.742
3700	2.911	2.975	2.997	3.000	2.964	2.703
3800	2.659	2.714	2.731	2.735	2.705	2.632
3900	2.433	2.476	2.489	2.494	2.464	2.564
4000	2.226	2.254	2.268	2.276	2.252	2.500
4200	1.868	1.885	1.896	1.902	1.893	2.381
4400	1.580	1.591	1.598	1.602	1.601	2.273
4600	1.349	1.355	1.359	1.362	1.362	2.174
4800	1.158	1.161	1.163	1.164	1.165	2.083
5000	1.000	1.000	1.000	1.000	1.000	2.000
5200	.869	.867	.866	.865	.864	1.923
5400	.759	.757	.754	.753	.752	1.852
5600	.666	.664	.659	.658	.657	1.786
5800	.587	.584	.579	.578	.578	1.724
6000	.519	.514	.509	.510	.510	1.667
6500	.386	.382	.376	.377	.378	1.538
7000	.293	.288	.284	.285	.286	1.429
7500	.226	.222	.218	.220	.220	1.333
8000	.178	.174	.171	.172	.172	1.250
8206V	.162	.158	.155	.156	.156	1.219
8206R	.172	.167	.162	.161	.159	1.219
8700	.138	.133	.129	.129	.127	1.149
9214	.110	.107	.103	.103	.102	1.085
10503	.067	.064	.062	.062	.061	.952
12213	.037	.036	.034	.034	.034	.819

distributions are compared. The models are all considered to represent main-sequence stars. Their equivalent spectral types are:

Model	*Spectral type*
63	B2
89	B1
97	B0.5
64	B0
98	O9

COMPARISON BETWEEN THEORY AND OBSERVATION

The differences between the observed distributions and that for model 98 at each selected wavelength are given in tables III and IV. A negative magnitude difference means that the star is brighter than the model by the given amount, the fluxes in each object, star, or model being measured in units of the flux at 5000 Å. A positive magnitude difference means that the star is fainter than the model at the listed wavelength.

TABLE III.—*Magnitude Differences Between Model 98 and Observed Intensity Distributions of ζ Ophiuchi and ε Orionis*

λ, Å	λ^{-1}, μ^{-1}	Magnitude difference between model 98 and—		λ, Å	λ^{-1}, μ^{-1}	Magnitude difference between model 98 and—	
		ζ Oph	ε Ori			ζ Oph	ε Ori
3390	2.950	+0.455	+0.160	5840	1.712	−0.225	−0.115
3448	2.900	+0.425	+0.132	6055	1.652	−0.272	−0.142
3509	2.850	+0.402	+0.132	6370	1.570	−0.325	−0.152
3571	2.800	+0.395	+0.122	6800	1.471	−0.418	−0.218
3636	2.750	+0.350	+0.098	7100	1.408	−0.498	−0.255
3704	2.700	+0.498	+0.232	7530	1.328	−0.550	−0.292
4032	2.480	+0.310	+0.152	7850	1.274	−0.603	−0.303
4167	2.400	+0.268	+0.132	8080	1.238	−0.638	−0.338
4255	2.350	+0.242	+0.102	8400	1.190	−0.670	−0.350
4464	2.240	+0.198	+0.092	8805	1.136	−0.675	−0.335
4566	2.190	+0.152	+0.062	9700	1.031	−0.758	−0.353
4787	2.090	+0.072	+0.032	9950	1.005	−0.790	−0.410
5000	2.000	+0.000	+0.000	10250	.976	−0.838	−0.448
5263	1.900	−0.088	−0.038	10400	.962	−0.835	−0.435
5556	1.800	−0.165	−0.080	10800	.926	−0.868	−0.468

The relative intensity distributions of models 98 and 64 are indistinguishable between 4000 Å and 6500 Å; thus it suffices to compare the observations with one model. The spectrum from model 98 is significantly brighter than that from model 64 at wavelength shorter than the Balmer limit.

TABLE IV.—*Magnitude Differences Between Model 98 and Observed Intensity Distributions of HD 154368 and HD 167971*

λ, Å	λ^{-1}, μ^{-1}	Magnitude difference between model 98 and—	
		HD 154368	HD 167971
4000	2.500	+0.798	+1.028
4200	2.381	+0.670	+0.839
4400	2.273	+0.505	+0.639
4600	2.174	+0.344	+0.396
4800	2.083	+0.172	+0.236
5000	2.000	+0.000	+0.000
5200	1.923	−0.164	−0.204
5400	1.852	−0.299	−0.385
5600	1.786	−0.436	−0.571
5800	1.724	−0.509	−0.681
6000	1.667	−0.654	−0.849
6500	1.538	−0.909	−1.177

From each set of data the color excess between the V and B points ($\lambda^{-1}=1.83$ and $\lambda^{-1}=2.29$, respectively) was found. It is 0.361 magnitude for ζ Ophiuchi, 0.180 magnitude for ϵ Orionis, 0.870 magnitude for HD 154368, and 1.110 magnitudes for HD 167971. The data were then normalized to an excess of 1.000 magnitude between V and B, and the points were plotted to give the composite reddening curve shown in figure 1.

Four conclusions are immediately evident:

1. The comparison with theoretical spectra has produced a reddening curve like that found by standard observational procedures. Consequently, it may be concluded that over the range from 4000 Å to 6500 Å at least, the spectrum from model 98 represents well the spectra from real stars of a type near O9.

2. A definite "knee" occurs in the reddening curve. The break appears to occur at $\lambda^{-1}=2.25$ (4450 Å).

3. If the decrease in gradient for $\lambda^{-1}>2.25$ is due to an anomalous brightening of the stellar spectrum and not to weaker interstellar extinction, the gradient for $\lambda^{-1}>2.25$ should be a function of color excess. This is not true, which means that the "knee" is not due to an anomaly in the stellar spectrum.

4. The stars ζ Ophiuchi and ϵ Orionis are considerably brighter in the Balmer continuum and in the Paschen continuum than predicted by the model. They appear to be surrounded by extended envelopes

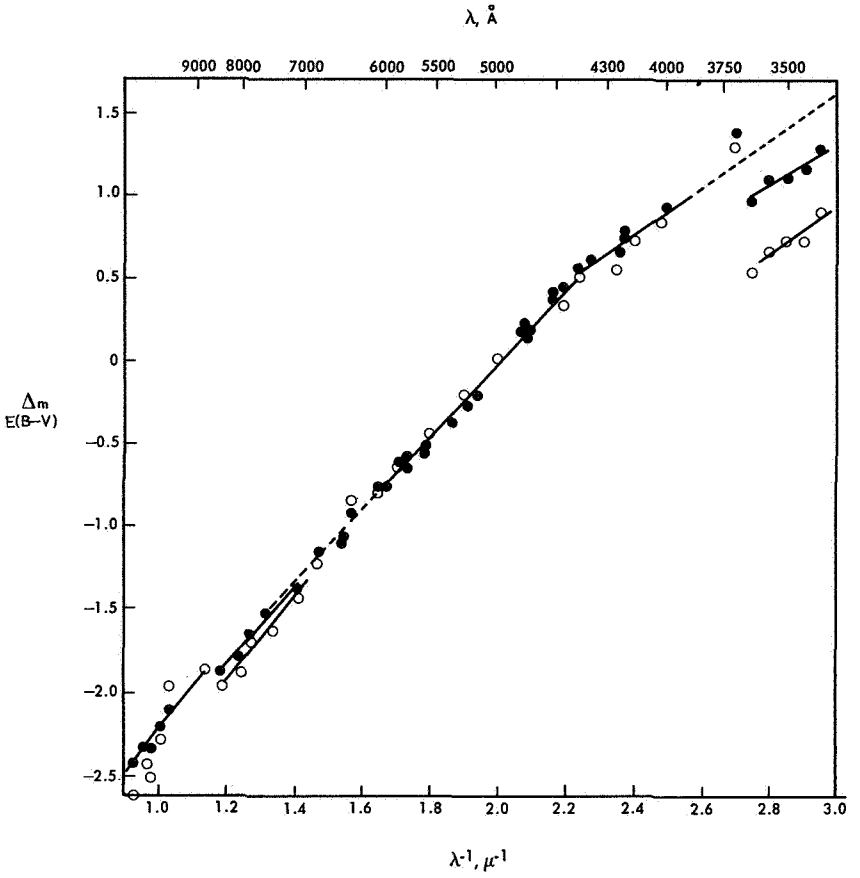

FIGURE 1.—Normalized interstellar reddening curve. Closed circles, HD 154368 and HD 167971 for 4000 Å $< \lambda <$ 6500 Å, and ζ Ophiuchi, for all values of λ; open circles, ϵ Orionis.

which give the Balmer continuum in emission, a not unlikely state of affairs for such early-type stars.

In the discussion the point at $\lambda^{-1} = 2.700$ (3704 Å) is ignored because the overlapping of the Balmer lines probably depresses the stellar continuum there.

The normalized reddening lines may be represented by the following equations:

$$\Delta m_\lambda = 2.23(1/\lambda - 4.46) \text{ for } 2.25 > \lambda^{-1} > 1.45 \quad (1)$$

$$\Delta m_\lambda = 1.42(1/\lambda - 2.65) \text{ for } 2.25 < \lambda^{-1} < 2.50 \quad (2)$$

These results may be compared with those of reference 10. The equations in this reference are normalized to give unit gradient for $2.25 < \lambda^{-1}$, and $\Delta m_\lambda = 1$ for $\lambda^{-1} = 2.22$. In this reference is found

$$\Delta m_\lambda = \lambda^{-1} - 1.22 \qquad \text{for } 1.0 \leq \lambda^{-1} < 2.30$$

$$\Delta m_\lambda = 0.64(\lambda^{-1} - 0.39) \text{ for } \lambda^{-1} > 2.30$$

Applying the same normalization conditions to equations (1) and (2) gives:

$$\Delta m_\lambda = \lambda^{-1} - 1.22 \qquad \text{for } 2.25 > \lambda^{-1} > 1.45 \tag{1}$$

$$\Delta m_\lambda = 0.64(\lambda^{-1} - 0.41) \text{ for } 2.25 < \lambda^{-1} < 2.50 \tag{2}$$

The agreement is excellent and strongly supports conclusions 1 and 3 given previously. Furthermore since the four stars being studied do not lie in the Cygnus region, but are scattered around the sky, the agreement between the reddening law found here and that of reference 10 lends support to the idea that the scattering properties of interstellar grains are the same in all parts of the galaxy.

REFERENCES

1. SHARPLESS, S.: Interstellar Reddening. Stars and Stellar Systems, vol. 3, Strand, ed., University of Chicago Press, 1963, p. 225.

2. OKE, J. B.: Photoelectric Spectrophotometry of Stars Suitable for Standards. Astrophys. J., vol. 140, 1964, p. 689.

3. WILLSTROP, R. V.: Absolute Measures of Stellar Radiation II. Roy. Astron. Soc., Memoirs, vol. 69, pt. 3, 1965.

4. MORGAN, W. W.; CODE, A. D.; and WHITFORD, A. E.: Studies in Galactic Structure II. Luminosity Classification for 1270 Blue Giant Stars. Astrophys. J., Suppl. Ser., vol. 2, 1955, p. 41.

5. NEUBAUER, F. J.: The Radial Velocities of Faint Class B Stars in the Declination Zone 0° to −23°. Astrophys. J., vol. 97, 1943, p. 300.

6. SANFORD, R. F.: Interstellar Calcium Lines in the Spectra of Stars in Open Clusters. Astrophys. J., vol. 110, 1949, p. 117.

7. UNDERHILL, A. B.: A Program for Computing Early-Type Model Atmospheres and Testing the Flux Integral. Pub. Dominion Astrophys. Obs., vol. II, no. 23, 1962.

8. UNDERHILL, A. B.: Concerning the Interpretation of Line Strengths in B-Type Spectra. Bull. Astron. Inst. Netherlands, vol. 17, 1963, p. 161.

9. UNDERHILL, A. B.: A Program for Computing the Theoretical Spectrum from a Model Atmosphere. Pub. Dominion Astrophys. Obs., vol. II, no. 24, 1962.

10. NANDY, K.: Observations of Interstellar Reddening I. Results for Region in Cygnus. Edinburgh Pub., vol. 3, no. 6, 1964.

DISCUSSION

Wickramasinghe: I would like to point out that the knee in Dr. Nandy's curve occurs rather strikingly at a wavelength where the refractive index for graphite begins to change considerably; from the infrared up to that point it remains reasonably constant, and then begins to vary.

Greenberg: Is there any good reason why the graphite index should change sufficiently to make such a drastic change in the extinction? These are two straight lines.

Wickramasinghe: What I have done is to perform Mie computations for graphite by using recently available refractive index data. For radii less than about 0.06 μ the extinction efficiency curves have the property of remaining closely like the curves for λ^{-1} in the wavelength range $0.8 < \lambda^{-1} < 2.4$, and thereafter deviating considerably from the λ^{-1} curve. The precise structure of the curves for shorter wavelengths appears to depend sensitively on the particle size. If I take a size distribution of graphite, I can simulate approximately Dr. Nandy's two-straight-line effect.

Greenberg: Then this effect will show up if there are many small graphite particles corresponding to this type of extinction?

Wickramasinghe: Yes. The straight-line segment for $\lambda^{-1} < 2.4$ could be obtained almost independently of size—provided it is less than about 0.06 μ. But, in order to get a specified ratio of slopes over the two segments, one has to be a bit careful in mixing sizes.

Greenberg: Why can this be observed in Perseus as well as in Cygnus? In one case one has pure graphite. Then I would expect that if something happened to the graphite that is pure and small, this effect would be observed.

If on the other hand one had to account for this large extinction in the UV by putting on dirty ice mantles, which we have had to do, these ice mantles or whatever we put on would then be sufficiently large to obscure this slope discontinuity. However, if I remember correctly, Dr. Nandy's curves had a change in slope with a rather sharp discontinuity, both for Perseus as well as for Cygnus. Can you explain these two?

Wickramasinghe: Yes; the point is that if we take the graphite core radius of the order of 2 to 3×10^{-6} cm and cover this core with an ice mantle of up to 1.5 times that radius, then 60 percent of the extinction in the visible and the *ultraviolet* comes from the graphite core. The reason is that one has to have a value of $(2\pi a)/\lambda$ of the order of unity where a is the outer mantle radius before one can get a significant contribution from the ice mantle. For example, if you have an ice grain with a radius of 0.05 μ, you won't get very much absorption in the visible compared with what you would obtain with a graphite core of radius 0.03 μ.

Greenberg: I disagree. We have computed also for 0.05-μ graphite cores covered with ice mantles of small as well as large dimensions and do not find this to be true.

Wickramasinghe: It depends on how much ice mantle you have.

Greenberg: I assume that the ice mantles are sufficient to give one good extinction in the UV. I think, however, that this is a very fundamental point, at least as fundamental as the character of the extinction at 2400 Å.

Wickramasinghe: At least it is the case in comparing the extinction cross section for an ice particle of radius 0.05 μ with that for a graphite core of radius 0.03 μ that the ice absorption is very much smaller. If one compares the cross section for the composite particle with that for the core itself, it turns out that the core absorption amounts to about 80 percent in the infrared, 70 percent in the visible, and 60 percent in the blue.

Borgman: Miss Underhill has criticized sometimes the practice of comparing stars of equal spectral classification with the purpose of deriving their reddening properties. Now I note with some satisfaction that you find the same results as these which were critical. Does this now satisfy you and Miss Underhill that the previous practices that have been used are satisfactory?

Walker: I don't quite understand. Did she normally criticize the use of stars which do not necessarily have exactly the same spectrum?

Borgman: Yes, and I do not think that the stars which you have analyzed here have the same spectral type.

Walker: No, I quite agree. I didn't get the impression when I was writing this with Miss Underhill that she felt there should be a change in viewpoint.

Borgman: The fact that you find the same results is at least encouraging.

Walker: Yes, I think one has to make a proviso that we have stipulated the range over which this has been satisfactory. There is no question that we can use this where continua are concerned. I think that obviously we must be quite cautious about anything which might involve shell emission. As I said before, this is the hottest stellar model Miss Underhill has computed so far and it looks as if it is satisfactory in the visual, ultraviolet, and red. I think we are bringing up the point of graphite too early. It might be worth deciding just how sharp the discontinuity of slope is. As far as I could make out in our work it was just a complete break. Now, we obviously do not have sufficient resolution to state that categorically. I don't know how you would find it in your results.

Nandy: It is difficult to say how sharp this discontinuity is from my results because the dispersion is too low. Another program is in progress using 60- and 120-Å dispersions, and the same stars will be studied; we hope to determine how sharp this change in slope is.

Greenberg: I wonder if Dr. Walker has any comments. This happens to be around 4430.

Walker: In the way that I drew it I found that it could coincide with the wavelength of 4430. But I don't think it is going to have anything to do with 4430. I think that one would expect for unit color excess a central depth of the order of 10 percent for the 4430 line. With the 50-Å resolu-

tion used in scanner results, one would not see the full 10 percent, but would probably see about 1 percent. This becomes something like one-hundredth of a magnitude and the discrepancy here, if one wants to draw in a smooth curve, is more of the order of one-tenth of magnitude.

Wampler: I would agree, I think. The wavelength 4430 is not the agent here.

Olson: One of your stars is very obviously a rapid rotator – ζ Ophiuchi; I think it is about 400 km/sec.

Walker: The apparent Balmer and Paschen emission might be due to that.

Wickramasinghe: Could you say something about how these stars are distributed in the galaxy?

Walker: There is one star in Orion and there are three in the Southern Hemisphere reasonably close together. I think Dr. Nandy showed them on his graph. Actually, I think it is a pity that we didn't proceed and go through the whole of Willstrop's list (ref. 3). But, of course, we couldn't do it in this way. I think probably one could go about it now in what I would call the classical fashion.

Field: Could I ask about the bump in the extinction at $\lambda = 6300$? Do you believe that?

Walker: I don't really know; it just happens to occur in both our graphs. It happens to be a kink in the same direction as far as our experimental errors are concerned. It looks like a significant thing. There is no strong interstellar absorption band there, and $\lambda = 6284$ is some distance away, but again this is something I just noticed in passing.

Wampler: We were doing some work at Lick in regard to stellar energy distributions, and we have had to find out what the extinction of the atmosphere is. It follows the curve for λ^{-4} very closely to about 5500 Å to 5800 Å; beyond that we quickly run into bumps and I wonder if there are regions in the atmosphere that might cause extinction in this spectral region. The extinction may not go as the secant of the altitude angle z region.

Walker: But surely there should be a scatter at this point. It should not be all in the same direction.

Wampler: All your stars with the exception of Orion are in the Southern Hemisphere, which means that they never pass overhead.

Walker: They were all measured at the same zenith distance, but Dr. Nandy's results show that there should only be a scatter around that point. His standard stars and his reddened stars presumably do not have a systematic difference in sec z.

Nandy: Yes, when they are on the same objective prism plates atmospheric extinction is not that important. But, when the reddened and comparison stars are not on the same plate, magnitude differences have been corrected for atmospheric extinction.

Optical Thickness of the Galactic Absorption Layer and Its Ratio of Total to Selective Absorption

HEINZ NECKEL
Hamburg Observatory
Hamburg, Germany

AS IS WELL KNOWN, the surface brightness within the galaxies decreases strongly with increasing distance from the center. Therefore, if the diameters of the galaxies are defined by the isophote of a distinct apparent surface brightness, these diameters become smaller and smaller with increasing galactic absorption. The diameters are defined in reference 1 in this manner (by the isophote $26^{m}.5/\text{sec}^2$); therefore, the mean surface brightnesses derived in that reference correspond more and more to the inner, brighter parts of the galaxies as the absorption increases. Consequently, in the derivation of the half optical thickness a of the galactic absorption layer from the variation of the mean surface brightnesses S of 113 spiral galaxies with galactic latitude β, the assumption in reference 1, $dS/d(\csc \beta)=a$, is not correct but has to be replaced by the more complicated formula

$$dS/d(\csc \beta)=\left[1-\frac{5 \log e}{m_{lim}-m_{center}}(1-R)\right]a$$

This formula holds for spirals whose brightness distribution may be represented by the law

$$m(\rho)=m_{center}+\frac{(m_{lim}-m_{center})\rho}{\rho_{lim}}$$

where

ρ	distance from center
ρ_{lim}	apparent radius of galaxy
m_{lim}	(photographic) surface magnitude at border
m_{center}	(photographic) surface magnitude at center
R	ratio of surface brightness at apparent border of galaxy to mean surface brightness within this border

The ratio R is small compared with 1 and may be neglected. Assuming $m_{lim}-m_{center}=5^{m}.0$ and taking the equation $dS/d(\csc\beta)=0^{m}.26$ from reference 1, one gets $0^{m}.46$ for the half (photographic) optical thickness of the absorption layer.

Similar values are found from the galaxy counts in references 2 and 3 if the loss of galaxies with decreasing galactic latitude is considered to be an effect of decreasing diameters rather than being determined by the limiting magnitude of the plates. Since the diameters of the faintest galaxies which can be found are only a little larger than the diameters of the stars, even a small decrease of their diameters due to absorption will make them indistinguishable from the stars. A thorough treatment of the problem shows that the decrease of the galaxy numbers with decreasing galactic latitude depends not only on the optical thickness of the absorption layer but also on the brightness distribution within the galaxies. For elliptical galaxies, whose brightness distribution may be approximated by the formula $m=m_0+5\log\rho$, one gets

$$\frac{d(\log N)}{d(\csc\beta)}=-\frac{3}{5(1+dK/dm_c)}a$$

while for the spirals, the corresponding expression

$$\frac{d(\log N)}{d(\csc\beta)}=-\frac{1.3}{(m_{lim}-m_{center})(1+dK/dm_c)}a$$

follows from their brightness distribution mentioned previously, where

$N=N(m)$ number of galaxies with magnitude less than m
K extinction
$m_c=m-a\csc\beta-K$

The differential quotient dK/dm_c considers the influence of the red shift. These two formulas have to be compared with the one used so far,

$$\frac{d(\log N)}{d(\csc\beta)}=-\frac{0.60}{1+dK/dm_c}a$$

which obviously holds only for point sources as, for example, the quasars and, more accidentally, the ellipticals.

Values of $m_{lim}-m_{center}=3$ magnitudes for the counts in reference 2 and $m_{lim}-m_{center}=2$ magnitudes for the Lick counts are used since corresponding photographs showed these values to be the most probable. If values of $\frac{d(\log N)}{d(\csc\beta)}$ of 0.15 for Hubble's counts and 0.24 for the

Lick counts are also assumed, one finds values of $0^m.40$ and $0^m.45$, respectively, for the half (photographic) optical thickness a. These values are in good agreement with the former value, $0^m.46$, derived from the data of reference 1.

The mean value of about $0^m.45$ is approximately twice as large as the former value, $0^m.25$, found in references 1 and 2 and also twice as large as the value which follows from the observations of: (1) the colors of galaxies by Holmberg and (2) the colors of globular clusters by Kron and Mayall (ref. 4) (at the galactic pole $E_{B-V}=0^m.05$ and $0^m.06$, respectively, for (1) and (2)), if one assumes a ratio $R_B=A_B/E_{B-V}=4$. Because these last observations need no corrections, a value of R_B of about 8 results from these considerations.

This result is in quantitative agreement with the work published in reference 5 and indicates that there may be an appreciable amount of neutral absorbing material whose relative abundance perhaps increases with increasing distance from the galactic plane. The observations of the galaxies are confined to higher galactic latitudes, whereas the "normal" ratio $R=A_VE_{B-V}=A_B/E_{B-V}-1=3$ in general is determined near the galactic equator, where

R_B ratio of total extinction in blue to color excess, A_B/E_{B-V}
A_B extinction in the blue
A_V extinction in the visual

However, for a final solution of this problem, further special observations are needed.

REFERENCES

1. HOLMBERG, E.: A Photographic Photometry of Extragalactic Nebulae I. A Study of Integrated Magnitudes and Colors of 300 Galaxies. Medd. Lund Obs., vol. II, no. 136, 1958.

2. HUBBLE, E.: The Distribution of the Extragalactic Nebulae. Astrophys. J., vol. 79, 1934, p. 8.

3. SHANE, C. D.; WIRTANEN, C. A.; and STEINLIN, U.: The Distribution of Extragalactic Nebulae III. Astron. J., vol. 64, 1959, p. 197.

4. KRON, G. E.; and MAYALL, N. Y.: Photoelectric Photometry of Galactic and Extragalactic Star Clusters. Astron. J., vol. 65, 1960, p. 581.

5. JOHNSON, H. L.: Interstellar Extinction in the Galaxy. Astrophys. J., vol. 141, 1965, p. 923.

DISCUSSION

Borgman: This result was a controversial one, but was expected from counts of galaxies and would indicate that there is some neutral absorption which does not show up in the more traditional methods.

Neckel: That is true. The neutral absorption probably is more important than was expected. The result agrees fairly well also quantitatively with Johnson's work (ref. 2).

Gehrels: I was wondering if the ratio A/E was assumed to be the same for E_{P-V} and E_{B-V}.

Neckel: The difference between total absorption A_B and A_P (where the subscript P refers to photographic extinction) can be neglected. The ratio of A/E_{P-V} to A/E_{B-V}, therefore, is approximately equal to the ratio E_{B-V}/E_{P-V}. This latter ratio has a value of about 0.8. From Holmberg's value of $0^m.06$ for the selective absorption at the galactic pole (ref. 1), one gets about $0^m.05$ in the BV system. This difference was taken into account, although it is not important in this case.

Wickramasinghe: Is it possible to separate completely the effects of absorption inside and outside the galaxy?

Neckel: It is not possible to separate the absorption inside and outside the galaxy. Only the absorption inside our galaxy can show up in the latitude variation of surface brightness and numbers of galaxies.

I first wanted to see if it was possible that the ratio A/E might vary with distance from the galactic plane. The adopted value of 3 for this ratio was derived from objects near the galactic plane. For the latitude variations of galaxy counts and brightnesses, the layers at larger distances from the plane are important. So far, I didn't doubt that within the galactic plane the ratio would be 3, because one can derive the spiral structure very well from early-type stars if one assumes this ratio when computing the distances.

The model I proposed was the following: A geometrically thin layer of selective ($A/E \approx 3$) absorption material near the galactic plane with an optical thickness of about $0^m.25$, and a geometrically thick layer of neutral absorbing material with the same optical thickness. While the contribution of the neutral layer in the galactic plane would be small because of the larger geometrical thickness, the total optical thickness would be $0^m.5$. This is the value derived from the galaxy counts. But this was only a first speculation. According to previous papers, there seems to be a large variation of the ratio A/E in the galactic plane. The value 3 seems to be the minimum value and, as a consequence, the average one will be larger than 3. This is exactly the result indicated by the galaxies.[1]

---

[1] Note added in proof: If the reddening law is uniform within the whole galaxy, one obviously gets the best spiral-arm structure when the distances of the stars are derived by using the true ratio A/E. If, however, the reddening law and the ratio A/E varies from star to star between two limiting values, but the distances are computed by using one single value of the ratio A/E for all stars, one gets the best concentration by using the smaller limiting value. Therefore, the fact that the best spiral-arm concentration is derived when reducing the distances of the stars with a value of 3 for the ratio A/E does not exclude the possibility of a general variable reddening law.

Wickramasinghe: I am wondering if the inference could be drawn that this is galactic absorption rather than absorption between galaxies.

Neckel: Our results depend on the variation with galactic latitude. I can't see how intergalactic absorption would depend on the galactic latitude.

Nandy: Are you assuming that there is no intergalactic absorption when you count the galaxies?

Neckel: If there were an appreciable amount of intergalactic matter, its influence could be considered in a first approximation as an increase of the term dK/dm_c, which so far only includes the loss of brightness due to the red shift. The result would be a still larger value for the optical thickness of the galactic absorption layer. But I think this would be an effect of the second order. The main assumption is that the intergalactic absorption does not depend on the direction.

Wickramasinghe: For directions close to the plane of the galaxy one would expect the dominant contribution to the extinction to come from dust grains inside the galaxy, but for directions at right angles to it one would expect the stuff between the galaxies to play the dominant role.

Greenberg: If this were true, the dependence of extinction on galactic latitude would be considerably different. The extinction depends on a geometrical configuration and is a function of the length of path in our galaxy. If there were intergalactic absorption in addition to that within the galaxy and it were uniform, an additional constant (independent of β) would result which could not be seen and which would have no effect on this function.

Borgman: What you actually get here is, in my opinion, the component in the galaxy which might be considered neutral with respect to every other component that has been found by variable extinction methods of color differences.

Behr: Is there not a discrepancy between these results and those of Johnson? Johnson finds that the neutral absorption is present especially in very young areas, or in areas near the galactic plane. At higher galactic latitudes we don't know any young regions.

Neckel: Johnson's observations of one star led to a value of A/E of about 15. The star was at a rather high latitude.

The Color Dependence of Interstellar Polarization

ALFRED BEHR
Göttingen University Observatory
Göttingen, Germany

MEASUREMENTS OF THE INTERSTELLAR POLARIZATION of starlight at different wavelengths have been reported by several observers in references 1 to 8. With a few exceptions the wavelength range of the measurements is still relatively small, and up to now only a few dozens of stars have been measured with high precision. There is still a remarkable discrepancy between the results of different observers, as can be seen in figure 1. The scattering of the individual values is significantly larger than the probable error given by the respective authors. One of the most serious error sources seems to be the instrumental polarization which itself is highly color dependent. (See ref. 9.)

Nevertheless, even if a much greater individual error is assumed, a remarkable conclusion can be drawn: the wavelength dependence of polarization is not the same for all stars. If the Davis-Greenstein mechanism (ref. 10) is assumed as a working hypothesis, theoretical considerations presented in references 11 and 12 show that, in general, a maximum of polarization should be expected at a certain wavelength for a given type of interstellar dust. In this case any individual color dependence can be understood as a combined influence of more than one cloud with different types of interstellar grains, and, if necessary, with depolarization if the planes of vibration are not parallel to each other. However, it still seems to be impossible to draw conclusions from the observed color dependence about the type of material producing the polarization.

On the other side, according to reference 12, a variation of the color dependence with the angle between the line of sight and the lines of magnetic force should be expected. In this instance a correlation with galactic longitude, or at least a significant difference between the Cygnus region and the Perseus region, should be observed, the effect of which, however, seems not to be very strongly indicated. Also, it is known that the small polarization in Cygnus is mostly due to depolarizing effects.

There is still another way to discuss the observed results. According to reference 10, the observed polarization p as a function of the interstellar extinction A_V and the angle σ between the line of sight and of the lines of force is

$$p/A_V = (p_0/A_V) \sin^2 \sigma$$

where p_0 is the polarization for $\sigma = 90°$

Absence of depolarization indicates that the lines of force are in the plane of vibration. The observations reported in reference 4 show that the polarization can always be represented by the expression

$$p/A_V \leqq 0.065$$

Small values should be observed when $\sigma < 90°$, or when depolarization occurs by different clouds with lines of force not in the same plane. For an individual star there is in general no possibility of deciding between the two cases. For large values of the ratio p/A_V, it can be easily assumed that σ is not very much different from 90°.

For small values of the ratio p/A_V, a majority of stars with small values of σ can be selected if stars with possible depolarization are excluded.

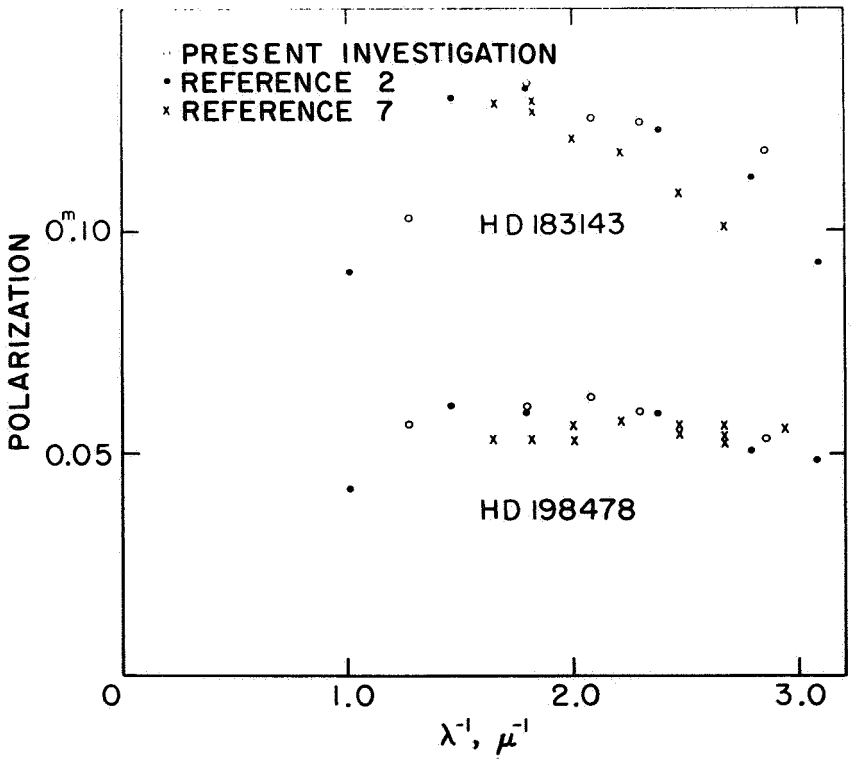

FIGURE 1.—Polarization as a function of wavelength for two stars.

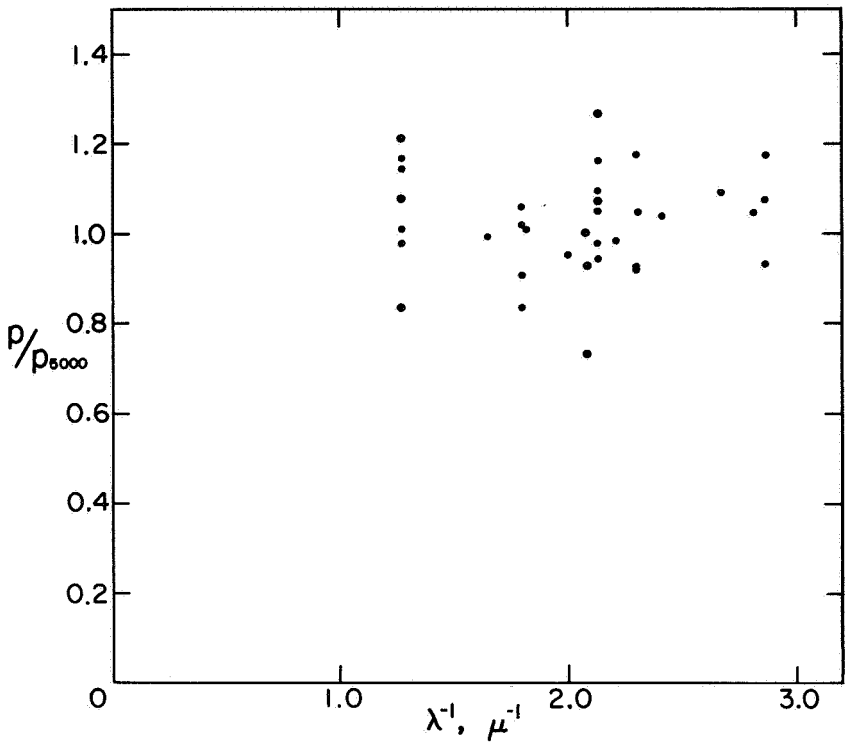

FIGURE 2.—Wavelength dependence of polarization for stars in group I.

This can be done if only polarizations with the plane of vibration parallel to the galactic equator are regarded. The material can therefore be divided into two groups:

group I: $p/A_V \leqq 0.027$ and $\theta = \pm 5°$

group II: all other stars

where θ is the angle between the plane of polarization and the galactic plane. In the first group are all stars with values of σ very probably small, and in the second group are all stars with values of σ certainly near 90° for large values of the ratio p/A_V and probably near 90° for small values of the ratio p/A_V due to depolarization. Although individual stars may deviate strongly, it can be concluded that the value of σ is significantly smaller in group I than in group II. The result is shown in figures 2 and 3, which contain results of references 2 and 7.

Figure 3 shows the color dependence as it was already known by Gehrels' measurements of six stars (all belonging to group II). Figure 2 does not show any significant color dependence, except perhaps for a weak minimum near $\lambda = 5000$ Å.

A comparison of these observations with results in the Orion aggregate obtained in 1965 by Appenzeller with the rotatable telescope at Yerkes Observatory in Williams Bay, Wisconsin, is shown in figure 4.

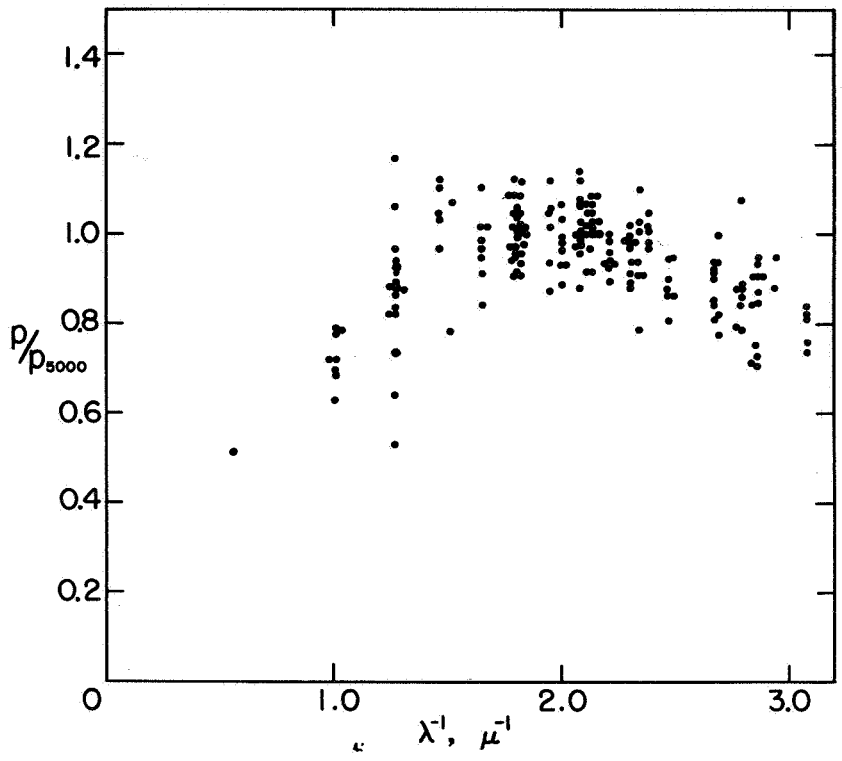

FIGURE 3.—Wavelength dependence of polarization for stars in group II.

Six Orion stars show a color dependence of polarization similar to that of group I; HD 43384, an Orion star in the background with larger polarization, HD 183143 in Sagitta used for comparison, and θ^2 Ori exhibit a behavior like the stars in group II. The polarization of θ^2 Ori may be influenced by the center of the bright Orion nebula.

In order to draw further conclusions from the results represented in figures 2 and 3, it should be assumed that the value of σ in the Orion aggregate, where the plane of vibration is nearly perpendicular to the galactic equator, is low, an assumption that seems to be in contradiction with the observations which yield a mean value for the ratio $p/3E_{B-V}$ of 0.040, where E is color excess. According to recent results (refs. 13 and 14), $A_V \approx 6E_{B-V}$ in the Orion aggregate; therefore, $p/A_V \approx 0.020$, a result which admits a low value of σ. This new value of p/A_V indicates that the plane of vibration does indeed appear perpendicular to the galactic equator.

REFERENCES

1. BEHR, A.: Beobachtungen zur Wellenlängenabhängigkeit der Interstellaren Polarisation. Zs. Astrophys., vol. 47, 1959, p. 54.

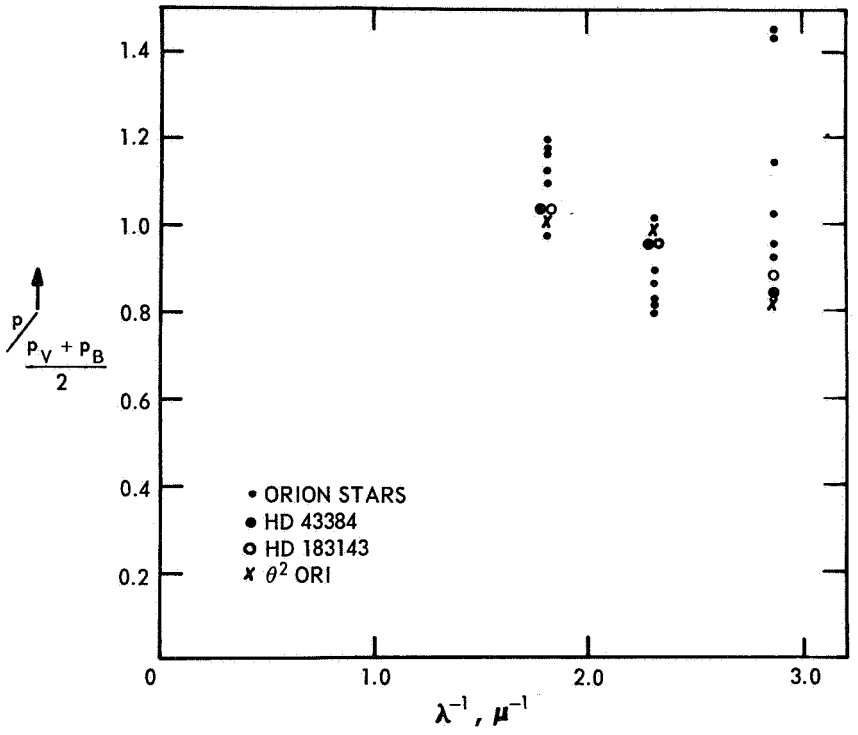

FIGURE 4.—Color dependence of six Orion stars. That of three other stars given for comparison.

2. GEHRELS, T.: The Wavelength Dependence of Polarization II. Interstellar Polarization. Astron. J., vol. 65, 1960, p. 470.

3. HILTNER, W. A.: On Polarization of Radiation by Interstellar Medium. Phys. Rev., vol. 78, 1950, p. 170.

4. HILTNER, W. A.: Photoelectric, Polarization, and Spectrographic Observations of O and B Stars. Astrophys. J., Suppl. Ser., vol. 2, 1956, p. 389.

5. SCHMAHL, G.: Die Wellenlängenabhängigkeit der Interstellaren Polarisation in der Umgebung der Assoziation VI Cygni. Zs. Astrophys., vol. 58, 1964, p. 165.

6. SERKOWSKI, K.: Polarization of Galactic Clusters M25, NGC 869, 884, 1893, 2422, 6823, 6871, and Association VI Cygni. Astrophys. J., vol. 141, 1965, p. 1340.

7. TREANOR, P. J.: Wavelength Dependence of Interstellar Polarization. Astron. J., vol. 68, 1963, p. 185.

8. VAN DEN BERGH, S.: Polarisation des Sternlichtes im Gebiet der Plejaden. Zs. Astrophys., vol. 40, 1956, p. 249.

9. BEHR, A.: On Some Improvement in the Polarization Technique. Lowell Obs. Bull., vol. 4, 1960, p. 292.

10. DAVIS, L.; and GREENSTEIN, J. L.: Polarization of Starlight by Aligned Dust Grains. Astrophys. J., vol. 114, 1951, p. 206.

11. DAVIS, L.: The Color Dependence of the Polarization of Starlight. Zs. Astrophys., vol. 47, 1959, p. 59.

12. GREENBERG, J. M.; and MELTZER, A. S.: The Effect of Orientation of Non-Spherical Particles on Interstellar Extinction. Astrophys. J., vol. 132, 1960, p. 667.

13. JOHNSON, H. L.; and BORGMAN, J.: The Law of Interstellar Extinction. Bull. Astron. Inst. Netherlands, vol. 17, 1963, p. 115.

14. JOHNSON, H. L.: Interstellar Extinction in the Galaxy. Astrophys. J., vol. 141, 1965, p. 923.

DISCUSSION

Greenberg: The formula $p/A_V = (p_0/A_V) \sin^2 \sigma$ is derived on the basis of the Rayleigh approximation. Actually, however, this formula is not quantitatively correct.

Behr: Do you mean that this formula is completely wrong now?

Greenberg: It is restricted to Rayleigh particles—very small particles.

Wickramasinghe: It depends entirely on the sizes one uses. I feel that the formula holds for graphite grains with sizes of a few hundredths of a micron.

Greenberg: A spheroidal type of characteristics in the orientation effects must also be assumed.

Wickramasinghe: Yes, I am thinking of the case of anisotropic oblate spheroids. One can get this type of relation by using the Gans approximation. Of course, the Gans approximation may not be valid here.

Donn: In order to get a high extinction for these small particles, the Rayleigh-Gans approximation cannot be used because a small extinction would result in this instance.

Wickramasinghe: No, I think in this instance that is not true. For small conducting particles the Rayleigh-Gans efficiency could get quite high.

Behr: If the angle σ is zero, then polarization is zero too; and if σ is 90°, then the polarization is a maximum; what happens between?

Greenberg: In between, the ratio of polarization to extinction doesn't follow $\sin^2 \sigma$.

Behr: Yes, I agree. I only assume this theory as a working hypothesis. A more correct one would probably change my separation limit of 0.027. My only argument is that in group I the angle may be significantly smaller than in group II, not larger. This is what I emphasized in the paper.

A Search for the Regional Variations in the Wavelength Dependence of Interstellar Polarization

K. SERKOWSKI, W. CHOJNACKI, AND S. RUCINSKI
Warsaw University Observatory
Warsaw, Poland

THE POLARIZATION OF 19 BRIGHT, HIGHLY POLARIZED STARS was measured from March until July 1965, with a differential polarimeter installed at the Cassegrain focus of the 90-cm telescope of the Toruń Observatory in Poland. The stellar light was split by the calcite Wollaston prism into two beams falling upon the cathodes of the photomultipliers. The observations were made at eight position angles of the polarimeter differing by 45°, alternately with and without the quartz depolarizer. The yellow 2-mm Schott GG 14 and the blue Schott BG 12 (1-mm)+GG 13 (2-mm) filters were used. No optical elements except the depolarizer were placed between the Wollaston prism and the telescope mirrors.

Usually only the Stokes parameters having the larger absolute values were accurately measured. The resulting polarization ratios p_V/p_B of the Stokes parameters expressed in magnitudes, measured with yellow and blue filters, are given in the ninth column of table I. They are followed by the number of nights that the star was observed; each observation lasted about an hour. Several nearby stars from the list published in reference 1 were also observed; these observations indicate that the instrumental polarization is negligibly small.

Table I contains all the stars for which the ratio of the amounts of polarization in yellow and blue spectral regions is known with a mean error not larger than ± 0.05. It includes the observations reported in references 2 to 5, and those made at the Toruń Observatory. The results of these references are followed in table I by their mean errors. The value p_{4290} is the average of the amounts of polarization measured by Treanor (ref. 4) at 4050 Å and 4530 Å, while p_{5250} is the average of those at 5000 Å and 5500 Å. In the last column of table I the arithmetic mean of the polarization ratios listed in preceding columns is given for each star. No appreciable systematic differences between the results of different authors are found.

TABLE I.—*Ratios of Interstellar Polarization in*

HD or cluster number	Star	l^{II} deg	$\frac{E_{V-I}}{E_{V-R}}$	$\frac{p_{5160}}{p_{4300}}$ (ref. 2)	$\frac{p_{5580}}{p_{4200}}$ (ref. 3)
147165	σ Sco	351	2.20	.....	.....
147933	ρ Oph	354	2.14	.....	.....
160529		356	.....	.....	.....
149757	ζ Oph	6	2.00:	1.09 ± .03	.....
M 25	77 stars	14	.....	.....	.....
161056		18	.....	.....	1.02 ± .02
154445		19	.....	.....	1.08 ± .01
183143		53	1.89	.....	1.07 ± .01
NGC 6823	16 stars	59	2.11	.....	.....
193237	P Cyg	76	1.75:	.....	.....
194279		78	.....	.....	.....
VI Cyg	27 stars	80	1.80	.....	.....
194057		81	.....	.....	.....
198478	55 Cyg	86	1.91	.....	1.00 ± .02
197770		93	.....	.....	.....
204827		99	.....	.....	.....
207260	ν Cep	102	1.82	.....	.....
213470		104	.....	.....	.....
217476		108	1.76	.....	.....
5394	γ Cas	123	1.86:	1.11 ± .05	.....
6811	φ And	126	1.7:	0.88 ± .05	.....
7927	φ Cas	127	1.98	.....	.....
10516	φ Per	131	1.86:	.92 ± .04	.....
13402		133	.....	.....	.....
+58°400		133	.....	.....	.....
Stock 2	10 stars	133	.....	.....	.....
17378		138	1.90	.....	.....
21291	2H Cam	141	2.15	.....	1.00 ± .02
21389		142	1.96	.....	.....
25443		143	.....	.....	.....
24912	ξ Per	160	1.94	1.16 ± .05	.....
24398	ζ Per	162	2.17:	1.04 ± .02	.....
NGC 1893	19 stars	174	.....	.....	.....
43384	9 Gem	188	2.08	.....	.....
41117	χ^2 Ori	189	2.00	.....	.....
37356	near M 42	208	.....	.....	.....

[a] Value for p_{5250}/p_{4550}.

Yellow and Blue Spectral Regions

$\frac{p_{5250}}{p_{4290}}$ (ref. 4)	p_V/p_B (ref. 5)	p_V/p_B (present paper)	Number of nights observed (present paper)	Mean value of p_V/p_B
1.13 ± .04	.....	.....	.....	1.13
1.11 ± .04	.....	.....	.....	1.11
[a] 1.10 ± .06	1.03 ± .02	.....	.....	1.06
1.08 ± .04	.....	.....	.....	1.08
.....	1.03 ± .02	.....	.....	1.03
1.13 ± .05	1.13 ± .05	1.11 ± .03	2	1.10
0.98 ± .04	1.19 ± .02	1.06 ± .02	4	1.08
1.10 ± .02	1.07 ± .02	1.09 ± .02	2	1.08
.....	1.08 ± .02	.....	.....	1.08
.....	.....	0.93 ± .05	2	.93
.....	.....	1.04 ± .03	2	1.04
.....	0.93 ± .02	.....	.....	.93
.....	.....	1.01 ± .04	2	1.01
0.95 ± .02	1.00 ± .04	1.02 ± .03	3	.99
.....	.....	1.01 ± .03	3	1.01
.....	.....	0.97 ± .02	5	.97
.....	.....	0.96 ± .04	2	.96
.....	.....	1.02 ± .04	2	1.02
0.97 ± .03	.....	0.98 ± .08	2	.97
.....	.....	.....	.....	1.11
.....	.....	.....	.....	.88
.....	1.03 ± .04	1.02 ± .02	2	1.02
.....	.....	.....	.....	.92
.....	1.03 ± .05	.....	.....	1.03
.....	1.02 ± .03	.....	.....	1.02
.....	1.09 ± .04	.....	.....	1.09
.....	.....	1.06 ± .04	1	1.06
.....	1.01 ± .02	.....	.....	1.00
.....	.....	1.00 ± .05	1	1.00
.....	.....	0.99 ± .03	1	.99
.....	.....	.....	.....	1.16
.....	.....	.....	.....	1.04
.....	1.03 ± .04	.....	.....	1.03
.....	1.08 ± .02	1.03 ± .03	3	1.06
.....	.....	1.09 ± .05	1	1.09
.....	.....	1.11 ± .05	4	1.11

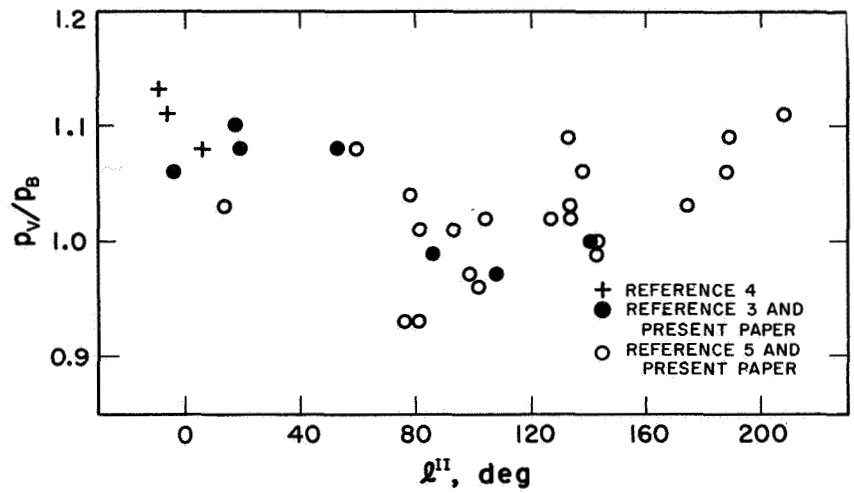

FIGURE 1.—Ratio of amount of polarization in yellow to amount in blue spectral region as a function of galactic longitude of the star.

The dependence of the mean ratios of yellow and blue amounts of polarization as a function of galactic longitude is shown in figure 1. The smallest values of this ratio occur in the Cygnus region.

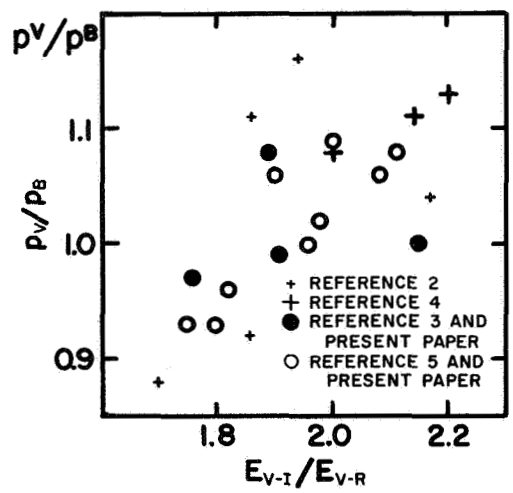

FIGURE 2.—Ratio of amount of polarization in yellow to amount in blue spectral region as a function of ratio of the color excesses E_{V-I}/E_{V-R}.

The ratio of polarizations is correlated with the color excesses ratio E_{V-I}/E_{V-R} as obtained in reference 6 in figure 2.[1] The ratios of the color

[1] *Note added in proof:* Recent observations of the wavelength dependence of interstellar polarization by G. V. Coyne and T. Gehrels (Astron. J., vol. 71, p. 355, 1966) and by K. Serkowski (unpublished) confirm the validity of this correlation.

excesses listed in table I and plotted in figure 2 are computed by using the observed values of $V-R$ and $V-I$ and intrinsic colors listed in reference 6, 7, or 8. In order to bring into agreement the results of these papers, the corrections 0.09 and 0.05 were added to the $V-R$ and $V-I$ colors observed by the authors of reference 8. For the Orion Sword region, the ratio E_{V-I}/E_{V-R} equals about 2.04 and is only slightly larger than the average for all the sky; similarly the ratio p_V/p_B is 1.11 for the star HD 37356 situated near the Orion trapezium. The ratio E_{V-I}/E_{V-R} is independent of galactic longitude for those stars in the catalogues of references 6 and 8 for which the amount of polarization is larger than 0.020 magnitude.

The polarimeter described previously was also used at the Haute-Provence Observatory in France for attempts to measure the circularly polarized component of stellar light in the yellow spectral region. The values obtained for the Stokes parameter p_v describing the circularly polarized component of stellar light expressed in magnitudes are listed with their mean errors in table II. They are accompanied by the amount of polarization p and the position angle of the plane of vibration θ observed in the yellow spectral region with the same instrument used for the stars with measured p_v. For none of these stars does p_v exceed 0.0004 magnitude, an indication that the degree of ellipticity does not exceed 0.02 percent. This may be considered as an argument against the interstellar grains with high iron content, as these are expected to introduce an appreciable circularly polarized component into the partially plane-polarized stellar light. (See ref. 1.)

TABLE II.—*Observations of the Circularly Polarized Component of Stellar Light*

HD number	Star	p	θ, deg	p_v, magnitude
21291	2H Cam	0.073	116	+0.0004±.0003
36371	χ Aur	.048	176	−.0002±.0002
109358	β CVn	.001	177	.0000±.0002
112185	ϵ UMa	.000	.....	−.0001±.0008
144217–8	β Sco	.017	91	+.0003±.0002
147165	σ Sco	.032	179	−.0001±.0006
149757	ζ Oph	.030	126	+.0001±.0003
174638	β Lyr	.016	156	+.0001±.0003
198478	55 Cyg	.061	3	−.0001±.0003

REFERENCES

1. SERKOWSKI, K.: Suggested Standards of Polarization. Lowell Obs. Bull., vol. 4, 1960, p. 317.

2. BEHR, A.: Beobachtungen zur Wellenlängenabhängigkeit der Interstellaren Polarisation. Zs. Astrophys., vol. 47, 1959, p. 54.

3. GEHRELS, T.: The Wavelength Dependence of Polarization II. Interstellar Polarization, Astron. J., vol. 65, 1960, p. 470.

4. TREANOR, P. J.: Wavelength Dependence of Interstellar Polarization. Astron. J., vol. 68, 1963, p. 185.

5. SERKOWSKI, K.: Polarization of Galactic Clusters M25, NGC 869, 884, 1893, Z422, 6823, 6871, and Association VI Cygni. Astrophys. J., vol. 141, 1965, p. 1340.

6. JOHNSON, H. L.: Interstellar Extinction in the Galaxy. Astrophys. J., vol. 141, 1965, p. 923.

7. IRIARTE, B.; JOHNSON, H. L.; MITCHELL, R. I.; and WISNIEWSKI, W. Z.: Five-Color Photometry of Bright Stars. Sky and Telescope, vol. 30, 1965, p. 21.

8. JOHNSON, H. L.; and BORGMAN, J.: The Law of Interstellar Extinction. Bull. Astron. Inst. Netherlands, vol. 17, 1963, p. 115.

Dispersion of Interstellar Polarization

THOMAS GEHRELS
University of Arizona
Tucson, Arizona

THE WAVELENGTH DEPENDENCE OF POLARIZATION as observed in 32 stars, for which the Henry Draper numbers are given, is shown in figure 1. Details of some of these observations are presented in reference 1.

The equipment is now being used with the new 154-cm Catalina reflector of the Lunar and Planetary Laboratory at the University of Arizona. The instrumental polarizations are nearly zero. The data processing and observing techniques have been further improved; the precision is mainly determined by statistics such that the internal probable error in the percentage polarization is ± 0.03 percent (± 0.0006 magnitude) for a half-hour observation per filter on objects brighter than about 7 magnitudes. The wavelength λ ranges from 0.33 to 0.95 μ, covered by seven filters of bandwidth of about 0.05 μ. The wavelength range is being extended to 1.2, 1.6, and 2.2 μ, and, with high-altitude ballooning, to 0.28 and 0.22 μ.

The calculations for perfectly alined infinite cylinders in chapter 15 of reference 2 are fitted to these observations. The fits represent a first reconnaissance for which size distributions are ignored and the refractive index of dirty ice is adopted; it is then found that the particle diameters range between 0.2 and 0.4 μ. One or more interstellar clouds having such a narrow distribution in the refractive indices and particle sizes may give a curve similar to the one obtained for HD 2905 (fig. 1).

A flatter curve, such as that for HD 18326 in figure 1, may be caused by light passing through various clouds that also contain smaller particles, thereby raising the amount of polarization at the larger values of λ^{-1}. An upturn in the ultraviolet appears in a few cases (see, for example, the curve for HD 218342 in fig. 1); this upturn may be interpreted as evidence for additional clouds with particle diameters of about 0.17 μ.

An upturn in the infrared is similarly explained as showing evidence of larger particles. The strongest case is that of HD 37202. It should be noted that HD 37041 in the Orion nebula is spectacularly different from the other stars.

271-992 O-67—5

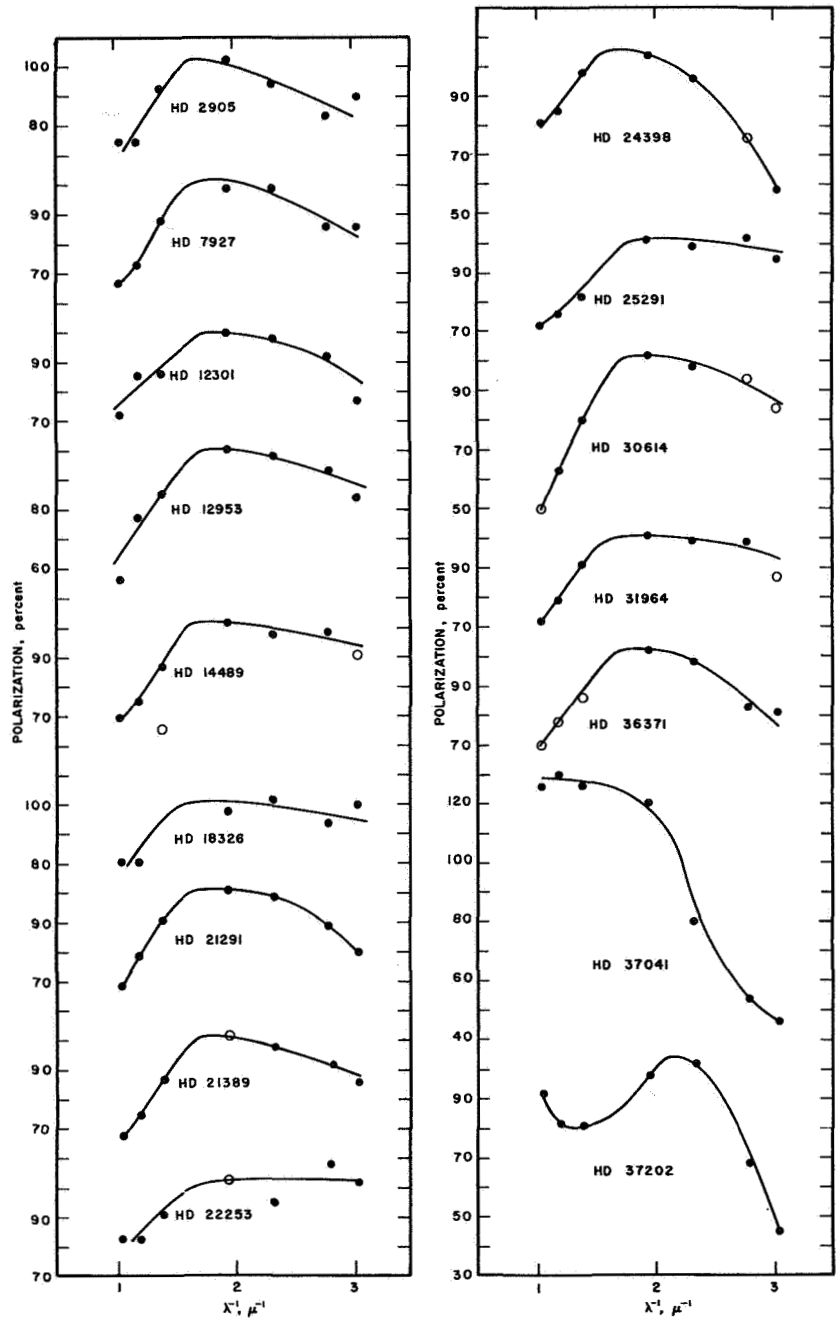

FIGURE 1.—Percentage polarization of selected stars, plotted after normalization to 100.0 for the straight average observed with filters at $\lambda^{-1}=1.95\ \mu$ and $\lambda^{-1}=2.33\ \mu$.

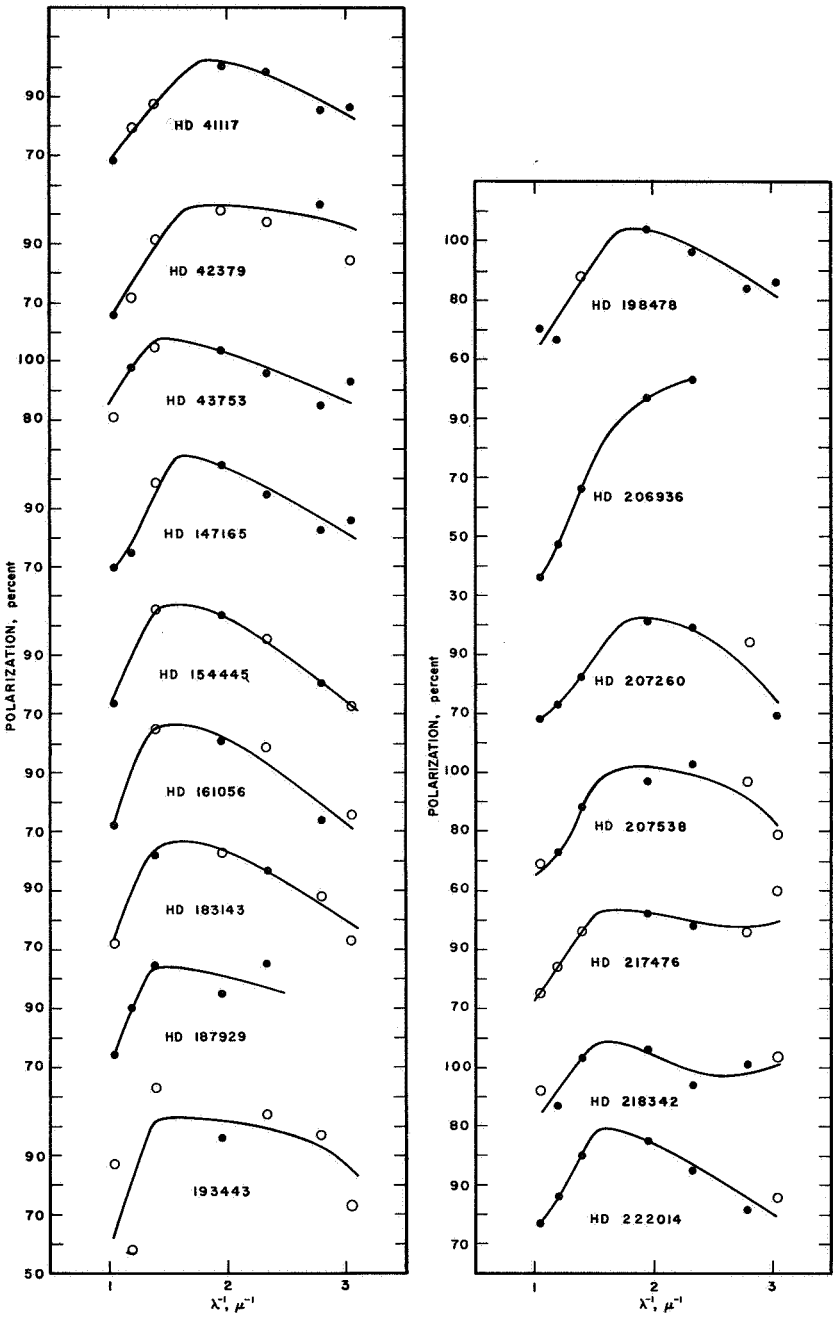

FIGURE 1.—Concluded.

Also unusual is the curve for HD 206936 which is μ Cephei; the polarization is intrinsic, that is, caused within or close to the star itself. The visual polarization of μ Cep varies, with time, between 0.3 and 2.3 percent.

Polarimetry is a sensitive tool for the study of grain parameters. For various galactic regions, the differences between polarization curves are much more pronounced than the differences between photometric results.

The position angles also show wavelength dependence. Of the 35 stars observed to date, 14 show the effect appreciably; these stars are listed with their galactic longitudes in table I. For each star, the difference of the position angle (at each filter) from the mean position angle (of all seven filters) is listed in the table. A solution of nickel sulfate was used in the filter listed in the last column in order to eliminate red leakage.

The rotation of the position angle with wavelength is very puzzling. For the 14 stars selected for table I, the position angles increase with decreasing wavelength until the point perpendicular to the local spiral arm (longitude = 144°) is reached; and beyond that point the position angles decrease with decreasing wavelength. This effect is reminiscent

TABLE I.—*Difference Between Position Angle at Seven Filters and Mean Position Angle for 14 Stars*

HD number	Galactic longitude, deg	Angular difference in degrees for—						
		Infrared filter (λ=0.95 μ)	Red filter (λ=0.84 μ)	Orange filter (λ=0.71 μ)	Green filter (λ=0.53 μ)	Blue filter (λ=0.43 μ)	Ultraviolet filter (λ=0.36 μ)	Filter using nickel sulfate solution (λ=0.33 μ)
147165	351	[a]−2	[a]−8	−2	[a]0	+1	[a]+6	+2
207538	102	−8	−2	[a]0	+2	+2	−1	+6
2905	121	−5	−3	[a]−4	−1	+1	+2	+8
7927	127	−3	−2	−2	0	[a]+2	+1	+5
12301	131	−3	−2	−2	+1	+1	+2	+3
12953	133	−6	−2	−2	+1	+2	+3	+4
14489	136	[a]−6	−2	−4	0	+1	[a]+1	+7
21389	142	−2	−1	−1	0	+1	+1	+2
30614	144	−3	−1	0	+1	+2	[a]+1	+1
22253	145	+6	+7	+6	0	0	−9	−10
24431	150	+7	+3	+2	−5	+1	−1	−8
36371	176	[a]+4	[a]+2	+4	[a]+2	[a]+1	−3	−5
37202	186	[a]+4	+4	+7	−1	+1	−4	−9
41117	190	+4	[a]+2	[a]+4	−1	−3	[a]−1	[a]−3

[a] Value obtained with poorer precision.

of a Faraday rotation, but Faraday rotation should be negligible at optical wavelengths. As yet no explanation for this effect is known.

REFERENCES

1. COYNE, G. V.; and GEHRELS, T.: Wavelength Dependence of Polarization. VIII. Interstellar Polarization. Astron. J., vol. 71, 1966, p. 355.

2. VAN DE HULST, H. C.: *Light Scattering by Small Particles*. John Wiley & Sons, Inc., 1957.

DISCUSSION

Greenberg: Apparently the wavelength dependence of polarization becomes less and less peaked as we view further away from the perpendicular to the magnetic field. This observation seems to fit in somewhat with the remarks that have been made earlier so that, for example, the ratio of the polarization in the yellow to that in the blue would tend to be less when the line of sight is not quite perpendicular to the magnetic field than it would be if the line of sight were perpendicular to the magnetic field (high polarization).

I would like to comment on the terminology "dirty ice." Many things are used to represent dirty ice, and we should have some idea of where the imaginary part of the index of refraction comes from. In the visible we have made some calculations to see if an imaginary index of 0.05 is reasonable. The only way to get as much as 0.05 imaginary part in the visible index of refraction is to take all the iron in its usual cosmic abundance and put it in clumps large enough so that it acts like little pieces of metal.

All the other materials that are used for dielectrics are all very clear in the visible. In order for something to be called dirty, it should have an imaginary part of the order of 0.01 to 0.05 in the visible. In other words, anything having an imaginary part as large as 0.2 is metallic or is at least characteristic of what one may find in the neighborhood of a resonance or absorption line. Did you use 0.2 for the imaginary part?

Gehrels: Yes, we tried imaginary parts as large as that. In the paper on the reflection nebulae I conclude that acceptable model particles would be graphite particles covered with a coated shell. The other particle model that would fit the observations of NGC 7023 has a large imaginary part to the refractive index; in view of what you now say, then, the only remaining possibility is that of graphite particles with the ice coating.

Greenberg: Dirty ice is relatively clear in the visible. Even if it had an imaginary part between 0.01 to 0.05 and would thus look rather muddy, it would still be fairly clear as far as Mie calculations go.

Gehrels: Would you agree with the conclusion that the coated graphite particles give a good fit in general to the interstellar polarization?

Greenberg: No.

Wickramasinghe: In order to get an imaginary part of 0.2, a great deal of solid iron would have to be embedded in the ice.

Greenberg: Yes, you would need a lot of very small particles, all having common characteristics. These calculations which I made several years ago showed that embedding a number of iron atoms in the grains that is proportional to their cosmic abundance gave rise to a negligible contribution to the absorptivity even when all the iron absorption lines are included. In other words, a thick chunk of ice, even bigger than an ice cube, with a lot of iron atoms embedded in it would still be transparent.

Spitzer: Is not θ^2 Orionis (HD 37041) the star which has long been known for the unusual variation of selective extinction with wavelength?

Gehrels: Yes.

Spitzer: So everything makes sense, and the unusual wavelength dependence of polarization in this star is consistent with the presence of large particles, already indicated by the wavelength dependence of the interstellar reddening curve.

Field: What about λ4430? If the particles really are 1 μ in diameter, the absorption for a wavelength of 4430 Å might be expected to be very anomalous; either it might be very weak or it might possibly even show up as an emission rather than absorption. What do the observations tell us?

Walker: The star HD 37041, if I remember correctly, shows a weak absorption for this wavelength.

Gehrels: Is there a correlation or connection between the 4430 Å wavelength and the upturn in the interstellar reddening curve?

Nandy: We have found no correlation with the line intensity of 4430 Å and the dispersion at that wavelength. If that upturn depended on λ4430 we would expect the dispersion in extinction at that wavelength to correlate with the intensity of λ4430.

Wickramasinghe: With regard to the isotropic conductivity assumption that you made, I think that, for a local region like the one you examined, all the graphite axes would almost surely be randomly oriented, and then I think that this assumption is as good as any other.

Nandy: Does the wavelength dependence of polarization depend on the galactic longitude, or is it just different for different groups of stars?

Gehrels: It is different for different stars. The curves for these different stars, including the relative errors, have been published in a series of papers in the Astronomical Journal.

Nandy: Is there any correlation between polarization and the wavelength of 4430 Å?

Gehrels: I do not know. We have not looked at that.

Spitzer: We have heard about the great differences in the wavelength dependence of extinction and about the differences in the wavelength dependence of the polarization. Is there any clear-cut correlation between these differences? Have enough data been obtained?

Gehrels: We have made only a preliminary analysis and we see no correlation yet. Actually, the data do not overlap enough to make a study feasible. In Orion, however, there is at least an indication of larger particles from both the photometry and from the polarization.

Spitzer: When you say Orion, are you referring primarily to the trapezium stars?

Gehrels: Yes.

Spitzer: As has already been emphasized, this is the region whose unusual properties have been known for some time. In this particular region there is a clear indication that these relatively large 1-μ particles are present. For the rest of the sky are there still some uncertainties as to the possible presence of these larger particles?

Gehrels: Yes. Not enough stars have been observed yet.

Behr: Do you find the same color dependence in Orion as Dr. Appenzeller does?

Gehrels: I have not made a comparison with Dr. Appenzeller's observations as yet.

Greenberg: Dr. Gehrels refers to 1-μ size particles; I assume that these particles are dielectric or dirty-ice particles. In other words, the wavelength dependence of polarization for HD 37202 implies that there are two distinct groups of particle sizes: one centered at about 0.4 μ and the other, at about 1 μ. Why is there a gap between the two sizes?

Greenberg: There is doubt as to whether or not a discontinuity in the size distribution exists. If one used a model for grain growth and assumed that a particular cloud had existed without collisions for a longer time than usual, one would find considerably larger grains in this cloud than ordinarily would be found. The assumption of simultaneously smaller than average and larger than average particles as an explanation of the wavelength dependence of polarization due to a single cloud would be difficult to justify. However, in two separate clouds, one might reasonably expect two different size distributions. The net result for viewing through these clouds would then be equivalent to that of viewing through a single cloud.

Donn: A possible explanation for the rather sharp variation in size could be that in growing plates, the plate particle sizes are much more sensitive to possible density fluctuations in the medium than are, for example, spherical particles.

Walker: Are these particles large enough to explain the μ Cephei results and the neutral absorption suggested from the galaxy counts, or would larger particles be required to cause these phenomena?

Greenberg: The polarization maximum at $\lambda^{-1} \approx 0.2\ \mu^{-1}$ implies a dielectric grain whose size is about 10 times the normal size limit. This conclusion is also valid for relative sizes of metallic type grains.

Walker: So we have three distinct types of clouds of particles at the moment?

Greenberg: If the upturn in the infrared extinction is real, then this is possible.

Scanner Observations of λ4430

E. JOSEPH WAMPLER
Lick Observatory
Mount Hamilton, California

THE INTERSTELLAR BAND AT λ4430 has been observed in over 100 stars by using the Lick Observatory scanning spectrograph mounted on both the 120-inch telescope and on the Crossley telescope. Although in some instances the feature is badly blended with stellar lines, particularly with early B supergiants, in general the central depth of λ4430 has been determined to an accuracy exceeding 0.5 percent of the stellar continuum.

The feature has been found to have a fairly symmetrical profile, although there may be changes in the profile from star to star. The extended wings reported by other observers were not detected, and also the feature does not seem to be polarized.

The correlation between the absorption band at λ4430 and color excess is not one-to-one. Even field stars lying in the galactic plane show much intrinsic scatter in the ratio of this absorption band to color excess. For some clusters, a change in the slope of the correlation between λ4430 and color excess can be interpreted as caused by local variations in the ratio of λ4430 absorption to interstellar dust absorption. However, these differences are not well correlated with the values of the ratio of absorption to color excess A_v/E that are reported in reference 1. Also there are quite large local variations in the ratio of λ4430 to color excess that cannot be interpreted as caused by local destruction of the source of λ4430 by hot stars.

The absorption band at λ4430 definitely appears to be weakened in dust clouds that lie outside the galactic plane. This weakness may indicate that the agent causing λ4430 is more closely confined to the plane than the dust, or that it has been destroyed in the high latitude clouds, or that the conditions for forming the atomic states responsible for λ4430 are unfavorable in these clouds. The scatter in the relationship between absorption at λ4430 and color excess as well as the probable detection of this absorption in ρ Leonis indicates that this absorption may be produced by an agent of the interstellar medium other than that which causes the extinction.

REFERENCE

1. JOHNSON, H. L.: Interstellar Extinction in the Galaxy. Astrophys. J., vol. 141, 1965, pp. 923–942.

DISCUSSION

Donn: Are there any instances of strong λ4430 but weak color excess?

Wampler: Possibly ρ Leonis. Also, in general, the regions in Monoceros have strong λ4430 for their color excess. There is no example as outstanding as ρ Leonis that I know of. This is just one case and, of course, the color excess of ρ Leonis may be in error because it is small.

Greenberg: In a recent calculation I have assumed that the λ4430 extinction is one-twentieth of the total interstellar extinction at $\lambda = 4430$Å. What is the maximum that has been observed?

Wampler: According to Dr. Herbig of the Lick Observatory, the absorption at λ4430 is probably 18 percent deep in HD 183143. I think the color excess is about 1.4. Assuming a ratio of total to selective extinction of 3 yields a value of A_v of 4.5 magnitudes. Another 1.4 magnitudes must be added because of the $B-V$ color.

Greenberg: Yes. Now, roughly speaking, the percentage is one-tenth of a magnitude.

Wampler: For λ4430 absorption of 0.18 and 6 magnitudes of extinction at $\lambda = 4430$ Å, the ratio of λ4430 to extinction would be 0.18/6, or approximately 0.03.

Greenberg: It looks like the maximum ratio is about 1:25.

Walker: I did observe one star with about 25 percent central absorption at λ4430 for 1 magnitude of color excess; it was HD 46711.

Greenberg: Maybe this could be checked later, because I would like to see whether the numbers that I have are meaningful in the sense that they can explain the maximum. If the 5 percent is a reasonable maximum, then a surface phenomenon is not unreasonable.

Wickramasinghe: What is a surface phenomenon?

Greenberg: I am assuming that various (as yet undetermined) molecules may form on the surface and may even be somewhat transient as long as they are present for a sufficient fraction of time. I can say either that they have to occupy roughly 5 percent of the surface all the time or that they have to cover the entire surface only 5 percent of the time.

Wampler: Because scatter is seen for stars in the galactic plane, one might assume that there is a difference in strengths of λ4430 absorption between clouds; that this difference could be rather large; and that it could produce the scatter. A fairly good mean relationship can be obtained by looking through several clouds. High galactic latitude clouds on both sides of the plane all show weak absorption at λ4430. Although some of them show the λ4430 as strong as the mean line,

none show λ4430 stronger than the mean line, and the majority show λ4430 considerably weaker than the mean line. Perhaps this is a clue.

O'Dell: In the case of NGC 2244, since the ratio of total to selective extinction can be different in certain regions, would it not be better to look at the strength of λ4430 as a function of absorption instead of color excess? This might provide a better measure of the total amount of dust, and would tend to shove NGC 2244 systematically over to the right. Would this make the overstrength of λ4430 tend to disappear?

Wampler: It would indeed. On the other hand, it would make λ4430 appear even weaker in Orion than it already appears.

Dressler: Is breaking some solid material up into very small grains equivalent to spreading it out into a thin layer as far as its optical absorption properties are concerned?

Greenberg: If the absorption occurs in a sufficiently thin layer, then to the first approximation the inside of the grain sees almost the undisturbed incident radiation; consequently, the extinction is additive. That is, the extinction at λ4430 and the extinction by the grains are additive.

Dressler: Hence, would some macromolecule which did have an absorption line at λ4430 show up in the same way either as a thin layer or as a very small grain?

Greenberg: I would think so. There are problems associated with shifts of the wavelengths when one material is embedded in a material of different optical properties.

Dressler: Were the photoelectric profiles that you showed for λ4430 raw data or were they corrected for stellar absorption lines?

Wampler: These profiles are not corrected for stellar absorption lines. The only change that has been made to the raw data has been to take out the slope of the continuum. Some of the scatter was due to stellar atomic lines. The star HD 183143 shows a little dip at λ4437 due to He I and some of the stars show O II. Of course, ρ Leonis shows very strong O II because it is an early B supergiant.

For illustration I picked stars in which there were no strong atomic features. I tried not to pick the B supergiants. A profile for B supergiants would have looked much messier.

Hall: What figures did you get for NGC 2244? Do you remember those?

Wampler: As well as I can remember the λ4430 is 6 percent. The λ4430 profile for all the stars in this cluster looks somewhat peculiar; it looks like the star has emission wings. The absorption at λ4430 becomes a little stronger if you assume that the continuum is on these "wings" than if you take a continuum as derived from points 50 or 100 Å away from λ4430.

Hall: Did you try polarization?

Wampler: I didn't try polarization for these stars. The only polarization I tried was for the two stars that I mentioned. The difficulty is that polaroids cut out a lot of light, and with a 6 Å exit slot there is not much light.

Walker: Could you possibly say anything more about the differences in profiles between different stars? In photographic reduction of plates for λ4430 I have frequently seen a kink near λ4471. I had assumed it was something caused by the emulsion response, but it looks as if it must be due to an astronomical effect.

Wampler: I have drawn some profiles that occur quite often. Typical profiles for NGC 2244 show that in some of the stars the blue wing is steeper than the red wing, but that in other stars the opposite is true. At present I am undecided as to whether this difference is due to λ4430 or perhaps to some other broad interstellar feature that might be overlapping λ4430, or due to the stars themselves. I have also compared the absorption in the ultraviolet wing with that in the red and plotted this as a function of the central depth of λ4430. The results showed very large scatter with a slight tendency for the red wing to be deeper. At the time, I decided that this trend could probably be explained in terms of the helium wings; but there may really be an asymmetry in the profile.

Nandy: Did you apply corrections for reddening when you derived the continuum?

Wampler: I think any effect is small. I can show you the observations in the raw form and you can draw your own conclusions. The continuum points were as follows: λ4285, λ4305, λ4310, λ4359, λ4378, λ4495, and λ4527. The choice λ4527 may not be a very good one because there are nitrogen features in early-type stars nearby. I suspect that they influence this point. In general, if one fits a straight line to these points, that line comes very close to the wings of λ4430. Although there may be some curvature, I think that this is less than 1 percent of the depth of the λ4430 absorption.

On the λ4430 Absorbers in "Normal" and in Perturbed Clouds

KURT DRESSLER
Princeton University
Princeton, New Jersey

REGIONS PERTURBED BY EARLY-TYPE STARS are characterized by the occurrence of high Ca II velocities and an increase in the abundance ratio Ca II/Na I (ref. 1), by a decrease in the λ4430 absorption to color excess (ref. 2), and possibly by a deficiency of small relative to large grains (large values of the ratio of total extinction to color excess, A/E). According to reference 3, the grain temperatures in the same regions are expected to be higher, and therefore may lead to selective evaporation of the smallest grains. Since these observations may be connected by way of λ4430 absorption originating in very small grains, it is of interest to compare the value of nf (number of absorbers times $f$value) of the λ4430 absorbers with the number of molecules n_{mol} in the grains responsible for extinction in the visible. Based on the observed mean equivalent width of 3 Å kiloparsec in the λ4430 band, the value of nf(4430) is

$$nf(4430) = 1.7 \times 10^{13}/\text{cm}^2\text{-kpc} = 6 \times 10^{-9}/\text{cm}^3$$

With a grain density of 10^{-26} g/cm^3 and 3×10^{22} molecules/cm^3 in the grain material, n_{mol} is

$$n_{mol} = 10^{18}/\text{cm}^2\text{-kpc} = 3 \times 10^{-4}/\text{cm}^3$$

Therefore, the relative abundance of λ4430 absorbers is

$$nf(4430) = 2 \times 10^{-5} n_{mol}$$

and the λ4430 band can be explained by reasonable $f$values and by moderately abundant species. In particular, it might be caused by resonance line absorption of some minor grain constituent, since, for example, 20 parts per million of Ca I or Ca II in the smallest grains would suffice to account for the observed absorption intensity. It should be

emphasized that this is a very ingenious hypothesis in that it speculates that among other possible atomic or molecular absorbers, the 4430 Å line might be caused by the resonance line of either Ca I or Ca II. Both of these qualify by having a resonance line very close to 4430 Å, and the resonance lines of both have *f*-values of the order of unity. Therefore, 4430 Å bands can be produced by putting calcium atoms or singly ionized calcium into some solid material. I think the kind of solid would be immaterial.

The hypothesis that the 4430 Å resonance line might be caused by Ca II would be quite difficult to disprove in the laboratory. The element Ca I might be a good suggestion also, but this hypothesis can be checked with relative ease in the laboratory by condensing neutral calcium atoms that are evaporating out of an oven onto a cold window simultaneously with some other material. Indeed, some preliminary observations have already been carried out; Dr. Schnepp in Israel found some more or less continuous absorptions in the visual and the ultraviolet by using calcium atoms in various ice-type solids while nothing showed up at 4430 Å. However, it was not known in those experiments whether the calcium atoms were single atoms or whether they tended to conglomerate into small calcium particles. In any case, I think Ca II is a very good suggestion.

In an investigation reported in reference 2, I found that the correlation between λ4430 absorption and color excess can be improved by separating stars into two groups: those showing high-velocity Ca II interstellar lines and those showing no such high velocity. With this separation one finds those stars showing the high-velocity clouds predominantly in the lower section of the diagram, whereas the remaining stars are predominantly in the upper part.

Another interesting way of improving this correlation would be to separate the stars according to the two types of reddening curves, as observed, for example, in Cygnus and in Perseus.

REFERENCES

1. ROUTLY, P.; and SPITZER, L., JR.: A Comparison of Components in Interstellar Sodium and Calcium. Astrophys. J., vol. 115, 1952, p. 227.

2. STOECKLY, R.; and DRESSLER, K.: On the Interstellar λ4430 Line. Astrophys. J., vol. 139, 1964, pp. 240–247.

3. GREENBERG, J. M.; and LICHTENSTEIN, P. R.: Absorption Lines Produced in Interstellar Grains. Astron. J., vol. 68, 1963, p. 279.

DISCUSSION

Spitzer: Your suggestion about Ca II brought to mind the similarity between Ca II and Mg II. Could you guess as to possible effects of Mg II?

Dressler: In order to produce a 4430 Å line, we need a fairly abundant

species or one that has a line with a very large *f*/value originating in the line is near 2800 Å.

Spitzer: I wasn't thinking of Mg II producing this line, but if Ca II produces the 4430 Å resonance line, Mg II might produce a line that we could measure in the ultraviolet.

Walker: I am not entirely convinced about the differences between the correlation of λ4430 and reddening for stars showing normal interstellar calcium velocities and those showing high calcium velocities. I find that if I introduce data that Dr. Münch obtained in Israel, the correlation you found disappears. The two lines in your diagram are actually parallel; they don't diverge from the origin.

Dressler: Yes, and we like that fact in particular because it indicates that the hot star affects just the material nearest to it, whereas all the rest of the material is unperturbed. There is just one cloud lacking the λ4430 absorption.

Walker: I just wanted to suggest that perhaps it depends on exactly how one chooses the data. I don't know what resolution you would want. The higher resolution plates which Münch used picked up more satellite lines of calcium; there practically all the associations show a relative expansion of calcium velocities, and so the correlation does disappear if you restrict it to the stars in the Milky Way. However, if one is only dealing with very strong expansion components, perhaps your conclusion is reasonable.

Dressler: Yes, it is just a question of where one does divide between stars having or not having sufficient power to produce high-velocity Ca II.

Borgman: It is always possible to explain the scatter by introducing a sufficient number of parameters that might have some influence, whether you understand the physical machinery or not. It is always dangerous to do this and one should be very careful.

Wampler: The star NGC 2244 shows strong 4430 Å resonance indeed, but I have measured several of the field stars in the neighborhood of NGC 2244, and they also show strong 4430 Å resonance. At one time I was rather excited about the possibility of a relation between longitude and the λ4430 absorption, and perhaps it is still there. Certainly the stars in the Taurus complex show weak 4430 Å resonance, but this type of change in the 4430 Å wavelength region greatly overwhelms any possible correlation of longitude.

Alinement of Solid Interstellar Particles by a Magnetic Field[1]

LYMAN SPITZER, JR.
Princeton University
Princeton, New Jersey
AND
R. V. JONES
Harvard University
Cambridge, Massachusetts

FOR A LONG TIME THE DAVIS-GREENSTEIN THEORY (ref. 1) has been generally considered an adequate explanation of the mechanism responsible for the alinement of interstellar grains and thus for the observed interstellar polarization. The magnetic field required to orient paramagnetic grains is apparently somewhat greater than 10^{-5} gauss, a relatively large field, but according to reference 2 ferromagnetic grains, proposed by the authors of reference 3, can be oriented by a field of only 10^{-7} gauss. These results indicate that orientation of interstellar grains is easily explained, even if the magnetic field in interstellar space is relatively weak.

Unfortunately, this relatively satisfactory state of affairs has been upset by two developments. Firstly, the basic mechanism of magnetic relaxation proposed by Davis and Greenstein has been questioned by Dr. C. Kittel of the University of California, who has pointed out that the disorienting effect associated with thermal fluctuations of magnetization within the solid particles is ignored in the formulation of this mechanism. In thermodynamic equilibrium this effect cancels out the effect of the average magnetic torques in alining the grains, and the distribution is isotropic. Secondly, further analysis of ferromagnetic relaxation (ref. 4) has led to numerical corrections in the results of

[1] The contents of this paper were published previously in the Astrophys. J. (published by the Univ. of Chicago Press), vol. 147, 1967, p. 943.

reference 2, and it now appears that if magnetic relaxation can aline particles at all, a field of 10^{-5} gauss will be required for ferromagnetic particles, a value not much less than that required for paramagnetic grains. The present paper explores these two difficulties, analyzing the fundamental basis for magnetic alinement and reexamining the strength of the field required with ferromagnetic grains.

A detailed discussion of grain orientation, in which thermal fluctuations of magnetization as well as steady torques are considered, is beyond the scope of the present paper. Suffice it to point out here that grain orientation can be understood in terms of a steady-state distribution in which the rotational temperature that characterizes the distribution of rotational energy tends to be different for different directions of the rotational momentum **J**. For **J** parallel to the magnetic field **B**, there is no magnetic torque and the temperature is about equal to the gas temperature T_g; for **J** transverse to **B**, a substantial magnetic torque can arise, and the kinetic temperature is somewhere between the gas temperature T_g and the internal temperature T_i of the grains. If these two temperatures are equal, there is no orientation of the rotational momentum, but if T_i is much less than T_g, the grains will spin primarily about axes parallel to **B** if collisions with gas atoms are sufficiently infrequent.

Orientation of the principal axes of the grains relative to the angular momentum direction also follows from simple equilibrium consideration. If prolate spheroids are considered, the condition that the kinetic energy of rotation about the principal axis equals that about each of the transverse axes leads directly to the result that the angular momentum is systematically greater about the transverse axes, with their greater moment of inertia. The net result is that for prolate spheroids in equilibrium the principal axes tend to be perpendicular to the angular momentum vectors of each grain. The combination of this tendency with the alinement of **J** parallel to **B** produces the grain alinement predicted by the Davis-Greenstein theory.

A more quantitative discussion of paramagnetic relaxation, based on an idealized model, gives an equation for the orientation parameter F introduced by Davis and Greenstein. The value of this parameter is 1/3 for complete orientation and it vanishes for an isotropic distribution. For weak orientation (F much smaller than 1/3) this equation becomes

$$F=\frac{\chi''B^2}{75a\omega n}\left(\frac{2\pi}{mkT_g}\right)^{1/2}(\gamma-1)\left(\frac{T_i}{T_g}-1\right) \tag{1}$$

where

χ'' imaginary part of magnetic susceptibility
a grain radius
n number density of H atoms

m mass of H atom
k Boltzmann constant

Except for a relatively minor change in numerical constants, equation (1) agrees with equation (90) of reference 1 except for the factor $(T_i/T_g)-1$. The value of the present theory is that it provides a sounder physical basis for this result and indicates how the alinement depends on the difference between T_i and T_g. It is assumed that similar results apply also for ferromagnetic and other anisotropic grains, although the present analysis has not been applied specifically to such particles.

A reexamination of ferromagnetic relaxation rates has led to a redetermination of the magnetic susceptibility, particularly its imaginary part χ'', which is responsible for a dissipation of energy when a particle rotates in a magnetic field. Theoretical and experimental research on this subject has much increased our knowledge since the original work of reference 2. The dissipation of energy results from scattering of energy out of a uniform rotation mode into other normal modes of the particle, particularly the lattice vibrations and spin fluctuations. A study of these scattering processes indicates that the value of χ'' adopted in references 2 and 4 was probably too small by several orders of magnitude. In view of the uncertainty as to the structure of interstellar grains, definite numerical values cannot be cited, but it appears quite likely that substantial orientation of interstellar grains can be achieved in magnetic fields of 10^{-6} gauss or less.

REFERENCES

1. DAVIS, L.; and GREENSTEIN, J.: Polarization of Starlight by Aligned Dust Grains. Astrophys. J., vol. 114, 1951, p. 206.

2. HENRY, J.: Polarization of Starlight by Ferromagnetic Particles. Astrophys. J., vol. 128, 1958, p. 497.

3. SPITZER, L.; and TUKEY, J.: A Theory of Interstellar Polarization. Astrophys. J., vol. 114, 1951, p. 187.

4. CUGNON, P.: Sur la Polarisation de la lumière des étoiles. Bull. Soc. Royale d. Sciences Liege, vol. 32, 1963, p. 228.

DISCUSSION

Field: Did you say that the effect of the thermal fluctuations would be small?

Spitzer: The effect of the thermal fluctuations is to cancel the orientation completely if the grain temperature is equal to the gas temperature. If these two temperatures are equal, the grains act as though they are in a thermodynamic enclosure as far as all rotational motions are concerned and there can be no orientation. The effect of thermal fluctuations is small, as assumed by Davis and Greenstein, if the grain temperature is much smaller than the gas temperature. As a first approximation, the orientation is determined by the difference between the grain temperature and the gas temperature.

Greenberg: If the grain temperature is 10° and the gas temperature is 100°, the effect is negligible. If, on the other hand, the grain temperature is comparable to the gas temperature, then one should get no polarization. This might be one of the distinguishing features of the various types of grains, because various models of grains adopt quite different grain temperatures.

There are two effects: magnetic susceptibility is itself temperature sensitive and this temperature sensitivity is different depending on whether the grains are paramagnetic or diamagnetic. Also, different kinds of grains have different grain temperatures relative to the temperature of the gas. Therefore, the dependence of polarization on the ambient physical (radiation) conditions would be different for various grain models.

Donn: If we did have some relatively hot cloud that was warmed up by some mechanism where the gas temperature got high but the grains were not destroyed, then this would be a mechanism whereby one may have a high or low polarization depending on the temperature of the cloud.

Spitzer: If the internal grain temperature exceeds the gas temperature, then the polarization is in the opposite direction.

Greenberg: Is this really true or is it only a first-order approximation?

Spitzer: I should emphasize, perhaps, that the model I have presented is really not exact, since a full solution of the Fokker-Plauck equation has not yet been possible, but it does at least give results for arbitrary values of the temperatures and other parameters involved. The model predicts a linear variation of alinement only when the alinement is weak.

Wickramasinghe: Do you expect the same analysis to apply to the graphite particles?

Spitzer: The analysis in its present form should be applicable to any isotropic particles, but not to anisotropic particles such as graphite. When the grain temperature is equal to the gas temperature, orientation must disappear for all types of particles. It should be possible to work out an approximate theory for graphite.

Elvius: Would these numbers for the magnetic field apply to paramagnetic particles?

Spitzer: For paramagnetic particles, one gets the same magnetic field strength that Davis and Greenstein originally found, which is an embarrassingly high 10^{-5} gauss. However, some believe that the interstellar magnetic field probably has this high value.

Greenberg: I once calculated the fields needed to orient the graphite type of particles and I did not find that the fields that were required significantly less than those for dirty ice particles.

Color and Polarization of Reflection Nebulae NGC 2068, NGC 7023, and Merope Nebula in Three Spectral Regions[1]

AINA ELVIUS
Uppsala Observatory
Uppsala, Sweden
AND
JOHN S. HALL
Lowell Observatory
Flagstaff, Arizona

A SURVEY OF THE POLARIZATION OF LIGHT by the nebulosity within 67 regions of the Pleiades cluster was made in early 1962. The survey was made without color filters. On two nights, however, some preliminary polarization measures were made with color filters; the results obtained in this investigation seemed to be promising enough to justify a more thorough study of polarization in three colors. The polarimeter used in 1962 was not suited for observations in the UV, however, because its polaroid analyzer would have absorbed most of the ultraviolet light.

In early 1963 color measures of nebulosity were made within the Pleiades cluster in the blue and yellow spectral regions. Later that year a few more observations of polarization were made in three colors with a polarimeter which contained a Glan-Thompson analyzer. An entirely new polarimeter with a Glan-Foucault prism was built in 1964. With this polarimeter three-color observations of the polarization were obtained in several regions of the nebulae NGC 7023, NGC 2068, and the Merope nebula, and of several other objects not discussed here. The polarization observations described here were mainly obtained in October, November, and December 1964, with the 69-inch Perkins Reflector of the Ohio Wesleyan and the Ohio State Universities at the Lowell Observatory in Flagstaff, Arizona. Colors of NGC 2068 and

[1] The contents of this paper were published previously in the Lowell Obs. Bull. No. 135, vol. VI, No. 16, 1966.

NGC 7023 were obtained from the data which had been secured primarily for the purpose of studying the wavelength dependence of polarization in selected regions of these objects.

EQUIPMENT

The nebulosity involved in these measurements was often fainter than the night sky; consequently, it was necessary to make many measures on the sky background during the course of the observations. Because of this it seemed worthwhile to use two telescopes simultaneously in such a way that both the sky and nebula-plus-sky could be recorded at the same time. This procedure should not only double the rate at which observations could be secured, but also improve the accuracy of the observations, because changes in the intensity of the sky background would be continuously recorded.

Figure 1 shows the arrangement of the equipment as it was intended to be used. A 12-inch telescope was attached to the centerpiece of the 69-inch Perkins telescope in such a way that it could be offset from the position of the 69-inch telescope by as much as 1° either way in the east-west direction and could be moved about half this range either north or south. Unfortunately, despite repeated trials, certain unforeseen technical difficulties made it impossible to take advantage of this dual-telescope arrangement. The main difficulty encountered with the 12-inch sky telescope stemmed from the deviation of the transmitted beam (2 minutes of arc) produced by the rotation of its Glan-Foucault prism, combined with a lack of symmetry in the image on the cathode due to the rapid convergence of an $f/8$ beam. (The 69-inch telescope was used at $f/18$.) This method is mentioned here because the difficulties encountered can be removed and the advantages to be obtained are well worth the additional effort and equipment required.

The two polarimeters were identical, and their analyzers were turned simultaneously and to similar position angles by means of two synchro-receivers coupled to a single sychrotransmitter operated by the observer.

The Glan-Foucault prisms were mounted in hollow cylinders centered on the optical axes. In each series of measures the analyzers were oriented at four predetermined position angles 45° apart, each angle being used twice in a symmetrical sequence. An offset guider, located above the focal plane of the 69-inch telescope, made it possible to determine the center of each observed area to an accuracy of about 1 second of arc.

The signals from the photomultipliers were recorded continuously on a dual-trace Brown Recorder. They were also integrated, usually for 30 seconds; and the integral was automatically printed on a white tape and simultaneously punched into a red tape, which was later used for reduction of the data with an electronic computer, the IBM 1620, in Uppsala, Sweden. After repeated trials, the 12-inch sky data proved

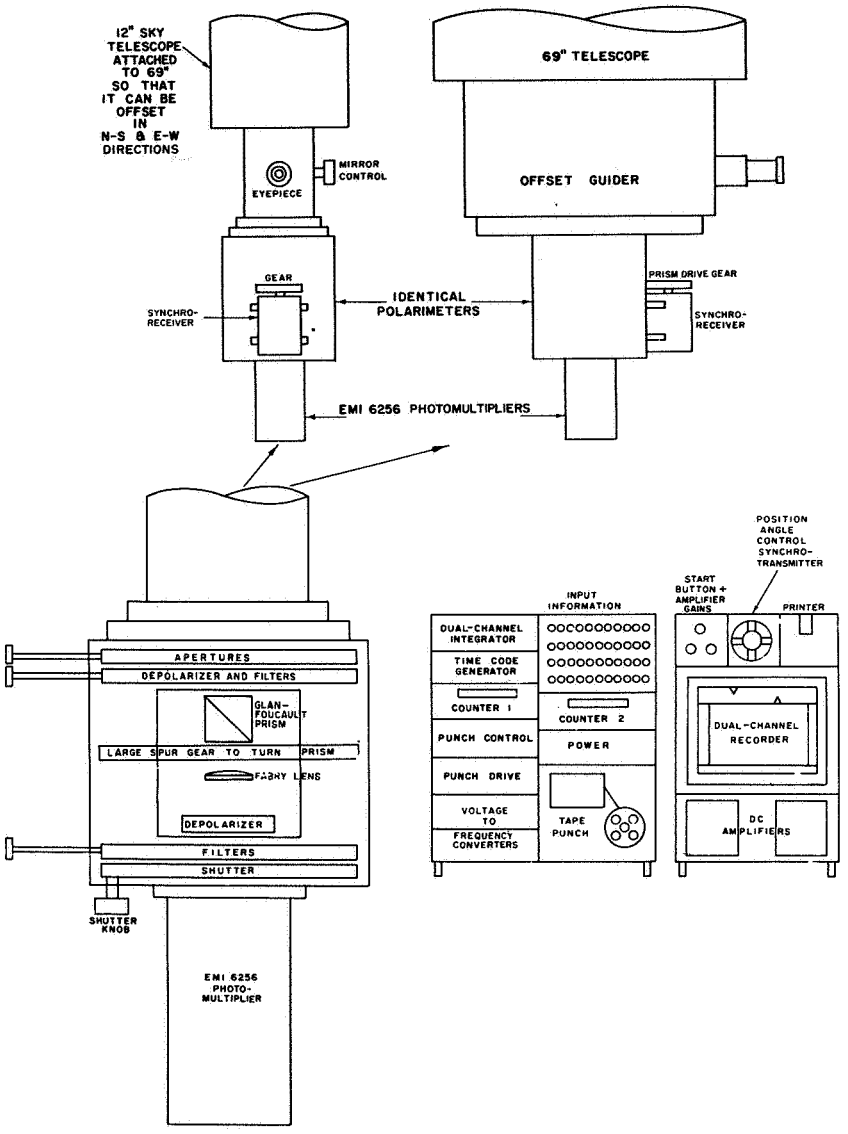

FIGURE 1.—Schematic drawing showing equipment which was intended to be used.

unreliable and only the 69-inch equipment was used for the remainder of the program.

Measures of polarization in three colors required about 20 minutes of observing time. Since a sequence on a nebula field was flanked by two similar sequences on the sky background, or vice versa, a complete set of polarization or color measures occupied about an hour and a half.

Since the color measures were considered to be of secondary importance, as a matter of convenience they were made without removal of the calcite analyzer. In order to be sure that polarized light from different regions did not systematically change the colors, a depolarizer was used together with the analyzer and the color filters. This quartz depolarizer was cemented with Canada balsam, which absorbs in the ultraviolet; consequently, special corrections, determined empirically, were applied.

Figure 2 shows the observed effective energy distribution for the entire light path using Vega as a source when each of the color filters was in position. (See ref. 1.) Energy from Vega was dispersed into focal-plane spectra by means of an objective fine-wire grating. Intensities were measured by accurately offsetting the entrance slit from the central image. The effective wavelengths determined from these data are at 3760 Å, 4460 Å, and 5740 Å. The scale of colors for each of the two systems exceeds that of the $U-B$ system by 5 percent and $B-V$ system by 10 percent. One advantage of this system of filters is that the wavelength bands transmitted by the filters are well separated; a small overlap exists near 4000 Å. Also, very little energy from H beta is transmitted by either the blue or yellow filter; and the response of the photomultiplier to H alpha is almost negligible.

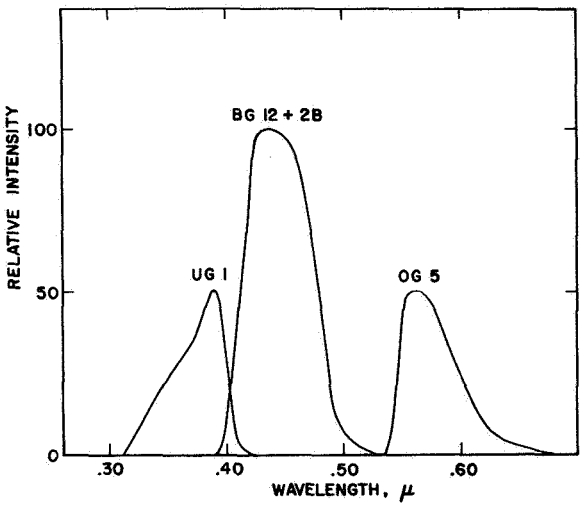

FIGURE 2.—Observed effective energy distribution for each of the three filters when Vega was the light source.

Focal-plane diaphragms with angular apertures corresponding to 29″ and 42″ were usually used. However, in order to obtain measures very close to the stars, special apertures, which are referred to as "baffles," were substituted for the diaphragms. Each baffle consisted

of a black central disk mounted on a quartz plate and surrounded by an open annular ring which was used to transmit the nebular energy. When stars were observed, apertures as small as 14″ were often used in order to include as little of the surrounding nebulosity as possible.

In order to eliminate the effects of scattered light from a nearby star, which passes through either the circular aperture or a baffle, special measurements were made in the vicinity of stars which were apparently situated in areas free from nebulosity. Some results obtained for measures of scattered light in each of the three colors using a 29″ circular aperture are presented in figure 3. In this figure, mean curves are shown for measures made through circular apertures equivalent to 29″ with two pairs of Cassegrain mirrors. For the freshly aluminized mirrors in the 72-inch system the scattered light was not only much smaller, but also was only slightly color dependent; the differences, indicated by circles, could only be detected close to the star.

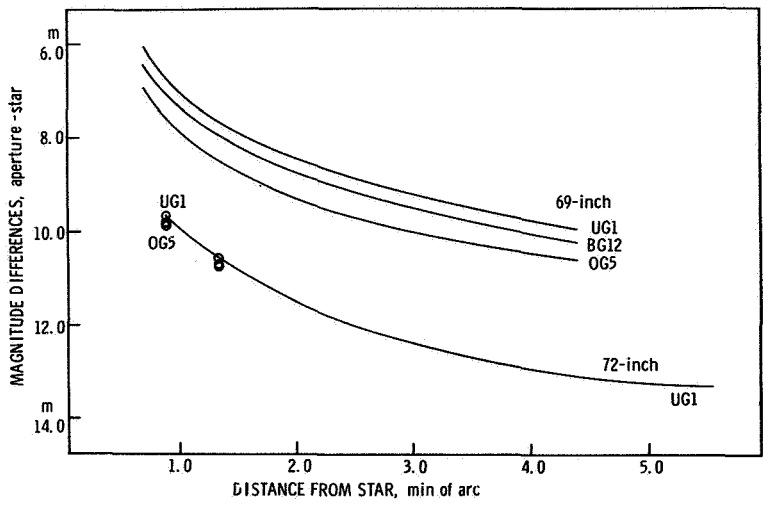

FIGURE 3.—Curves showing amount of scattered light at different distances from a star. Circles indicate areas where noticeable differences for different colors could be detected for the 72-inch system.

As can be seen in figure 3, the scattered light increased substantially toward the shorter wavelengths and varied from night to night. Furthermore, it was 10 or 20 times greater for the 69-inch optics than for the new, freshly aluminized 72-inch mirrors. The 69-inch mirror was last aluminized in 1961. Parts of this mirror had become noticeably etched during resilvering operations since it was polished 34 years ago.

The influence of scattered light on observations of color of the nebulos-

ity south of Merope was found to be so strong for the 69-inch optics that these colors were entirely rejected for this discussion. Special color observations of this region were made in the fall of 1965 by using the new 72-inch optics. Even for these observations, it was found necessary to make calibration runs on each night in order to obtain reasonably consistent results for the nebulosity within a few minutes of arc of Merope. (The analyzer and depolarizer had been removed when these observations were made.)

The colors of NGC 2068 and NGC 7023 presented here were measured with the 69-inch optics only. Because of the much more favorable ratio of nebula-to-star brightness, the scattered light corrections were small or negligible. It is difficult, however, to estimate the effect of the surrounding nebulosity on any observed region (and vice versa)—certainly gradations in color would not be as pronounced as would otherwise be true. Also, because of the wavelength dependence of scattering, the true color of the illuminating star cannot be accurately determined. As a result, the difference in color between star and nebulosity may be systematically in error—perhaps by as much as a tenth of a magnitude.

For the polarization data, the effects of the scattered light (although wavelength dependent) do not influence the results so strongly. The trends, showing wavelength dependence of polarization presented here, are not as reliable for regions close to Merope as for the more distant regions.

Measures with the baffles were less accurate because they are very sensitive, not only to scattering but also to seeing conditions present at the time. For a 29″ occulting disk surrounded by a transparent annular ring 13″ wide, the percentages of scattered light (for the 69-inch optics) were found to be 2½, 2, and 1½ percent for the *UV*, *B*, and *V* regions, respectively. No measures with baffles were obtained with the 72-inch optics.

Extinction corrections were applied to all colors in order to reduce them to unit air mass. The coefficients used were average values obtained during various photometric programs at the Lowell Observatory in recent years and were $0^{m}.250$ and $0^{m}.125$ for the $U-B$ and $B-V$ colors, respectively.

All color data presented have been reduced to the *UBV* system. A number of *UBV* standard stars were observed during each dark run. It was found that the same linear transformations for the two sets of colors could be used for each of the three runs made in 1964. The transformation coefficients which were found when the 72-inch system was used to measure colors near Merope were quite similar to those used for the 69-inch optics. The zero points of the observed colors were, however, about $0^{m}.20$ bluer for the freshly coated mirrors.

OBSERVATIONAL DATA AND RESULTS

The Pleiades

The polarization data in three colors obtained for the Pleiades in the fall of 1964 seem generally to agree well with the data obtained during 1962 and 1963, even though the different techniques were used during the different observing seasons. The polarization survey without filters in 1962 gave a general picture of the polarization of light from the nebulosity near Merope in the Pleiades cluster. This picture of the variation of the polarization with the distance from Merope has been confirmed by later observations. (See ref. 2.) For the regions close to Merope the polarization is small and seems to be of the so-called "radial" type. The data for regions within 5 minutes of arc from Merope are not very accurate, however, because of the strong influence of light from this bright star scattered in our atmosphere and instrument, the scattered light being sometimes as strong as the nebulous region itself.

Measurements of the polarization of light from this part of the Merope nebula have been published in reference 3. The data in that reference for three regions around Merope were obtained with a 12-inch telescope under poor observing conditions and they differ widely from our results.

In the fainter regions of the nebula south of Merope the polarization seems to be systematically higher than near the star; and the direction of the polarization does not depend so strongly on the direction to the illuminating star, but seems to be related to the direction of nebulous filaments in this area. This fact indicates that the light is scattered by nonspherical particles oriented in a magnetic field associated with the filaments. Hall (ref. 4) pointed out that the starlight transmitted through this system of filaments shows polarization parallel to the filaments, an indication that magnetic fields are present along the filaments. More extensive polarization measurements of stars in the Pleiades reported in reference 5 and some made by us more recently tend to confirm this conclusion, although there is not always a complete correspondence, presumably because of the complexity of the nebular structure in many areas.

A similar relationship between the directions of polarization and bright filaments in several other reflection nebulae has been pointed out in the comprehensive study of the polarization of light from reflection nebulae reported in reference 6.

The polarization vectors for scattered nebular light south of Merope were found to be nearly perpendicular to those of the starlight transmitted by the nebula. This evidence seems to strengthen the arguments given in references 7 and 8 that the polarization of scattered light is in some cases strongly correlated with the polarization of transmitted starlight, the two processes being complementary. It should be noted, how-

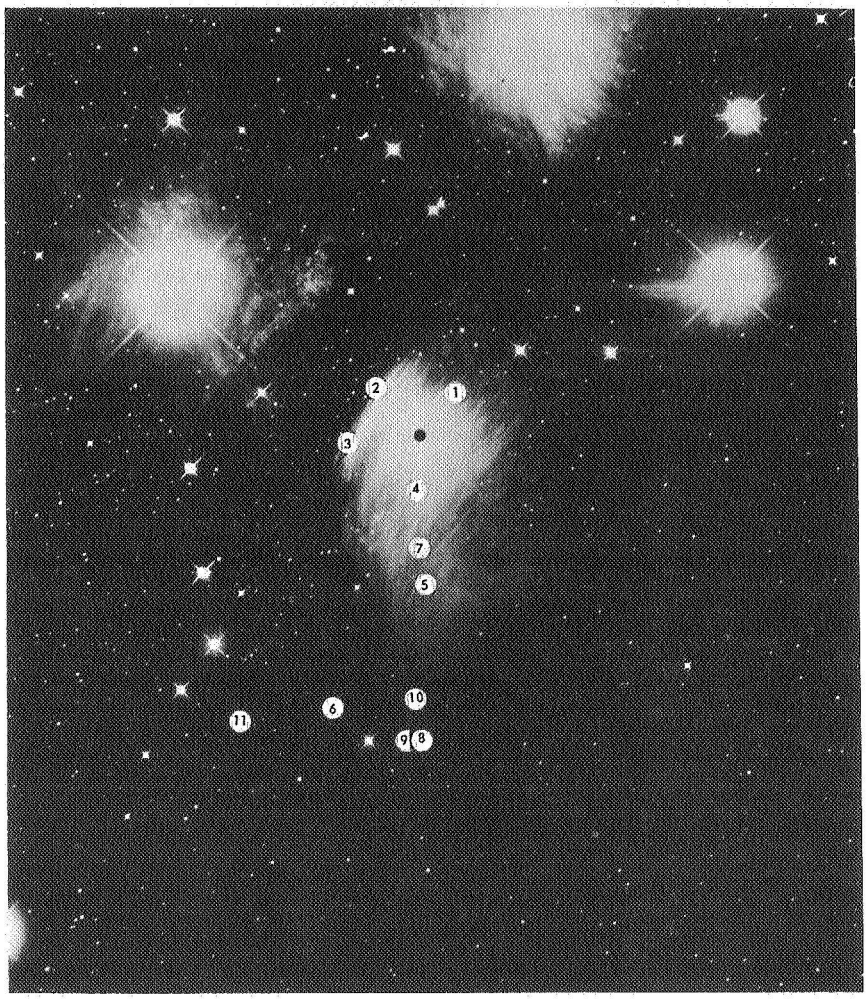

ever, that the schematic model used in these references is oversimplified and needs revision as soon as enough data are obtained to make a more elaborate model meaningful.

Preliminary results of polarization measurements in three colors are indicated in figure 4, which also shows the regions on a photograph where the measures were made. The degree of polarization has been plotted as a function of λ^{-1} with the effective inverse wavelengths: 2.66 for UG, 1, 2.24 for BG+2 B, and 1.74 for OG 5, which were obtained from the data of figure 2.

Figure 5 shows a plot of the degree of polarization (measured with the yellow and the blue filter) as a function of distance from Merope. There is a fairly strong correlation between polarization and distance.

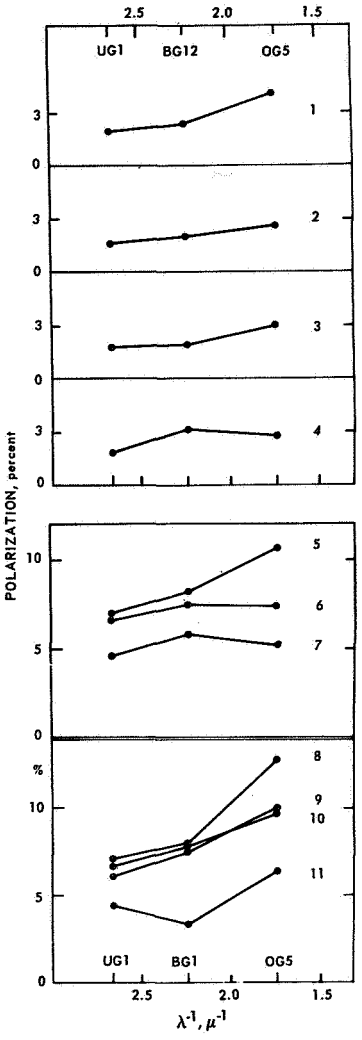

FIGURE 4.—Photograph of Merope nebula and polarization observed at different wavelengths in selected areas. The white disks with identification numbers have twice the diameter of the largest areas measured. The diagrams at the right show the increase of polarization found at three effective wavelengths with increasing distance from Merope (represented by black disk). Official U.S. Navy photograph obtained by E. Roemer with the 40-inch Ritchey-Chrétien telescope.

The degree of polarization increases with distance to a maximum, and then seems to decrease again at greater distances. The curves are drawn in a tentative way to illustrate this general relation. Data obtained in the ultraviolet would result in a similar curve with a lower maximum and are omitted from the diagram to avoid overcrowding.

The degree of polarization probably depends strongly on the scattering angle so that the relation between polarization and distance mainly reflects this dependence on scattering angle. Since the nebula are not expected to be entirely symmetrical, the scattering angles cannot be expected to vary smoothly with distance; thus, it is not surprising that the points in the diagram deviate more or less from the mean curve.

As must be expected from the close correlation between polarization

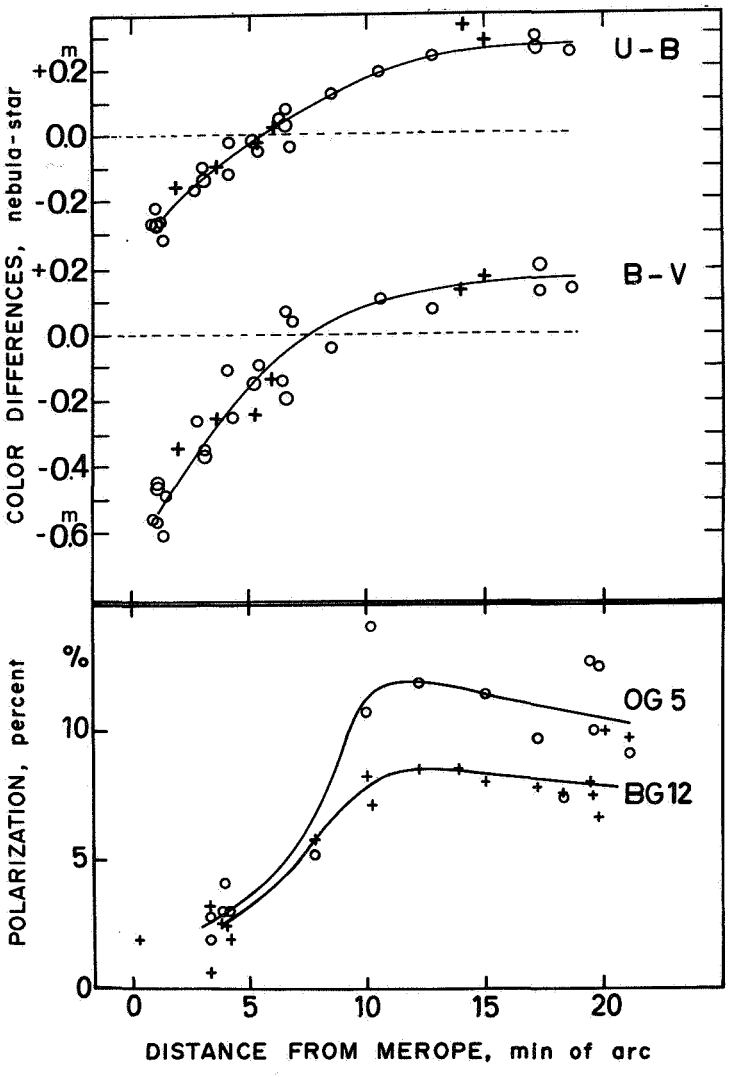

FIGURE 5.—Variation of color and polarization with distance from Merope. The data plotted in the upper part of the figure pertain to areas south of Merope; the crosses (upper plot only) represent data from reference 12. Polarization data for UG 1 are not shown but indicate the same trends as the data for OG 5 and BG 12.

and distance and the even closer correlation between color and distance, there is also a fairly close relation between polarization and color. This correlation is not considered important, however, as it seems to be quite different for different objects.

Two photographic investigations of the color of the nebulosity in the Pleiades conducted about 30 years ago are reported in references 9 and

10. The net result of these investigations was that the nebulosity was bluer than the illuminating star. Another photographic study of the Merope nebula (ref. 11) was made later. The results clearly indicated that the color of the Merope nebula increased with increasing distance south of Merope. The zero point of the colors in this investigation was not determined accurately, an indication that the nebula was always redder than Merope.

The color observations of reference 3 were made with an aperture corresponding to 12 times the area included by the largest diaphragm of the present investigation. There is little correlation between the color data of reference 3 and those of the present investigation, which were obtained for much smaller regions.

The colors of six selected regions near Merope are presented in reference 12. Interference filters were used to make measurements at four wavelength regions between 3400 Å and 5620 Å. Their equivalent widths were not greater than 250 Å. These photoelectric observations were obtained at the 82-inch telescope at the McDonald Observatory in Texas with a 63″ focal-plane diaphragm. The six regions were generally south of Merope at distances between 127″ and 885″.

The $U-B$ and $B-V$ color differences observed on four nights with the new 72-inch optics in the Perkins telescope (circles) are compared with those differences obtained in reference 12 (crosses) in the upper part of figure 5. Despite the difference in aperture size and in the positions of the areas measured, the agreement with the data of the present investigation is excellent. Shifts of only 80 Å in effective wavelength could explain the discrepancies.

The observations plotted in figure 5 show that at a distance of 1′ from Merope the nebulosity in $U-B$ and $B-V$ is about 0.3 and 0.6 magnitude bluer, respectively, than the star. In $U-B$ the color of the nebula becomes about equal to the color of Merope at 5′ south of the star; in $B-V$ the corresponding separation is 7.5.

NGC 7023

The NGC 7023 reflection nebula, shown in figure 6, subtends a much smaller angle in the sky than does the Merope nebula. The illuminating star is 7.3 magnitudes and has a color excess of 0.6 magnitude, indicating a total absorption of two magnitudes.

The polarization of light from NGC 7023 has been studied by several astronomers; however, in reference 13 is published the only data indicating the wavelength dependence of polarization for this object. These were obtained in three wavelength bands in a single region of the nebula.

Figure 6 gives a general picture of the direction of the electric vectors and the degree of polarization found for the areas that have been observed.

TABLE I.—*Color and Polarization*

Observed area offset from star	Aperture, mm	Colors		Polarization data			
				UG 1			BG 12 +2 B
		$U-B$	$B-V$	Region, sky	Polarization, percent	Position angle θ, deg	Region, sky
Star HD 200 775	.....	$-0^m.41$	$+0^m.40$	.....	0.7	85	.....
Around star	.....	−0.34	+0.20	8.1	1.5	175	11.7
5 mm S	4	−0.72:	+0.19:	4.1	4.2	91	4.3
10 mm S	4	−0.68	+0.16	2.5	11.2	92	3.9
20 mm S	4	−0.53	+0.02	0.9	3.5	90	1.2
20 mm S, 11 mm E	6	−0.68	−0.06:	0.9	9.9	62	1.0
10 mm E	6	−0.74	−0.12	1.1	4.3	5	1.1
20 mm E	6	−0.77	−0.13	0.6	6.5	162	0.45
25 mm E	6	−0.72	−0.03	0.7	7.1	172	0.9
28 mm E	6	−0.56	−0.30	0.7	8.1	178	0.7
38 mm E	6	−0.80	−0.22	.....	.....	.....	.....
10 mm N	4	−0.46	+0.38	1.5	11.8	81	2.3
4 mm N, 4 mm E	4	−0.56	+0.16	5.5	7.4	126	5.7
5 mm N, 5 mm E	4	−0.42	.....	1.8	9.5	129	2.5
6 mm N, 6 mm E	6	−0.62	−0.04	1.7	6.4	125	2.2
10 mm N, 10 mm E	6	$-0^m.72$	+0.04	1.1	4.1	125	1.1
30 mm W	6	.....	$-0^m.21$	.....	.....	.....	0.27

[a] Colons denote unconfirmed data.

[b] 6 mm = 42 sec of arc.

Data for NGC 7023 [a]

Polarization data – Continued					Distance from star, sec of arc	Remarks
BG 12 +2 B−Con.		OG 5				
Polarization, percent	Position angle θ, deg	Region, sky	Polarization, percent	Position angle θ, deg		
1.4	85	.....	1.3	85:	.....	Data are mean values of observations with 2-, 4-, and 6-mm apertures [b]
1.0	175	3.9	1.5	1	20	Observed with baffle aperture, 8-mm opening with 4-mm black disk in center; two observations with BG 12 and OG 5 filters
8.2	88	1.3	12.9	87	33	
15.8	92	1.5	19.1	91	67	Two observations with BG 12 and OG 5 filters
9.0	92	0.45	13.3:	81	133	Two observations with each filter
8.9	68	0.35	10.1	57	152	Two observations with each filter
6.3	174	0.35	11.0	1	67	Two observations with BG 12 filter
3.0	154	(0.12:	13:	20:)	133	
9.5	178	0.26	14.4	173	166	Two observations with each filter
13.1	179	0.18	20.3	179	186	Two observations with OG 5 filter
.....	.....	.....	.....	.....	253	
13.4	86	1.2	18.1	85	67	
9.5	126	2.1	12.6	125	38	Two observations with each filter
10.0	122	0.9	14.0	122	47	
7.5	123	0.6	12.6	126	57	Mean of two observations with each filter; one series with aperture of 6-mm opening with black disk of 2-mm diameter in center (by mistake)
3.9	121	0.35	5.8	131	94	
7:	171	0.07	(35:	174:)	200	

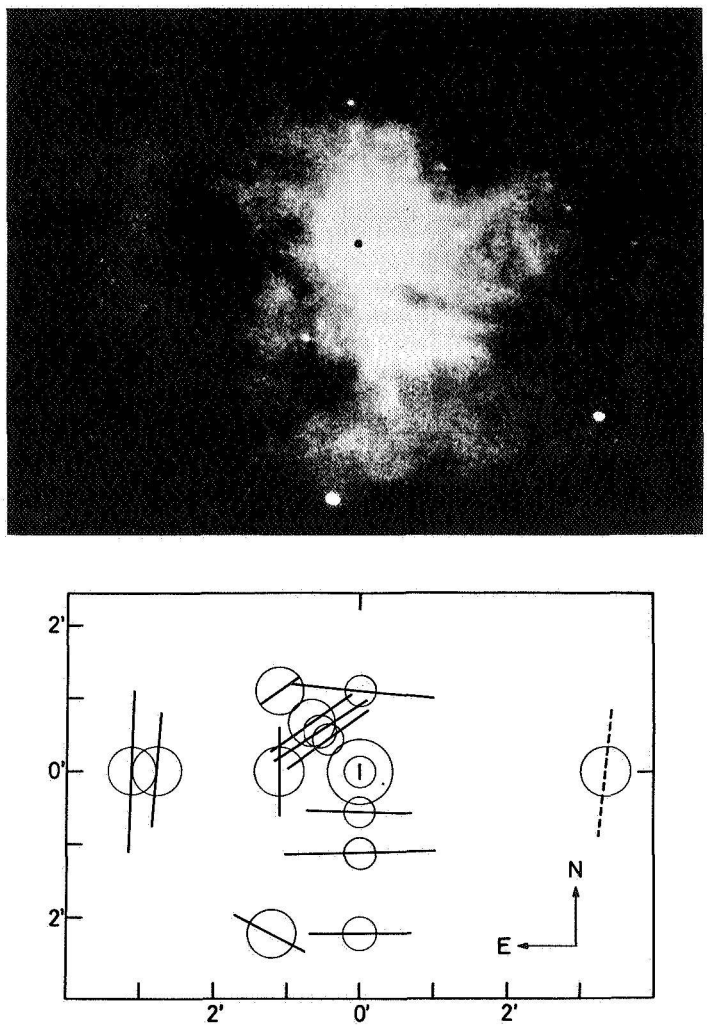

FIGURE 6.—Photograph of NGC 7023 and diagram, printed to same scale, showing polarization found in different regions. The illuminating star, HD 200775, is represented by a black disk on the photograph. The polarization of the nebulosity surrounding the star, corresponding to the area within the annular ring, is represented by the vector at the center of this ring. The open circles represent areas observed, and the length and direction of the electric vectors represent degree and direction of observed polarization. These vectors are consistently perpendicular to the direction to the star. Photograph obtained using Crossley Reflector, Lick Observatory.

The results of observations on NGC 7023 are demonstrated in table I. The data given in this table have been corrected for scattered light from the central star HD 200775 by means of the upper curves shown in figure

3 as described in the text. Because of the unknown variations of atmospheric and instrumental scattering from one night to the other, the values in table I may have been slightly overcorrected or more probably undercorrected by an amount of about the same order of magnitude as the corrections already applied. In order to make it possible for the reader to estimate the uncertainty due to variations in scattering, the values obtained for the same regions without any corrections for scattered light are given in table II.

TABLE II.—*Color and Polarization Data for NGC 7023 Uncorrected for Scattered Light* [a]

Observed area offset from star	Colors		Degree of polarization, percent		
	$U-B$	$B-V$	UG 1	BG12+2B	OG 5
Star HD 200 775	$-0^m.41$	$+0^m.40$	0.7	1.4	1.3
Around star	−0.48	+0.16	0.6	0.1	0.4
5 mm S	−0.73	+0.07	3.8	7.3	11.5
10 mm S	−0.54	+0.15	10.3	14.8	17.9
20 mm S	−0.62	+0.06	3.2	8.4	12.5
20 mm S, 11 mm E	−0.69	−0.05	9.3	8.4	9.6
10 mm E	−0.75	−0.12	3.4	5.1	8.9
20 mm E	−0.86	−0.22	6.0	2.2:	11:
25 mm E	−0.71	−0.05	6.6	9.0	13.5
28 mm E	−0.60	−0.26	7.8	12.5	19.2
38 mm E	−0.77	−0.28			
10 mm N	−0.40	+0.33	10.4	12.2	16.9
4 mm N, 4 mm E	−0.58	+0.13	6.9	8.7	11.5
5 mm N, 5 mm E	−0.43	+0.06	8.3	8.7	12.4
6 mm N, 6 mm E	−0.60	−0.04	5.5	6.5	10.9
10 mm N, 10 mm E	−0.74	−0.02	3.6	3.4	5.1
30 mm W		$-0^m.24$		6.4:	31:

[a] Colons denote unconfirmed data.

In table III a comparison is made of the data of the present investigation with those of references 6, 14, and 15. The overall agreement is good. However, in the present tests, none of the very faint areas where the authors of reference 14 reported extremely high polarization have been observed. It may be of interest to point out that yellow-sensitive plates were used in the tests of reference 14 and the effective wavelength was estimated to be 5800 Å. The work of reference 14 was criticized by the author of reference 16, who found the polarization to be much smaller. Unfortunately, he did not mention the effective wavelength at which his measures were made. If he used ordinary blue-sensitive plates without any filter, his measures were made at much shorter wavelengths than those of reference 14; and thus

TABLE III.—*Comparison of Polarization Data Given in Table I With Those of References 6, 14, and 15 for Adjacent Areas in NGC 7023*[a]

Source	Area	Color	Polarization, percent	Position angle, deg
Present paper	25 mm E mean	Blue	11	179
	28 mm E mean	Yellow	17	176
Refs. 6 and 15	A	Blue	11±9	0±25
	XVI	Yellow	12	
Ref. 14	3	Yellow	14±5	
	4	Yellow	8±6	
Present paper	10 mm N	Blue	13	86
		Yellow	18	85
Refs. 6 and 15	F	Blue	8±4	90±11
	I	Yellow	19	
Present paper	10 mm S	Blue	16	92
		Yellow	19	91
Refs. 6 and 15	S	Blue	16±5	95±6
	VIII	Yellow	17	
Present paper	20 mm S	Blue	9	92
		Yellow	13	81:
Refs. 6 and 15	IX	Yellow	25:	
Ref. 14	16	Yellow	13±3	
Present paper	20 mm S, 11 m E[b]	Blue	9	68
		Yellow	10	57
Refs. 6 and 15	P	Blue	36±8	45±6
Ref. 14	9	Yellow	21±7	
	10	Yellow	21±4	

[a] Colon denotes unconfirmed data.
[b] This is a faint region surrounded by much brighter regions.

the polarization naturally would come out smaller. This point is clearly illustrated by the data presented in figure 7, showing how the observed polarization changed with the ratio λ^{-1} in different parts of NGC 7023. In any given direction, the polarization for each wavelength region seems to increase with distance and then decrease again, as was found for the Merope nebula. The maximum polarization, however, in different directions occurs at widely different distances from the illuminating star.

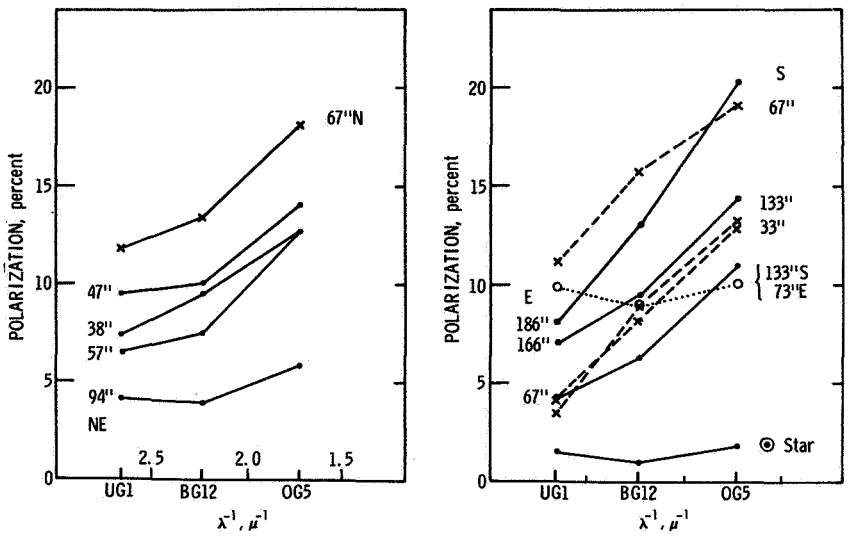

FIGURE 7.—Polarization observations obtained in various areas of NGC 7023 in three different wavelength regions.

The single region previously observed by the author of reference 13 is situated about 38″ NE of the star HD 200775, which illuminates the nebula. The present results show almost exactly the same slope of the line joining the points in UV and yellow as those reported in reference 13 for the same region, but the degree of polarization is systematically smaller in the present observations.

In NGC 7023 there is not such a simple relationship between polarization and distance as in the Merope nebula. It is true that when one starts out in any one direction from the star in NGC 7023 the polarization seems to increase, reach a maximum, and then decrease again, as was found for the Merope nebula. But the maximum polarization will be reached at widely different distances from the star in different directions. This is probably because of the very complicated three-dimensional structure of NGC 7023. No correlation between polarization and $B-V$ colors was detected for this object.

Photographic measures of the color of the nebula in eight regions were reported in reference 17. Some areas were found to be bluer and some were found to be redder than the illuminating star.

Photoelectric color measures were made by Mme. Martel in six regions situated 0'.8 and 1'.6 from the star. The present color measures were made at a dozen points, with that farthest from the star centered in a faint filament on the eastern edge of the nebula. The agreement between the two sets of data is quite satisfactory. She concluded that the nebula is bluer than the star and that the color index increases with increasing distance from the object. Her conclusion that the nebula is bluer than the star does not necessarily contradict that of reference 17, because the regions studied were not the same.

More recently photoelectric colors obtained during three scans across the nebula in an east-west direction have been published in reference 18. These data show a general increase in color as one scans away from the star, with maximum negative color excess to the southeast.

Our observed color differences on the $B-V$ system in the sense, region-minus-star, are shown in figure 8. When a baffle was used to eliminate the direct light from the illuminating star, the observed color

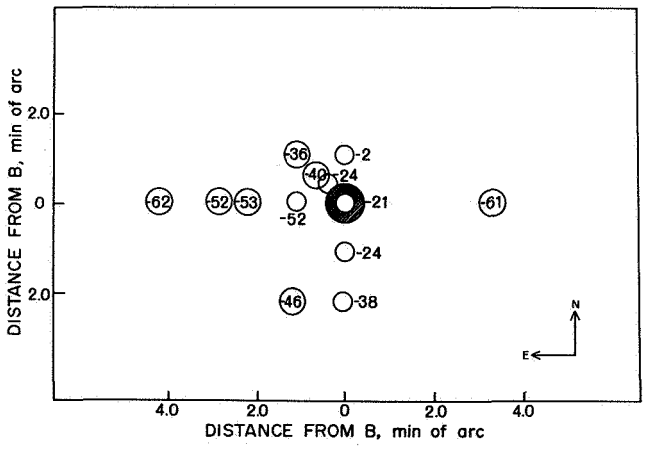

FIGURE 8.—Color differences (nebula minus star) found for NGC 7023 in different areas. Size and position of circles represent areas observed. The color of the nebulosity found for the annular ring surrounding the illuminating star is $0^m.21$ bluer than the star itself. Unit, $0^m.01$.

of the nebulosity immediately around the star was found to be $0^m.21$ bluer than the star. The degree of bluing in the east-west direction is about 0.6 magnitude in $B-V$ at a distance of 4′ from the central star. However, the color 1 minute of arc north of the object is only slightly bluer than the star, a result which agrees with the color observed near this region by Mme. Martel. Much farther to the north, Keenan (ref. 17)

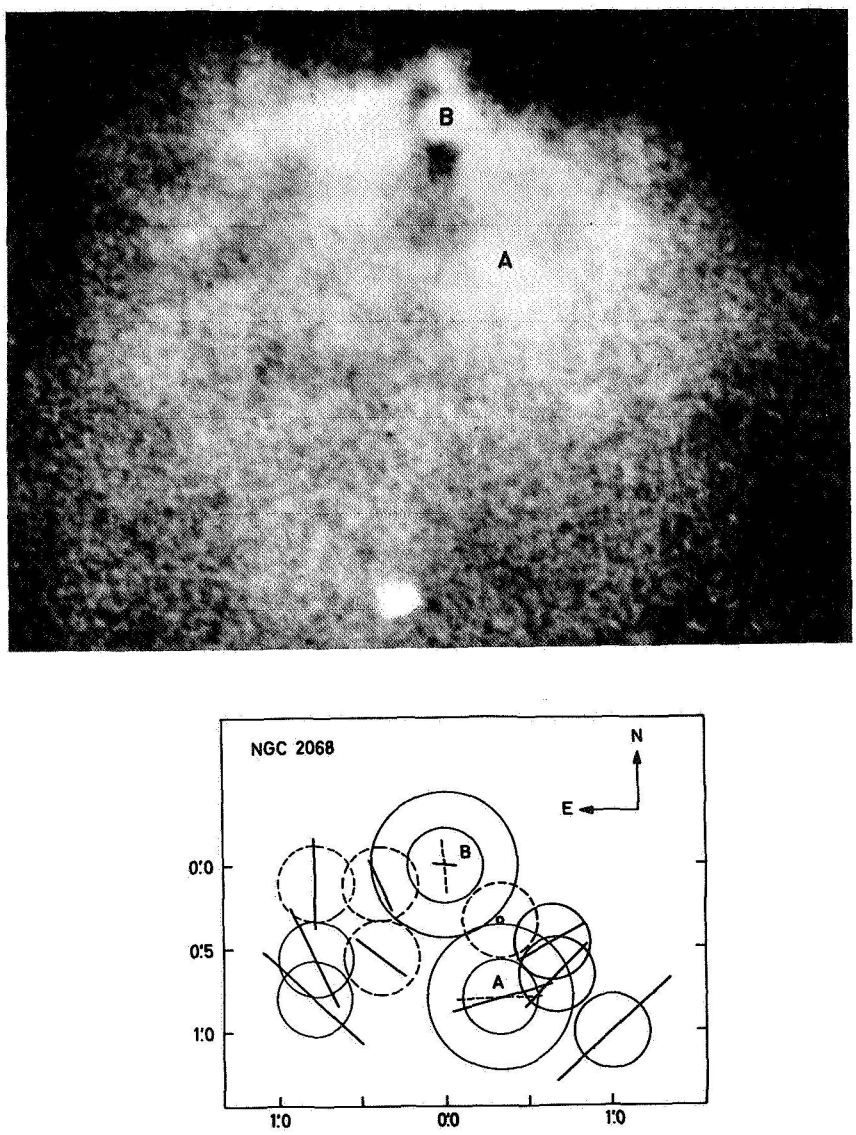

FIGURE 9.—Photograph of NGC 2068 and diagram showing observed polarization found for different areas. The positions of stars B and A are indicated together with the observed electric vectors. These correspond to yellow light and are represented by straight lines which pass through the centers of circles outlining the observed areas. The polarization found within the annular rings surrounding the two stars is similarly represented by vectors. The dotted lines describe the polarization found for the stars A and B themselves. The data clearly show that star B illuminates the nebulosity—even in the area "surrounding" A. Photograph obtained using Crossley Reflector, Lick Observatory.

TABLE IV.—*Color and Polarization*

Object or area offset from B	Colors		Polarization data			
				UG 1		BG 12 +2 B
	$U-B$	$B-V$	Region, sky	Polarization, percent	Position angle θ, deg	Region, sky
Star A	−0.06	+0.65	.....	3.4	92	.....
Star B	+0.20	+1.26	1.4	0.5:	.....	3.5
Around star B	−0.45	+0.37	2.3	0.9	81	3.5
3 mm S, 3 mm W	.....	.....	.....	.....	.....	.....
4.2 S, 5.7 W	−0.44	+0.28	2.1	3.5	116	3.1
6.0 S, 6.0 W	−0.39	+0.24	2.6	3.6	129	2.8
9.0 S, 9.0 W	−0.53	+0.13	2.1	4.6	134	2.5
7.2 S, 7.1 E	−0.47	+0.25	1.9	2.5	76:	2.7
5.0 S, 7.0 E	−0.54	+0.25	1.8	4.5	34	2.2
1.0 S, 7.0 E	.....	.....	.....	.....	.....	.....
5.0 S, 3.5 E	.....	.....	.....	.....	.....	.....
1.0 S, 3.5 E	.....	.....	.....	.....	.....	.....
Around star A	−0.54	+0.21	4.5	4.9	96	5.2

[a] Colons denote unconfirmed data.

NOTE: When not otherwise stated the aperture used was 4 mm (29″) in diameter and the area was observed only once with each filter.

Data for NGC 2068 [a]

Polarization data—Continued					Distance from star B, sec of arc	Remarks
BG 12+2 B—Continued		OG 5				
Polarization, percent	Position angle θ, deg	Region, sky	Polarization, percent	Position angle θ, deg		
4.0	90	.....	4.3	96	52	Color observation with 2-mm aperture. Polarization measures with 2-mm and with 4-mm aperture.
1.3	175:	7.8	2.4	179:	0	Color observation with 2-mm aperture. Polarization measures with 2-mm and with 4-mm aperture.
0.6:	.....	1.8	0.9	81	20	Mean values of three observations with baffle; 8-mm opening with 4-mm black dot in center.
.....	.....	2.3	0.2	.....	28	
3.4	119	1.3	4.2	118	47	
4.4	144	1.6	4.9	137	57	
5.5	132	1.0	8.3	133	85	Mean of three observations.
5.5	47	1.5	7.5	36	67	Polarization in BG 12 and OG 5 mean of two observations.
4.8	11:	1.5	6.1	29	57	Polarization in OG 5 mean of two observations.
.....	.....	1.8	5.5	1	47	Polarization in OG 5 mean of two observations.
.....	.....	1.8	3.5:	52:	41	
.....	.....	2.2	3.1	24	24	
4.4	106	2.8	5.6	107	52	8–4 mm baffle.

found the nebulosity to be redder than the star. Consequently, the presently available data indicate that this object does not have the same nearly symmetrical properties which characterize the Merope nebula. Because of differences in the regions observed, apertures used, and possible differing influence of emission lines, it is not possible to make close comparison of present results with those of reference 18.

NGC 2068

The NGC 2068 reflecting nebula is interesting from several points of view. Two tenth-magnitude stars, situated within the nebulosity A and B, are only 50″ apart, yet show polarization of almost "opposite" direction, as has been pointed out in reference 19. The electric vector has a po-

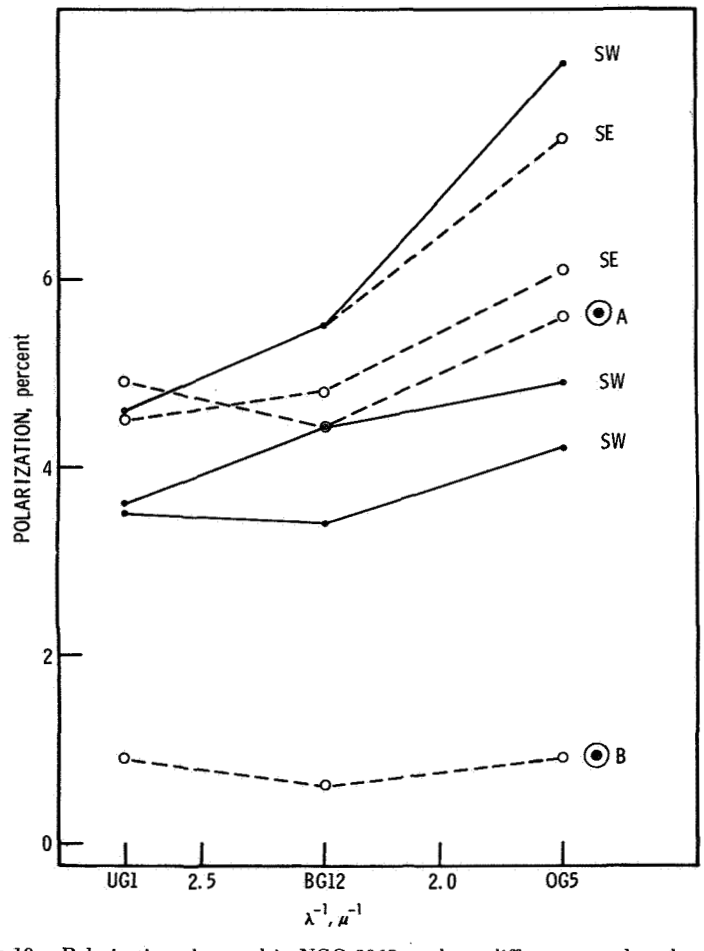

FIGURE 10.—Polarization observed in NGC 2068 at three different wavelength regions in different directions from star B.

sition angle close to 90° for star A and close to 0° for star B. It has been suggested in reference 20 that the nebula is being illuminated by the star B, which is seen in figure 9 to be very close to the northern edge of the visible nebula.

This assumption of reference 20 is verified by present polarization measures which indicate a strong correlation between the polarization vectors and position relative to star B. Even the nebulosity "around" star A seems to be illuminated mainly by the star B. It is not clear how much of the dark matter which causes the sudden change in brightness just north of star B also influences the polarization of the two stars and the nebulosity. Perhaps the dark patch close to star B, which is elongated in a north-south direction, may contribute both to the obscuration of star B and to the change in polarization relative to star A.

The polarization found for NGC 2068 is shown in table IV as a function of the ratio λ^{-1} in figure 10. The degree of polarization seems to be related to distance, as shown in figure 11, in much the same way as was found for the Merope nebula. It should be noted that the distances are small and the apertures relatively large. The relation between polarization and $B-V$ color seems to be almost opposite to that found for the Merope nebula, if there is any significant correlation at all.

In reference 20 the illuminating star is classified as B1 and its color excess is found to be 1.5 magnitude in the $B-V$ system. Since the position of the object in the Orion association places it 15° from the galactic plane, it is reasonable to assume that most of the heavy absorption is in some way associated with the nebula.

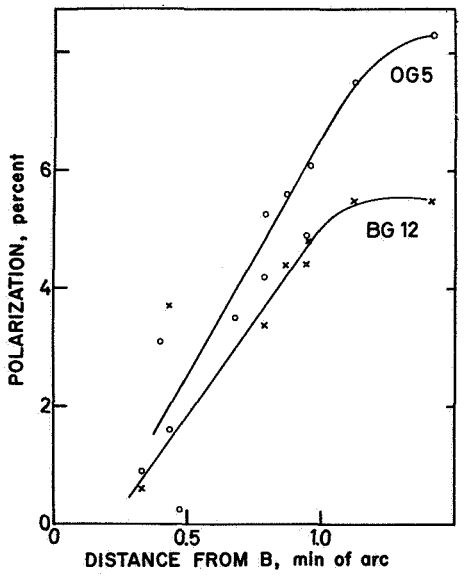

FIGURE 11.—Increase of polarization for blue and yellow regions, with increasing distance from star B in NGC 2068.

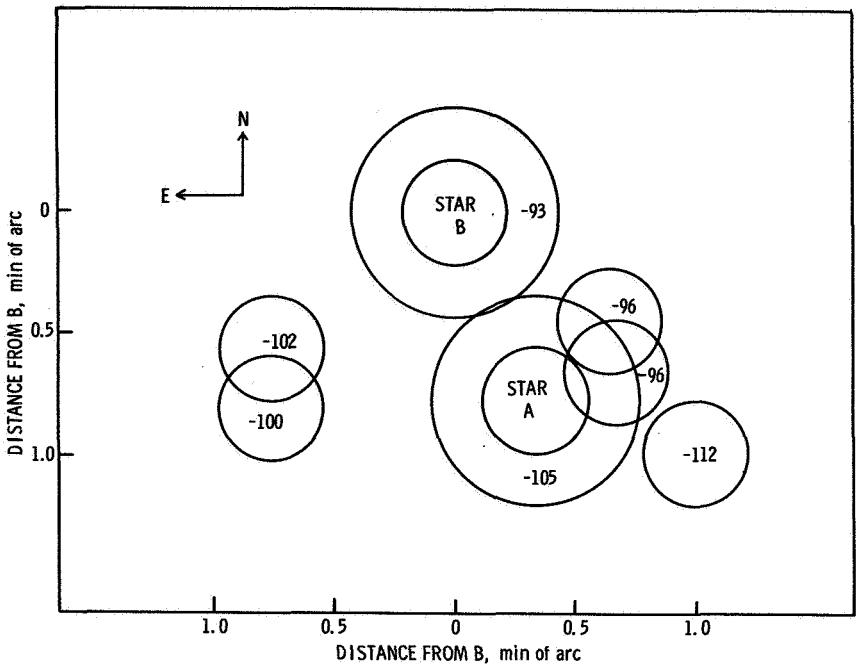

FIGURE 12.—The $B-V$ color differences (nebula minus star) found for NGC 2068. Unit, $0^m.01$.

The $B-V$ color differences (nebula minus star) found for this object are shown in figure 12. The nebulosity appears to become bluer with increasing distance from star B. These color differences are much more pronounced in NGC 2068 than in the Merope nebula and in NGC 7023; it is near 1.0 magnitude, rather than 0.6 magnitude. This larger difference must be due at least in part to very strong reddening of star B within the nebula.

TABLE V.—*Color Excesses, Spectra, and Magnitudes of Illuminating Stars*

Nebula	Data for illuminating star			
	E_{B-V}	Spectrum	V	Ref.
Merope Nebula	$+0^m.08$	B6 IV nn	$4^m.2$	21, 22
NGC 7023	+0.6	B3 ne (V)	7.3	6, 18, 23, 24
NGC 2068	$+1^m.5$	B1 V	$10^m.7$	20

Pertinent data concerning the color excesses and spectra of the illuminating stars for the three objects discussed in this paper are outlined in table V.

CONCLUSIONS

1. The data obtained in three colors indicate that the polarization varies with wavelength in approximately the same way for the three objects studied, although small variations which might be significant do occur from one region to the other within each object.

2. The polarization data show that the fainter (northern) of the two tenth-magnitude stars in NGC 2068 is the illuminating star.

3. No general correlation between the degree of polarization and the $B-V$ color of the nebulosity seems to exist.

4. The expected change in polarization with scattering angle is observed as a systematic change in polarization with distance from the illuminating star, at least in areas where the structure of the nebula is not too complicated. The shape of the curve relating polarization and angular distance, and especially the position of maximum polarization, may be helpful in solving the geometrical problems concerning the arrangement of various parts of the nebulosity relative to the position of the star.

5. It is highly probable that Merope is near the front side of the nebula and there is a rather uniform increase in color index with angular distance southward from the star. One minute of arc south of Merope the nebulosity is 0.3 and 0.6 magnitude bluer than Merope in $U-B$ and $B-V$, respectively. The angular distances at which the $U-B$ and $B-V$ colors are equal to those of the star are, respectively, 5′ and 7′.5.

6. For NGC 7023 the color excess of the nebulosity seems to decrease slightly with angular distance from the illumination star in the east-west direction. However, much more extensive color data, free from possible influence by hydrogen emission lines, should be secured before a clear picture can be obtained.

7. For NGC 2068 (M78), where the illuminating star has a color excess of 1.5 magnitude and therefore is behind heavy absorption, the color of the nebulosity decreases very slowly with increasing distance.

8. This color and polarization survey of parts of three objects suggests that for NGC 2068 and NGC 7023 the interpretation of the data is far more complicated than for the nebulosity south of Merope. The proximity and the relative symmetry of the Merope nebula suggest that it is a favorable object for intense study by several different observational techniques. The region also offers one of the best possibilities to study the relationship between the polarization due to extinction of transmitted starlight and that due to scattering of light in the same clouds.

REFERENCES

1. HALL, J. S.: Spectrophotometry of 67 Bright Stars with a Photoelectric Cell. Astrophys. J., vol. 94, 1941, p. 72.

2. ELVIUS, A.; and HALL, J. S.: Three-Color Observations of Polarization in the Light From the Reflection Nebulae NGC 2068, 7023, and IC 349, the Crab Nebula and the Galaxies NGC 1068, 3034, and 7814. Astron. J., vol. 70, 1965, p. 138.

3. JOHNSON, H. M.: Photoelectric Photometry of Diffuse Galactic Nebulae and Comet Arend-Roland. Astron. Soc. Pacific, Pub., vol. 72, 1960, p. 10.

4. HALL, J. S.: The Polarization of Light From Stars Behind Filamentary Structure. Mem. in 8° Soc. Roy. Sci. Liège, ser. 4, vol. 15, 1955, p. 543.

5. VAN DEN BURGH, S.: Polarisation des Sternlichtes im Gebiet der Plejaden. Zs. Astrophys., vol. 40, 1956, p. 249.

6. MARTEL, T. M.: Polarisation de la Nébuleuse du Crabe. Polarisation et Couleur des Nébuleuses Diffusantes. Pub. Obs. Haute-Provence, vol. 4, no. 20, 1958.

7. ELVIUS, A.: Polarization of Light in the Spiral Galaxy NGC 7331 and the Interpretation of Interstellar Polarization. Stockholm Obs. Ann., vol. 19, no. 1, 1956.

8. ANON.: On the Polarization of Light in Reflection Nebulae with Filamentary Structure. Uppsala Astron. Obs. Medd., 1959, p. 121.

9. STRUVE, O.; ELVEY, C. T.; and KEENAN, P. C.: On the Colors of Diffuse Nebulae Having Continuous Spectra. Astrophys. J., vol. 77, 1933, p. 274.

10. GREENSTEIN, J. L.; and HENYEY, L. G.: The Spectra of Two Reflection Nebulae. Astrophys. J., vol. 89, 1939, p. 647.

11. SCHALÉN, C.: The Colour Distribution in the Nebula Surrounding the Star Merope in the Pleiades. Uppsala Astron. Obs. Ann., vol. 2, no. 5, 1948.

12. O'DELL, C. R.: Photoelectric Spectrophotometry of Gaseous Nebulae II. The Reflection Nebula Around Merope. Astrophys. J., vol. 142, 1965, p. 604.

13. GEHRELS, T.: Measurements of the Wavelength Dependence of Polarization. Lowell Obs. Bull., vol. 4, 1960, pp. 105, 300.

14. GLIESE, W.; and WALKER, K.: Polarisationsuntersuchungen am Reflexionsnebel NGC 7023. Zs. Astrophys., vol. 29, 1951, p. 94.

15. MARTEL, T. M.: Polarisation de la Lumière Diffusée de NGC 7023. Pub. Obs. Haute-Provence, vol. 2, no. 17, 1951.

16. WESTON, E. B.: Polarization of the Reflection Nebula NGC 7023. Astrophys. J., vol. 57, 1952, p. 28.

17. KEENAN, P. C.: Photometry of the Diffuse Nebula NGC 7023. Astrophys. J., vol. 84, 1936, p. 600.

18. VANÝSEK, V.; and SVATOŠ, J.: Solid Particles in Reflection Nebulae I. Acta Univ. Carolinae-Math. and Phys., no. 1, 1964, p. 1.

19. HALL, J. S.: Polarization of Starlight in the Galaxy. Pub. U.S. Nav. Obs., vol. 17, 1958, p. 275.

20. SHARPLESS, S.: A Study of the Orion Aggregate of Early-Type Stars. Astrophys. J., vol. 116, 1952, p. 251.

21. JOHNSON, H. L.; and MORGAN, W. W.: Fundamental Stellar Photometry for Standards of Spectral Type on the Revised System of the Yerkes Spectral *Atlas*. Astrophys. J., vol. 117, 1953, p. 313.

22. MENDOZA, E. E.: A Spectroscopic Study of the Pleiades. Astrophys. J., vol. 123, 1956, p. 54.

23. GREENSTEIN, J. L.; and ALLER, L. H.: Spectra of Stars in Diffuse Nebulae. Astron. Soc. Pacific, Pub., vol. 59, 1947, p. 139.

24. MENDOZA, E. E.: A Spectroscopic and Photometric Study of the B Stars. Astrophys. J., vol. 128, 1958, p. 207.

DISCUSSION

O'Dell: I have obtained results that indicate that the regions at distances of about 15′ from Merope observed through narrower filters show a sharper decrease; that is, the nebula becomes even redder than the authors have indicated. This trend might be explained by the rather wide band-pass filter employed for the ultraviolet measurement of your tests. However, in general the results are the same.

Wickramasinghe: Isn't it true in general that the total color of a nebula tends to be bluer than that of the exciting star?

Elvius: I think that the integrated color of the nebula was bluer than the star. We did not measure the very faint regions far away from the star, however. You may remember that the color of the Merope nebula becomes redder with increasing distance from the star (fig. 4). Thus, the integrated color of this complete nebula may not differ much from that of the star.

Wickramasinghe. It seems this should tell us something about the nature of the grains.

Greenberg: I think that when Mr. Roark talks he will be able to point out that the color is strongly dependent on the geometry.

Wickramasinghe: The total integrated color?

Greenberg: Yes. The total color is a function of the geometry of the nebula.

Nandy: Did you study whether bluing or reddening depends upon the spectral type of the exciting star?

Elvius: The spectral types were rather similar in the cases we observed from B1 to B6.

Nandy: Are the illuminating stars of these nebulae all of the same spectral type?

Elvius: They are almost the same types; they are usually B stars.

Greenberg: Mr. Roark has noted a significant difference to be expected for the total intensity of the light for different grain models. This is another feature by which one can investigate the character of the grains. This is all, of course, a function of the albedo.

Elvius: I think we should clarify our definition of "bluing." With what do you compare the color of the nebula? The starlight we observe is often reddened. Do you compare the color of the nebula with the original color of the star?

Wickramasinghe: Yes.

Elvius: Then you get quite a bit of reddening if the light of the illuminating star is very reddened, as in NGC 2068.

Wickramasinghe: You get both bluing and reddening.

Elvius: Yes; it depends on the geometry.

Serkowski: Is the plane of polarization of the Merope nebula perpendicular to the plane for the transmitted starlight?

Elvius: Yes, the polarization vectors for the scattered light are perpendicular to those of the transmitted starlight except close to Merope, where the direction to the star is more important. We have not yet used the data to determine the albedo or to construct any models. I think the geometry problem is important, particularly in cases with nonisotropic scattering.

Greenberg: The geometry here is simplest in Merope. This seems to be the prevailing opinion.

Hall: But I don't see how you can deduce the albedos without making half a dozen assumptions.

Wickramasinghe: Yes, the situation is very difficult here. Very special models must be made before the albedos can be computed.

O'Dell: It might be important to put an error on the albedos, considering, possibly, the role of second-order scattering. If an attempt is made to fit this nebula, which becomes much redder in the outer regions, to an optically thick nebula, the fact that second-order scattering is important becomes obvious. This constitutes one more term of complication in addition to considering the geometry in obtaining a meaningful albedo.

Strömgren: I believe Dr. Hall emphasized that the Merope is the simplest case, not only because of the geometry but also because we can be fairly certain that there is no foreground absorption.

Dressler: Are there any other similar cases?

Hall: Several stars other than Merope in the Pleiades are unreddened. It looks as if the nebulosity is mostly behind the stars.

Dispersion of Polarization in Reflection Nebulae

THOMAS GEHRELS
University of Arizona
Tucson, Arizona

A FEW OBSERVATIONS WERE MADE IN NGC 7023 with filters at 0.36, 0.56, and 0.74 μ. The wavelength dependence of polarization fitted with a straight line shows an appreciable rise with longer wavelengths. (See refs. 1 and 2.) The observations at the three filters were compared with Mie calculations obtained from Dr. B. M. Herman and General S. R. Browning of the University of Arizona for various refractive indices and particle sizes. Only single particle sizes have been considered, and therefore the results are preliminary. The present work represents a first reconnaissance to learn the techniques and some of the geometrical conditions.

A firm conclusion, however, is reached in ruling out purely graphitic and purely metallic interstellar grains. The reasoning is as follows: The polarizations in various reflection nebulae (observed by Elvius and Hall) are "positive" and strong, and the color dependence is strong, with a fairly steep rise toward longer wavelengths; this behavior occurs for scattering angles from 20° to 70°. Such behavior is found in the Mie calculations at $2\pi a/\lambda \cong 1.5$. (See ref. 3.) Diagrams similar to those in reference 3 were made in the present investigation for a large imaginary component added to the refractive index, and the conclusion is unchanged. The behavior is observed at $\lambda \cong 0.56$ μ, so that $2a \cong 0.3$ μ where a is the particle radius. Such particle sizes fit the interstellar reddening and polarization-wavelength results exclusively for dielectric substances, and not for substances with a high imaginary component added to the refractive index, such as graphite and metallic particles (the latter would fit only for much smaller diameters, $2a \cong 0.06$ μ; see table III of ref. 4). This conclusion pertains to grains in the interstellar medium in general. Graphite nuclei might be generated near late-type stars and thus cause the peculiar polarizations of, for example, μ Cephei.

The Mie calculations were integrated over various ranges of the scattering angles, and self-extinction within the nebula was included. The cloud

271-992 O-67—8

was assumed to be a uniform spherical nebula, and the particles were assumed to be spherical. Some of the photometry by Mme. T. M. Martel of France was also used. It is obviously important to combine polarimetry and photometry instead of treating them separately in these problems in which solutions must be made for many parameters.

Good fits of the theory and the observations have been obtained for both homogeneous particles with a refractive index of about 1.4, an imaginary component (between 0.1 i and 0.4 i), and particle diameters of about 0.3 μ; and composite particles that have the outer shell with a refractive index of about 1.4, a negligible imaginary component, and a nucleus of diameter of about 0.06 μ consisting of a metallic or graphitic substance.

If the star is in front of the reflection nebula, no fit can be obtained. The computed wavelength dependence is too steep regardless of the refractive index used. The conclusion drawn, therefore, is that the illuminating star (HD 200775) is either inside or behind the nebula. An estimate of about 0.5 is made of the visual albedo, and the directivity $< \cos \theta >$ is about 0.6.

The distance to HD 200775 is 0.29 kiloparsec, and the space density in the nebula is about 4×10^{-10} grains/cm^3.

In general, from the work on these problems and from the fits of the interstellar polarization observations, one gains the impression that the best fit is obtained for the coated grains: a condensation nucleus of a material with a high imaginary component included in the refractive index and having a diameter of the order of 0.06 μ, coated with a material of refractive index of about 1.4 with an imaginary component that is very small. A graphite core, coated with essentially pure ice to an outer diameter of about 0.3 μ, satisfies the requirements.

REFERENCES

1. GEHRELS, THOMAS; and TESKA, THOMAS M.: The Wavelength Dependence of Polarization. Appl. Opt., vol. 2, 1963, p. 67.

2. GEHRELS, T.: Measurements of the Wavelength Dependence of Polarization. Lowell Obs. Bull., vol. 4, 1960, p. 300.

3. VAN DE HULST, H. C.: Light Scattering by Small Particles. John Wiley & Sons, Inc., 1957, pp. 152–153.

4. GEHRELS, T.: The Wavelength Dependence of Polarization II Interstellar Polarization. Astron. J., vol. 65, 1960, p. 472.

DISCUSSION

Behr: Did you find any dependence of your observed curve on the apparent distance of the nebula point from the illuminating star?

Gehrels: No, we made calculations for only one distance from the central star.

Behr: I do not understand how you draw these conclusions without knowing anything about the geometry of the nebula.

Gehrels: For the density estimate, the distance and the geometry must be known. However, for the polarimetry, there are two important factors involved. Let a scattering element having a scattering angle θ be the space confined by the observed beam, and consider discrete intervals of the scattering angle. With increasing θ the volume V of the element decreases and the distance R to the central star decreases. The weighting factor for the intensities V/R^2 is constant. This situation facilitates the use of the Mie calculations, and the value of R does not have to be known.

The other factor that is important for the polarization work is the strong forward scattering of these particles. Only the range near small values of θ is important.

Wickramasinghe: I think I am right in assuming that the geometry doesn't enter. It is only a solid-angle effect.

Greenberg: Dr. Hall mentioned that there were approximately 1.5 magnitudes of extinction. Now, was any account taken of the extinguishing of the light that gets from the star to the particles and from the particles to the observer? This would play an important role. Furthermore, if the extinction is 1.5 magnitudes from the star in this spherical geometry, I would expect that there would be a considerable difference from the single scattering that you have done.

Wickramasinghe: I don't think this would affect the polarization, which is produced essentially by the cloud particles.

Greenberg: I will get to the polarization later, but that would certainly affect the amount of light, and I think it also would affect the amount of polarization because the contributions due to different parts would be differently affected—different angles have different polarization contributions. This particular V/R^2, which is simply a solid-angle effect, is fine, but there is an additional attenuation of the radiation coming from the different parts. Therefore, different angles of scattering have contributions which are modified by the different amounts of attenuation.

Gehrels: The extinction of the light from the star to the nebular particles has been accounted for. The nebula is small and the optical depth is small; therefore, only single scattering occurs.

The dimension of the nebula must be known only approximately, for some limitation on the range of scattering angles. It makes little difference whether we stopped at a scattering angle of 20° or 10°.

The 1.5-magnitude extinction occurs mostly between the nebula and the observer, and it is the same for the starlight and for the particle-scattered light. It does not affect the polarization, and the effect on brightness and color has been accounted for.

Greenberg: Errors could also result from the interpretation in terms of single sizes. For example, in determining the wavelength dependence of polarization produced by infinitely alined cylinders, one finds for the typical Oort-van de Hulst size distribution that the value of $2a$ is about 0.6. However, the single size of cylinder that would produce essentially the same type of polarization is a value of $2a$ of about 0.4. There is a difference factor of 2 in treating a single particle and a size distribution. This situation arises because the contribution at the various wavelengths is a different function of the size for polarization than it is for extinction.

Wickramasinghe: I would like to comment on the point which Professor Greenberg raised about the effect of grains outside the cloud. If you assume that the number density of spherical grains in the line of sight outside the cloud is much less than the number density inside the cloud, then Dr. Gehrels' conclusions follow.

Greenberg: In other words, the total extinction is inside the cloud.

Wickramasinghe: What really enters is the angle with the line of sight that the starlight reaches a grain. Inside the cloud all the grains are going to be scattering into different cones producing the polarization. The grains far away from the cloud in the line of sight receive the light at zero angle and, therefore, there is no interstellar polarization.

Greenberg: Yes, but the major part of the polarization is produced by the grains in the cloud. This is where I think he may be making a mistake in his calculations.

Voice: No, he is taking this into account. He is saying that all the stuff in the cloud is producing the polarization; isn't it?

Greenberg: Yes, it is on this basis that I say that the extinction within the cloud is ignored.

Voice: I also do not understand how you can draw conclusions regarding particle size. Why couldn't you decrease the calculated polarization from the 100 percent that you would get with isotropic Rayleigh scattering? Also, introducing a somewhat larger optical depth would tend to reduce the polarization.

Gehrels: The optical depth inside the cloud is very low and the multiple scattering is negligible.

Voice: Can it possibly fit with 1.5 magnitudes?

Gehrels: The 1.5-magnitude extinction occurs on the way; that is, from the observed cloud to the observer. The starlight and the nebular scattered light are affected by the same processes.

Elvius: Have you studied the thesis written by C. J. van Houten in 1961 at the Leiden University? Do you think that the optical depth of two magnitudes in the blue quoted by him is wrong?

Gehrels: Yes. The optical depth from nebula to the observer is large, but within the cloud the optical depth is small.

Nandy: Why did you use the value 4.2 instead of 3.0 for the ratio of interstellar extinction to color excess?

Gehrels: This value was determined by H. L. Johnson.

Nandy: Do all your calculations depend upon this value?

Gehrels: The 4.2 value had nothing to do with the polarization conclusions.

Nandy: What about the distance of the star?

Gehrels: This factor did not affect the polarization conclusions, but did affect the density conclusions.

Nandy: Would the weighting factor $V/R^2=0.23$ be different if the distance were known?

Gehrels: Only in the first approximation, and it is of no consequence for the polarization work.

Elvius: As I pointed out, we found a lower polarization than you found. If your values were two-thirds lower, would that influence your conclusions?

Gehrels: It would affect the particle size; instead of the mean 0.30, the grain diameter may be 0.24 μ. But this is well within the uncertainties of the measurements and of the analysis. After all, we are dealing with spherical particles. If the interstellar particles were snowflakes, for example, none of this would hold.

Wickramasinghe: How did you get these estimates of the optical depths?

Gehrels: The optical depth is obtained as the product of the scattering efficiency, the path length, the cross section, and the number density of the grains. A mean density through the nebula was adopted; and the nebula is assumed to be a uniform spherical one.

Donn: Your analysis suggests that polarization does not depend very much on the angle; this implies that polarization would not vary across the nebula.

Gehrels: I did not say that polarization is independent of the scattering angle; near $\theta=5°$ or $\theta=20°$ it does not make much difference whether the nebula is twice as large or not. We studied rather extreme scattering angles of 10° and 20°, and the value of the angle did not affect the fits. However, for larger values of θ, near 60°, the polarization depends strongly on θ.

Donn: Do you have similar measurements at different distances from the central star at which you could carry out the same analysis?

Gehrels: No, but Elvius and Hall do. The distance is very important. For large values of θ near 90° there is a very small range of scattering angles.

Nandy: How bright is the nebula?

Gehrels: I was working at about the 14th magnitude level with a diaphragm of 23″ in diameter. The sky brightness was about one-third of the brightness of the spot.

Models of Reflection Nebulae

T. P. ROARK and J. MAYO GREENBERG
Rensselaer Polytechnic Institute
Troy, New York

A FEASIBILITY STUDY FOR AN OBSERVATIONAL PROGRAM was made to investigate models of reflection nebulae. Specifically, for a relatively simple model of an interstellar dust cloud with a source of illumination nearby, predictions of the color of the nebula, relative to the source color, at points along any radial direction from the source are sought. Furthermore, from these color differences, the possibility is studied of discriminating between the effects produced by the cloud-source-observer geometry and those due to the assumed optical properties of the scattering particles. If such discrimination is feasible, the types of observations that would be most useful in separating the effects must be known to the investigator.

Plane-parallel slab models similar to those of reference 1 in which the scattering particles are distributed isotropically and homogeneously were used. The scattering properties of the particles were assumed to be those obtained by using the Mie theory of electromagnetic scattering.

Single scattering by an ensemble of particles was assumed; a correction factor was applied to allow for the fact that the incident source-light and the light scattered in the nebula are both extinguished exponentially in passing through the nebula. Equation (1) gives the intensity of monochromatic light scattered in a direction ϕ regardless of the overall geometrical situation.

$$I_n(\phi, \lambda) = I_s(\lambda) \frac{r^2}{4k^2} \sec \alpha \, d\omega \times \int_0^T \int_{a_1}^{a_2} \frac{1}{R^2} F(\Theta, \lambda, a, n) n(a) \, da \, dz \, e^{-\kappa(\lambda)[L_s(z) + L_n(z)]} \qquad (1)$$

where

I_n nebular intensity
ϕ viewing angle (see fig. 1)

I_s source intensity in a vacuum
κ wave number, $2\pi/\lambda$
r radius of the source
$d\omega$ solid angle subtended by viewing device
R distance from source to scattering volume at point B
F scattering amplitude
Θ scattering angle, $180-\theta$
a radius of scattering particle
n index of refraction of scattering particle

The exponential term on the right-hand side of equation (1) is the single scattering modification term; $\kappa(\lambda)$ is a linear absorption coefficient; $L_s(z)$ is the distance $\overline{AB}$ in figure 1; and $L_n(z)$ is the distance $\overline{BP}$.

The function $n(a)$ is a distribution function for the scattering particle radii. Two forms are assumed for $n(a)$; one yields scattered intensities from a single size particle, and the other is an exponential distribution given by (see ref. 2)

$$n(a)=n_0 \exp\left[-5\left(\frac{a}{a_0}\right)^3\right] \tag{2}$$

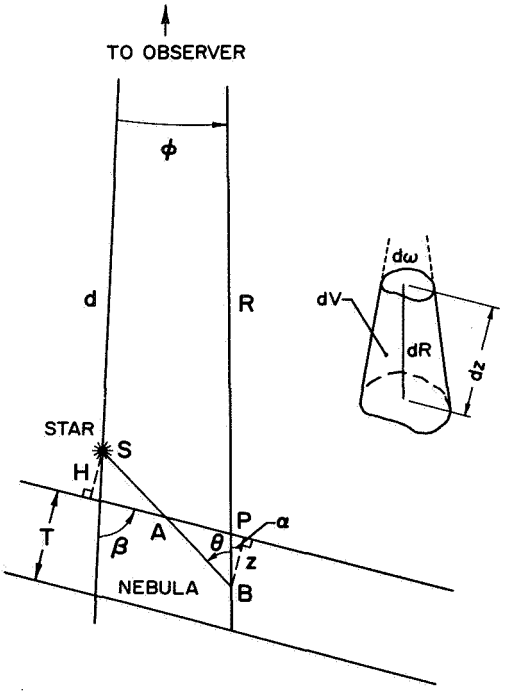

FIGURE 1.—Basic geometrical configuration for star in front of plane-parallel nebula. Sketch on the right shows detail of scattering volume dV at B.

For a value $a_0 = 0.50\ \mu$, the distribution represented by equation (2) closely parallels that determined in reference 3.

Ratios of the nebular intensities $I_n(\lambda)$ at different wavelengths may be taken and a nebular color obtained. The $B-V$ color difference between the star and nebula is then defined as

$$\text{Color difference} = 2.5 \log \left(\frac{\overline{I_s(\lambda)_V}}{\overline{I_s(\lambda)_B}}\right) - 2.5 \log \left(\frac{\overline{I_n(\lambda)_V}}{\overline{I_n(\lambda)_B}}\right) \tag{3}$$

The integrated light in each band is defined by

$$I(\lambda)_i = \int I(\lambda) Q_i(\lambda)\ d\lambda \tag{4}$$

where $Q_i(\lambda)$ is the filter-detector transmissivity function for the color "i" ($i = U, B, V$). In equation (3), the subscript s refers to the source and n, to the nebula. It should be noted that when the source is inside or behind the model nebula an exponential attenuation is introduced in the expression for $I_s(\lambda)$. Thus the source colors are those as seen by an observer and are intrinsic source colors only when the source is in front of the nebula. A positive color difference indicates that the nebula is bluer than the source of illumination.

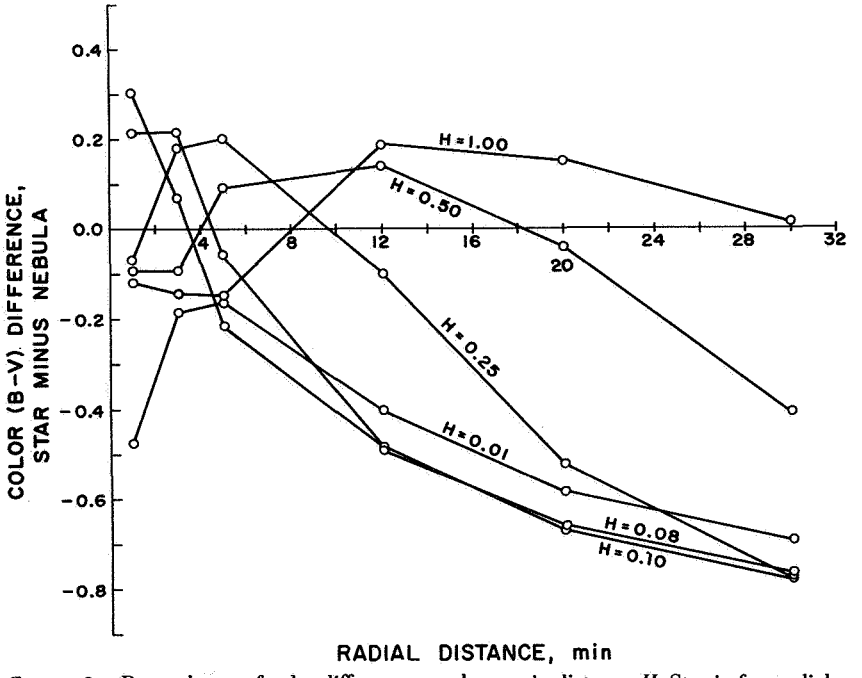

FIGURE 2.—Dependence of color difference on changes in distance H. Star in front; dielectric spheres: $a_0 = 0.50\ \mu$; $T = 1.0$ pc; $d = 160$ pcs; $\beta = 90°$; $\kappa(\lambda)_V = 1.2$ magnitudes/pc.

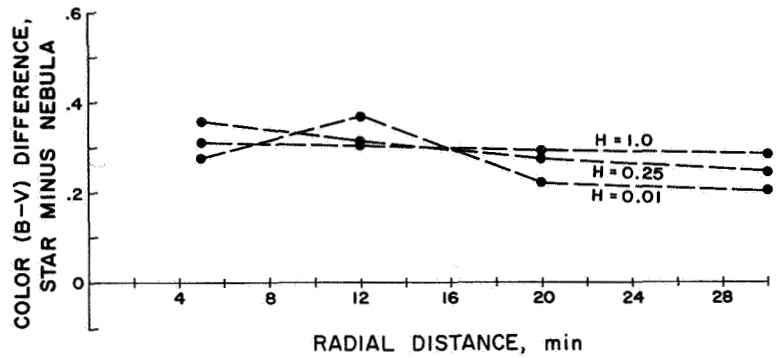

FIGURE 3.—Dependence of color difference on changes in distance H. Star in front; graphite spheres: single size, $a = 0.05\ \mu$; $T = 1.0$ pc; $d = 160$ pcs; $\beta = 90°$; $\kappa(\lambda)_V = 1.2$; magnitudes/pc.

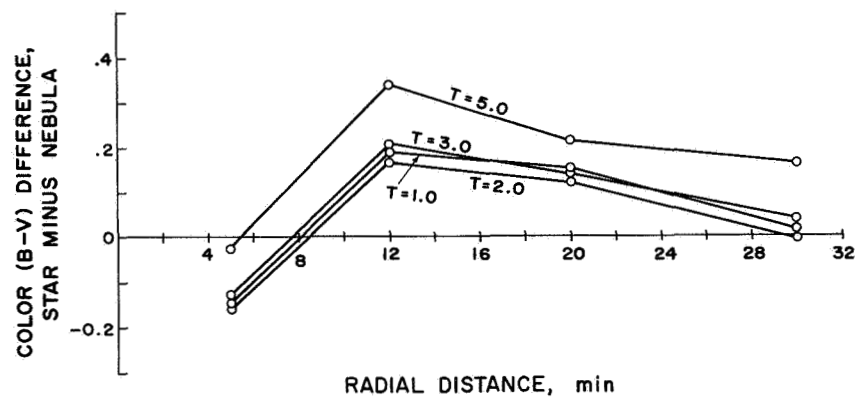

FIGURE 4.—Dependence of color differences on changes in model thickness T. Star in front; dielectric spheres: $a_0 = 0.50\ \mu$; $H = 1.0$ pc; $d = 160$ pcs; $\beta = 90°$; $\kappa(\lambda)_V = 1.2$ magnitudes/pc.

Figures 2 to 10 are representative samples of the results. Three types of spherical scattering particles have been used and all three give satisfactory theoretical fits, in the visible region, to the normalized interstellar reddening curve of reference 4. First are dielectric spheres with a real part to the refractive index of 1.30, independent of wavelength, and no imaginary part. Their radii are assumed to be distributed according to equation (2) with $a_0 = 0.50\ \mu$. Graphite spheres which all have a radius of $0.05\ \mu$ are considered next. The refractive indices of reference 5 were used. Schalèn's refractive indices for iron, as quoted in reference 6, were employed. The iron particles were considered because of their historical interest and for comparison with the graphite predictions.

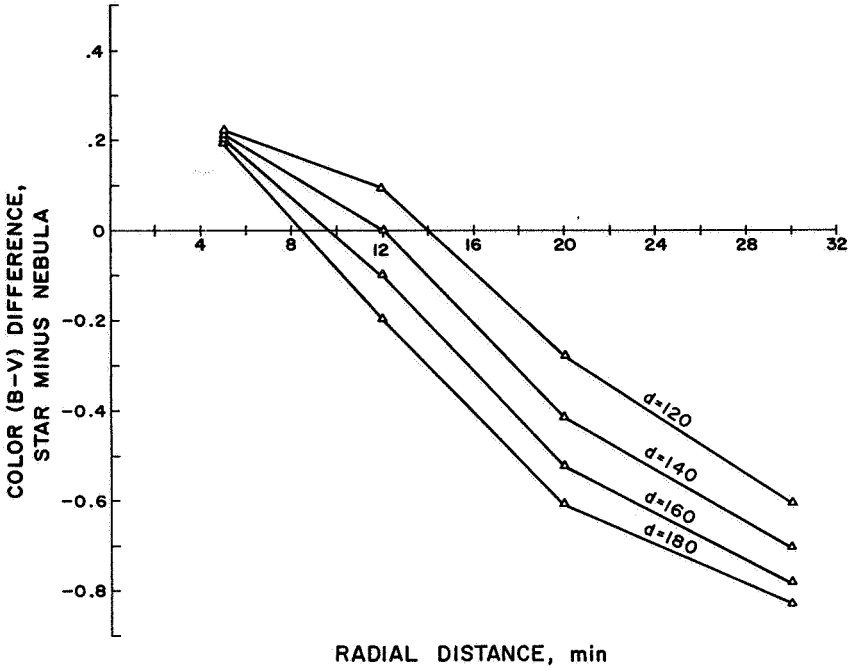

FIGURE 5.—Dependence of color differences on changes in observer-nebula distance d. Star in front; dielectric spheres: $a_0 = 0.50\ \mu$; $T = 1.0$ pc; $H = 0.25$ pc; $\beta = 90°$; $\kappa(\lambda)_V = 1.2$ magnitudes/pc.

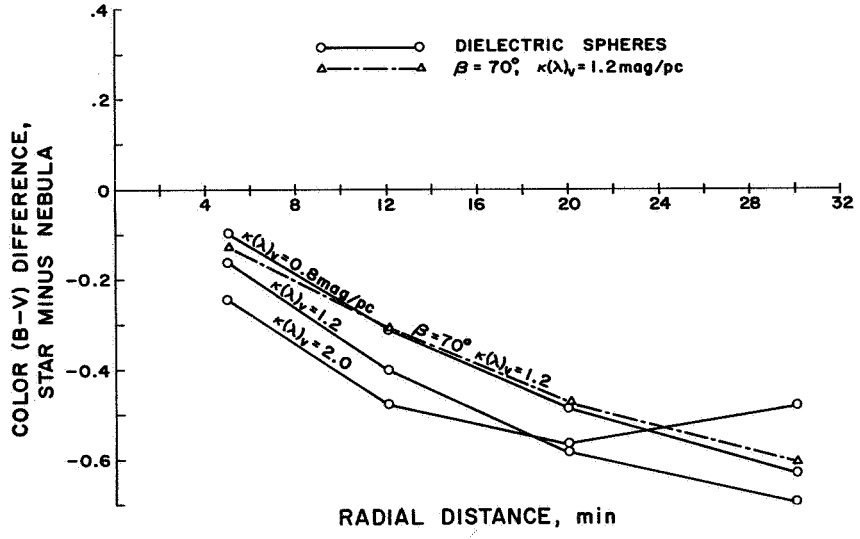

FIGURE 6.—Dependence of color differences on changes in linear absorption coefficient $\kappa(\lambda)$ and tilt angle β. Dielectric spheres: $a_0 = 0.50\ \mu$; $T = 1.0$ pc; $H = 0.01$ pc; $d = 160$ pcs; solid curves: $\beta = 90°$.

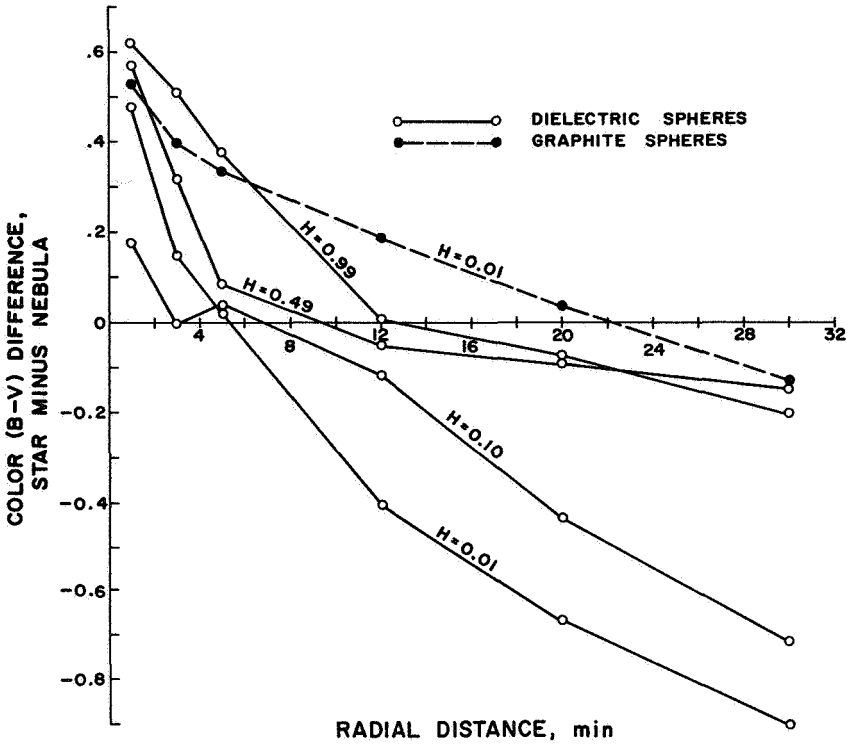

FIGURE 7.—Dependence of color differences on changes in distance H. Star inside; a_0 (dielectric spheres)$=0.50$ μ; a (single size graphite spheres)$=0.05$ μ; $T=1.0$ pc; $d=160$ pcs; $\beta=90°$; $\kappa(\lambda)_V=1.2$ magnitudes/pc.

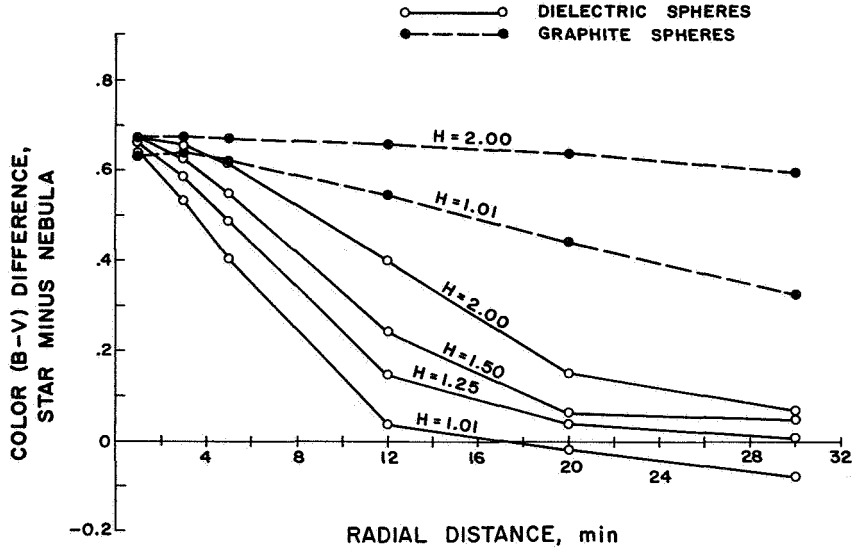

FIGURE 8.—Dependence of color difference on changes in distance H. Star behind: a_0 (dielectric spheres)$=0.50$ μ; a (single size graphite spheres)$=0.05$ μ; $T=1.0$ pc; $d=160$ pcs; $\beta=90°$; $\kappa(\lambda)_V=1.2$ magnitudes/pc.

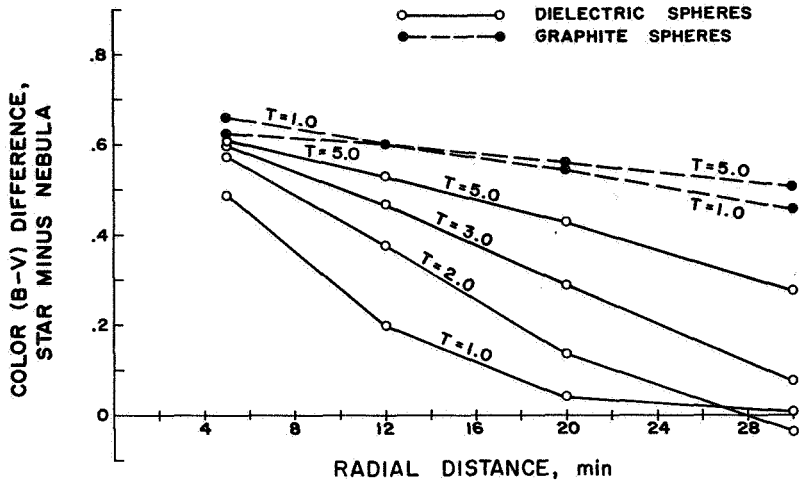

FIGURE 9.—Dependence of color difference on changes in model thickness T. Star behind; a_0 (dielectric spheres) = 0.50 μ; a (single size graphite spheres) = 0.05 μ; $H = T + 0.25$ pcs; $d = 160$ pcs; $\beta = 90°$; $\kappa(\lambda)_V = 1.2$ magnitudes/pc.

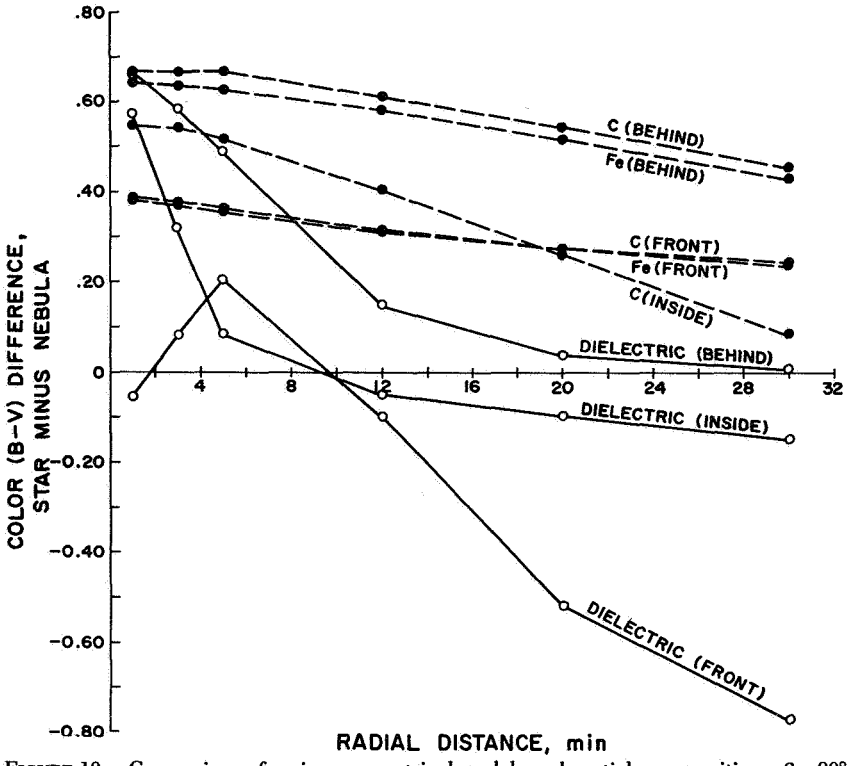

FIGURE 10.—Comparison of various geometrical models and particle compositions. $\beta = 90°$; $T = 1.0$ pc; $d = 160$ pcs; $\kappa(\lambda)_V = 1.2$ magnitudes/pc; H (front) = 0.25 pc; H (inside) = 0.49 pc; H (behind) = 1.25 pc.

The spectral energy distribution for α Eri given in reference 7 was used for $I_s(\lambda)$. This is a B5 V star and thus is typical of those stars illuminating reflection nebulae. It was found that it made very little difference in the $B-V$ color differences whether a B5 V or A0 V star was used.

Three geometrical configurations are considered. Figure 1 illustrates the case of the star in front of the nebula. Results are also presented for the cases of star inside and star behind. In all the figures, the abscissa is in minutes of arc offset from the illuminating star.

Figure 2 is for the case of a star in front of the nebula with a tilt angle β (see fig. 1) of 90°. The extreme sensitivity of the theory to the parameter H, the distance from the star to the front surface, is well shown here and in figures 7 and 8. It can be seen that the predicted nebular colors may be either bluer or redder than the illuminating star or a mixture of both, depending on the value of H.

Figure 3 shows results for a model geometrically identical to that for figure 2, but these data are for single size ($a=0.05\ \mu$) graphite particles. The curves illustrate the general qualitative behavior of graphite nebulae in that they have little slope or structure and do not go to red color difference values for star in front.

The model sensitivity to a change in nebular thickness T is shown in figures 4 and 9 for star in front and star behind, respectively. The curves for $T=5$ parsecs are probably unrealistic within the framework of the approximate nature of our theory.

Figure 5 indicates the sensitivity of the model to the distance d, from the observer to the illuminating star. This parameter is often fairly well known and a small uncertainty in d is of minor importance compared with the changes effected by a variation in H.

Figure 6 indicates the effects produced by variation of the linear extinction coefficient $\kappa(\lambda)$. It can be seen that by changing the tilt angle β and $\kappa(\lambda)$, one may duplicate color difference curves rather closely. This fact is not surprising when one considers the large number of free parameters entering into the models.

Figure 10 is a composite diagram illustrating many of the changes in color differences due to overall geometry changes and due to scattering particle changes. Two curves for iron particles are also included.

The theoretical models of the present study indicate that the most fruitful observational approach would be to observe the nebula very close to the illuminating star and at moderate to large offset distances. These are the most difficult regions to measure: The first region is difficult because of the necessity of subtracting starlight scattered by the telescope optics, and the second region, because the nebular intensity is rapidly decreasing to less than that of the night sky.

REFERENCES

1. SCHALEN, CARL: Studies of Reflection Nebulae. Uppsala Obs. Ann., vol. 1, no. 9, 1945.

2. GREENBERG, J. M.: The Optics of Interstellar Grains. Proceedings of the I.A.U. Symposium No. 24: Spectral Classification and Multicolor Photometry (Saltsjobäden, Sweden), 1964.

3. OORT, J. H.; and VAN DE HULST, H. C.: Gas and Smoke in Interstellar Space. Bull. Astron. Inst. Netherlands, vol. 10, 1946, p. 187.

4. WHITFORD, A. E.: An Extension of the Interstellar Absorption Curve. Astrophys. J., vol. 107, 1948, p. 102.

5. HOYLE, FRED; and WICKRAMASINGHE, N. C.: On Graphite Particles as Interstellar Grains. Roy. Astron. Soc., Monthly Notices, vol. 124, 1962, p. 417.

6. VAN DE HULST, H. C.: Light Scattering by Small Particles. John Wiley & Sons, Inc., 1957.

7. ALLER, L. H.; FAULKNER, D. J.; and NORTON, R. H.: Photoelectric Spectrophotometry of Selected Southern Stars. Astrophys. J., vol. 140, 1964, p. 1609.

DISCUSSION

Elvius: When you compare the color of the nebula with the color of the star, are you talking about the star as you actually see it?

Roark: We consider the fact that we are viewing the star through the nebulosity if it is behind or inside the front surface.

Elvius: Do you view the reddened star?

Roark: Yes. We tried to formulate this so that as few adjustments as possible to the observed data would have to be made.

Hall: Have you carried the computations very close to the star, within 2 or 3 seconds?

Roark: No, we have carried it only up to 1 minute offset.

Wickramasinghe: Have you used any graphite-core–ice-mantle grains in your model computations?

Roark: We are working on that. We have a program written but we're not satisfied with the results we are getting.

O'Dell: Have you treated this over a broader wavelength base than *UBV* colors?

Roark: No.

O'Dell: The reason I ask is that any of these calculations, because of the shape of the size distribution, would be far more sensitive to a wider wavelength base; therefore, would it not be just as well to calculate color differences for an ultraviolet wavelength?

Roark: Yes. We plan to obtain $U-B$ color-difference models soon.

O'Dell: Could you indicate, at least in a qualitative manner, what the effects of second-order scattering would be? In the case of Merope the nebula is obviously optically thick, because the star count is very low when we look through the center of the nebula. I wonder if this is not something to worry about before one starts detailed interpretations?

Roark: This is quite right.

Wickramasinghe: Concerning the expression for the size distribution you used: did you use a size distribution for the graphite as well?

Roark: No, one size for graphite and iron, 0.05 μ, was used.

Wickramasinghe: What is the effect of changing size here?

Roark: There is very little structure to most of the metallic color-difference curves. Most are relatively flat, although some have a rather mild slope. If one uses your new refractive indices for graphite and a particle of 0.015-μ radius, the color differences become about 0.4 bluer, but the shape of the curve does not change.

Wickramasinghe: I see. The trouble with the graphite case is that you are essentially looking at scattering from different angles, and here you would really have to take into account the anisotropic properties of graphite.

Field: Is it fair to summarize qualitatively some of those graphs by saying that graphite always showed bluing, whereas the other particles did not always show bluing?

Roark: This is correct. We have many more graphs than we have shown and in no case yet can I get graphite or iron to go below the zero line. We cannot be sure why this occurs.

Wickramasinghe: In a qualitative treatment of reflection nebulae that Hoyle and I presented, we were able to get bluing as well as reddening for the nebula. We didn't use such a detailed model as yours, but we took into account the possibility of multiple scattering by Rayleigh scattering particles. The result was reddening for a large optical depth and bluing for a small optical depth.

Hall: Is there any combination for which the sort of reddening we observed in Merope would occur with only graphite particles.

Roark: Using our model and graphite parameters, we have not been able to get reddening, and we cannot obtain kinks in the color-difference curve.

Hall: Then these color data suggest, perhaps, that the nebular material is not graphite.

Roark: That is the conclusion that I am tempted to draw.

Elvius: Could anything be said about the albedo of these graphite particles? Can you compare the brightness of the nebula with that of the star in your models?

Roark: We have not looked into the problem of albedos as yet.

Elvius: I think the albedo of the graphite particles differs considerably from that of the dielectric particles. This might help in your interpretations.

Wickramasinghe: Did you do a calculation for a size distribution of graphite of the same sort as Oort-van de Hulst's?

Roark: I think in the early stages we did, but since then I had some

reconsiderations of our theory and I would rather not quote the values. Our computation program is not complete. We want to try many size distributions which have been in the literature.

Wickramasinghe: It is important that computations for various size distributions of graphite be made before anything definite is concluded about the bluing or the reddening on the basis of this simple model. You might use different expressions for your ice-grain size distribution to see how sensitive your effect is going to be. It is not completely clear that the Oort-van de Hulst distribution which you have used is the correct one.

Roark: We used it because it was convenient, and it does give a good fit to the observed interstellar extinction law when used with dielectric spheres.

Wickramasinghe: For completeness, I think one ought to do other sorts of size distributions.

Greenberg: I agree, but in the present study, which is only a beginning, essentially two different models of grains were used; a single size graphite and a size distribution of the dielectric grains. Different models of clouds were studied within that framework.

Roark: One of the basic unknown parameters in this work is the linear extinction coefficient. I would like to have some independent means to get this.

Hall: Perhaps one could get some idea by studying the stars behind the nebulosity.

Strömgren: In that connection perhaps it is interesting to go back to Struve's work, in which rough estimates of the optical depths of reflection nebulae were made. I am sure that they are comparable to the Palomar Atlas, Dr. Hall.

Hall: Binnendijk has done this for Merope.

Strömgren: Well, Merope is a case where it appears big but even to an optical depth of 0.2 or so this would be reasonably within the range of your theory.

Roark: Yes, I think our theory would apply there.

271-992 O-67—9

Interstellar Grains in Reflection Nebulae

VLADIMIR VANÝSEK
Charles University
Prague, Czechoslovakia

REFLECTION NEBULAE are suitable objects for studying the physical nature of interstellar grains. Unfortunately, there exist only a few sufficiently bright objects, the most widely studied being nebula NGC 7023. This nebula has been studied photographically and photoelectrically by many authors, and therefore it is best suited for the verification of some theoretical conclusions. Earlier measurements (refs. 1 to 3) have already shown unambiguously that almost all nebulae exhibit a negative color excess in comparison with the color of the illuminating star. This fact has been verified photoelectrically in reference 4. In the $B-V$ system the average difference between the color of the star and that of a nebula is -0.2^{m}. These facts have been known for a long time, but the distribution of the color excess in the nebula itself has not been studied very intensively.

In the years from 1961 to 1965 we made a series of photoelectric measurements of the NGC 7023 nebula. Photometric measurements were compared with theoretical models computed for different particles of a dielectric nature. Some results have already been published in reference 5. Recently, these published measurements have been completed by measurements in the ultraviolet spectral region. It appears that considerable differences in the color excess in different regions of the nebula are observable. Nevertheless, there exists an evident decreasing trend of the color excess toward the edge of the nebula. This trend is true particularly for the color excess $U-B$ which, as the $B-V$ color excess, is defined according to the relation

$$E=(B-V)_{neb}-(B-V)_{st} \tag{1}$$

where $(B-V)_{st}$ is the color index of the star and $(B-V)_{neb}$ is the color index of the nebula in the UBV system.

The decrease of the negative color excess toward the edge of nebulae

also follows from photographic results of reference 6 for NGC 7023 and from those of reference 7, as well as from the photoelectric measurements in reference 8 of the Hubble variable nebula 2261 in Monoceros.

The increasing trend of blue color of nebulae bearing from the illuminating star to a certain distance, as observed by Hall and Martel, is obviously caused by instrumental scattering of the starlight. However, the "return" of color to the color of the star in the area near the edge of the nebula is caused by the intrinsic nature of the nebular particles.

Measurements can be interpreted by comparison with theoretical models based on the following assumptions:

1. The nebula is rather thin, optically, at greater distances from the star.

2. The gradient of the decrease of the density at greater distances is very slow, and for computational purposes, the average density is assumed to remain constant.

3. The nebula itself can have various forms; for the computation of models, the form of a spherical layer with different thicknesses is assumed. Such a model is very suitable from the mathematical point of view, as relations for analogous models can be deduced from it.

Let a mass of homogeneous density be distributed around an illuminating star in the form of a spherical layer. Consider an element in the direction of observation and of unit cross section and length dy, containing the point P. (See fig. 1.) The scattered light in this element, contributing to the scattered light in the direction $\overline{PQ}$, is given by the expression

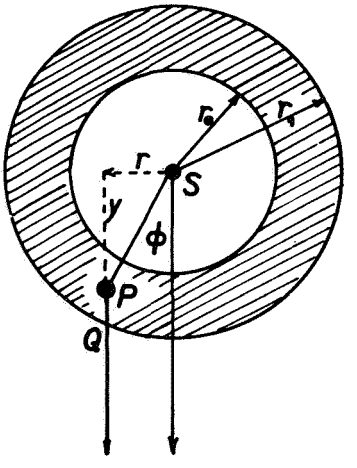

FIGURE 1.—Model of star with surrounding spherical shell of dust.

$$dI(r) = I_s \omega \, dy \, e^{-\kappa(\overline{SP} - r_0 + \overline{PQ})} F(\phi) \tag{2}$$

where

I_s energy emitted by the star into a unit solid angle
ω solid angle under which element is seen from point S
κ coefficient of absorption
$F(\phi)$ function following from Mie coefficient

Substituting the relations

$$\begin{aligned} \overline{SP} &= r \csc \phi \\ \overline{PQ} &= r_1^2 - r^2 - r_0 \cot \phi \\ \omega &= \frac{1}{r^2 \csc^2 \phi} \\ y &= r \cot \phi \\ dy &= r \csc^2 \phi \, d\phi \end{aligned} \tag{3}$$

into equation (2) gives

$$dI(r) = I_s r^{-1} \exp\left(-\kappa r_1^2 - r - r_0\right) \exp\left(-\kappa r(\csc \phi - \cot \phi)\right) F(\phi) \, d\phi \tag{4}$$

The total brightness of the nebula at a distance r from the center of the nebula S is given by integration

$$\begin{aligned} I(r) = I_s \frac{1}{r} e^{-\kappa(\sqrt{r_1^2 - r^2} - r_0)} \Bigg[& \int_{\sin^{-1} r/r_1}^{\sin^{-1} r/r_0} e^{-\kappa r(\csc\phi - \cot\phi)} \; F(\phi) d\phi \\ & + \int_{\pi - \sin^{-1} r/r_0}^{\pi - \sin^{-1} r/r_1} e^{-\kappa r(\csc\phi - \cot\phi)} \; F(\phi) d\phi \Bigg] \quad \text{for } r < r_0 \\ I(r) = I_s \frac{1}{r} e^{-\kappa r(\sqrt{r_1^2 - r^2} - r_0)} & \int_{-\sin^{-1} r/r_1}^{\pi - \sin^{-1} r/r_1} e^{-\kappa r(\csc\phi - \cot\phi)} \; F(\phi) d\phi \\ & \text{for } r \geq r_0. \end{aligned} \tag{5}$$

It is evident that the second of equations (5) is actually the formula for the spherical nebula. Analogous relations hold for other models.

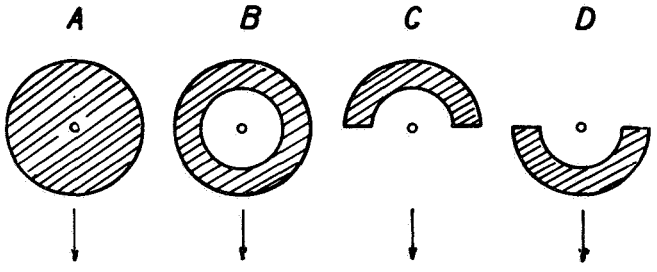

FIGURE 2.—Models of reflection nebulae.

On the basis of these relations, the following models (see fig. 2) of nebula have been used for computation of the theoretical color excess $E(r)$ which depends on the distance r:

A a spherical nebula
B a basic model; i.e., the nebula in the form of a spherical layer
C a nebula in the form of a curved layer with the illuminating star before the nebula
D a model analogous to model C with the illuminating star behind the nebula.

The effective radius of an actual nebula (NGC 7023) r_1 is assumed to be 720 seconds of arc. The size-distribution function

$$\left(\frac{a}{a_0}\right)^{-\gamma}$$

in these models is very steep. If $\gamma \geq 4$ and the limits of smallest diameters are near a_0, then the mean diameters $\bar{a} \approx a_0$ may be used for the practical computation.

It is impossible to get an unambiguous and exact answer to the question of the composition and size of particles of the nebula from the computed and measured color excesses because the real conditions in nebulae do not satisfy all the limiting assumptions on which the computation was performed. Photoelectric measurements also have their limitations. At greater distances from the center the nebula is too weak, while the measurements very near the center are affected by the scattered light of the illuminating star in the telescope. The photoelectric measurement described previously was performed for a distance approximately 0.1 to 0.4 r_1 from the center.

The full integration over the scattering function is impossible without the assumption of some particular models. Therefore, in the preliminary research the models with which no agreement between the observed and computed color excess $E(r)$ was found were ruled out. For this purpose the method of fitting the computed course of $E(r)$ to the observed values was used. In this method, the steepness of $E(r)$ is considered the most important parameter. An example of the results of such a fitting is shown in tables I and II and figure 3 for dielectric particles with a radius of 3.3 μ. The distribution of measured values of $E(r)$ is illustrated by the crosshatched area in figure 3. After preliminary comparison, the spherical dielectric particles with radii of $a < 0.2\,\mu$ and $a > 0.33\,\mu$ are disregarded if the refractive indices 1.33, 1.55, and 2 are used.

Although it is not possible mathematically to represent all the influences acting on a real nebula, the model of a spherical cloud where there is single scattering, at least at greater distances from the nebula, can be regarded as sufficiently satisfactory. The results obtained justify

the conclusion that the model containing particles of a dielectric nature with a refractive index of 2 and a radius of 0,3 μ is the most satisfactory for NGC 7023. The interpretation concerning particles with refractive index 1.33 and $a=0.2\ \mu$ is somewhat questionable since for this model it was necessary that the nebula have larger dimensions than follows from the apparent observable radius. However, this refractive index and particle size is in good agreement for NGC 2261.

These investigations are suitable for the qualitative delimitation of probable sizes of particles. The sizes found in this investigation are somewhat larger than the supposed sizes of particles ascertained from the interstellar absorption.

TABLE I.—*Results of Fitting Observed Color Excess* E(r) *in Reflection Nebulae on Theoretical Values NGC 7023*
[$a=0.33\ \mu$]

Model	Type of agreement for refractive index of —		
	1.33	1.50	2.0
A	Good if r_1 of nebula is larger than observed	Poor	Very good
B	Poor	None	Good
C	None	None	None
D	Poor	None	Poor

TABLE II.—*Comparison of Color Distribution Between Computed Models and Observations*
[*Diameter of nebula= 18 minutes of arc*][a]

a, μ	Refractive index m	Correlation of color distribution between computations and observations for model—		
		A	C	D
0.30	2	Good	None	Good
.18	2	Poor	None	Poor
.30	1.55	Poor	Good	Poor
.18	1.55	None	None	None
.30	1.33	None	None	None
.18	1.33	None	Good	None
.30	1.33	Good	None	Good

[a] In last row, adopted diameter of nebula extended to 27′.

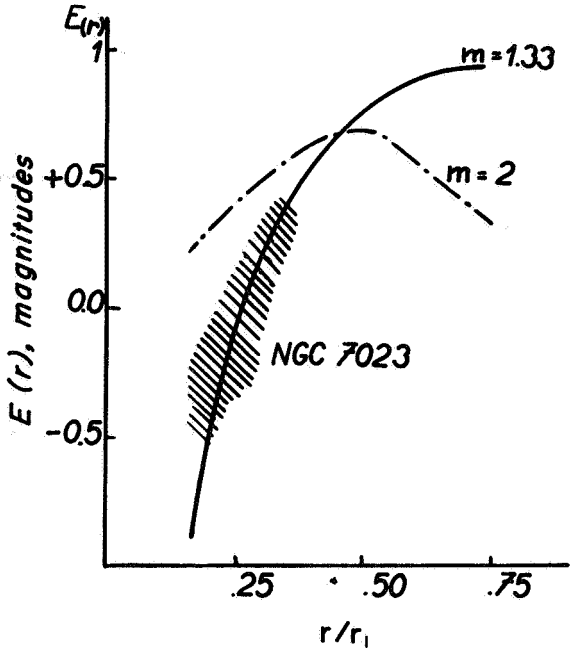

FIGURE 3.—Color excess as function of r/r_1 for refractive indices m of 1.33 and 2.

REFERENCES

1. KEENAN, P. C.: Photometry of the Diffuse Nebula NGC 7023. Astrophys. J., vol. 84, 1936, p. 600.

2. COLLINS, O. C.: Color Indices of Reflection Nebulae. Astrophys. J., vol. 86, 1937, p. 529.

3. HENYEY, L. G.; and GREENSTEIN, J. L.: The Theory of the Colors of Reflection Nebulae, Astrophys. J., vol. 88, 1938, p. 580.

4. JOHNSON, H. M.: Photoelectric Photometry of Diffuse Galactic Nebulae and Comet Arend-Roland. Astron. Soc. Pacific, Pub., vol. 72, 1960, p. 10.

5. VANÝSEK, V.; and SVATOŠ, J.: Solid Particles in Reflection Nebulae I. Acta Univ. Carol. No. 1, 1964.

6. KATCHIKIAN, E.: Akademiia Nauk Armianskoi SSR, Izvestiia, Seriia Tekhnicheskikh Nauk. vol. 10, No. 5, 1957.

7. MARTEL, T. M.: Polarisation et Coleur des Nébuleuses Diffusantes. Ann. Astrophys., Suppl. 7, 1958.

8. HALL, R. C.: Polarization and Color Measures of NGC 2261. Astron. Soc. Pacific, Pub., vol. 77, 1965, p. 158.

DISCUSSION

Wickramasinghe: Why is there such a sharp discontinuity of trend between $m = 1.33$ and $m = 1.55$ in table II?

Vanýsek: The refractive index is very important because an increase in its value produces a shift of nebular diameter. I think these results

are very similar to those of the previous paper, but the geometric configuration is different. I believe that our geometry is much closer to that of the real nebula.

Lind: Could the diameter of the cloud affect the results?

Vanysek: We say that the diameter of the whole nebula is 1 and we take into consideration the fact that the nebula has a diameter (effective diameter) of about 18 minutes of arc.

Lind: You didn't change the diameter then?

Vanýsek: If we take into consideration that the nebula itself is much greater than the observed diameter, 25 or 75 percent greater, we can find good agreement between the theory and the observation if the index of refraction is 1.33 and the diameter of the particles is about 0.3 μ.

Greenberg: I think that what is bothering all of us is a lack of continuity in the sense that one would expect to get progressively better or progressively worse results within a particular framework if the value of m is increased from 1.33 to 1.55 to 2. What bothers us is the fact that the trend is not monotonic. However, it may well be that this is just some property of this type of geometry.

Vanýsek: I think that our main problem is that we made all the computations for spherical particles with real indices only. I am not sure what the effect would be of introducing an imaginary part to the refractive index smaller or larger than 1 or of using other types of particles. The experimental measurements of real clouds of small particles as made many years ago by Richter are not representative enough because they were for very large particles. I think that the experimental measurements Dr. Greenberg has in mind for ellipsoids may be useful for reflection nebulae computations.

Accreted Molecules[1]

THOMAS GEHRELS
University of Arizona
Tucson, Arizona

IN SOME OF THE PLOTS OF THE INTERSTELLAR POLARIZATION (for example, fig. 1 of first paper by Gehrels in the present compilation) a striking feature is noted in a discontinuity that frequently occurs near $\lambda^{-1}=1.3$. The following explanation of the shape of the curve of interstellar polarization as a function of wavelength is proposed in terms of physical optics.

Far in the infrared, light passes the particle with relatively little interaction. At shorter wavelengths (red light), scattering by the molecules at the particle skin increases and consequently the amount of polarization rises. The rise with increasing values of λ^{-1} is steep (although not necessarily with λ^{-4} for polarization).

Prediction of the wavelength at which the rise becomes evident would necessitate a knowledge of the optical depth or scattering cross sections. These factors have not yet been evaluated. Qualitatively, the larger the particles, the larger the wavelength at which the polarization rise becomes manifest because of greater molecular optical depth near the skin.

A maximum in the amount of polarization is reached at larger values of λ^{-1}. The wavelength at which this maximum occurs and the maximum percentage polarization itself also depend on the total optical depth (that is, the size of the particle as well as the number of particles along the line of sight) along with such other factors as aspect, degree of magnetic alinement, and so forth.

At still larger values of λ^{-1} the amount of polarization decreases because of dilution by multiple scattering. This part of the process is fully understood. The dilution is seen in the calculations of multiple molecular scattering, as discussed in reference 1. The dilution is also

[1] The contents of this paper were published previously in the Astron. J., vol. 71, 1966, p. 62.

seen in the polarization-wavelength dependence of the multiple scattering of atmospheric molecules. (See ref. 2.)

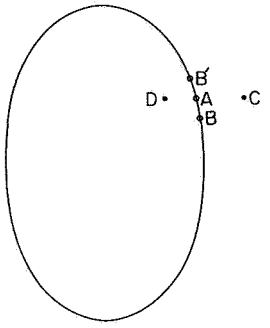

FIGURE 1.—Cross section through an interstellar particle.

Figure 1 depicts a cross section through an interstellar particle, with the illuminating star infinitely distant behind the center of the particle. As the starlight is incident on a molecule at A, the dipole vibration is exclusively in the DAB-plane, perpendicular to the direction of the incoming light. After secondary scattering by a neighboring molecule at B or B′, the vibrations occur exclusively perpendicular to the skin of the particle because, again, the vibration at B can only be perpendicular to the direction of the light from A to B. The vibration at B and B′ is observed edge-on, or 100 percent polarized.

Secondary scattering occurs more often from A in the directions of B and B than in the direction of C, because toward C the radiation is lost to the observer. In the direction of D the light (if it reaches the observer at all) experiences higher order scattering that dilutes the amount of polarization. The predominant electric-vector maximum, therefore, is perpendicular to the skin of the particle. The resulting predominant vibration is perpendicular to the long axis of the particle. This latter conclusion is compatible with the direction predicted by the Mie theory for the whole particle and with our present ideas on alinement of the particles, by the Davis-Greenstein mechanism, and the alinement of the galactic magnetic fields.

A very interesting, and as yet unresolved, problem is whether or not the particles have to be loosely accreted. More generally, this brings up the problems of coherent radiation. Interference effects appear insignificant at least for the polarization. These topics are discussed in reference 3. The scattering by loosely accreted molecules, that still have motion relative to one another, may not be greatly different from that in the gaseous state of the blue sky, in the Earth's atmosphere, for instance. The density of the molecules differs between the two cases by a factor of the order of 10. The temperatures are, of course, grossly different.

The physical mechanism of molecular scattering within the particles is not meant to replace the mathematical results such as those made by van de Hulst for long cylinders. The two models appear compatible. The advantage of the present ideas is that they at least qualitatively explain the sharp turnover at $\lambda^{-1} \cong 1.3$ and the smooth decline in the ultraviolet for the interstellar polarization curves. Furthermore, the molecular absorption bands such as interstellar $\lambda = 4430$ Å appear to follow rather logically within the proposed amorphous skin structure.

This mechanism may also be used to explain the upper limit to the particle size. Apparently, the nucleation of graphite cores is well understood. The graphite cores may be generated by and near late-type giants such as μ Cephei. The accretion of interstellar H, C, N, O, and other molecules onto the nuclei to make the particles grow further is an effective mechanism for increasing the size of the particles rapidly up to a limit. This limit may be partly determined by the multiple molecular scattering and the local radiation field. As the particle size increases, the optical depth of the molecules at the skin increases, and more light is absorbed by nonconservative scattering, causing wavelengths of 4430 Å. The particle temperature rises, causing increasing evaporation of the molecules from the skin, and, ultimately, the evaporation rate balances the growth rate.

REFERENCES

1. COULSON, J. L.; DAVE, J. V.; and SEKERA, Z.: Tables Related to Radiation Emerging From a Planetary Atmosphere With Rayleigh Scattering. Univ. of California Press, Berkeley, 1960.

2. GEHRELS, THOMAS: Wavelength Dependence of the Polarization of the Sunlit Sky. J. Opt. Soc. Am., vol. 52, 1962, p. 1164.

3. VAN DE HULST, H. C.: Light Scattering by Small Particles. John Wiley & Sons, Inc., 1957, pp. 87, 396.

DISCUSSION

Donn: With regard to the relative intensity of this secondary scattered Rayleigh light compared with the light scattering of the particles, do you require that they be equivalent in orders of magnitude? The polarization from the particles has to be small now compared with the polarization produced by molecules, and this does not seem plausible.

Greenberg: Have you calculated the amount of intensity of radiation, assuming a certain number of molecules? This shouldn't be too difficult. We know the cross sections are approximately of atomic dimensions.

Wickramasinghe: You would still want these grains to be alined, wouldn't you?

Gehrels: Definitely.

Wickramasinghe: So we still can't get over that part.

Strömgren: By what criteria do you distinguish between these different molecules; that is, the ones on the outside or surface and those inside?

Gehrels: I think the same mechanism takes place also for the molecules farther inside, but deeper inside the polarization will be diluted by high-order scattering; that is, a further zigzag path results before the light gets out.

Strömgren: It would, of course, be important that one not count the same particles twice. That is why I asked for the criterion by which you distinguish the particles.

Elvius: Does your model imply that the scattered light from a nebula around the star would have the properties of molecular scattering?

Gehrels: That is an interesting thought. I don't know.

Wickramasinghe: Could you give us the wavelength at the point of the peak?

Gehrels: The value of λ^{-1} is 1.3 at this point. I should perhaps emphasize that the discontinuity appears to be sharp. When we are looking through various clouds we have depolarization, and the effect vanishes. But for nearby stars, and perhaps a single cloud, one observes a sharp effect.

Behr: We don't have the color dependence in any nearby stars. The nearest stars for which we have color dependence are at a distance of several hundred parsecs. Your curve is drawn for stars that are more than 1 kiloparsec distance.

Gehrels: "Close" is used as a relative term. Light from stars farther away goes through so many clouds that these effects are washed out. But for stars relatively closer, the curve becomes progressively sharper.

Nandy: What polarization do you predict in the far infrared for this model?

Gehrels: Zero.

Nandy: And in the ultraviolet?

Gehrels: Zero. By complete washing out due to higher order multiple molecular scattering.

Donn: Are you really suggesting here that the entire interstellar polarization is due to these attached molecules and not due to the grain itself?

Gehrels: No, this is not a substitute for the Mie theory.

Donn: I don't quite understand. You have to superimpose on this again the polarization produced by the particle. Mie scattering is, physically, scattering by the entire grain. And you are talking here about polarization produced by molecules loosely adsorbed on the grain. Therefore, you have two scattering particles and the resultant polarization is due to a superposition produced by these two effects. What I am asking

is what is the contribution of the grain? You are avoiding the contribution due to Mie scattering.

Gehrels: If you carried the molecular scattering through rigorously, numerically, and also for the molecules inside, you might come up with the ensemble results of the Mie theory.

Nandy: Would it matter whether the particles are graphite or ice?

Gehrels: It would matter in the numbers, I'm sure. But qualitatively, this could hold, because they are still molecules.

Wickramasinghe: It depends on how strongly bound the ice molecules are.

Hallam: I think the saturation effect you mentioned must be very strong to make such a strong discontinuity at $\lambda^{-1}=1.3\ \mu^{-1}$.

Gehrels: But any single scattering by molecules will go to a maximum, which is 100 percent; then follows the dilution by the higher order scattering. We do not observe 100 percent because of the geometry involved, and because of many other factors. The number of particles, their shape, and their aspect, all enter into it.

Strömgren: Can you say that this is a λ^{-4} effect?

Gehrels: No, it is not in the amount of polarization.

Strömgren: If you consider an ideal spherical particle you can work on it in microscopic or macroscopic terms. In fact, the Mie theory gives only the macroscopic effects. The question I have is how to single out or distinguish the effects due to the particles on the skin and those due to the particles inside the grain?

Scattered Light in H II Regions

C. R. O'DELL
Yerkes Observatory
Williams Bay, Wisconsin

THE POSSIBLE ROLE OF INTERSTELLAR PARTICLES in the determination of the ionization structure of H II regions, the transfer of the Lyman line radiation, and the early stages of stellar contraction have stimulated an investigation of the properties and relative abundance of the scattering particles that exist within the boundaries of a number of bright galactic diffuse nebulae. It is interesting to note that the conclusion reached in reference 1, based on crude observations, was that there does not seem to be any scattered light in the bright H II regions; this conclusion is in contradiction to the results of the study presented herein. Results of the present investigation show that, in general, dust is an important constituent of the diffuse nebulae; that certain anomalies in the gas-to-dust ratio can be explained in a straightforward manner through the interaction of the particles and stellar radiation; and that the anomalies are closely related to the deviations known to exist in the interstellar reddening law.

The apparent surface brightnesses in the emission line Hβ and the strengths relative to Hβ of the continuous radiation at optical wavelengths have been investigated in 15 diffuse nebulae by using the methods of photoelectric filter photometry. Of these 15 nebulae, NGC 1976 (ref. 2), NGC 6514, NGC 6523, and NGC 6611 (ref. 3) have been investigated in detail across the apparent surface, enabling us to study the nature and amount of material inside the region of ionized gas. It was seen that almost all the nebulae investigated have a continuum that is stronger than that which is predicted from purely atomic processes; the excess is attributed to light scattered within the nebulae. Figure 1 gives the relevant data for the nebulae observed. The strength of the continuum can be given as an equivalent width relative to Hβ in emission and should be compared with the theoretical value of 1150 Å. This measure is in the sense that a smaller equivalent width denotes a stronger continuum and is not affected by the amount of interstellar extinction. The surface brightnesses given are not corrected for the effects of ex-

271-992 O-67—10

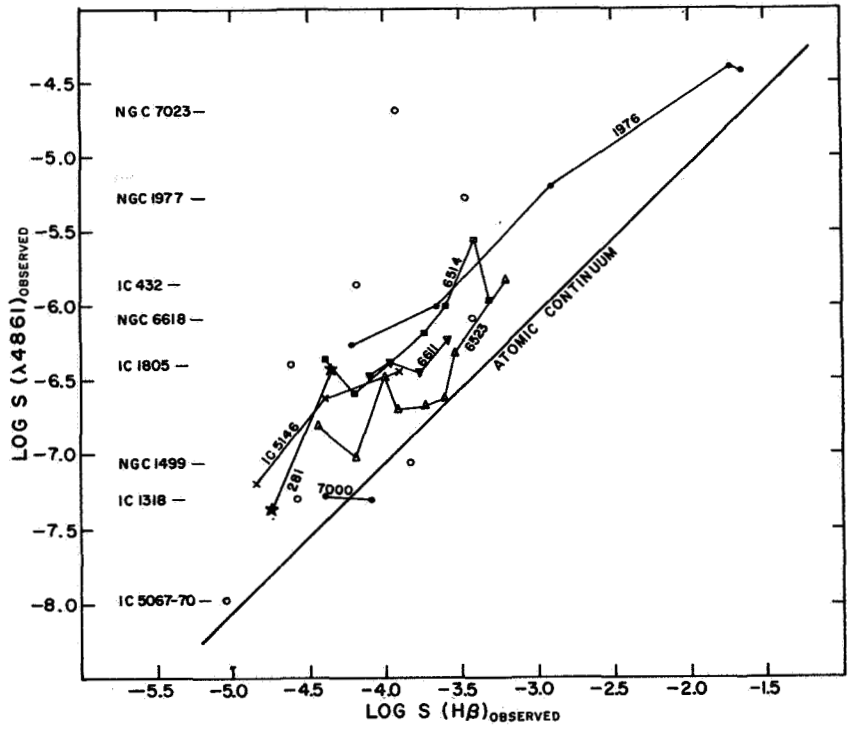

FIGURE 1.—Surface brightness of galactic nebulae in the continuum at λ4861 (ergs/cm²/sec/steradian/Å) as a function of surface brightness in the emission line Hβ (ergs/cm²/sec/steradian). Observations of multiple points in the same nebula are connected by a thin solid line. The heavy line labeled "atomic continuum" shows the predicted relation for a purely gaseous nebula.

tinction. The multiple positions for individual nebulae refer to different distances from the exciting star (or stars). The equivalent widths are generally about 400 and range from 59 Å to 1670 Å.

The effective gas-to-dust ratio can be determined from the following equation:

$$N_{\mathrm{H}}/N_d\sigma_\lambda = N_{\mathrm{H}}\Big/\int_0^\infty N(a)\pi a^2 Q(a/\lambda)\mathrm{d}a$$

where

N_{H}	density of ionized hydrogen
N_d	density of dust
σ_λ	extinction cross section for a dust particle
$N(a)$	size distribution of particles of radius a
$Q(a/\lambda)$	scattering efficiency at wavelength of the continuum measures

The detailed investigations show that the effective gas-to-dust ratio is very similar in both the nebulae NGC 6523 and NGC 6611 and in the general interstellar medium, attaining a value of $N_H/N_d\sigma_\lambda = 20 \times 10^{20}/\text{cm}^2$. The Trifid Nebula (NGC 6514) seems to be particularly dusty, with $N_H/N_d\sigma_\lambda = 4 \times 10^{20}/\text{cm}^2$. The most interesting object is NGC 1976, where there is a wide variation in the effective gas-to-dust ratio from $144 \times 10^{20}/\text{cm}^2$ in the inner regions to $5 \times 10^{20}/\text{cm}^2$ in the outer regions of the nebula. This variation occurs because there is a smaller effective scattering cross section per ionized hydrogen atom in the inner regions of the nebula. It is significant that the most deviant reddening curve known is also found in the inner region of the Orion Nebula (ref. 4). a fact utilized in the interpretation of these observations.

This new material is evaluated under rather simplified considerations of the interaction of the grain and the radiation inside the nebulae. There seem to be two main processes that can produce the observed characteristics; grain evaporation and grain repulsion by radiation pressure. In determining the rate of evaporation, we have considered the input of energy through absorption of both the stellar radiation and the Lyman line radiation and through electron impact. The energy input by these mechanisms is counteracted by infrared thermal emission by the grains and is used to find the rate at which the particles are heated above the temperature required for evaporation to occur. The procedure adopted in reference 5, where evaporation is assumed to occur when the vapor pressure exceeds the stoichiometric pressure of the particles, is followed to evaluate the grain temperatures necessary to evaporate grains composed mostly of CH_4, NH_3, and H_2O; temperatures of 28° K, 75° K, and 105° K, respectively, were found for the low densities of the interstellar medium critical grain. The two principal energy-input mechanisms are through absorption of the stellar radiation and absorption of resonance line radiation; the energy input by complete transfer of energy from free electrons is small compared with these processes. The absorption efficiency of particles with radii about the wavelength of visual radiation is quite high since most of the radiation is coming out at much shorter wavelengths. The energy input by the stellar continuum is very sensitive to the effective temperature and radius of the exciting star and is strongly concentrated to the central nebular regions because of the inverse square dilution factor. On the other hand, the energy input due to absorption of Lyman line radiation is fairly homogeneous because of the nearly constant Lyman α flux density. Except for the innermost regions, the energy input by absorption of Lyman α radiation dominates by a factor of about 2. Since the radiating efficiency decreases for decreasing grain size, the smaller grains are at a higher equilibrium temperature. If all grains smaller than a critical size a_e have a temperature higher than that necessary for evaporation, then very

soon all such grains would disappear, while the larger, cooler grains would not be modified significantly. For the Orion nebula the critical size would be $a_e(\mu) = 0.03/\phi^2$ for H_2O, $a_e(\mu) = 0.17/\phi^2$ for NH_3 grains, and $a_e = 22.7/\phi^2$ for CH_4 grains, where ϕ is the apparent displacement from the Trapezium cluster in arc minutes. Since the most effective size in scattering photons of wavelength 4861 Å is about 0.2 μ, grain evaporation may be considered unimportant in this nebula unless the grains are destroyed when CH_4 is evaporated, a result not consistent with the observations of grains in other H II regions. Since this is the most favorable case, the conclusion is very likely generally valid.

The effects of radiation pressure expulsion of grains promise to be far more important in most H II regions. This effect, selectively being stronger for the smaller particles, causes grains to be pushed out of the vicinity of the most luminous stars. One would expect the grains to be accelerated to a velocity approaching that where the drag caused by collisions with the gas particles equals the force of radiation pressure. Since the drag increases as the square of the relative velocity, the particles will rapidly accelerate until they reach a velocity close to the terminal velocity and then proceed at nearly the terminal velocity—which depends upon the gas density and the distance from the central star (or stars). If the age of the Orion Nebula is 10^5 to 10^6 years, then one can explain the observed variation in the effective gas-to-dust ratio on the basis of radiation pressure expulsion.

This interpretation of the scattered light observations is strengthened from the known peculiarities of the reddening law for the stars in and close to the Trapezium. The selective acceleration of the smaller particles would mean that they have been pushed out of the most dense region, preferentially leaving the larger grains behind where most of the reddening occurs. If the reddening law for Orion before the illumination occurred were similar to that found in the Cygnus region of the Galaxy, then this selective depletion of small particles would cause the original reddening curve to be modified into the flat curve that is now observed. This same mechanism must also be operating in the other diffuse nebulae; but, in the case of the other nebulae investigated in detail, one can show that the most luminous stars have shown for an insufficient time to cause drastic changes in the amount of dust. However, the stars have been bright long enough to have caused some small changes in the dust, a fact consistent with Johnson's observations that the reddening curve is slightly modified in these regions.

The fact that the amount of dust in the outer regions of NGC 1976 and in NGC 6514 is greater than that in the general interstellar medium may be interpreted as evidence for accelerated grain growth in regions of higher density. It would appear that gradual accretion by sticking collisions is very important in the growth of grain nuclei, a process which

depends upon the mean temperature and density of the region in which the grains are found. Since it is very likely that grains existed in the original clouds which now constitute these larger H II regions, the rate of growth should have been accelerated. For grains composed of ices, in a cloud of temperature 100° K and having final radii of 0.2 μ, the grain growth time is about $6\times10^8/N_H$ years. For the Trifid Nebula this time-scale becomes about 10^7 years, sufficiently short that we are now probably observing regions where the grains have recently grown rapidly in size but where the illuminating stars have not had time to push out many of the smaller grains. If grain growth is accelerated in the neutral clouds of material, then what we see in the other H II regions may be the combination of recent grain growth and radiative expulsion. It is interesting to note that a substantial fraction of the common heavy elements are tied up in the grains if they are icelike. For the values of the cosmic abundance usually assumed, the limiting value would be $N_H/N_d\sigma_\lambda = 3\times10^{20}/\text{cm}^2$ if the effective grain radius is 1000 Å and all O, C, and N are in grains. This value is very close to the values observed in the outer Orion Nebula and the Trifid Nebula. Possibly in these regions the accretion has gone close to completion, a hypothesis that could be tested by accurately determining the relative atomic abundances.

The question that remains is: How important are these grains in the study of the H II regions; specifically, what are their roles in the determination of the ionization structure, the transfer of resonance radiation, and the evolution of the nebulae? If the effective gas-to-dust ratio is $20\times10^{20}/\text{cm}^2$ (probably an overestimate due to recent grain growth) at $\lambda=4861$ Å, the total optical depth at Hβ for an H II region illuminated by a single O5 star will be 1.0. Since the radiation causing the ionization of hydrogen falls at a much shorter wavelength, the ultraviolet optical depth will be considerably larger—an effect counteracted in part by the fact that only the true absorption component will be important. This means that significant fractions of the energy from the star, that otherwise would go toward ionization of neutral hydrogen, will be lost by grain absorption and reradiation into the infrared. This would cause the degree of ionization to decrease more rapidly in the inner regions and make the total Strömgren sphere smaller. The problem for the transfer of Lyman α radiation is even more extreme because the photons are scattered by the absorption-emission process of hydrogen. This scattering causes the average Lyman α photon to traverse a total path inside the nebula that is larger than the radius by a factor of at least 10, and possibly much larger because of the effects of back scattering by the outer neutral shell. (See refs. 6 and 7.) The probability that a Lyman α photon will be destroyed by absorption by a grain is, therefore, almost certain. This fact can also be true for other optically thick Lyman line photons and can cause a significant deviation from the elementary conditions of statistical

equilibrium that are assumed in the calculation of the emissivities in Balmer radiation. Finally, the continued rapid grain growth in the outer, un-ionized regions of an interstellar cloud can modify the nature of the structure and evolution of the H II region because of the expected sharp discontinuity in the relative opacity in the continuum. In this instance, the ionization front would not grow as rapidly as expected in a grain-free nebula, and the shock front concentration of material (bulldozing) ahead of the ionization boundary would be of greater importance and relatively thicker than previously calculated for a pure gas nebula.

The present results have shown that interstellar grains do exist in abundance in the ionized regions of the interstellar medium; mechanisms have been outlined that may be important in understanding the nature of the particles. The need to extend this work to regions of the galaxy known to have anomalous scattering properties is obvious. It would appear that, to a first approximation, Hubble's division of nebulae into emission-line and reflection objects is because of the nature of the ionization field and does not constitute an intrinsic difference as suggested in reference 1.

REFERENCES

1. SHAJN, G. A.; HAZE, V. T.; and PIKELNER, S. B.: Proceedings of the Liège Symposia, vol. 15, 1954, p. 441.

2. O'DELL, C. R.; and HUBBARD, W. B.: Photoelectric Spectrophotometry of Gaseous Nebulae I. The Orion Nebula. Astrophys. J., vol. 142, 1965, p. 591.

3. O'DELL, C. R.; HUBBARD, W. B.; and PEIMBERT, M.: Photoelectric Spectrophotometry of Gaseous Nebulae III. Scattered Light in Three Bright H II Regions. Astrophys. J., vol. 143, 1966, p. 743.

4. JOHNSON, H. L.: Interstellar Extinction in the Galaxy. Astrophys. J., vol. 141, 1965, p. 923.

5. GAUSTAD, J. E.: The Opacity of Diffuse Cosmic Matter and the Early Stages of Star Formation. Astrophys. J., vol. 138, 1963, p. 1050.

6. O'DELL, C. R.: Photoelectric Spectrophotometry of Gaseous Nebulae II. The Reflection Nebula Around Merope. Astrophys. J., vol. 142, 1965, p. 604.

7. YADA, B.; and OSAKI, T.: The Radiation Field in a Galactic Nebula with an H I Envelope I. Astron. Soc. Japan, Pub., vol. 9, 1957, p. 82.

DISCUSSION

Walker: How do you compare the observed continuum emission with that to be expected from free-free emission? Did you actually look at any planetary nebulae?

O'Dell: This was done before. The level of the emission there is generally that found, within the observational errors.

Walker: The values should fall on the theoretical straight line in your diagram, of course. I think that would be very crucial for your argument.

O'Dell: Yes. In the case of some of these very strong continuum objects for which the continuum is 10 times too strong, the argument is very safe; however, in the case of NGC 7000, for which the continuum accords with the predicted amount using the excess Hβ to define light scattered within the nebula becomes very dangerous. That is why I haven't tried to interpret most of these nebulae but have limited myself to the ones that did have a strong continuum. They have a strong continuum because of the low dilution factors, and accurate values can be derived for these parameters. The other 11 nebulae were not discussed in detail because they do not have strong continua, and because I did not get enough observations to make any valid discussion.

Donn: Is there any evidence that the CNO lines in the outer regions of the Orion nebula are weaker in the spectrum than in the center? Another point related to this is that the study of the radial volocity indicated a high degree of turbulence in the Orion nebula. What about this material over extensive regions of the nebula? Would this be an important factor in your argument?

O'Dell: It would if the turbulence had a scale the size of the nebula. But the turbulence rather has a scale the size of seconds of arc; that is, 10 to 20 seconds of arc rather than 5 to 10 minutes of arc. In answer to your first question, I don't know about the CNO lines.

Wickramasinghe: I would like to point out that you have to be a little careful in the radiation pressure arguments. Very small particles would not necessarily be pushed out. It depends upon the index of refraction.

O'Dell: This I omitted because of a lack of time. We have investigated the Mie theory scattering for particles. What we've done is to try to fit the Cygnus law by using the wavelength dependence of the index of refraction in the most accurate manner possible with programing, and we used only the wavelength-dependent Q that is relevant to radiation pressure.

Greenberg: Certainly at 30 000° K to 50 000° K, for example, the as the ultraviolet (these are the dominant ones in these cases I believe), we have found that the small particles are pushed out more than the big ones as long as the stellar temperatures are high.

O'Dell: What is high and low?

Greenberg: Certainly at 30 000° K to 50 000° K, for example, the small grains will be pushed out.

O'Dell: But that is what we are talking about in the H II regions.

Voice: Are you thinking of ices?

Greenberg: Yes. I have a question: what size scale do you use to say whether or not the radiation pressure is effective in the cases you have given here? For example, what is the size scale that you have used for the inner portion of Orion?

O'Dell: The radius, the apparent radius.

Greenberg: What is that in terms of parsecs? You need a time scale and a distance scale.

O'Dell: I derived the distance for each of these nebulae independently, except for Orion where I adopted 430 parsecs.

Greenberg: What did you call the inside of Orion?

O'Dell: I called that the innermost 4 arc minutes.

Greenberg: How much is that in parsecs?

O'Dell: That is 1/2 parsec, or more exactly 4/7 of a parsec. Orion is special because it has a much lower dilution factor, that is, the material is much more concentrated than is typical for H II regions.

Nandy: What bearing does your finding have on the rate of star formation? This is a very good related subject.

O'Dell: I am not trying to speculate in these directions, except for the fact that if star formation is accelerated by an increase in the optical depth in the continuum produced by grain growth, then perhaps NGC 6514 and the outer parts of Orion show that the grain growth can occur on a short time scale and that dust would tend to accelerate the mechanism.

Nandy: Could we say that the rate of star formation would be different in different regions?

O'Dell: You could say that.

Wickramasinghe: I think some theoretical work has been done by W. Fowler and E. Hoyle on star formation and its relation to grain opacity. They came to the conclusion that the opacity of the grains played a very crucial role in determining whether or not you get certain types of contraction processes. Also, they concluded that the nature of the dust plays an important role in determining the luminosity function.

O'Dell: Thank you. All that I can say is that the dust would probably accelerate stellar contraction.

Hall: Will you say how far out the outer regions are that you are talking about?

O'Dell: In Orion? I think 18.3 arc minutes is generally considered the outermost region.

Hall: Are there any polarization measurements?

O'Dell: No. The regions of overlap, actually my regions two and three, were the regions that had a very strong continuum.

Field: Concerning your calculations of the atomic continuum to which, I believe, Dr. Walker referred: I am not sure I understand your answer to that. Did you account for the 2-photon emission?

O'Dell: Yes. Essentially the atomic continuum that I considered was the free-bound, the free-free, and the 2-photon, from 2s to 1s, emission.

Field: Doesn't the 2-photon emission depend upon the degree of Lyman α trapping, because Lyman α can populate the 2s level via 2s–2p collisional transitions?

O'Dell: Only in the case of extremely large optical depths for Lyman α.

Field: That's true.

O'Dell: I would rather assume that the grains never let the penetration depth get this large. In other words the Lyman alpha radiation would be destroyed before 10^6 scatterings would occur.

Field: Yes, but unfortunately you can't use the presence of the grains in this argument, because, if indeed the continuum is due to the 2-photon process, there would be no grains at all.

O'Dell: The color of the continuum is not consistent in low density regions. Sometimes the extra continuum is red while the 2-photon component is extremely blue.

Field: Another question concerns the general calculation of radiation pressure. I didn't understand whether in fact the grains did come to a terminal velocity or not in the times available.

O'Dell: All have achieved a terminal velocity.

Field: I see. If that is true, and they have reached terminal velocity, then I think your statement that the small grains would be pushed out faster may not be correct.

O'Dell: That is right, if you let the process of grain ejection run long enough.

Field: If you let it run long enough, the terminal velocity will be that of the larger grains because the extinction efficiency is greater. The point is that the drag force is proportional to the area and the radiation pressure is proportional to the area times the efficiency. For the small grains the efficiency would be small; therefore, the velocity of the small grains would be smaller than that of the large ones.

O'Dell: That is certainly true.

Field: I have one more question. In your calculation of the heating of the grains you didn't go into details. Did you account for the fact that beyond the dissociation limit of water the absorptivity of the particle is going to go up very drastically and therefore, presumably, the particle would heat up more effectively? What did you assume about the absorptivity?

O'Dell: I assumed that it was quite high, essentially 1. I used the value obtained from simple Mie scattering, the Mie absorption in this case. I didn't consider the effects of bands here.

Donn: You now have this grain in a high energy medium with a temperature of the order of a few thousand degrees in the Orion nebulae. The density that you get is on the order of 1000 or 10 000

electrons/cm^3. Now what contribution does this provide to the energy of the particle?

O'Dell: I computed the energy input assuming that for every electron collision the electron gave up the total amount of its kinetic energy. This is small compared with the other two mechanisms of energy input.

Donn: What about particle collisions?

Greenberg: They are negligible.

A Unified Model of Interstellar Extinction and Polarization[1]

J. MAYO GREENBERG AND G. SHAH
Rensselaer Polytechnic Institute
Troy, New York

THE MOST COMPLETELY OBSERVED CHARACTERISTICS OF INTERSTELLAR GRAINS are their ability to dim and polarize the light of distant stars in our own galaxy. The principal limitation in previous theoretical models of interstellar dust clouds has been the fact that the extinction and polarization have been calculated for different particles, the connection between these types of particles being semiquantitative at best.

A knowledge of the electromagnetic scattering properties of the various proposed grains is a fundamental ingredient of any theory of extinction and polarization. All the types of grains which have been suggested, except those of reference 1, scatter electromagnetic radiation by a classical process, i.e., a process which is characterized by a classical application of Maxwell's equations and for which the particles are defined by a size, shape, and index of refraction. In spite of the fact that the methods of application of the classical theory are completely understood, numerical results for the particular range of application which appears to be needed in the interstellar dust problem have been somewhat limited.

Most of the previous calculations of extinction have been performed on spherical particles of various types: dielectric (dirty ice), metallic, graphite, and core-mantle (graphite plus dirty ice or metal plus dirty ice). Regardless of whether one tries to fit the observed extinction curves with a single size of particle or a distribution of sizes, one arrives at a characteristic size depending on the particular optical properties chosen for the grains. In all cases the particle dimension is such that incomplete numerical (analytical or experimental) results were available for the extinction cross sections of arbitrarily oriented nonspherical particles of the appropriate dimension. For example, the only really quantitative

[1] The contents of this paper were published previously in the Astrophys. J. (pub. by the Univ. of Chicago Press), vol. 145, 1966, p. 63.

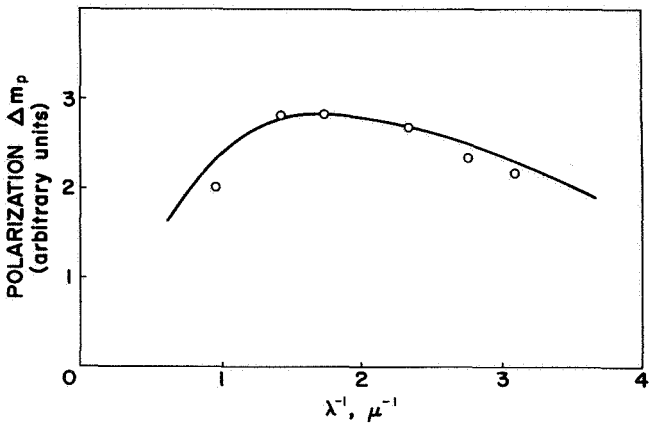

FIGURE 1.—Observed percentage polarization (each point is average for eight stars) as a function of inverse wavelength. (See ref. 3.) Solid curve is calculated for perfectly oriented dielectric (index of refraction = 1.70) cylinders with a distribution of radii according to an Oort-van de Hulst size distribution which, for spheres, reproduces a standard extinction curve.

calculations of the wavelength dependence of polarization could be made for perfectly alined circular cylinders. By choosing a distribution of radii for dielectric cylinders which is the same as that for the spheres which give a good representation of the extinction, it was indeed possible to achieve a good fit to the observed wavelength dependence of polarization. (See ref. 2 and figs. 1 and 2.) Semiquantitative calculations have also been made on the polarization—its amount and wavelength dependence—produced by dielectric spheroidal particles. The results are given in reference 4. However, in no case has it been possible to

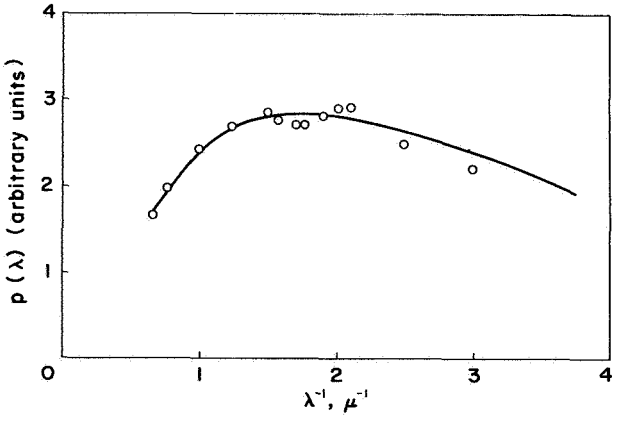

FIGURE 2.—Comparison between theoretical wavelength dependence of polarization produced by a distribution of sizes of cylinders (solid curve) with that produced by a single size cylinder of radius $a = 0.20\ \mu$ (open circles).

perform a simultaneous and equally quantitative calculation of extinction and polarization.

A complete computing scheme, equivalent to the Mie theory for spheres, for the scattering by arbitrarily oriented infinite cylinders is given in references 5 and 6. These new schemes have made it possible to calculate simultaneously the extinction and polarization by realistically oriented particles. The justification for the infinite cylinder model lies in the fact that the extinction and polarization by infinite cylinders differ quantitatively but not qualitatively from the extinction and polarization produced by finite elongated particles. (See ref. 4.) Furthermore, if the grains are indeed needlelike in structure or perhaps consist of loose agglomerations of needles, this representation would be fully realistic.

In this paper we consider particles whose index of refraction m is 1.33, and the application, therefore, is most reliably made to the wavelength region where icelike materials are nonabsorbing; namely, $1 \lesssim \lambda^{-1} \lesssim 3\ \mu^{-1}$. The orientation is treated from the point of view of the Davis-Greenstein mechanism (ref. 7).

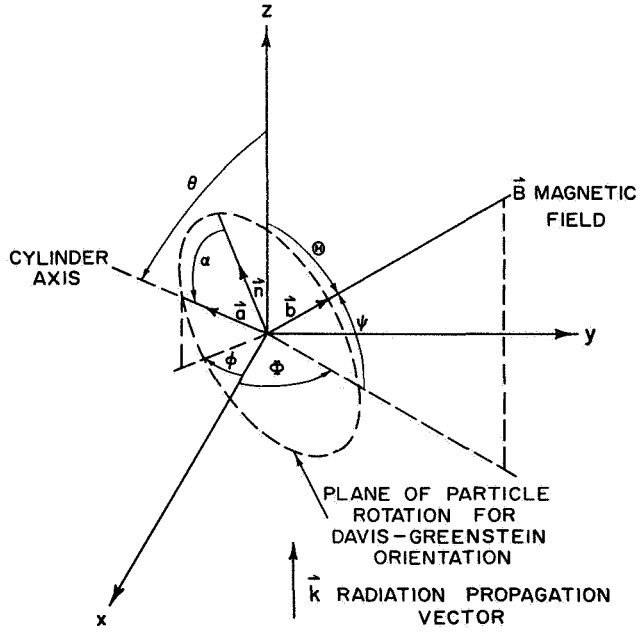

FIGURE 3.—Geometrical configuration for axially symmetric elongated particle spinning about its short axis which is alined with the magnetic field direction. Radiation is propagated along z-direction.

GENERAL FORMULATION FOR EXTINCTION AND POLARIZATION BY AXIALLY SYMMETRIC PARTICLES

The extinction and polarization are determined by the optical depths τ_x and τ_y corresponding to radiation polarized along appropriate rotated x- and y-directions and propagated along the z-direction. (See fig. 3.) For axially symmetric particles the most general form for these optical depths is given by (see ref. 2)

$$\tau_{x,y}=\int_0^L dz \int_0^\infty da \int_0^\infty de \int_0^\pi \sin\theta\, d\theta \int_0^{2\pi} d\phi\, n(z, a, e) \times f(z, \theta, \phi, a, e) C_{x,y}(\theta, \phi, a, e, \lambda) \quad (1)$$

where

L	total path length
a	a characteristic linear dimension
e	ratio of length to width
λ	wavelength of radiation
$C_x(\theta, \phi, a, e, \lambda)$	extinction cross section
$C_y(\theta, \phi, a, e, \lambda)$	extinction cross section
$n(z, a, e)$	size distribution function
$f(z, \theta, \phi, a, e)$	angular distribution function

The extinction is related approximately to the optical depths by

$$\Delta m = 1.086 \frac{\tau_x + \tau_y}{2} \quad (2)$$

where the approximation is based on the fact that, in practice, the ratio of polarization to extinction is considerably less than 1.

The polarization is given exactly by

$$\Delta m_p = 1.086\ (\tau_x - \tau_y)_{\max} \quad (3)$$

where the subscript "max" denotes that τ_x represents the maximum optical depth and τ_y, the minimum optical depth as the plane of the analyzer is rotated.

Although it is now within the realm of possibility to consider the fully general form of equation (1), it is probably more instructive, and certainly simpler to visualize, if we consider its implications in gradually increasing complexity.

Throughout this paper, unless otherwise stated, the integrations over z, a, and e are ignored. This reduces equation (1) to the form

$$\tau_{x,y}=\int_0^{\pi}\int_0^{2\pi} \mathrm{d}\phi \sin\theta \,\mathrm{d}\theta f(\theta,\phi)C_{x,y}(\theta,\phi) \tag{4}$$

Insofar as infinite cylinders are concerned, it is only the elongation factor which needs to be suppressed. The simplest orientation is that in which all particles are lined up in the same direction. To denote such perfect alinement the letters P.F. (picket fence) are used and all the particles are assumed to point along the x-direction:

$$f_{\text{P.F.}}(z,\theta,\phi,a,e)=\delta(\cos\theta)\ \delta(\phi)$$

where δ is the Dirac delta function.

For perfect Davis-Greenstein orientation the particles all spin with their short axes along the direction of the magnetic field. In figure 3, $\mathbf{B}$ is defined by the angles Θ and Φ with respect to the z- and x-axes. If $\mathbf{b}$ is a unit vector along $\mathbf{B}$ and $\mathbf{a}$ is a unit vector along the particle symmetry axis, then the plane of rotation of the axis is defined by $\mathbf{a}\cdot\mathbf{b}=0$. If the symmetry axis makes the angles Θ and ϕ with respect to the xyz frame and the angle a with respect to some fixed direction $\mathbf{n}$ in its plane of rotation, we may write

$$\mathbf{b}\cdot\mathbf{n}=0, \qquad \mathbf{a}\cdot\mathbf{n}=\cos a, \qquad \mathbf{n}\cdot\hat{\mathbf{z}}=\sin\Theta,$$

where $\hat{\mathbf{z}}$ is a unit vector along the z-axis.

The appropriate vector relations yield

$$\cos\theta=\sin\Theta\cos a \tag{5}$$

$$\cos\phi=\frac{\cos\Theta\cos\Phi\cos a-\sin\Phi\sin a}{\cos\Theta\sin\Phi\cos a+\cos\Phi\sin a}. \tag{6}$$

For any axially symmetric particle, the cross sections for arbitrary orientations with respect to the direction and state of polarization of the incident radiation can be derived from two basic cross sections, $C_E(\Theta)$ and $C_H(\Theta)$, where Θ is the angle between the incident radiation and the symmetry axis. The cross section C_E is that for which the electric vector of the radiation is in the plane containing the direction of propagation and the symmetry axis. The cross section C_H is similarly defined for the magnetic vector of the radiation. For the configuration in figure 3, with incident unpolarized radiations, it can be shown that

$$C_x=C_E(\theta)\cos^2\phi+C_H(\theta)\sin^2\phi \tag{7}$$

$$C_y=C_E(\theta)\sin^2\phi+C_H(\theta)\cos^2\phi \tag{8}$$

The extinction and polarization are derived from the sum and difference of these two quantities given by

$$C_x + C_y = C_E(\theta) + C_H(\theta) \tag{9}$$

$$C_x - C_y = [C_E(\theta) - C_H(\theta)] \cos 2\phi \tag{10}$$

Substitution of equations (9) and (10) into equation (4) and use of the appropriate forms for the angular distribution function f yields

Perfect alinement

$$\frac{2}{1.086} (\Delta m)_{\text{P.F.}} = C_E\left(\frac{\pi}{2}\right) + C_H\left(\frac{\pi}{2}\right) \tag{11}$$

$$\frac{1}{1.086} (\Delta m_p)_{\text{P.F.}} = C_E\left(\frac{\pi}{2}\right) - C_H\left(\frac{\pi}{2}\right) \tag{12}$$

Perfect Davis-Greenstein alinement

$$\frac{2}{1.086} (\Delta m)_{\text{D.G.}} = \frac{1}{\pi}\int_0^{\pi} d\alpha [C_E(\theta) + C_H(\theta)] \tag{13}$$

$$\frac{1}{1.086} (\Delta m_p)_{\text{D.G.}} = \left\{ \frac{1}{\pi}\int_0^{\pi} d\alpha [C_E(\theta) - C_H(\theta)] \cos 2\phi \right\}_{\max} \tag{14}$$

where θ and ϕ are defined by equations (5) and (6).

The maximum value of the integrand in equation (14) is, for symmetry reasons, obviously obtained for $\Phi = \pi/2$ ($\mathbf{B}$ in the yz-plane in fig. 3). Under more general conditions, such as, e.g., would hold when the radiation passes through several clouds in each of which the orientation is different, it is convenient to define for each cloud the quantities

$$C = \frac{1}{\pi}\int_0^{\pi} d\alpha [C_E(\theta) - C_H(\theta)] \cos 2\phi, \tag{15}$$

$$S = \frac{1}{\pi}\int_0^{\pi} d\alpha [C_E(\theta) - C_H(\theta)] \sin 2\phi, \tag{16}$$

in terms of which the polarization due to a single cloud would be given by

$$(1.086)^{-1} (\Delta m_p)_{\text{D.G.}} = (C^2 + S^2)^{1/2} \tag{17}$$

and the polarization due to several clouds is determined by summing the quantities over all clouds involved.

EXTINCTION CROSS SECTIONS FOR SMALL SPHEROIDS AND FOR INFINITE CYLINDERS

For very small particles satisfying the condition for validity of the Rayleigh approximation $[(2\pi a)/\lambda \ll 1]$ the direction of the electric field of the incident radiation relative to the particle completely defines the cross section independent of the direction of the radiation. For an axially symmetric particle $C_{||}$ and $C_{\perp}$ are defined as the extinction cross sections when the electric vector is parallel to the symmetry axis and perpendicular to the symmetry axis, respectively. For spheroids, the formulas for $C_{||}$ and $C_{\perp}$ may readily be obtained, for example, from reference 8.

For arbitrary orientation,

$$C_E(\theta) = C_{||} \sin^2\theta + C_{\perp} \cos^2 \theta \tag{18}$$

$$C_H(\theta) = C_{\perp} \tag{19}$$

$$C_E + C_H = (C_{||} + C_{\perp}) + (C_{\perp} - C_{||}) \cos^2 \theta \tag{20}$$

$$C_E - C_H = (C_{||} - C_{\perp}) \sin^2 \theta \tag{21}$$

The basic cross sections for infinite cylinders are obtained from equations analogous to, but somewhat more complicated than, the ones used for computing cross sections of spheres. The pertinent equations used in computing the cylinder cross sections are summarized in the following equations. (Note that these cross sections are normalized to be cross sections per unit length.)

$$C_E(\theta) = \frac{4}{k} Re \left[b_0^E(\theta) + 2 \sum_{n=1}^{\infty} b_n^E(\theta) \right] \tag{22}$$

$$C_H(\theta) = \frac{4}{k} Re \left[a_0^H(\theta) + 2 \sum_{n=1}^{\infty} a_n^H(\theta) \right] \tag{23}$$

where

$$b_n^E(\theta) = R_n \frac{A_n(\mu) B_n(\epsilon) - n^2 S^2 \cos^2 \theta}{A_n(\epsilon) A_n(\mu) - n^2 S^2 \cos^2 \theta}$$

$$a_n^H(\theta) = R_n \frac{A_n(\epsilon) B_n(\mu) - n^2 S^2 \cos^2 \theta}{A_n(\epsilon) A_n(\mu) - n^2 S^2 \cos^2 \theta}$$

$$R_n = J_n(la)/H_n(la)$$

$$A_n(\xi) = \frac{H_n'(la)}{laH_n(la)} - \xi \frac{J_n'(l_1 a)}{l_1 a J_n(l_1 a)}$$

$$B_n(\xi) = \frac{J_n'(la)}{laJ_n(la)} - \xi \frac{J_n'(l_1 a)}{l_1 a J_n(l_1 a)}$$

271-992 O-67—11

S	$(la)^{-2}-(l_1a)^{-2}$
l	$k \sin \theta$
l_1	$k\sqrt{(m^2-\cos^2\theta}$
a	cylinder radius
J_n	cylindrical Bessel function of the first kind
H_n	cylindrical Hankel function of the second kind
ϵ	dielectric permeability
μ	magnetic permeability

In the present calculations, restricted to nonabsorbing, nonmagnetic particles, $\epsilon=m^2$ and $\mu=1$. Some sample results of the computations of equations (22) and (23) are presented in figures 4 to 6 as extinction efficiencies (i.e., cross sections per unit area; $Q=C/2a$). Figure 4 contains the well-known curves for the variation of extinction efficiency with wavelength for an infinite cylinder whose axis is perpendicular to the direction of the incident radiation. Figures 5 and 6 demonstrate the effect of obliqueness on the extinction efficiencies over a range of selected values of ka. With regard to subsequent application to the problem of interstellar extinction and polarization, the most obviously interesting results are: (1) the average polarizing ability of cylinders, as exhibited by the average of Q_E-Q_H with angle θ, undergoes the greatest reduction relative to its maximum value at $\theta=\pi/2$ for small values of ka (long wavelength); and (2) the average value of Q_E+Q_H, relative to its value at $\theta=\pi/2$, tends to decrease more or less uniformly with increasing ka.

EXTINCTION AND POLARIZATION RESULTS

The various polarization and extinction measures for the very small Rayleigh particles can be analytically obtained. Substituting equations (20) and (21) into equations (11) and (14), performing the required integration, and denoting the appropriate quantities by the superscript R (for Rayleigh), yield

Perfect alinement

$$\left|\frac{2}{1.086}\,(\Delta m)^R_{\text{P.F.}}\right| = C_{\|}+C_{\perp}, \tag{24}$$

$$\left|\frac{1}{1.086}\,(\Delta m)^R_{\text{P.F.}}\right| = C_{\|}-C_{\perp}, \tag{25}$$

$$\left(\frac{\Delta m_p}{\Delta m}\right)^R_{\text{P.F.}} = 2\,\frac{C_{\|}-C_{\perp}}{C_{\|}+C_{\perp}}; \tag{26}$$

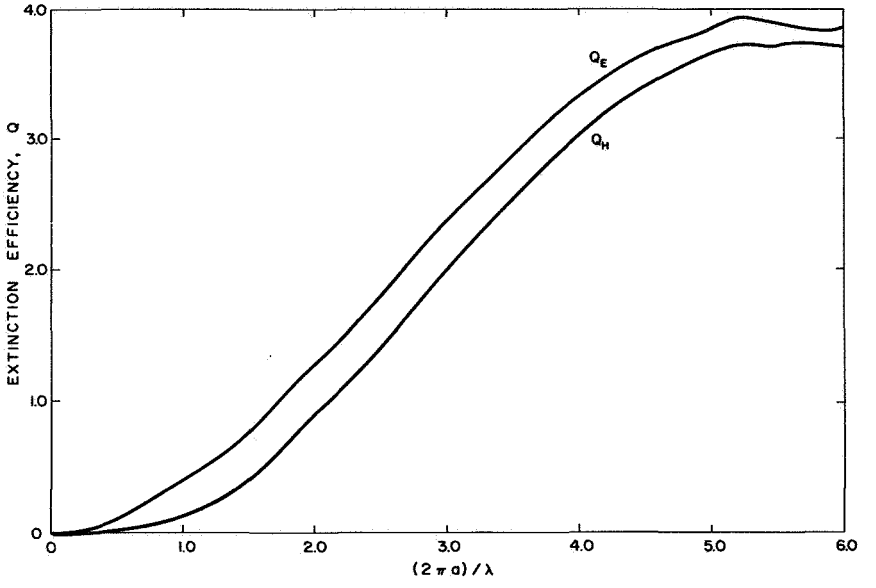

FIGURE 4.—Extinction efficiencies as a function of $ka = 2\pi a/\lambda$ for infinite dielectric ($m = 1.33$) circular cylinder whose axis is perpendicular to direction of propagation of radiation. Subscripts E and H refer, respectively, to the cases in which E and H are parallel to the cylinder axis.

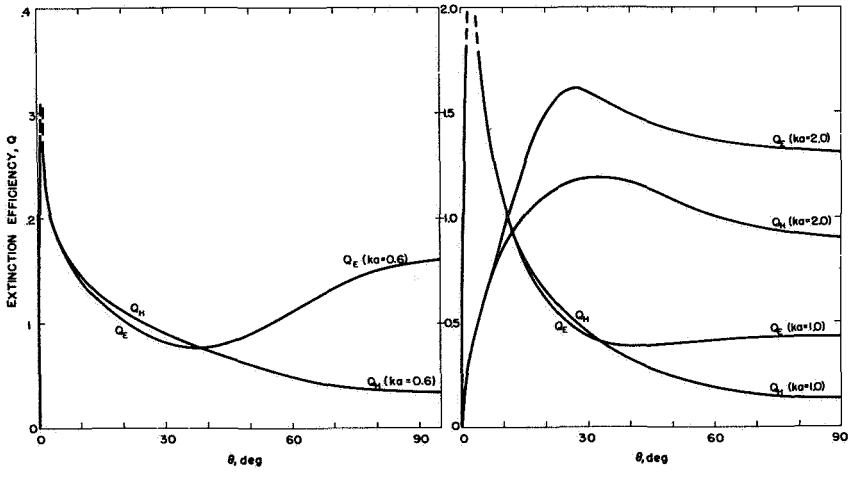

FIGURE 5.—Extinction efficiencies as a function of orientation angle for infinite dielectric ($m = 1.33$) circular cylinders. Normal incidence is given by $\theta = 90°$. The peak value of Q for $ka = 0.6$ is 3.33, and for $ka = 1.0$, it is 3.1. Note the crossing of the curves for Q_E and Q_H (and consequent polarization reversal) as the obliqueness increases (θ decreasing).

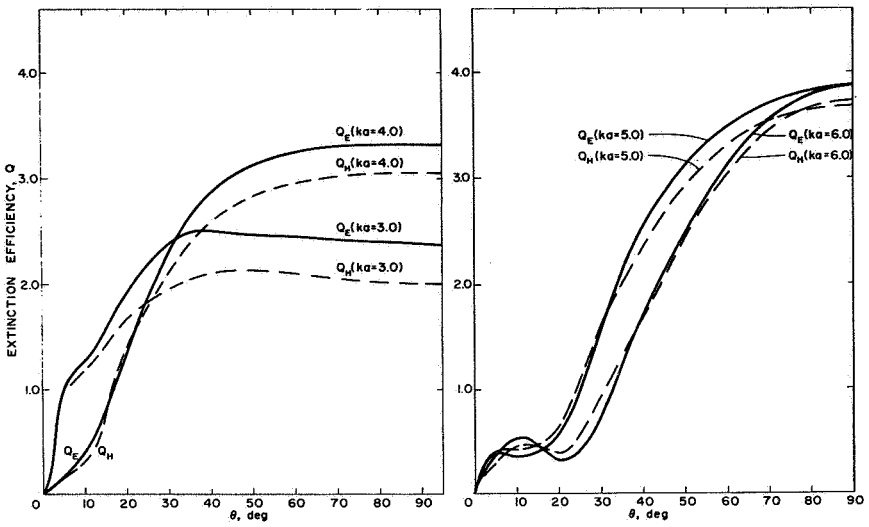

FIGURE 6.—Extinction efficiencies for infinite dielectric ($m=1.33$) circular cylinders as a function of orientation angle. Normal incidence is given by $\theta=90°$. Note the several crossings of the curves for Q_E and Q_H (representing polarization reversals).

Perfect Davis-Greenstein alinement

$$\frac{2}{1.086}(\Delta m)^R_{\text{D.G.}} = C_{||}(1-1/2\cos^2\psi) + C_\perp(1+1/2\cos^2\psi), \quad (27)$$

$$\frac{1}{.086}(\Delta m_p)^R_{\text{D.G.}} = 1/2(C_{||}-C_\perp)\cos^2\psi, \quad (28)$$

$$\left(\frac{\Delta m_p}{\Delta m}\right)^R_{\text{D.G.}} = \frac{(C_{||}-C_\perp)\cos^2\psi}{C_{||}[1-1/2\cos^2\psi]+C_\perp[1+1/2\cos^2\psi]}. \quad (29)$$

The analogous results for infinite cylinders whose index of refraction is $m=1.33$ are presented in figures 7 and 8. These curves (except for the uppermost one in fig. 8) are obtained by numerically evaluating the cross sections defined in equations (22) and (23), substituting these values into equations (13) and (14), respectively, and finally evaluating these expressions by numerical integrations. The uppermost curve in figure 8 is the wavelength dependence of polarization if the cylinders are in picket-fence alinement and is obtained by taking the difference between the extinction efficiencies Q_E and Q_H as given in figure 4.

It is readily seen by comparing the results of figures 7 and 8 with the observed extinction and polarization curves that, even for a single size particle (all cylinders of the same radius), there is a good resemblance between theory and observation. The scale to be chosen corresponds

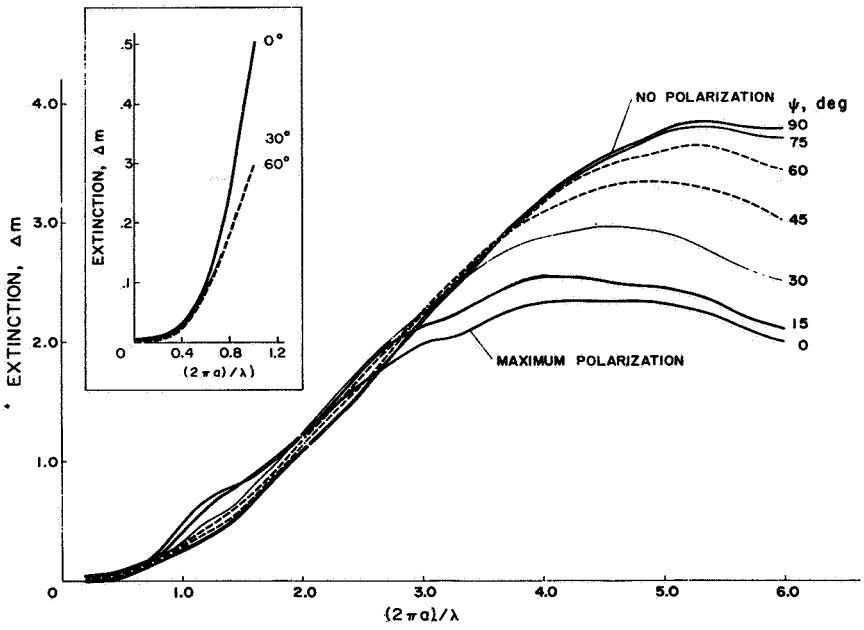

FIGURE 7.—Variation with $ka=(2\pi a)/\lambda$ of extinction produced by infinite dielectric cylinders spinning in planes which make various angles ψ with respect to direction of incident radiation. The angle $\psi=0°$ corresponds to the case in which the spinning plane contains the propagation vector and thus gives rise to the maximum degree of polarization.

roughly to associating an inverse wavelength, $\lambda^{-1}=1$, with a value of ka in the range $1.1 \leqslant ka \leqslant 1.25$. In view of the fact that the calculations are for a pure real index of refraction as well as for a single size of particle, only qualitative inferences can be made particularly in the infrared and ultraviolet where dielectric particles may be expected to be absorbing.

In the range of ka (or λ^{-1}) corresponding to high polarization ($2 \lesssim ka \lesssim 3$ in fig. 8) it is interesting to note that all the extinction curves in figure 7 are similar in magnitude and that, as a consequence, the ratio of polarization to extinction varies almost entirely according to the amount of polarization. The oscillations in the polarization curves occur because only one size of particle is considered. These oscillations will certainly disappear when a distribution of sizes is considered.

It is instructive at this point to compare the results for small particles with those for cylinders insofar as the amount of polarization depends on the kind of orientation. According to equations (26) and (29), one would predict that the ratio of polarization to extinction would drop by a factor of 1/2 (approximately—assuming that the ratio $C_{\parallel}/C_{\perp}$ is not much larger than 1) in going from picket-fence alinement to perfect Davis-Greenstein orientation (B perpendicular to line of sight, $\psi=0°$);

however, as one sees in figure 8, the reduction is only by a factor of about 3/4. A previous estimate of the reduction factor as being about 0.6 was made in reference 4 for spheroids of elongation 2.

According to figures 7 and 8, the obvious consequences of decreasing the angle between the magnetic field and the line of sight (increasing ψ) are: (1) reducing the amount of polarization; (2) broadening of the wavelength dependence of polarization; and (3) increasing extinction in the ultraviolet relative to the visible (assuming a reasonable scale of λ^{-1} relative to ka). Item (3) has already been predicted in references 9 and 10 on the basis of various approximations. The advantage of the present calculation is that one may hope to correlate not only the amount but also the wavelength dependence of polarization with variations of the wavelength dependence of extinction, particularly in the ultraviolet.

The effect of reducing the amount of polarization (item (1)) may be examined and compared with the equivalent effect for small particles by considering equation (28) (assuming as before that the denominator of eq. (29) varies only slightly with ψ). The Rayleigh approximation predicts that, as the magnetic field makes an angle $\pi/2-\psi$ with respect to the line of sight, the polarization is reduced by the factor $\cos^2\psi$.

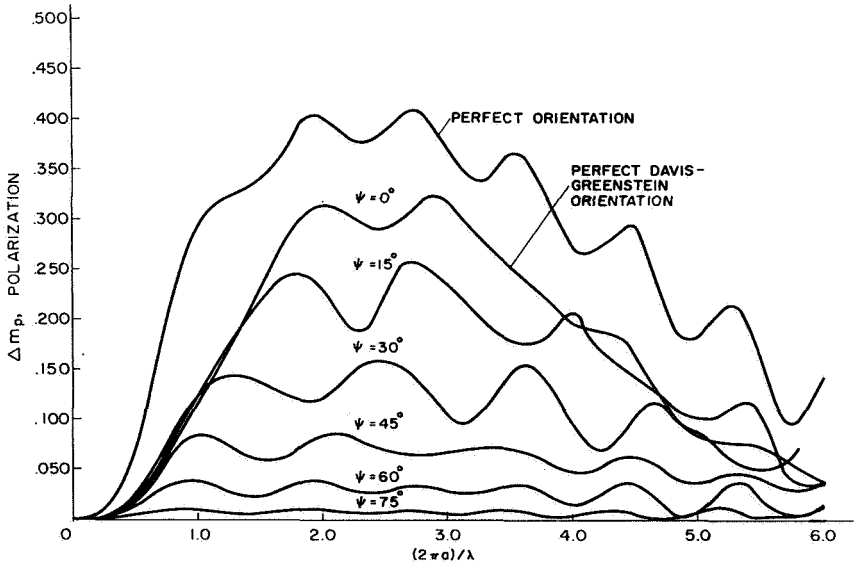

FIGURE 8.—The uppermost curve is the variation of polarization with $ka=(2\pi a)/\lambda$ for perfectly alined infinite dielectric cylinders (Q_E-Q_H in figure 4). The other curves give the variation of the wavelength dependence of polarization produced by cylinders spinning in planes which make various angles ψ with respect to the direction of incident radiation. The case $\psi=0°$ corresponds to the case in which the spinning plane contains the propagation vector. The angle $90°-\psi$ is the angle between the magnetic field and the direction of light propagation.

TABLE I.—*Dependence of Amount of Polarization on Magnetic-Field Direction*

ψ, deg	$\cos^2\psi$	$[(\Delta m_p)_\psi/(\Delta m_p)_0]/\cos^2\psi$ [a]	[a,b] $(\Delta m_p)_\psi/(\Delta m)$
0	1	1	0.16
15	0.93	0.9	.13
30	.75	.7	.08
45	.5	.5	.04
60	.25	.5	.....

[a] Values of $(\Delta m_p)_\psi$ and $(\Delta m_p)_0$ are peak values.

[b] The value of Δm is chosen at $ka=3$ which is probably an overestimate. This means that the ratios in this column are perhaps conservatively estimated.

The data of table I show that, as the magnetic field angle ψ increases, the polarization reduction factor for the cylinders is more drastic than that for Rayleigh particles. This is shown in the third column by the fact that the ratio of reduction factors is always less than 1. On the other hand, the ratio of polarization to extinction as given in the fourth column is greater than the maximum observed value of $(\Delta m_p/\Delta m)_{\max} \equiv 0.065$ (ref. 11) for values of ψ even beyond $\psi=30°$. In figure 9 is shown the ratio of polarization to extinction for the oriented cylinders as a function of size (ka). Comparison of these curves with the maximum observed value of this ratio indicates that a size distribution of such

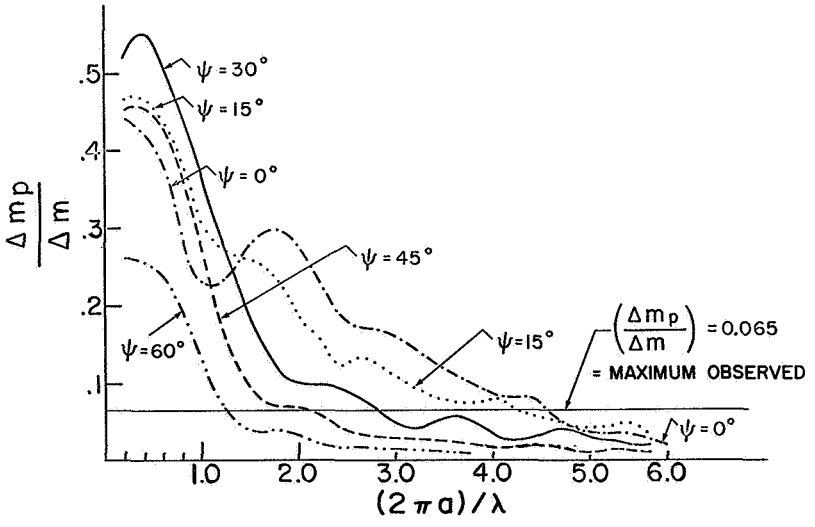

FIGURE 9.—Polarizing capabilities of Davis-Greenstein-oriented cylinders as a function of $(2\pi a)/\lambda$. The horizontal line is the maximum observed polarizing capability of interstellar grains.

grains would be able to produce sufficient polarization. Furthermore, the calculated ratio of polarization to extinction is apparently sufficiently large at the smaller angles that one may well tolerate relatively incomplete orientation (as given by letting the B direction be contained within some cone) and still achieve a rather high degree of polarization. Because more detailed calculations of this averaging are in process, further discussion of this point is deferred

CONCLUDING REMARKS

On the basis of the limited theoretical model of a cloud of interstellar grains consisting of elongated particles (infinite dielectric cylinders) of a single size, some hitherto unexpected correlations between variations in the wavelength dependence of polarization and variations in the wavelength dependence of extinction have been demonstrated. This investigation, although only preliminary, represents the first completely self-consistent theoretical approach to two of the manifestations of interstellar grains—extinction and polarization.

Calculations are either in progress or being planned that will take into account wavelength dependence of index of refraction (including absorption), distribution of particle sizes, variations in particle size dis-

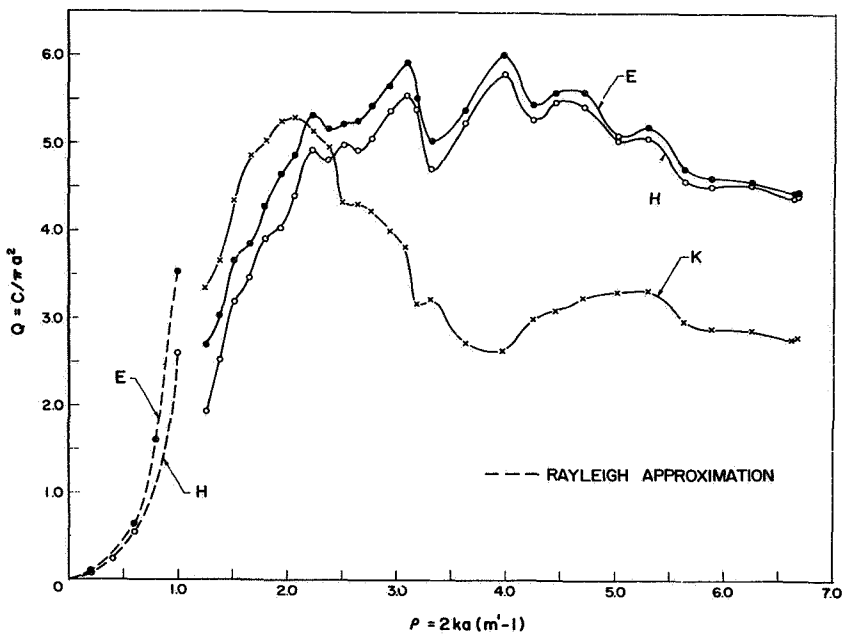

FIGURE 10.—Extinction efficiencies for three orthogonal orientations of prolate spheroids. $b/a = 2.0$; $m = 1.33 - 0.05i$.

tribution, and incomplete Davis-Greenstein orientation. It is within the realm of possibility to uncouple the extinction and polarization through different clouds along the line of sight via the effect of variations of polarization angle with wavelength. (See refs. 12 and 13.)

Of the many questions which need to be considered, there is one which does not exhibit itself in the single size model but which is quite important when one has a distribution of sizes. This question is the distribution of elongations with particle size. Basically, the answer to this question lies in the physics and chemistry of grain growth. Phenomenologically it exhibits itself in determining the wavelength dependence of

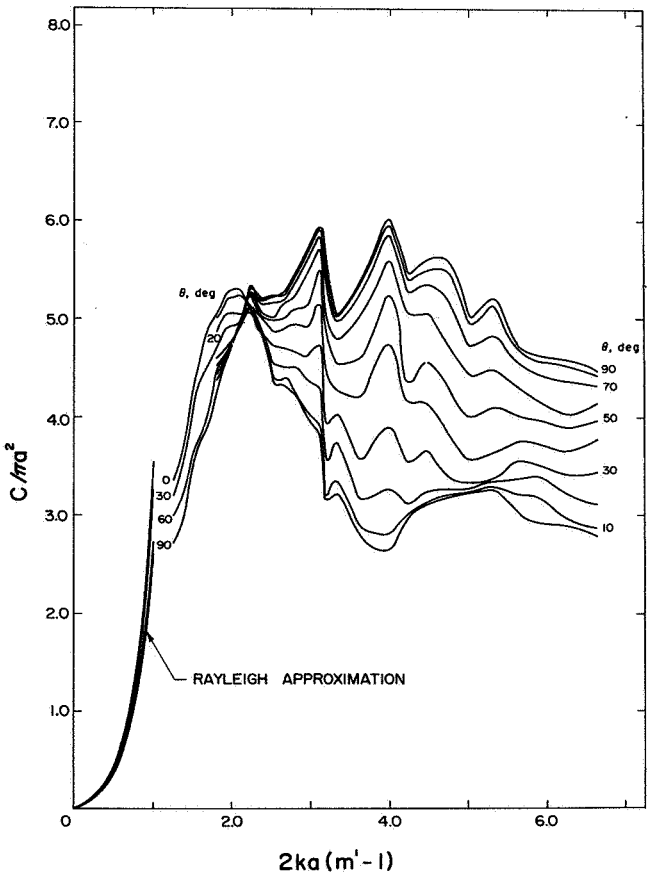

FIGURE 11.—Extinction efficiencies for prolate spheroids whose symmetry axes are tilted in the plane containing electric and propagation vectors of incident radiation.

Tilt angle of 90° corresponds to case *E* of figure 10.
Tilt angle of 0° corresponds to case *K* of figure 10.
$b/a=2.0$; $m=1.33-0.05\,i$; *E* plane.

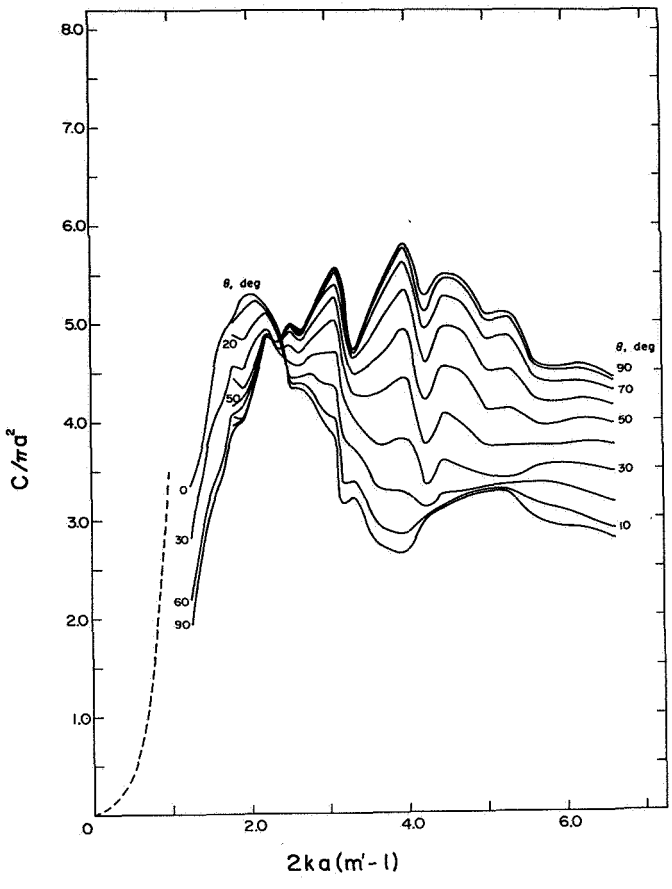

FIGURE 12.—Extinction efficiencies for prolate spheroids whose symmetry axes are tilted in the plane containing magnetic and propagation vectors of incident radiation.
Tilt angle of 90° corresponds to case *H* of figure 10.
Tilt angle of 0° corresponds to case *K* of figure 10.
$b/a = 2.0$; $m = 1.33 - 0.05i$; *H* plane.

extinction and polarization. Initially two extremes will be considered; namely, that in which all particles either have the same elongation or the same length.

Finally, with the improved microwave scattering techniques now available (ref. 14) the finite particle model will be subjected to detailed scrutiny in the near future. Figures 10 to 12 show some results already obtained for arbitrarily oriented prolate spheroids.

REFERENCES

1. PLATT, J.: On the Optical Properties of Interstellar Dust. Astrophys. J., vol. 123, 1956, p. 486.

2. GREENBERG, J. M.: Interstellar Grains. Ann. Rev. Astr. and Ap., vol. 1, 1963, p. 267.

3. GEHRELS, T.: Astron. J., vol. 65, 1960, p. 466.

4. GREENBERG, J. M.; LIND, A. C.; WANG, R. T.; and LIBELO, L. F.: The Polarization of Starlight by Oriented Non-Spherical Particles. Electromagnetic Scattering. Proceedings of ICES I (New York), Pergamon Press, 1963, p. 123.

5. LIND, A. C.; and GREENBERG, J. M.: Electromagnetic Scattering by Obliquely Oriented Cylinders. J. Appl. Phys., vol. 37, 1966, pp. 3195–3203.

6. GREENBERG, J. M.; LIND, A. C.; WANG, R. T.; and LIBELO, L. F.: Scattering by Nonspherical Particles. Proceedings of ICES II (Amherst, Mass.), 1965.

7. DAVIS, L., Jr.; and GREENSTEIN, J. L.: The Polarization of Starlight by Aligned Dust Grains. Astrophys. J., vol. 114, 1951, p. 206.

8. VAN DE HULST, H. C.: Light Scattering by Small Particles. John Wiley & Sons, Inc., 1957.

9. GREENBERG, J. M.; and MELTZER, A. S.: The Effect of Orientation of Non-Spherical Particles on Interstellar Extinction. Astrophys. J., vol. 132, 1960, p. 660.

10. WILSON, R.: The Relation Between Interstellar Extinction and Polarization. Roy. Astron. Soc., Monthly Notices, vol. 120, 1960, p. 51.

11. SCHMIDT, T.: Zur Analyse des Zusammenhangs zwischen interstellarer Polarisation und interstellarer Verfärbung. Zs. Astrophys., vol. 46, 1958, p. 145.

12. GEHRELS, T.; and SILVESTER, A. B.: Wavelength Dependence of Polarization V. Position Angles of Interstellar Polarization. Astron. J., vol. 70, 1965, p. 579.

13. TREANOR, P. J.: Wavelength Dependence of Interstellar Polarization. Astron. J., vol. 68, 1963, p. 185.

14. LIND, A. C.; WANG, R. T.; and GREENBERG, J. M.: Microwave Scattering by Non-Spherical Particles. Appl. Opt., vol. 4, 1965, p. 1555.

DISCUSSION

Wickramasinghe: Do those extinction curves go up at all in the far ultraviolet? Is there a point of inflection in the curve after which the slope increases? Are they concave upward?

Greenberg: For sufficiently small values of $(2\pi a)/\lambda$ they are concave upward.

Wickramasinghe: Is the abscissa λ^{-1}?

Greenberg: This abscissa is $(2\pi a)/\lambda$.

Wickramasinghe: Did you make the computations for a particular value of the radius in order to compare the result with the observed extinction curve?

Greenberg: You could say that we made computations for a particular radius and then let the wavelength vary, but since we used a constant index of refraction, it doesn't make any difference.

Wampler: Did I understand you correctly that, for small-diameter infinite cylinders, the direction of the polarization vector can change with the wavelength?

Greenberg: Yes, but only for orientations such that the particle axis is directed close to the direction of the radiation.

Wampler: I think the case for a conducting particle is different in that you would get different polarization with wavelength because of plasma oscillations in the particle.

Greenberg: It is true that a reverse polarization results if a particle is too large. If the particle is very small compared with the wavelength, the polarization is just as you would intuitively predict (except for certain orientations). If the particle is about the size of the wavelength or bigger, whether dielectric or metallic, then reversals of polarization occur. But at that point, in general, the polarization is very small; in fact, it is approaching zero. In the limit, since the wavelength is small compared with the size, the polarization is identically zero.

Wampler: Do you have a feeling about whether this would be observable if a normal Oort-van de Hulst size distribution is assumed?

Greenberg: In the case we have presented here, we have not reached the point of reversal in any of the particle sizes.

Nandy: Do you still believe that the longitudinal dependence of the extinction law is a test to discriminate whether the particles are dielectric or not?

Greenberg: If all other effects could be eliminated it would be a legitimate criterion. However, even that criterion would have to be quantitative. I would expect that the wavelength dependence of extinction by particles which are anisotropic in optical and shaped properties such as graphite would also exhibit variations in the wavelength dependence of extinction because of orientation. However, I think that these differences in the ultraviolet would not be as large for anisotropic as for dielectric particles. There may be significant but small, differences in the visible.

Wickramasinghe: In matching these experimental curves does one have to use a very special size in order to get the peak of the polarization curve to fit?

Greenberg: I use the Oort-van de Hulst size distribution.

Wickramasinghe: Yes, but you nevertheless have to choose a size parameter so that the peak comes in the right place.

Greenberg: Yes, but I don't think the peak is that well defined, because if I shift by 5 percent I get a small shift in the peak. But you are saying that the peak is sensitive to the size. I agree; but it is not as sensitive to the size parameter in a size distribution as it is to a single size. That's a very important point. For a single size, a shifting in size by 5 percent shifts the peak by 5 percent. However, for a size distribution, various particles in the size distribution give a different contribution. Therefore, even if we took a larger size distribution, the smaller particles would still give relatively larger contributions and the wavelength dependence would not be modified by the amount in which the parameter in the Oort-van de Hulst type of size distribution is changed.

Gehrels: Suppose for figure 8 you had assumed the Oort-van de Hulst distribution to peak at $2a=0.3$ instead of at $2a=0.6$. Have you tried this?

Greenberg: No.

Gehrels: You might have gotten a slightly better fit.

Greenberg: It wouldn't have shifted by a factor of 2, but it would have shifted the peak toward the shorter wavelength.

Gehrels: That is just where your fit is deficient.

Greenberg: That is possible. I can't say how much of a modification I would need.

Gehrels: Why did van de Hulst consider the ratio of polarization to extinction insufficient in the calculations?

Greenberg: The basis for doubting dielectric particles as sufficiently good polarizers was founded on insufficient knowledge of the dependence of polarizing ability on (1) particle elongation; (2) imperfect orientation, i.e., Davis-Greenstein spinning type (ref. 7) as a function of perfect full (picket-fence) alinement; and (3) incomplete orientation of the spin axis of the particles. Let me summarize here the pertinent results contained in reference 4.

Let C_E and C_H be cross sections for particles whose symmetry axis is perpendicular to the direction of propagation of the radiation and parallel to the electric and magnetic fields (E and H), respectively, of plane-polarized radiation. By $C_{E(\chi)}$ and $C_{H(\chi)}$ we denote the cross sections when the symmetry axis makes an angle χ with respect to the propagation direction.

With regard to elongation, in the range of particle sizes relative to wavelength characteristic of the visual spectrum, the average ratio (C_E/C_H) for prolate spheroids of elongation 2 and index of refraction $m=1.33-0.05i$ is the same as that for infinitely long cylinders with index of refraction $m=1.30$; namely, $(C_E/C_H)\approx 1.16$. Clearly, finite elongated particles may well be as effective as infinitely elongated particles in polarizing radiation.

In the matter of orientation, the ratio

$$R_{\text{D.G.}}=\frac{\int_0^{\pi}[C_E(\chi)-C_H(\chi)]\,d\chi}{\frac{1}{2}\int_0^{\pi}[C_E(\chi)+C_H(\chi)]\,d\chi}$$

is, for a single particle size, equal to the ratio of polarization to extinction $\Delta m_p/\Delta m$ for perfect spinning orientation. For picket-fence orientation, this ratio is

$$R_{\text{P.F.}}=\frac{C_E-C_H}{\frac{1}{2}(C_E+C_H)}$$

Averaging both of these quantities yields $R_{\text{P.F.}}\approx 0.15$ and $R_{\text{D.G.}}\approx 0.09$, a reduction by a factor of 0.6.

Concerning partial Davis-Greenstein orientation, if the angle between

the spin axis (normal to symmetry axis) and the direction of propagation is ψ, the ratio of polarization to extinction is reduced by the factor (approximate) cos 2ψ. If the spin axes are distributed within this angle, then the reduction is somewhat less. Noting that the maximum observed ratio of polarization to extinction is $\Delta m_p/\Delta m \cong 0.6$ and combining this with $R_{\text{D.G.}} \cong 0.09$, one finds an allowable half-angle $\psi \approx 20°$ to $30°$ for the cone containing the spin axes.

Wickramasinghe: One should really remember that the grains are spinning in cones. They are all alined about some direction, only to the extent of spinning in small cones about this direction.

Greenberg: I considered the worst possible case. If I put them within a cone, they are going to give a higher polarization than the case considered by us.

Wickramasinghe: But isn't it more realistic to take the case where the alinement has some sort of statistical effect? Then you would get out of one of the difficulties that van de Hulst was worrying about.

Greenberg: No, that is not what he was worried about; he was worried about getting the polarization. If I get this with random magnetic-field orientation, this is equivalent to some sort of a distribution in cone angle.

Behr: If we go down in the λ^{-1} direction, the cross sections in the H-plane and E-plane will go down to zero. Is the ratio also going to zero?

Greenberg: As a matter of fact, the ratio will approach a finite limit.

Graphite Grains and Graphite-Core-Ice-Mantle Grains

N. C. WICKRAMASINGHE
California Institute of Technology
Pasadena, California

AMONG THE FIRST REQUIREMENTS FOR A GRAIN MODEL is that it should explain the observed interstellar extinction law or laws as they are now understood; a desirable feature of such a model is that as few ad hoc assumptions be made as possible.

A criticism of the classical ice grain theory is that a very narrow range of grain sizes (or a size distribution with a size parameter specified to within a few percent) must be postulated in order to obtain a fit with the mean extinction law. (See refs. 1 and 2.) While it is true that regional variations in the extinction law have recently been detected (refs. 3 and 4), the best available evidence indicates that the extinction law is quite uniform when averaged over individual large regions which are widely distributed in the galaxy. (See ref. 5 and paper by Nandy in the present compilation.) The restriction of particle size to a radius within a few percent of an arbitrarily specified value ($r \approx 3 \times 10^{-5}$ cm) demanded on the basis of pure ice absorption is therefore considered quite unsatisfactory, particularly in view of the fact that no characteristic size parameter emerges from the Oort-van de Hulst theory for the formation and destruction of grains. (See ref. 6.)

In the original graphite model for interstellar extinction (refs. 7 and 8) this difficulty was overcome quite simply. In reference 7, the situation was that the mean extinction law as given in reference 9 was reproduced with graphite particles which were small enough ($r < 5 \times 10^{-6}$ cm) for a Rayleigh scattering approximation to the extinction cross section to be valid. This upper limit to the grain size was derived on the basis that there was insufficient time to build bigger grains, for example, in the pulsation cycles of N stars. Although now the situation for graphite is not as simple as it then seemed, the results of the present study show that one needs only to specify an upper limit to the graphite core radius and have an equilibrium distribution of ice mantles in order to reproduce the observed extinction laws.

Another important feature of graphite grains is that they can explain simply the phenomenon of interstellar polarization, as suggested originally by the authors of reference 10. The reason is that graphite is a strongly anisotropic substance with an electrical conductivity about a hundred times greater in directions parallel to the basal planes than at right angles to them. Because of this feature, graphite crystals have strongly polarizing properties. Furthermore, graphite is diamagnetic, and thus graphite flakes are easy to aline in a galactic magnetic field. In reference 10, however, only a small fraction of all the grains in the line of sight of a star were assumed to be polarizing graphite flakes—the others were taken to be nonpolarizing ice grains which gave rise only to the selective extinction. For such a model the total alinement of all the graphite flakes present was required in order to produce the observed ratio of polarization to extinction p/A_v; and to accomplish this alinement one needs a galactic magnetic field of about 10^{-5} gauss. (See ref. 11.) This value is probably greater than the best available estimates for the galactic magnetic field. If, however, one assumes that graphite particles (or graphite particles with ice mantles) produce the extinction as well as the polarization, the situation is much better. The grains then need to be alined only to a very slight extent—about 2 percent—in order to produce the observed p/A_v ratio, and the magnetic field required to produce such alinement is less than 10^{-6} gauss. (See refs. 12 and 13.) Magnetic fields of this general order are now considered far more satisfactory than the fields of 10^{-4} to 10^{-5} gauss which are required to aline "dirty ice" grains. (See ref. 14.)

MIE COMPUTATIONS FOR GRAPHITE

At the time of the original extinction computations for graphite grains (refs. 7 and 8), the available optical data on graphite were still very limited. The complex refractive index in directions parallel to the basal planes was given by (ref. 7)

$$m^2 = K - (2i\sigma\lambda)/c, \tag{1}$$

where c is the velocity of light. The dielectric constant K and the optical conductivity σ had to be specified at a given wavelength λ. The following values were suggested on the basis that they were consistent with earlier data on the reflectivities of polished graphite surfaces:

$$\left.\begin{aligned} \sigma &\cong 1.2 \times 10^{15}/\text{sec} \\ K &\cong 2 \end{aligned}\right\} \tag{2}$$

These values used in equation (1) yielded

$$m^2 = 2 - 8i\lambda, \tag{3}$$

where λ is the wavelength expressed in microns.

Mie computations performed on the basis of this model refractive index in references 8 and 15 substantiated the general conclusion, already reached in reference 7 by a simple Rayleigh approximation, that the extinction law as given in reference 9 could easily be reproduced for very small graphite particles—provided the radii are all less than about 5×10^{-6} cm. The assumption of a wavelength-independent conductivity for graphite, however, was rather unsatisfactory, although it was the best possible at the time. (See ref. 16.) These original Mie computations were, therefore, subject to revision when better data became available.

The first direct measurements of the wavelength dependence of the refractive index of graphite single crystals were made by the authors of reference 17, who measured the absorptive index κ in the wavelength range 2100 Å $< \lambda <$ 5500 Å. Their results showed a sharp peak in κ near 2600 Å, typical of a resonance phenomenon, which could not be explained in terms of a constant conductivity. This absorption peak centered at 2600 Å arises because of a transition of π-electrons into the conduction band, the precise position of the peak corresponding to the energy difference (4.8 eV) between the state of maximum density in the conduction band and the adjacent valence band of graphite. Such an effect was, in fact, predicted theoretically for graphite in reference 18.

The qualitative features of the measurements of reference 17 seemed to be consistent with a model of the refractive index based on the Drude-Lorentz theory of anomalous dispersion. (See ref. 19.) This model was then used to extrapolate to values of λ outside the measured range 2100 Å $< \lambda <$ 5500 Å, and Mie computations were performed. The extinction curves for very small particles showed a steep rise toward 2200

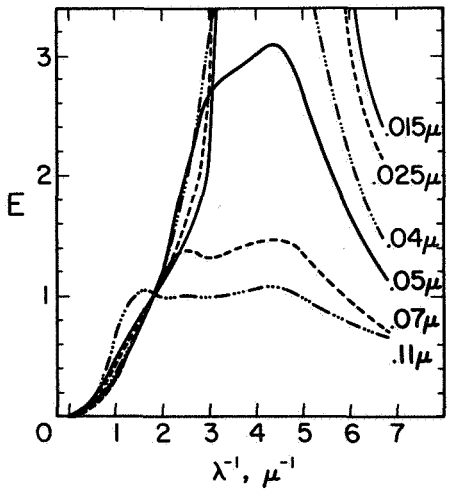

FIGURE 1.—Extinction curves for graphite spheres of various radii. Normalization: $E = Q_{ext}(\lambda)/Q_{ext}(5470\ \text{Å})$.

Å, exhibiting the qualitative features of the rocket UV observations (refs. 20 and 21).

More recently, however, direct measurements of both the real and imaginary parts of m^2 have been made (refs. 22 and 23) over wavelengths ranging from the far infrared to the far ultraviolet. There is little doubt that these measurements represent the best available optical data on graphite, and rigorous Mie computations have been performed for this case as well (refs. 1 and 24). Normalized extinction curves defined by

$$E = Q_{ext}(\lambda)/Q_{ext}(5470\ \text{Å}) \tag{4}$$

for various particle radii (Q_{ext} is the extinction efficiency), are plotted in figure 1. (See also refs. 1 and 24.) For particle radii less than about 0.06 μ, the extinction curves follow an approximately λ^{-1} dependence in the wavelength range $0.8\ \mu^{-1} < \lambda^{-1} < 2.4\ \mu^{-1}$ and show considerable variation for shorter wavelengths. The precise shape of the ultraviolet portion of the curve depends on the particle radius, but small particles produce a sharp ultraviolet quenching effect centered at ~ 2200 Å. This feature may be of importance in explaining the recent ultraviolet observations

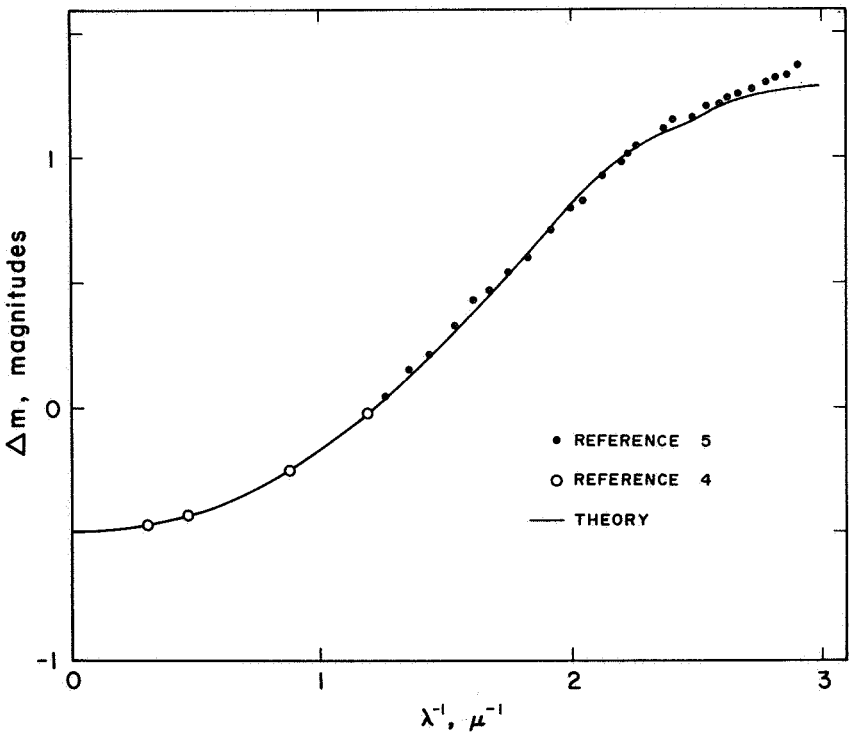

FIGURE 2.—Comparison of theoretical curve for a gaussian distribution of graphite spheres centered at 0.55 μ with dispersion 0.01 μ with observational points for Perseus region. Normalization to $\Delta m = 0$ at $\lambda^{-1} = 1.22$, $\Delta m = 1$ at $\lambda^{-1} = 2.22$.

presented in references 20 and 21. It is further of interest that the characteristic wavelength $\lambda^{-1}=2.4\ \mu^{-1}$ obtained by Nandy (see refs. 3 and 25 and paper by Nandy in the present compilation), at which both the Cygnus and Perseus extinction laws deviate from a λ^{-1} dependence, also turns out to be the wavelength at which extinction curves for small graphite spheres begin to deviate markedly as a function of λ^{-1}, as can be seen in figure 1.

The situation then is that the recent ultraviolet observations of a peak in extinction at 2200 Å and also a knee at $\lambda^{-1}=2.4\ \mu^{-1}$ in the curves of references 3 and 25 emerge as properties of the recently measured refractive index of graphite.

Detailed fits have been obtained on the basis of graphite grains and graphite grains covered with ice for the best available observational extinction curves. (See ref. 5.) In figure 2 is given a comparison of the Perseus curve of references 4 and 5 with the theoretical curve for a Gaussian distribution of graphite grains with dispersion $\sigma=0.01\ \mu$ centered at $0.055\ \mu$.

ICE MANTLES

The premise that graphite grains ejected from stars tend to grow ice-like mantles in interstellar clouds is presented in references 2, 8, and 26. A simple model for such growth can be constructed on the assumption that a certain fraction α of heavy atoms such as O, C, or N which hit a grain stick on as "icelike" molecules. The rate of increase of radius r is then given by

$$\frac{dr}{dt}=\frac{\alpha n}{s}\left(\frac{kTm}{2\pi}\right)^{1/2} \tag{5}$$

where

- n number density of O, C, or N, in ambient gas
- m mean atomic weight of heavy atoms
- α sticking probability
- T kinetic temperature of gas
- s mean density of grain material
- k Boltzmann constant

Taking $m\cong 18$, $s\cong 1.1\ \text{g/cm}^3$, $T\cong 100°\ \text{K}$, $n_H\cong 10/\text{cm}^3$ and $n/n_H\cong 10^{-3}$ as representative values for a cloud yields

$$\frac{dr}{dt}\cong 7\alpha\times 10^{-14}\ \text{cm/yr} \tag{6}$$

If $\alpha\cong 1$, as is commonly supposed, a graphite grain of initial radius 3×10^{-6} cm will grow an ice mantle to about 3×10^{-5} cm in a few times 10^8 years. The light scattering properties for such a grain will be almost

the same as those for a pure ice grain of radius 3×10^{-5} cm, except perhaps in the far infrared where core absorption may become dominant. Although it is possible that such icelike grains may be able to grow from graphite nuclei in localized regions, in general it is unlikely. According to reference 26, the proportion of grains with large mantles in the line of sight of the star is likely to be very small because of the disruptive effect of cloud collisions and because of the limited supply of O atoms which are responsible. These effects are discussed in the following paragraphs.

Mantle destruction by sputtering

On the average, an interstellar cloud is involved in a collision with a similar cloud once every 10^7 years. If such collisions are adequately inelastic, a cloud may be heated to 3000° to 4000° K and remain at that temperature for a length of time determined by the cooling rate. The best estimates of the cooling rate give a time scale

$$t \cong 10^4/n_{H_2} \text{ yr} \tag{7}$$

where n_{H_2} is the number density of H_2 in the colliding clouds. (See ref. 26.) If $t > 10^6$ years, the available data relating to the sputtering of ice by H impacts (ref. 26) indicate that all the ice mantles present may be destroyed. However, the condition $n_{H_2} < 10^{-2}/\text{cm}^3$ required for this does not seem likely to be realized for collisions between H I clouds, but would be realized for cloud collisions following closely upon cloud encounters with O and B stars. The other type of collision (collisions between H II clouds) has been estimated to occur with a frequency of once every 10^8 years per cloud, so that the chance of random destruction of an ice mantle is

$$P = 10^{-8}/\text{yr} \tag{8}$$

Graphite cores are not destroyed by this process.

A possible exhaustion of oxygen

A further restriction on the sizes of ice mantles might arise because of a limit of the available O atoms relative to the mass of condensed graphite cores. Graphite cores appear to be indestructible by ordinary interstellar processes, while O atoms tend to flit to and fro between mantles and gas. The characteristic time scale for the release of an O atom from a mantle is about 10^8 years; this is also the time scale for the growth of an ice mantle up to a radius of about 10^{-5} cm. An equilibrium in

$$O_{\text{grains}} \rightleftarrows O_{\text{gas}}$$

is therefore likely to be reached during the age of the galaxy in which

$$n[\mathrm{O}_{\mathrm{grains}}] \approx n[\mathrm{O}_{\mathrm{gas}}]$$

The process

$$\mathrm{C}_{\mathrm{gas}} \rightarrow \mathrm{Stars} \rightarrow \mathrm{C}_{\mathrm{grains}}$$

on the other hand, is likely to proceed predominantly one way, and an appreciable fraction of the available interstellar C atoms may eventually become locked up in grains. If this happens, the size of a typical ice mantle can be computed. Assuming an interstellar composition similar to the solar case,

$$\frac{\text{Mass of ice mantles}}{\text{Mass of C cores}} \cong \frac{18\times 2.9\times 10^{7}}{12\times 1.7\times 10^{7}} \cong 2.6$$

For graphite with a mean core radius of 3×10^{-6} cm and a density of 2.5 g/cm^3, a typical mantle can grow to at most $x\times 3\times 10^{-6}$ cm, where

$$\left(\frac{1}{2.5}\right)\left(\frac{x^3-1}{1}\right) \cong 2.6$$

$$x \cong 2$$

A typical graphite core of radius 3×10^{-6} cm is therefore able to grow to only about 6×10^{-6} cm with ice.

Equilibrium size distribution of mantles

On the assumption that the processes of mantle growth and destruction have reached an equilibrium state, one can obtain an equilibrium size distribution of ice mantles and perform extinction computations for such a distribution.

First suppose that the graphite cores are all of one radius r_0. Let $n(r,t)\,\mathrm{d}r$, $r \geqslant r_0$ be the number of grains with mantle radii in the range r, $r+\mathrm{d}r$ at time t. The total number of grains with mantles of radius less than r is then

$$N(r,t) = \int_{r_0}^{r} n(r,t)\mathrm{d}t \tag{9}$$

Denoting by P the destruction probability of a mantle per unit time, the conservation of cores gives

$$N(r+\mathrm{d}r, t+\mathrm{d}t) = N(r,t) - P\,\mathrm{d}t N(r,t)$$

$$\frac{\partial N}{\partial r}\,\mathrm{d}r + \frac{\partial N}{\partial t}\,\mathrm{d}t = -PN\mathrm{d}t$$

In a steady state $\partial N/\partial t = 0$, so that

$$\frac{\partial N}{\partial r}\dot{r} = -PN$$

$$n(r)\,\dot{r} = -P\int_{r_0}^{r} n(r)\mathrm{d}r$$

$$\frac{1}{n}\frac{\mathrm{d}n(r)}{\mathrm{d}r} = -P/\mu$$

where $\mu = \mathrm{d}r \equiv \dot{r}$, the rate of growth of grain. Thus

$$n(r) = n(r_0)\exp\left[-\frac{P}{\mu}(r-r_0)\right] \tag{10}$$

For a given value of r_0 and a known value of the ratio P/μ (determined from equations (6) and (8)), equation (10) gives the equilibrium size distribution of ice mantles. However, both these estimates are uncertain to within factors of order unity, and the ratio P/μ can therefore also be specified only to within a factor of order unity.

Two representative cases are considered:

(1) $P/\mu = 14.28\ \mu^{-1}$
(2) $P/\mu = 33.33\ \mu^{-1}$

Case (1) corresponds to $P = 10^{-8}$/yr and $\mu = 7\times10^{-14}$ cm/yr, and case (2) corresponds to $P = 2\times33\times10^{-7}$/yr and $\mu = 7\times10^{-14}$ cm/yr; but only the ratio P/μ is relevant for determining the size distribution. The functions $n(r)/n(r_0)$ for these two cases are plotted in figure 3.

Rigorous extinction computations are given in reference 27 for these two size distributions of mantles. The computations were initially made for a single value of the core radius $r_0 = 0.03\ \mu$, but it was subsequently verified that the resulting normalized extinction curves drawn in figure 4 were insensitive to the precise value of the core radius, provided $r_0 < \sim 0.06\ \mu$. Therefore, one only has to impose an upper limit $r_0 < 0.06\ \mu$ on the sizes of graphite cores to produce the normalized curves plotted in figure 4. It turns out that curve (2) (fig. 4), corresponding to $P/\mu = 33.33\ \mu^{-1}$, reproduces the Cygnus law given in reference 25, and it also qualitatively gives the observed ultraviolet absorption peak. (See ref. 21.) The detailed agreement with the observational points of reference 21 is shown in figure 5. The agreement is seen to be very good. In the near ultraviolet, the agreement can further be improved by adjusting the value of P/μ; but the theoretical curve already passes through the root-mean-square dispersion of the near UV points among the large number of stars observed by the author of reference 25.

Another question of interest concerning graphite-core–ice-mantle grains is: What fraction of the total extinction from a given graphite-

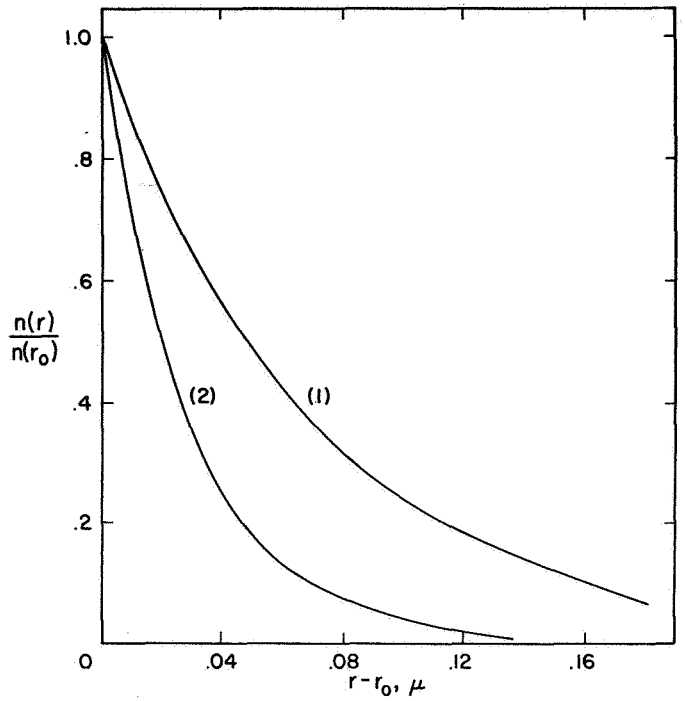

FIGURE 3.—Equilibrium distribution function for mantle radii $n(r)/n(r_0)$ for the two cases (1) $P/\mu = 14.28$ micron^{-1}, and (2) $P/\mu = 33.33$ micron^{-1}.

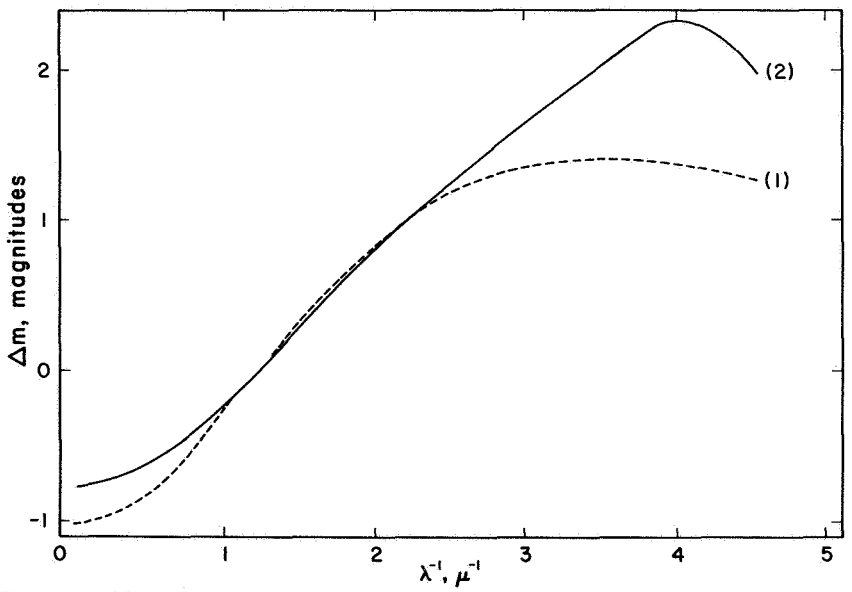

FIGURE 4.—Normalized extinction curves for the two ice-mantle size distributions sketched in figure 3, for graphite cores with $r_0 < \sim 0.06\ \mu$. Normalization to $\Delta m = 0$ at $\lambda^{-1} = 1.22$; $\Delta m = 1$ at $\lambda^{-1} = 2.22$. $\mu = 7 \times 10^{-14}$ cm/yr; curve (1): $P = 10^{-8}$/yr; curve (2): $P = 2.33 \times 10^{-7}$/yr.

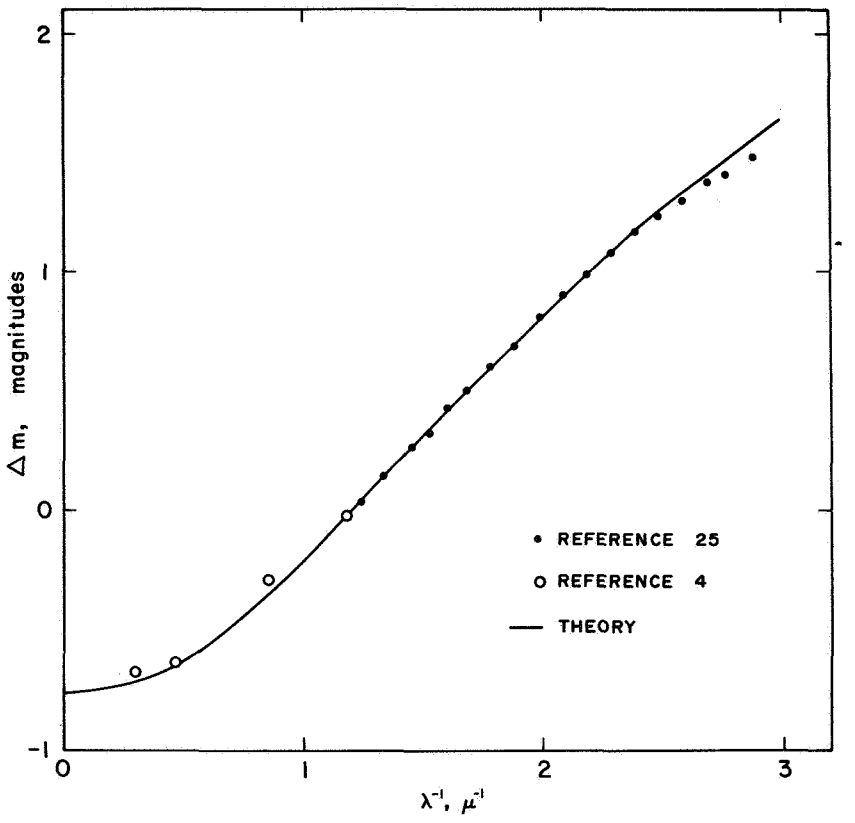

FIGURE 5.—Comparison of theoretical curve for equilibrium distribution (curve for case (2) in fig. 3) with observational points for Cygnus region. Normalization to $\Delta m=0$ at $\lambda^{-1}=1.22$; $\Delta m=1$ at $\lambda^{-1}=2.22$.

core–ice-mantle grain arises from core absorption? Figure 6 presents the total extinction cross sections for a graphite core of radius $r_0=0.02\ \mu$ covered to varying extents with ice. It is seen that for such a core covered with ice up to twice its own radius ($D\equiv r/r_0=2$), the extinction in the infrared and visible comes mainly from absorption in the graphite core. At about 6000 Å, in the red, graphite core absorption makes up about 70 percent of the total cross section (comparing ordinates with $D=1$ case), while in the blue and ultraviolet, it contributes to about 45 to 50 percent of the total.

These considerations have a direct bearing on recent infrared observations made in reference 28 as a result of sending up rocketborne equipment designed to detect a strong absorption band at 3.1 μ; such a strong absorption band at 3.1 μ is characteristic of ice and is expected on the basis of ice absorption. The fact that such a band was not detected led to the conclusion that ice absorption cannot account for more than 25

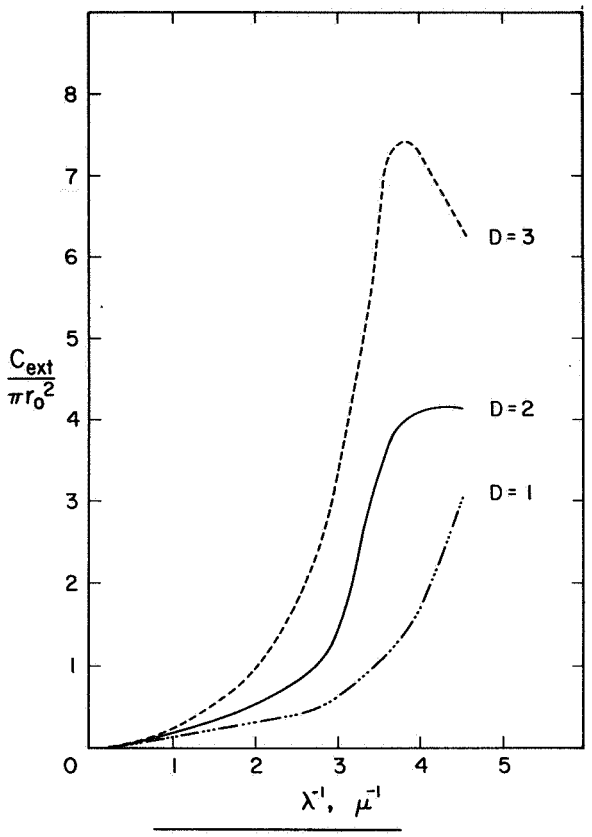

FIGURE 6.—Extinction cross sections for graphite cores with radii $r_0 = 0.02\ \mu$ covered with ice up to $D \equiv r/r_0 = 2$ and $D = 3$. $D = 1$ corresponds to pure graphite core.

percent of the total absorption at the visible wavelengths. Although absorption by pure graphite grains would meet this requirement, it is also of interest that the graphite-core–ice-mantle grains considered previously are not incompatible with the observations of reference 28.

For the Mie computations of the present investigation, spherical particles possessing an isotropic refraction index m have been assumed. The value of the refractive index that was adopted is appropriate for light polarized with an electric vector parallel to the basal planes. Since the absorption cross section for light with an electric vector at right angles to the basal planes is likely to be considerably less than that for light with an electric vector parallel to the basal planes, the present model of spherical isotropic grains is likely to give a good representation for actual graphite flakes provided they are in nearly random orientation. This conclusion, which has been checked for very small anisotropic graphite spheroids by using a Gans approximation (ref. 13), is likely to hold for grains with dimensions less than a few times 10^{-6} cm.

FORMATION OF GRAPHITE PARTICLES

In reference 7 it was suggested that graphite particles are formed during the pulsation cycles of N stars and ejected into interstellar space by the radiation pressure. Among the difficulties which had to be overcome before making graphite particles was the possibility that 0 might compete severely for the C to form CO. Consider the following thermochemical data:

$$C + O \rightarrow CO + 11.2 \text{ eV}$$
$$O + O \rightarrow O_2 + 5.25 \text{ eV}$$

Since CO is more strongly bound than O_2, it is likely that the formation of CO may prevent the formation of polyatomic carbon molecules and of graphite at 2000° K, if there is an excess of oxygen over carbon. However, if there is an excess of carbon over oxygen, as is likely to be true in carbon stars, this difficulty would not arise and solid graphite would be able to condense. The size of grains is limited by the time scale available for condensation during the pulsation cycle of an N star. It turns out that the maximum permitted radius is about 5.10^{-6} cm, close to the limit essential for the extinction curves.

The conditions for nucleation and growth appear to be considerably more favorable for graphite grains than for ice grains. For ice grains, one is in a better position to redo the calculations of references 29 and 30 using more reliable data. Preliminary calculations indicate that the nucleation problem for icelike grains in interstellar space now looks quite hopeless. The reason is that one cannot form stable diatomic and triatomic molecules at an adequate rate in interstellar space. Even if one formed such molecules in stars, the physical processes that could lead to their growth to "dirty ice" grains are still obscure.

Although the N stars are probably barely adequate to provide the necessary graphite grain density (ref. 7), it is also worth exploring other possible sites where such grains may be able to form. Preliminary computations which I have made in collaboration with B. Donn and T. P. Stecher indicate that graphite grains may be able to form in the expanding envelopes of certain red giant stars. Even though $n(O)/n(C) = 1$ in such envelopes, the lower temperature ($\sim 1000°$ K) permits a certain fraction of the available C atoms to be stable in the form of bulk graphite.

ALBEDO

Another requirement usually demanded of interstellar grains is that they possess a high visual albedo. Although the condition $\gamma \geq 0.5$ is frequently quoted, it is difficult to estimate how strong a requirement this must be. Graphite grains of radius of about 0.05 μ have an albedo $\gamma \sim 0.3$ at 5000 Å, and smaller graphite grains have lower albedos.

The presence of ice mantles, however, has the effect of considerably

enhancing the visual albedo, as discussed in reference 27. In table I the albedos of graphite-core–ice-mantle grains with core radii $r_0=0.03\ \mu$ and $r_0=0.05\ \mu$ are given. There is clearly no difficulty in meeting the conventional albedo requirement with graphite-core–ice-mantle grains.

TABLE I.—*Albedo at Representative Wavelengths*

λ^{-1}, μ^{-1}	Albedo for $r/r_0=$		
	1	2	3
r_0(core)$=0.03\ \mu$			
1.56	0.04	0.17	0.51
1.83	.06	.23	.59
2.30	.11	.34	.67
3.01	.19	.43	.68
r_0(core)$=0.05\ \mu$			
1.56	0.14	0.40	0.69
1.83	.20	.47	.71
2.30	.30	.53	.74
3.01	.42	.52	.80

REFERENCES

1. WICKRAMASINGHE, N. C.; and GUILLAUME, C.: Interstellar Extinction by Graphite Grains. Nature, vol. 207, 1965, p. 366.

2. VAN DE HULST, H. C.: Light Scattering by Interstellar Grains. Pub. Roy. Obs. Edinburgh, vol. 4, 1964, p. 13.

3. NANDY, K.: Observations of Interstellar Reddening II. Results for Region in Perseus. Pub. Roy. Obs. Edinburgh, vol. 5, 1965.

4. JOHNSON, H. L.: Interstellar Extinction in the Galaxy. Astrophys. J., vol. 141, 1965, p. 923.

5. NANDY, K.; and WICKRAMASINGHE, N. C.: A Survey of Recent Interstellar Reddening Observations. Pub. Roy. Obs. Edinburgh, vol. 5, 1965.

6. OORT, J. H.; and VAN DE HULST, H. C.: Gas and Smoke in Interstellar Space. Bull. Astron. Inst., Netherlands, vol. 10, 1946, p. 187.

7. HOYLE, F.; and WICKRAMASINGHE, N. C.: On Graphite Particles as Interstellar Grains. Roy. Astron. Soc., Monthly Notices, vol. 124, 1962, p. 417.

8. WICKRAMASINGHE, N. C.: On Graphite Particles as Interstellar Grains II. Roy. Astron. Soc., Monthly Notices, vol. 126, 1963, p. 99.

9. WHITFORD, A. E.: The Law of Interstellar Reddening. Astron. J., vol. 63, 1958, p. 201.

10. CAYREL, R.; and SCHATZMAN, E.: Sur la Polarisation Interstellaire par des Particules des Graphite. Ann. Astrophys., vol. 17, 1954, p. 555.

11. CUGNON, P.: Sur la Polarisation de la Lumière des Etoiles. Bull. Soc. Royale d. Sciences Liège, vol. 32, 1963, p. 228.

12. WICKRAMASINGHE, N. C.: A Note on Interstellar Polarization by Graphite Flakes. Roy. Astron. Soc., Monthly Notices, vol. 125, 1962, p. 87.

13. WICKRAMASINGHE, N. C.: Ph.D. thesis, Cambridge, 1963.

14. DAVIS, L.; and GREENSTEIN, J. L.: Polarization of Starlight by Aligned Dust Grains. Astrophys. J., vol. 114, 1951, p. 206.

15. MARGERUM, E. A.; and VAND, V.: Light Scattering by Small Graphite Spheres. Roy. Astron. Soc., Monthly Notices, vol. 128, 1964, p. 431.

16. HOYLE, F.; and WICKRAMASINGHE, N. C.: On the Deficiency in the Ultraviolet Fluxes from Early Type Stars. Roy. Astron. Soc., Monthly Notices, vol. 126, 1963, p. 401.

17. ERGUN, A.; and MCCARTNEY, J. T.: Proceedings of the Fifth Conference on Carbon, vol. 2, Pergamon Press, 1963, p. 167.

18. COULSON, C. A.; and TAYLOR, R.: Studies in Graphite and Related Compounds I Electronic Band Structure in Graphite. Proceedings of the Roy. Soc. London, vol. A65, 1952, p. 815.

19. WICKRAMASINGHE, N. C.: On the Growth and Destruction of Ice Mantles on Interstellar Graphite Grains. Roy. Astron. Soc., Monthly Notices, vol. 131, 1965, pp. 177–190.

20. BOGGESS, A.; and BORGMAN, J.: Interstellar Extinction in the Middle Ultraviolet. Astrophys. J., vol. 140, 1964, p. 1636.

21. STECHER, T. P.: Proceedings of IAU Colloquium on Grains. 1965.

22. TAFT, E. A.; and PHILIPP, H. R.: Optical Properties of Graphite. Phys. Rev., vol. 138A, 1965, p. 197.

23. CARTER, J. G.; HUEBNER, R. H.; HAMM, R. N.; and BIRKHOFF, R. D.: Optical Properties of Graphite in the Region 1100 to 3000 Å. Phys. Rev., vol. 137A, 1965, p. 639.

24. GREVESSE-GUILLAUME, C.; and WICKRAMASINGHE, N. C.: On the Optics of Small Graphite Spheres. III. Roy. Astron. Soc., Monthly Notices, vol. 132, 1966, pp. 471–473.

25. NANDY, K.: Observations of Interstellar Reddening I. Results for Region in Cygnus. Pub. Roy. Obs. Edinburgh, vol. 3, no. 6, 1964.

26. WICKRAMASINGHE, N. C.: On the Optics of Small Graphite Spheres. I. Roy. Astron. Soc., Monthly Notices, vol. 131, 1966, pp. 263–269.

27. WICKRAMASINGHE, N. C.; DHARMAWARDHANA, M. W. C.; and WYLD, C.: Light Scattering by Graphite Core–Ice Mantle Grains. Roy. Astron. Soc., vol. 134, 1966, pp. 25–36.

28. DANIELSON, R. E.; WOOLF, N. J.; and GAUSTAD, J. E.: A Search for Interstellar Ice Absorption in the Infrared Spectrum of μ Cephei. Astrophys. J., vol. 141, 1965, p. 116.

29. TER HAAR, D.: On the Origin of Smoke Particles in the Interstellar Gas. Bull. Astron. Inst. Netherlands, vol. 10, no. 1, 1943, p. 361.

30. KRAMERS, H. A.; and TER HAAR, D.: Condensation in Interstellar Space. Bull. Astron. Inst. Netherlands, vol. 10, no. 137, 1946, p. 371.

DISCUSSION

Dressler: You have shown that oxygen may not necessarily compete for the carbon in the stellar envelopes you have considered. Could you comment on the effect of hydrogen in the formation of graphite? In others words, can you show that the hydrogen also does not compete with the carbon?

Wickramasinghe: I do not know about hydrogen. The binding energy of CH is 3.5 electron volts, and the binding energy of H_2 is about 4.5

electron volts. Thus, about 1 eV more strongly bound than CH. For this reason I thought the H_2 molecule would begin to form before the CH molecule, but with the high hydrogen abundance in the stars one cannot be sure unless one performs equilibrium calculations for a CH system. I am hoping to study this.

Donn: Chemical equilibrium depends upon other factors besides the binding energy. A few years ago Dr. Bauer of Cornell made a very extensive calculation of the equilibrium of the CH system at high temperatures—temperatures of the order of 1500° to 5000° K. One of his results was an estimate of the temperature at which carbon would condense as a function of the C/H ratio and the total pressure. Dr. Bauer considered C/H ratios as low as 1/10 and pressures from 1/10 atmosphere. Extrapolation of their results to the case which Hoyle and Wickramasinghe discussed for a carbon star yields a condensation temperature of about 2100° K. This I think is at the minimum of the cycle of variation; therefore, there might be doubt as to whether grains would really grow. In view of the importance of the very suggestive calculations on carbon, it seems desirable to try to make some measurements on the extinction of small carbon grains. One could clarify the problem that Wickramasinghe pointed out about the anisotropy of carbon by measuring the extinction on both carbon black particles, which are more or less spherical polycrystalline material, and graphite flakes. We have begun some preliminary experiments to investigate this problem.

One can also, I think, modify this experiment to include the effect of an ice mantle by coating some of these particles. Although I am very dubious about getting particles being coated by ice in interstellar space, I certainly think it would be of interest to try to actually make these measurements.

Field: In your first curves, where you are considering graphite alone, there were extraordinary effects in the extreme UV which would not permit a fit to the $\lambda = 2200$ Å and $\lambda = 2600$ Å extinctions. Do you think that ice mantles form the only explanation for these data?

Wickramasinghe: No. If one ignored the farthest infrared points of Johnson, one could get a fit all the way up to the points of Boggess and Borgman. One has to take a size distribution of pure graphite to do this. It is to obtain a fit in the far infrared that one needs to coat the graphite particles.

Field: You have a number of curves; some of them seem to go too high and some go too low.

Wickramasinghe: To produce a good fit, or to go through both UV points, either a particular size or a particular size parameter in a size distribution is required. But all the curves for single sizes have the property of possessing peaks centered at 2200 Å.

Voice: I think that unity is a very optimistic assumption for the value

of the sticking coefficient, especially in the early stages of growth before the ice on the surface of the graphite has been nucleated. There is a nucleation problem here, in that graphite is not a very good nucleating agent for this absorption of water.

Wickramasinghe: Yes, the question of whether or not the accommodation coefficient is small is in doubt, and if it is small, not much ice will form. I think there is a very recent paper by Krishna Swamy in which he has a larger size parameter in an Oort-van de Hulst distribution of ice grains which fits the Orion curve very well.

O'Dell: The same result can be obtained if the small particles are removed. But what you say now seems inconsistent with what you said about sputtering, because if grain destruction can occur, then the situation in Orion would be ideal for this process and the grains would tend to be smaller rather than larger than average.

Wickramasinghe: For the Orion nebula, it would depend on the available time scale. I think it requires from 10^4 to 10^5 years to sputter the ice mantle if the gas temperatures are about 10 000° K. What would you say is the age of Orion?

O'Dell: I would say less than 2×10^6 years.

Wickramasinghe: The mantle destruction time would certainly be less than 2×10^6 years.

O'Dell: The fact that you are seeing scattered light in the other H II regions indicates that this grain destruction mechanism is not extremely important. Orion may be different. Now, does this mean that the remaining particles are graphite?

Wickramasinghe: The graphite particles wouldn't be sputtered. It would require a long time to sputter them if the gas temperature were 10 000° K. But with ice I imagine you would get the whole thing sputtered in 10^5 years.

O'Dell: By the same token I wonder whether Orion is more important or more suitable for sputtering than these others?

Wickramasinghe: Isn't the gas density also fairly high in Orion? Therefore, one really has to take a balance between the condensation as well as the sputtering. I don't know.

Greenberg: Did I miss a point in understanding the sputtering process? The relative fraction of condensing atoms and of atoms lost by sputtering is a function of the velocity distribution only. If the sputtering process is more effective than the condensing process at low density, the rate of loss by sputtering will certainly be greater as the density is increased.

Wickramasinghe: Yes, this is probably true.

Stecher: I would like to point out, as shown in the graph, that for larger particles the extinction does become neutral (wavelength independ-

ent). Thus, as you get about three times the size that is necessary to fit Perseus, even in the Oort-van de Hulst distribution, you might find at $\lambda^{-1}=3$ that the extinction is decreasing slightly in the ultraviolet.

Wickramasinghe: Yes. I think one could get a better fit in the ultraviolet by adding small particles unless one insists upon a very close fit in the infrared. By a very close fit I mean a fit through all the circles that Johnson and Borgman have. We did this using pure graphite distributions for Perseus and Cygnus, and the fits are as good as the ones for grains that have mantles.

Stecher: I should think that there would be some justification for adding the effects of several different size distributions to make the theory fit all the features completely. The basis for this justification is that each cloud is different and each region in a cloud is probably different.

Wickramasinghe: With regard to the graphite formation process, Dr. Donn mentioned earlier about the importance of CH formation. Perhaps a temperature below 2100° K is required in order for graphite grain formation to occur. Temperatures as low as this are available in the N stars. Also, it does seem that several of the carbon stars have opaque atmospheres in the infrared and some emit material similar to that emitted in R Corona Borealis.

Donn: There is a question in this respect of whether, in R Corona Borealis stars, the variation is due to some condensation process; that is, whether the catastrophic drop of these stars may be caused by an extensive condensation of graphite grains, as O'Keefe considered many years ago.

Wickramasinghe: I don't claim to have solved the formation problem. But I think that the formation of large molecules or of grains is very much more favorable near stars than in interstellar space.

Donn: Concerning the emphasis that has been given in all the calculations of the Oort-van de Hulst distributions, I think that there is no real theoretical reason for this distribution, especially when one talks about carbon grains. It is a good model in which one gets more small grains than large grains, and this is not an unreasonable assumption to work with. But I don't think one ought to feel that the precise distribution it gives is significant, and therefore, if one wants to get a different distribution he must assume that there is a series of clouds. We must certainly be free to modify this distribution in almost any way without the fear of violating a fundamental law of nature.

Donn (Communicated note (1966)): Wickramasinghe, Hudson, Stecher, and I have now reconsidered the formation of graphite in cool stars by using Tsuji's detailed calculations of molecular equilibrium. Tsuji found carbon to be highly supersaturated, a conclusion which we confirm for the regions in the atmosphere where graphite can grow to

the required radii in sufficient time. Calculations of the nucleation rate indicate that a sufficient number of grains will form to account for the interstellar extinction. These will be ejected by radiation pressure and carry molecules along with them. Free molecules and molecules adsorbed on grains may affect the optical properties of grains and Johnson's hypothesis of the origin of diffuse bands. Graphite opacity also seriously affects the structure of the atmosphere.

Infrared Radiation From Interstellar Grains

WAYNE A. STEIN
Princeton University
Princeton, New Jersey

DURING THE PAST SEVERAL YEARS there has been a growing interest in the possibility of observing infrared radiation at wavelengths greater than 10 μ from various astronomical objects. For example, Gould in references 1 and 2 has suggested trying to observe several lines in the infrared with emphasis on the 12.8-μ line of Ne^+ and the 28-μ line of molecular hydrogen. The possibility of being able to observe the emission from interstellar grains in the wavelength region between 10 μ and 100 μ was suggested in a discussion presented in references 3 and 4. The intensity expected from thermal emission by the grains has also been investigated by F. D. Kahn at Manchester.

The present paper indicates information about interstellar grains that could be gained by measuring the intensity as a function of wavelength and the polarization of radiation emitted by the grains in the far infrared. Because of uncertainties in the knowledge of the radiation field from stars in space and in the composition and temperatures of the grains, the models for the far infrared radiation calculated herein may not agree in detail with the results of the observations. It is the purpose of the present discussion to indicate the kind of measurements that should be made in order to gain better knowledge of these quantities.

EXPECTED INTENSITY

The total radiation flux incident on the grains is about 5.3×10^{-3} erg/cm^2-sec. (See ref. 5.) If one-tenth of this radiation is absorbed by the grains, it must be reemitted in the far infrared. If the infrared radiation is emitted isotropically over 4-π steradians, the intensity observed at the Earth would be

$$\left(\frac{5.3 \times 10^{-4}}{4\pi}\right) 4\pi r^2 nl \text{ ergs/cm}^2\text{-sec-sr}$$

where r is the grain radius, n is the density of grains, and l is the path

length. For $n=2\times10^{-13}/cm^3$, $r=2\times10^{-5}$ cm, and $l=20$ kpc, the intensity of radiation in the galactic plane is 2.5×10^{-10} watt/cm^2-sr. This intensity could be detected with modern far infrared detectors.

The most obvious difficulty involved in making these observations is the interfering effects of emission from water vapor in the Earth's atmosphere. The observations could possibly be made from balloon altitudes, but the detectors more likely would have to be flown above the Earth's atmosphere by rockets.

TEMPERATURES AND SPECTRA OF THE GRAINS

Four extreme types of interstellar grains are considered: metal, graphite, dielectric (ice), and Platt particles. The large molecules proposed by Platt (ref. 6) could immediately be distinguished from the other models of the grains by the presence or absence of far infrared radiation. These large molecules, because of their size, would contribute no radiation in the far infrared.

The equation of energy balance (ref. 7) leads to the temperatures and spectra of radiation from the grains. As a simplified example of the results one might expect, consider the spectral distribution for a dilution factor of 10^{-14} and an absorption efficiency of 1/10. The temperatures of grains of radius 0.2 μ would be 74° K for a good conductor, 30° K for graphite, and 15° K for ice under these conditions. The wavelengths of maximum emission would then be 28 μ for a good conductor, 70 μ for graphite, and 125 μ for ice, as shown in figure 1.

The spread of these spectra due to variations in dilution factor W and radius of particles can be shown for metal particles by the result

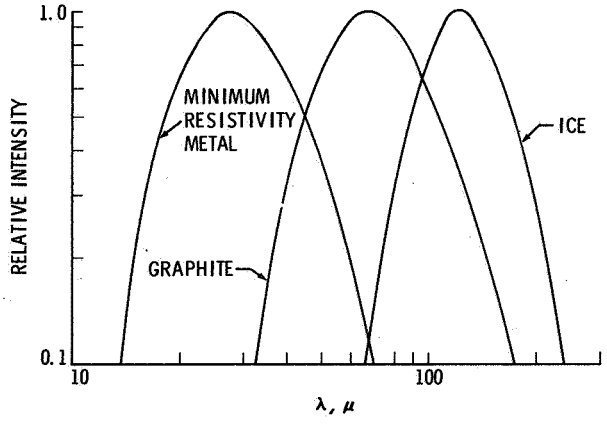

FIGURE 1.—Expected spectra of emission from interstellar grains of various compositions normalized to 1 at the wavelength of maximum intensity.

of the equation of energy balance in which the particle temperature T_p varies as $(W/r)^{1/6}$ or slower. A change by a factor of 100 in W would then result in a change by a factor of 2.15 in temperature. A similar result for dirty ice grains is presented in reference 8. For ice, a change by a factor of 100 in dilution factor resulted in a change by a factor of from 2 to 2.5 in temperature. The extreme examples of a good conductor and ice are separated by a factor of 5 in temperature. Thus it seems possible that under some circumstances, low temperature, high conductivity grains might be difficult to distinguish from high conductivity, low temperature grains, but extreme fluctuations in W or r would be necessary to lose the contrast between the spectra of high conductivity grains and ice. At least the temperature of the grains would be determined. Further calculations of details of spectra for composite grains and other complications should probably await observation of the radiation.

POLARIZATION

If the true source of the polarization of starlight at visible wavelengths is absorption of light by alined, elongated, interstellar grains, then the far infrared radiation from the grains should also be polarized. In order to compare the percentage of polarization from the two mechanisms, only the case of perfectly alined grains was considered.

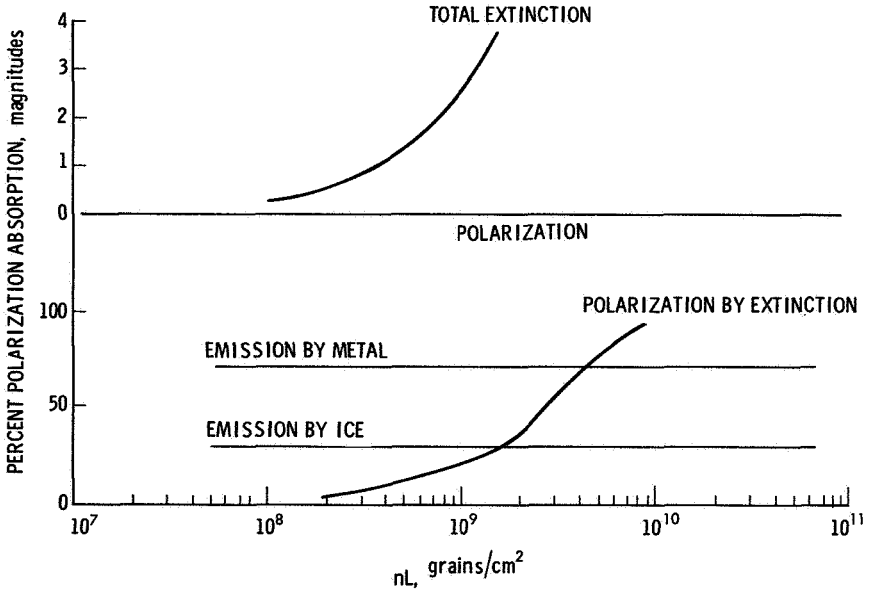

FIGURE 2.—Total extinction and polarization at visible wavelengths due to extinction by grains compared with the polarization of emitted infrared as a function of the number of grains per square centimeter in the line of sight for grains with ratio of axes of 2.

Figure 2 shows an example of the total extinction and polarization of starlight at visible wavelengths as a function of the number of grains per square centimeter in the line of sight for grains with a *ratio of axes of 2*. The polarization of the emitted far infrared as calculated for ice and metal grains is shown for comparison. It can be seen that the polarization of emitted infrared radiation from the grains for this example would be larger than the polarization of starlight at visible wavelengths under practically all conditions. In addition, it should be pointed out that since the absorption of far infrared radiation is small, observations of polarization could be made to large distances from the Earth. Thus the far infrared distribution of energy with wavelength and the polarization of radiation from interstellar grains would yield new information in the study of the grains.

REFERENCES

1. GOULD, R. J.: Infrared Emission Lines from H II Regions. Astrophys. J., vol. 138, 1963, p. 1308.

2. GOULD, R. J.: The Contraction of Molecular Hydrogen Protostars. Astrophys. J., vol. 140, 1964, p. 638.

3. SPITZER, L.: Proceedings of Third Symposium on Cosmical Gas Dynamics. Part VIII: Summaries and Conclusions. Rev. Mod. Phys., vol. 30, 1958, p. 1107.

4. DRAKE, F.: Proceedings of Third Symposium on Cosmical Gas Dynamics. Part VIII: Summaries and Conclusions. Rev. Mod. Phys., vol. 30, 1958, p. 1107.

5. ALLEN, C. W.: Astrophysical Quantities, Univ. of London, The Athlone Press, 1963.

6. PLATT, J. R.: On the Optical Properties of Interstellar Dust. Astrophys. J., vol. 123, 1956, p. 486.

7. VAN DE HULST, H. C.: Optics of Spherical Particles. Rech. Astron. Obs. Utrecht, vol. 11, pt. 1, 1946.

8. GREENBERG, J. M.: Interstellar Grains. Ann. Rev. Astron. Astrophys. vol. 1, 1963, p. 267.

DISCUSSION

Field: It occurs to me that one expects the distribution of the infrared to mimic that of reflection nebulae because reflection nebulae represent combinations of dust concentration and stellar radiation which give detectable scattered light. The same combination gives detectable infrared emission; therefore, such emission will probably be very patchy, as is the scattered light. The surface brightness may well be much higher than the average value you have computed for certain regions often associated with reflection nebulae.

Stein: Yes, I agree. One might be able to see individual clouds, depending upon how the numbers of particle density and path length are estimated. The wavelength of emission in particular regions might occur at shorter wavelengths also.

Field: The point is that it may not be the diffuse light you want to look for, but rather those patches which are quite near the stars; their angular dimensions are very much smaller.

Stein: Yes. But then also one would look at shorter wavelengths than the 100-μ region.

Donn: Do you have an estimate for the background light from the stars in the far infrared?

Stein: I don't know anything about stars at 100 μ. I have made estimates of the radiation at these wavelengths by extrapolating radio spectra of radio sources. I think one might be able to see the Sag A radio source. I think that the emission from the Zodiacal light would occur at shorter wavelengths, somewhere in the 1-μ to 10-μ range.

Hall: Have you made any estimates of how many watts per steradian would be received from these three types of grains at the Earth's surface after passing through the water vapor in the atmosphere?

Stein: It's hopeless.

Hall: Even at the shorter wavelengths? There is a window at 8 μ to 14 μ and one at 22 μ to 24 μ.

Stein: Oh, but the latter window is very small. One needs a very wide band in order to collect a lot of radiation. The problem isn't so much the absorption, but the fact that the water vapor in the Earth's atmosphere absorbs radiation from the Earth and then reemits; it is that flux of emission from the Earth's atmosphere that would cause the problem.

Hall: For the background?

Stein: That's right. This is what makes me very dubious about whether it can be done from balloons or not. One might have to use rockets to get above the water vapor.

W. E. Thompson: Is there any problem of infrared radiation from the instrument itself in the far infrared?

Stein: This involves chopping techniques and cooling of components. When one observes far infrared radiation like this, one chops the region he is observing against the background. The direct-current component is no problem; the problem involves cooling of the detectors and other components.

Nucleation and Grain Growth in Interstellar Space

BERTRAM DONN
NASA Goddard Space Flight Center
Greenbelt, Maryland

THE FIRST DETAILED STUDIES to determine the processes by which interstellar grains may form were made by a group of Dutch astronomers in the 1940's. (See refs. 1 to 5.) Since that time very little systematic work on this problem has been done until very recently when Hoyle and Wickramasinghe (ref. 6) investigated graphite formation in cool stellar atmospheres. Van de Hulst's paper in 1949 (ref. 5) represents the culmination of an intensive attack which had considerable influence on astronomical thought about interstellar grains.

Somewhat ironically, beginning about 1949 many significant advances in physics and chemistry having a direct bearing on this problem were made. In 1949, Frank in reference 7 presented a theory which explained how real crystals tend to grow, and much work, both theoretical and experimental, has been done since then. (See ref. 8.) Recent extensive research in chemical reactions at low temperatures both in solids and on surfaces is reported in reference 9. These investigations prompted renewed interest in investigating the origin of interstellar grains, and the present paper discusses part of the continuing study. Developments in stellar and galactic evolution indicate that a continuous source of grains is necessary. The interchange of interstellar material that is needed to explain the rate of star formation was studied in references 10 and 11, and a turnover time of 10^9 years was estimated. The fact that this time is short compared with the age of the galaxy, which is of the order of 10^{10} years, indicates that the interstellar material has been pretty well circulated through stars. Primordial grains that formed at some early stage of the galaxy should have disappeared. Other destructive processes such as collisions and passage near hot stars further shorten the lifetime.

This paper deals with the question of nucleation and subsequent growth in interstellar space. When ter Haar considered this problem in 1944, the accepted kinetic temperature for the interstellar gas was

10 000° K. Since the "temperature" corresponding to the internal energy of molecules and grains would be less 100° K, he was faced with a situation representing an extreme deviation from thermodynamic equilibrium. It was necessary, therefore, to resort to a mechanistic treatment of particle formation with all the complications and uncertainties of such a method.

Today investigators face a different problem because of the recognition (ref. 12) that extensive low temperature regions occur, with kinetic temperatures near 100° K. It is in these H I regions where all temperatures are below 100° K that grain formation takes place. Although thermodynamic equilibrium does not hold exactly, the temperatures for all degrees of freedom are sufficiently close that thermodynamic results may be expected to yield reasonable answers.

NUCLEATION THEORY

Comprehensive discussions and nucleation theory are given in references 13 to 15, and a more concise treatment including later developments as well as crystal growth is discussed in reference 8.

The rate of nucleation in a vapor is determined by the rate at which single molecules add to clusters of critical size to form stable nuclei. The frequency distribution of clusters and the condition of stability is determined by the free energy of formation of a cluster because entropy as well as energy changes must be accounted for. For the frequency distribution, one finds

$$m_i = m \exp(-\Delta G_i/kT) \tag{1}$$

where

m_i number of clusters of i molecules per cm^3
m number of molecules per cm^3
ΔG_i free energy of formation of ith cluster
k Boltzmann constant
T temperature

The factor ΔG_i may be represented by the equation

$$\Delta G_i = 4\pi r^2 \sigma + 4/3\pi r^3 \Delta G_v \tag{2}$$

where

σ surface energy
r nuclear radius (assumed spherical)
ΔG_v free energy difference per unit volume of liquid between supersaturated vapor at ambient pressure P and bulk liquid at its equilibrium vapor pressure

The term ΔG_v is given by

$$\Delta G_v = -\frac{kT}{\Omega} \ln \frac{P}{P_v} \tag{3}$$

where

Ω molecular volume
P ambient pressure
P_v equilibrium vapor pressure of bulk phase

One of the weak points of the theory is the assumption that macroscopic thermodynamic properties apply to the small clusters. Equations (1) and (3) hold for crystals as well as drops when the necessary changes in defining the various quantities have been made.

Initially, ΔG_i increases as molecules add to a cluster, with the result that clusters represent unstable fluctuations that form and decay. Equation (3) shows that the second term in equation (2) is negative, and the free energy of a cluster has a maximum value obtained by setting

$$\frac{d\Delta G_i}{dr}=0$$

This procedure yields the characteristics of the cluster of critical size for which further growth decreases the free energy. Clusters larger than the critical size will not tend to decay spontantously and are the condensation nuclei.

The critical parameters are as follows:

$$r^*=\frac{2\sigma\Omega}{kT\ln(P/P_v)} \tag{4}$$

$$i=\frac{4\pi r^3}{3\Omega} \tag{5}$$

$$\Delta G^*=\frac{16\pi\sigma^3}{3(kT/\Omega)^2\ln^2(P/P_v)} \tag{6}$$

The nucleation rate is the rate at which molecules collide with and stick to clusters of the critical size. This rate is given by:

$$J=\alpha Z 4\pi(r^*)^2\frac{P}{(2\pi mkT)^{1/2}}m\exp(-\Delta G^*/kT) \tag{7}$$

where

J number of nuclei formed per cm^2 per sec
α sticking coefficient
Z nonequilibrium factor

The factor Z arises because critical clusters are reduced from their equilibrium concentration by the growth of stable nuclei into droplets or crystallites.

INTERSTELLAR NUCLEATION

Equations (3) to (7) show the fundamental role of the supersaturation ratio P/P_v in the nucleation process. Consequently, this ratio must be determined in the interstellar medium for all elements of interest. The partial pressure P_i of the ith element is given by

$$P_i = m_i kT \tag{8}$$

where m_i is the interstellar concentration of the element. Table I displays concentrations, partial pressures at 100° K, and impact frequencies per cm² for the more abundant elements and observed radicals. Relative abundances are from reference 16; uncertainties of these values are not sufficient to affect the results of this analysis.

TABLE I.—*The Interstellar Gas*

Element	Atomic number	m_i, atoms/cm³	P_i, torr	Impact frequency no./cm²-sec
H	1	1	10^{-17}	4×10^{4}
He	4	1×10^{-1}	10^{-18}	2×10^{3}
O	8	5×10^{-4}	5×10^{-21}	5
Ne	10	2×10^{-4}	2×10^{-21}	2
N	7	2×10^{-4}	2×10^{-21}	2
C	6	10^{-4}	10^{-21}	1
Si	14	3×10^{-5}	3×10^{-22}	2×10^{-1}
Mg	12	2×10^{-5}	2×10^{-22}	2×10^{-1}
Fe	26	2×10^{-5}	2×10^{-22}	10^{-1}
S	16	10^{-4}	10^{-22}	7×10^{-2}
Ar	18	3×10^{-6}	3×10^{-23}	3×10^{-2}
Al	13	3×10^{-6}	3×10^{-23}	2×10^{-2}
Ca	20	10^{-6}	10^{-23}	6×10^{-3}
Na	11	10^{-6}	10^{-23}	7×10^{-3}
Ni	28	10^{-6}	10^{-23}	5×10^{-3}
CH, CN, OH		10^{-8}	10^{-25}	10^{-4}
		10^{-7}	10^{-24}	10^{-3}

The elements to which this calculation applies and whose vapor pressure is of interest are carbon, silicon, and the metals which condense directly and require no recombination reactions first. These are all of low volatility, and vapor pressures cannot be measured at low temperatures.

Vapor pressures can be calculated theoretically by using capacities for the solid and molecular energy levels for the vapor. The procedure is discussed in references 17 to 19. The resulting equation for the vapor pressure is

$$\ln P_v = -\frac{L_0}{RT} + \frac{5}{2}\ln T - \int_0^T \frac{dT}{RT^2}\int_0^T (C_{p_s} - C_i)\,dT + i \tag{9}$$

where

L_0 heat of vaporization at 0° K
C_{p_s} specific heat of solid
C_i internal specific heat of gas
h Planck's constant
i chemical constant $= \ln g_0 \dfrac{(2\pi m)^{3/2} k^{5/3}}{h^3}$
m molecular mass
g_0 statistical weight of molecule
R gas constant

Vapor pressures, listed as equilibrium constants for solid-vapor transition, are given in reference 20 for 100° intervals starting at 100° K. The 100° K data are appropriate for an H I region. Vapor pressures P and the supersaturation ratio $\rho = P/P_v$ in the interstellar medium are given in table II.

TABLE II.—*Interstellar Pressure and Supersaturation*
[$T = 100°$ K]

Element	log P, dynes/cm^2	ln ρ
Al	−157	315
C	−358	780
K	−35	32
Na	−45	57
S	−130	250
Si	−217	450

In order to find the critical cluster size and number of atoms from equations (4) and (5), the molecular volume Ω and surface energy σ for the elements under consideration must be determined. The molecular volume is given by:

$$\Omega = \frac{M}{N_0 n} \tag{10}$$

where

M atomic weight
N_0 Avogadro's number, 6×10^{23}
n density of bulk material, g/cm^3

Surface energies are difficult to measure with high accuracy, although results sufficient for these calculations are available for some materials in references 21 and 22. Data for carbon are discussed in references 23 and 24. Table III presents the crystal properties for nucleation calculations.

TABLE III.—*Crystal Properties*

Element	Atomic weight	Density, g/cm^3	P, torr	Temperature, °K
Carbon	12	2.2	1.0×10^{-23}	130 to 1000
Iron	56	7.9	1.2	> 1800
Silicon	28	2.4	2.0	1240
Sodium	23	1.0	4.0	150
Zinc	65	7.1	1.5	105

The application of equations (4) and (5) yields $r = 1.7 \times 10^{-8}$ for sodium and $r = 4 \times 10^{-9}$ for carbon with $\sigma = 1000$ ergs/cm^2. In each case the value of r^* is less than unity. A straightforward interpretation would be that a single atom acts as a nucleus for continued growth. However, the proper equivalent of such macroscopic properties of matter as surface energy, for clusters of a few molecules, is one of the stumbling blocks to the development of a rigorous nucleation theory. Although the evaluation of the critical cluster or nucleus is uncertain here, it seems reasonable to conclude that in interstellar space a nucleus will consist of a very small number of atoms. Physically, this comes about because of the low interstellar temperature which leads to a very low vapor pressure for the elements. The low temperature also causes all molecular aggregates to have high stability, and independent of an interpretation as a nucleation process we expect any diatomic molecules to be stable against spontaneous decay. As shown in reference 3, the steady-state molecular concentration is determined by photodissociation. The photodissociation probability of the molecules will be approximately independent of size or even increase for larger molecules as longer wavelengths tend to be effective. (See ref. 25.) This behavior is quite different from the decay of clusters in nucleation where the decay probability decreases with size until a critical size corresponding to the stable nucleus is reached.

Some preliminary estimates of the formation rate of interstellar grains based on the preceding analysis can be made. This stage seems to be the same as that from which ter Haar began his analysis. However, several features show that this is not actually true. By restricting the

analysis to crystal growth without recombination among different elements, only the heavier elements already indicated are involved. Also, the aggregates in the present study are stable molecules undergoing photodissociation, not the spontaneously disintegrating clusters. In ter Haar's paper (ref. 2), crystalline properties of the clusters play important roles. In addition to the uncertainties already noted about using these macroscopic properties for small clusters, it does not appear that the growth mechanism presented in reference 2 is consistent in assuming that it would lead to crystalline grains. This point will be considered later.

INTERSTELLAR MOLECULAR PROCESSES

In order to examine the kinetics of the formation of pure grains, carbon is used as a significant illustration, and chemical reactions involving other species are neglected. If recombination reactions incorporate other atoms the process is the alternative mechanism of ter Haar. Should the reactions remove carbon, somewhat akin to the molecular formation process proposed in reference 26, the growth rate becomes even slower than found here and interstellar formation of crystalline grains still less likely.

In reference 27 is obtained a rate coefficient for the reaction

$$C^+ + H \rightarrow CH^+ + h\nu \tag{11}$$

given by

$$\frac{dm_{CH^+}}{dt} = 10^{-18} m_C + m_H \tag{12}$$

The inclusion of other formation and decay processes yields a steady-state value of 10^{-10} to 10^{-11} molecules/cm^3. For CN^+, the estimates of a total production in 10^9 years in references 3 and 27 are 5×10^{-6}/cm^3 and 5×10^{-7}/cm^3, respectively. These numbers neglect photodissociation, and the actual density by this process must be less. If photodissociation for CN^+ is comparable to that for CH^+, a steady-state density of about 10^{-14}/cm^3 is obtained. In the absence of more direct evidence it is assumed that C_2 would behave similarly.

A third atom still has a low probability of adding to a diatomic molecule as stabilization against rapid dissociation remains low. (See ref. 28.) Consequently, for the reaction

$$C_2 + C \rightarrow C_3 + h\nu \tag{13}$$

$$\frac{dm_{C_3}}{dt} = 10^{-16} m_C m_{C_2} \tag{14}$$

When four molecules are involved the frequency with which the newly formed bond attains the recombination energy and can break becomes comparable to the reciprocal radiative lifetime. The probability of capture of a fourth carbon is somewhat less than for normal reaction probabilities and will be about normal for additional carbon atoms.

Consider the rate coefficient for the formation of four carbons

$$\frac{dm_{C_4}}{dt} = 10^{-13} m_{C_3} m_C \tag{15a}$$

For all succeeding reactions let the rate coefficients be

$$\frac{dm_{C_{j+1}}}{dt} = 10^{-12} m_{C_j} m_C \quad j \geq 4 \tag{15b}$$

These rate coefficients are given by the products 0.01 σv (eq. (15a)) and 0.1 σv (eq. (15b)), where σ is the collision cross section (10^{-15} cm^2) and v is the average relative velocity (10^4 km/sec).

The formation rate of a species containing j atoms is given by:

$$\frac{dm_j}{dt} = \gamma_{j-1} m_{j-1} m_1 - \beta_j m_j - \gamma_j m_j + \beta_{j+1} m_{j+1} \tag{16}$$

The γ's are the formation rate coefficients and the β's are the photodissociation rates whose values have been discussed previously. An approximate solution may be obtained for the steady state by solving each equation sequence starting with the first and dropping the last term in each equation. It will turn out that the m_j terms decrease rapidly enough to make this legitimate.

The procedure leads to the following solution for the m_j terms:

$$m_1 = 10^{-13}$$
$$m_2 = 10^{-12}$$
$$m_3 = 10^{-20}$$
$$m_4 = 10^{-24}$$
$$m_5 = 10^{-28}$$

For successively larger molecules the frequency is multiplied by 10^{-4} for each additional carbon atom added until the values of the adopted coefficients change. This will probably occur in the photodissociation process and effect β_j, which determines the rate of destruction. Although the building process may well be more efficient than the result obtained here indicates, two neglected factors make it less efficient.

The dissociation will not always consist of the removal of a single atom, and the broken bond in some instances will yield larger fragments than single atoms. More significant is the fact that all elements to which our mechanism applies will be largely ionized, leading to a positively charged carbon polymer and a reduction in the resultant capture rate of additional carbon ions. It follows, therefore, that the uncertainties in the calculations will probably not yield the required grain density for conducting grains, which for an extinction of 1 magnitude kpc is about $10^{-11}/cm^3$.

Ter Haar implied in his 1944 paper that the building process may consist of a sequence of the form

$$C \rightarrow CH \rightarrow CH_2 \rightarrow CH_2O \rightarrow CH_3O \rightarrow CH_3NO$$

and so on. This is the growth mechanism suggested in references 29 and 30 which leads to the so-called Platt particle.

STELLAR SOURCES

Because of the problem of forming grains in interstellar space, other sources require consideration. A significant contribution was made by the investigation reported in reference 6 concerning graphite formation in cool carbon stars. The graphite formation problem must consider the complete chemical equilibrium in a stellar atmosphere taking all constituents into account; hydrogen is clearly the most important. Fortunately, the chemical equilibrium of the CH system including graphite stability was investigated in reference 31. Seventy hydrocarbons are included, and the temperature at which graphite becomes stable as a function of the C/H ratio for several pressures is determined. These results are shown in figure 1, modified from the original diagram for

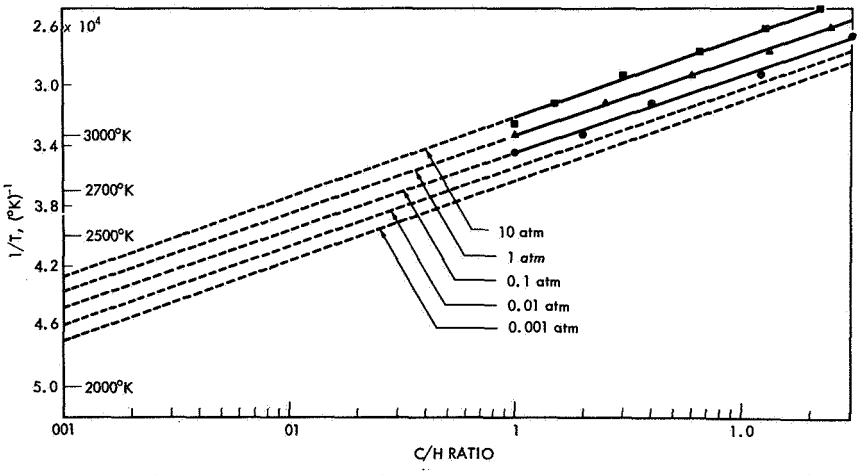

FIGURE 1.—Sublimation temperature of graphite as function of C/H ratio of atmosphere. Points are taken from reference 31. Dashed lines are extrapolations.

better extrapolation. Solid lines are drawn through the computed points and the dashed lines are extrapolated to a C/H ratio of 10^{-3}, adapted by Hoyle and Wickramasinghe. For a pressure of 10^{-3} atmospheres, the considerable extrapolation yields a sublimation temperature of graphite of about 2100° K. Professor Bauer has said that the pressure extrapolation should be valid.[1] At a temperature of 2100° K, conditions are less favorable for graphite formation and the mechanism becomes rather doubtful.[2]

An important feature of the molecular equilibrium in carbon stars of type N is the array of hydrocarbon molecules and radicals present in the atmosphere. If the observed mass ejection for M stars exists for carbon stars also, then a significant quantity of these species is carried into interstellar space. It is conceivable that they may serve as nuclei for further growth and that the growth process may compete favorably with photodecomposition of the molecules. As already discussed, the probability that a molecule of five or more atoms will add another is high. Whether this scheme would lead to graphitic grains or more nearly resemble the composition and structure of a Platt particle is not now clear. In examining this problem, the possibility that aggregates might develop beyond the normal atmospheric boundary, perhaps in an expanding envelope, needs to be considered.

It cannot be said that the nucleation problem has been solved. There are many uncertainties in the present discussion and several possibilities have yet to be investigated.

CRYSTAL GROWTH

With regard to particle growth on a preexisting nucleus, on the hexagonal or "C" face of a graphite lattice carbon atom, bonds are highly saturated and the captured surface atom is held by the relatively weak van der Waals' forces. These nonlattice atoms would be capable of diffusing over the surface. Experiments on the formation of carbon whiskers (ref. 33) indicate that this does occur. A study of the kinetics of graphite formation in interstellar space at low temperatures (ref. 34) indicates that the captured atoms become trapped at the edge of a "C" face so that a platelet or needle would tend to grow. The growth rate depends upon the surface area of the grain over which atoms are collected. This produces exponential growth until the size becomes larger than the mean diffusion distance, and then linear growth occurs.

---

[1] Later work in reference 32 extended the calculations to C/H = 0.008 and experimentally studied graphite equilibrium in a hydrocarbon atmosphere. The theoretical and experimental results are in agreement with the earlier work and our extrapolation. There is a suggestion that sublimation temperatures would be greater by somewhat less than 50°.

[2] See, however, the Donn comment following Wickramasinghe's paper in the present compilation concerning a recent detailed analysis of this problem by Donn, Wickramasinghe, Hudson, and Stecher.

Growth of a graphite platelet on a 10^{-7}-cm nucleus is shown in table IV.

TABLE IV.—*Growth of Graphite Platelet*

Time, yr	Radius, for hydrogen number density of—	
	$1/cm^3$	$10/cm^3$
10^7	10^{-7}	10^{-6}
10^8	10^{-6}	10^4
10^9	10^{-4}	-------

With a density of 1 hydrogen atom/cm^3, practically no change occurs in 10^7 years. In 10^8 years the grain reaches a radius of 10^{-6} cm and the rate increases very rapidly for greater time intervals because of the exponential behavior. The figure of 10^{-4} in column 2 is obtained by using the exponential growth expression and obviously is meaningless except to show how rapidly the size increases once growth begins. Column 3 shows the size attained for the intervals indicated in denser regions where the hydrogen number density is $10/cm^3$.

It can be seen that the change in size is much greater than the density increase for grains of 10^{-6} cm. This theory can provide for grain size distribution which changes discontinuously from small to large grains in different regions of the Galaxy. These results neglect effects of adsorbed atoms or attack by atomic hydrogen and oxygen which may remove carbon atoms.

A point related to the question of coating grains, or graphite cores with ice mantles, should be emphasized. To have an efficient substrate for condensing a different molecule, the two species should have similar crystal properties, in particular with regard to crystal structure and lattice spacing. Silver iodide has a hexagonal structure similar to ice I (normal ice) and is an effective nucleating agent for ice. A solution of silver iodide was cooled under sufficient pressure such that ice III was the stable phase in reference 35; however, ice I was again obtained. Silver iodide and ice III have dissimilar structure and spacing and silver iodide will not nucleate ice III even in the pressure-temperature domain where ice III is the stable phase. In another type of experiment (ref. 36), the sticking coefficient dropped from unity to about 0.65 as the lattice spacing mismatch increased from 0 to 15 percent for cubic crystals.

These phenomena indicate the necessity of detailed analysis of particle formation; it is not as simple as saying that material condenses. An extensive body of theoretical and experimental data exist which must be incorporated into a theory of interstellar grain formation.

271-992 O-67—14

Much more experimental work is needed, particularly for conditions appropriate to astrophysics.

It should be emphasized that only tentative conclusions have been presented herein. A study of interstellar grain formation can now be carried out which is on a sounder basis than was possible in the period from 1940 to 1950. It is necessary, however, to do this in successive stages. This paper discussed the nucleation process in some detail and more briefly, the crystal growth process. Some attention was also given to the role of chemical reactions. A program for continuing study of the origin and structure of interstellar grains is outlined in reference 37.

REFERENCES

1. OORT, J. H.; and VAN DE HULST, H. C.: Gas and Smoke in Interstellar Space. Bull. Astron. Inst. Netherlands, vol. 10, 1946, p. 187.

2. TER HAAR, D.: Astrophys. J., vol. 100, 1944, p. 288.

3. KRAMERS, A. H.; and TER HAAR, D.: Condensation in Interstellar Space. Bull. Astron. Inst. Netherlands, vol. 10, no. 137, 1946, p. 371.

4. VAN DE HULST, H. C.: Optics of Spherical Particles. Rech. Astron. Obs. Utrecht, vol. 11, pt. 1, 1946.

5. VAN DE HULST, H. C.: The Solid Particles in Interstellar Space. Rech. Astron. Obs. Utrecht, vol. 11, pt. 2, 1949.

6. HOYLE, F.; and WICKRAMASINGHE, N. C.: On Graphite Particles as Interstellar Grains. Roy. Astron. Soc., Monthly Notices, vol. 124, 1962, p. 417.

7. FRANK, F. C.: Disc. for Soc. No. 5, vol. 48, 1949, p. 67.

8. HIRTH, T. P.; and POUND, G. M.: Condensation and Evaporation. Macmillan Co., New York, 1963.

9. ANON.: Formation and Trapping of Free Radicals (A. N. Bass and H. B. Broida, eds.), Academic Press, New York, 1960.

10. SCHWARTZSCHILD, M.: Structure and Evolution of Stars. Princeton University Press, Princeton, New Jersey, 1958.

11. SCHWARTZSCHILD, M.: In the Distribution and Motion of Interstellar Matter in Galaxies. (L. Woltjer, ed.) W. A. Benjamin, New York, 1962, p. 266.

12. SPITZER, L.; and SAVEDOFF, M.: Astrophys. J., vol. 111, 1950, p. 593.

13. FRENKEL, J.: Kinetic Theory of Liquids. (Ch. 7), Dover Publications, New York, 1955.

14. TURNBALL, D.: In Solid State Physics, vol. 3, Academic Press, Inc., New York, 1956, p. 266.

15. FEDER, J.; RUSSELL, K. C.; LOTHE, J.; and POUND, G. M.: Advances in Physics, Phil. Mag. Suppl., vol. 15, 1966, p. 111.

16. SUESS, H. E.; and UREY, H. C.: Rev. Mod. Phys., vol. 28, 1956, p. 53.

17. ZEMANSKY, M. W.: Heat and Thermodynamics. (4th ed.), McGraw-Hill Book Co., Inc., 1952.

18. STATES, J. C.: Introduction to Chemical Physics. McGraw-Hill Book Co., Inc., 1939.

19. GURNEY, R. W.: Introduction to Statistical Mechanics. McGraw-Hill Book Co., Inc., 1949.

20. JANAF: JANAF Thermochemical Data. Dow Chemical Co., Midland, Mich., 1961–1965. (Presently available from Clearinghouse for Fed. Sci. and Tech. Information, U.S. Department of Commerce, Doc. No. PB 168 370–1.)

21. ADAMSON, A. W.: Physical Chemistry of Surfaces. Interscience Pub., New York, 1963.

22. GEGUZIN, Y. E.; and OVCHARENKO, N. N.: Soc. Phy. Uspekhi, vol. 5, 1962, p. 129.
23. UBBELOHDE, A. R.; and LEWIS, F. A.: Graphite and Its Crystal Compounds. Oxford Univ. Press, London, 1960.
24. SEARS, G. W.: J. Chem. Phys., vol. 31, 1959, p. 358.
25. CALVERT, J. G.; and PITTS, J. N.: Photochemistry. John Wiley & Sons, Inc., New York, 1966.
26. STECHER, T. P.; and WILLIAMS, D.: Astrophys. J., vol. 146, 1966, p. 88.
27. BATES, D. R.; and SPITZER, L.: Astrophys. J., vol. 113, 1951, p. 441.
28. TROTMAN-DICKENSON, A. F.: Gas Kinetics. Butterworth's, Sci. Pub., London, 1955.
29. PLATT, J. R.: On the Optical Properties of Interstellar Dust. Astrophys. J., vol. 123, 1956, p. 486.
30. PLATT, J. R.; and DONN, B. D.: Astron. J., vol. 61, 1956, p. 11.
31. DUFF, RUSSELL E.; and BAUER, S. H.: Equilibrium Composition of the C/H System at Elevated Temperatures. J. Chem. Phys., vol. 36, 1962, p. 1754.
32. CLARKE, J. T.; and FOX, B. R.: Reaction of Graphite Filaments with Hydrogen above 2000° K. J. Chem. Phys., vol. 46, 1967, p. 827.
33. MEYER, L.: Proceedings of Third Carbon Conference (Buffalo, New York), Pergamon Press, New York, 1959.
34. DONN, B. D.: Astron. J., vol. 70, 1965, p. 137.
35. EVANS, L. F.: Requirements of an Ice Nucleus. Nature, vol. 206, 1965, p. 822.
36. YANG, L.; SIMNAD, M. T.; and POUND, G. M.: Acta Metallurgica, vol. 2, 1954, p. 470.
37. DONN, B. D. Astron. J., vol. 58, 1953, p. 38.

DISCUSSION

Field: With regard to your comment that interstellar material gets recycled about every 10^6 years, I believe that the theory of stellar evolution, as it stands now, suggests that this recycling does occur through the red giant phase. Therefore, if nucleation takes place, it would have to take place by the agency of the red giants.

Donn: Yes, this is true. If the main ejection is from these cool stars, then one ought to look at these stellar atmospheres or clouds around these stars as being a source for the formation of possible condensation nuclei.

Field: Isn't it true that there are some observations that bear directly on the veiling of certain red giant stars?

Donn: The point that I made yesterday was that R Corona Borealis shows this very precipitous drop in intensity. A suggestion which has been analyzed in detail by O'Keefe was that this may be due to the sudden condensation of carbon which forms. There has been very little further work done. G. Herbig has a paper on the spectra of R Cor Bor during a decline. I looked through that and it didn't seem to me that his spectra, as I recall, at the various stages of cycle showed anything that indicates what is happening. I think that these phenomena ought to be studied observationally very carefully, as such observations are very important for understanding the cause of the decline and possible condensation processes in stellar atmospheres.

Wampler: A student in Los Angeles is working on these stars and he is trying to get the energy distribution from 4000 Å to a micron. But it

is difficult to separate reddening from temperature effects. You might have to look into some of the bands to determine temperatures.

Wickramasinghe: For the case of the gas clouds going out of red giants at 6000° at the surface, one finds that you don't have to go up to 2700° in order to find condensation, or in order for the vapor pressure to exceed the gas pressure. Therefore, the gas clouds undergo an adiabatic expansion.

Donn: Yes. As a matter of fact, I think that an interesting point that Dr. Hudson introduced in our discussions is that adiabatic expansion of a nozzle is one of the new techniques that shows very great applicability of studying homogeneous nucleation. In a sense the atmosphere is an adiabatically expanding cooling cloud, and this is often very favorable.

Hudson: This technique is making possible use of the adiabatic expansion in the nozzle area to study the nucleation of various gases. Both the crystal nucleation and the growth theory assume that once a molecule reaches a growth site near the nucleus or a macroscopic crystal, it is immediately incorporated. It is an additional complication that you might have a thermal activation barrier to incorporate at a growth center.

Nandy: Do you account for the change of density of the interstellar medium? A star is formed and the metal enrichment changes as a constant with time. When you consider the figure of 10^8 you have to account for this change.

Donn: You mean a change in the composition due to the heavy elements formation?

Nandy: Yes.

Donn: Strictly, of course, one ought to worry about all these things, but the problem is complicated enough without that. As I recall the evidence on the building up of heavy elements, the interstellar medium in the B stars in 10^8 years doesn't show any marked enhancement.

Wickramasinghe: I think there is very strong evidence that the ultraviolet emission from carbon stars is very low.

Donn: I don't think the problem is solved; one needs to look at further refinements and developments of the problem. One of the disturbing things is that the advancements in our understanding of the theory of interstellar grains that have taken place in the last quarter of a century have been relatively small. The idea of grain formation in carbon stars is certainly a significant contribution.

Hemingway: One of the characteristics that we have observed in the high-altitude particles is that when we heat them in an electron beam they appear to be unstable; that is, a phase change appears to take place. After this, electron diffraction which can give a particle chemical analysis is seen. Can you shed any light on why such instability can occur?

Donn: It is possible to form a nucleus that would grow an amorphous particle rather than a crystal; it ought to be spherical, because then there is no favored direction of growth. The formation phase is usually an unstable one. Now, if one heated the particle and annealed it, he would expect it to recrystallize. The question is: what were the conditions under which these initially were formed without a crystal structure? This is the interesting aspect.

Field: I do not understand the exponential growth. Could you explain that very simply?

Donn: It is an exponential growth as long as the particle grows by adding at an edge the material striking the surface. Larger surfaces collect more material and, therefore, growth is faster. The rate of growth is thus exponential. This procedure concerns growing a plate or a needle; it will not work for a sphere. It applies if the material that falls on the surface adds on in the same direction. It only works in a limited region because there is only a certain mean life for diffusion before the particle evaporates. Once the crystal grows larger than this, then linear growth will occur because the material that imparts at a distance that is greater than the diffusion distance will not reach the edge. One of the reasons that very large particles are unrealistic is that the mean free path of the material is much less than this distance.

Wickramasinghe: Did you try to redo the ter Haar computations on the rate of formation of triatomic molecules?

Donn: No. I assumed that the estimate ter Haar made was not altogether unreasonable and used it. (In the paper the rate of formation of triatomics is based on Bates' diatomic rate and its extension using unimolecular decomposition theory.)

Wickramasinghe: In spite of this, do you find that the nucleation rate is very small?

Donn: I think it would be too small by this process unless there are some factors that have not been accounted for.

Wickramasinghe: I tried to use the Bates-Spitzer data on the recombination coefficient and found that the rate of formation of absorbed CH was in error by a factor of 10^5.

Donn: Yes, I think it will be small. I think if the process does occur, it would probably go through an ion-molecular reaction like $CH^+ + H \rightarrow CH_2^+$ for which the cross section can be a factor from 10 to 100 larger than straight kinetic cross sections because of the polarization effects.

Lind: Is it impossible for whisker-type growth to occur in interstellar space?

Donn: A platelet is essentially a form of whisker growth. Whisker growth implies that growth is taking place along a single axis in which there is a screw dislocation; that is, a trapping center, which preserves

itself as the crystal grows so that there is always a place to trap the atom and it keeps growing. Now, if there is a two-dimensional set of dislocations growing out, a platelet results. For three-dimensional arrays a more equiaxial crystal would be the result.

We did some scattering measurements on zinc oxide particles to see how the scattering from irregular particles compares with that from spheres. These particles are grown from vapor and they look like nuclei with four needle-like arrays sticking out. One conclusion appears to be that when these particles are oriented in a random pattern the scattering measurements are similar to those of spheres of somewhat similar characteristics, if a suitable dimension parameter that is related to the shape is used. The polarization and the angular dependence of the particles are similar to those of spheres. Therefore, for reflection nebulae, for example, the use of the Mie scattering function of the spheres is useful even though the particles may be quite irregular. Van de Hulst showed that for a cylinder, the extinction curve closely resembles that of a sphere.

I had hoped when we started these measurements that we might find some effects that deviated so markedly from spheres that something about the shapes could be determined. We were thinking here of comet tails in particular. We could discover no significant deviations, however.

Effects of Absorption Spectra of Ices on the Ultraviolet Extinction by Interstellar Grains

G. B. FIELD, R. B. PARTRIDGE, AND H. SOBEL
Princeton University
Princeton, New Jersey

IN SPITE OF MANY YEARS OF RESEARCH ON INTERSTELLAR GRAINS, their composition is still unknown. Evidently it can be found only through the interaction of the grains with radiation, and one is led to the spectroscopic study of the solids composing the grains. If discrete lines, bands, or other spectral features can be discovered, they may be of great importance in the chemical analysis of the grains. So far, data of this type include the diffuse interstellar lines, the optical lines of CH, CH^+, and CN (almost certainly once part of the grains), the radio lines of OH, and the distinct "kink" or curvature in the optical extinction curve (see paper by Nandy in present compilation), which may reflect spectral variations in refractive index and hence indicate a specific material.

The advent of ultraviolet and infrared techniques suggests that consideration be given to new features to be expected in those regions. In the present paper is presented a calculation of features to be expected in the 1000- to 2000-Å range for particles of ice. Although the calculation is crude and almost certainly in error at certain points, it serves as an example of any case in which photons of 5 to 10 electron volts can cause internal transitions which profoundly affect the optical properties at wavelengths specific for the material. Other investigators will certainly find such effects for other materials.

While this work was in progress, a similar investigation which also included observational data was being carried out for the infrared. (See ref. 1.) By an examination of the 3.1-μ line of H_2O ice in the spectrum of μ Cep, the authors of reference 1 concluded that lack of a detectable line implies that less than 25 percent of the mass of the interstellar grains between the Sun and that star is H_2O, compared with the expected 64 percent (fig. 1). This seems to be the first definitive indica-

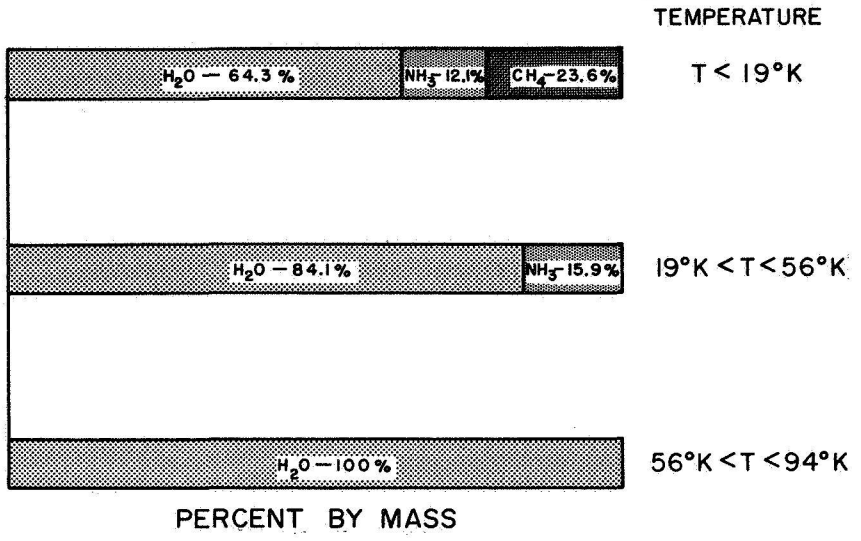

FIGURE 1.—Chemical composition of grains. Cosmic abundance ratios assumed for non-evaporated components. The three chemical compositions used were water, ammonia, and methane in cosmic proportions, as modified by evaporation of methane and ammonia at the indicated temperatures.

tion that grains predominantly of ice may not be responsible for the optical extinction and is an example of the power of the spectroscopic method. This early quantitative result should not be taken too literally, however. For example, an alternative calculation of the mass of ice grains required to explain the optical extinction of μ Cep, based on an exponential distribution of radii with $\bar{a}=0.05\ \mu$, is somewhat smaller than was assumed in reference 1, with the result that the upper limit on H_2O is revised upward to 45 percent.

CALCULATIONS

The effects studied here concern the dissociation continua of ices of water, ammonia, and methane discussed in reference 2. Figure 2 shows the values of n' (imaginary part of refractive index) for the pure ices implied by their measurements. These values of n' were weighted in accordance with the mixtures of figure 1, which were derived on the assumptions of complete binding of C, N, and O in the form of CH_4, NH_3, and H_2O in proportion to cosmic abundance, with successively less volatile components evaporating as the temperature was raised in accordance with the equilibrium calculations of reference 3. These mixtures were taken as representative of variations one might encounter successively closer to an early star (see paper by O'Dell in present compilation for a discussion of evaporation).

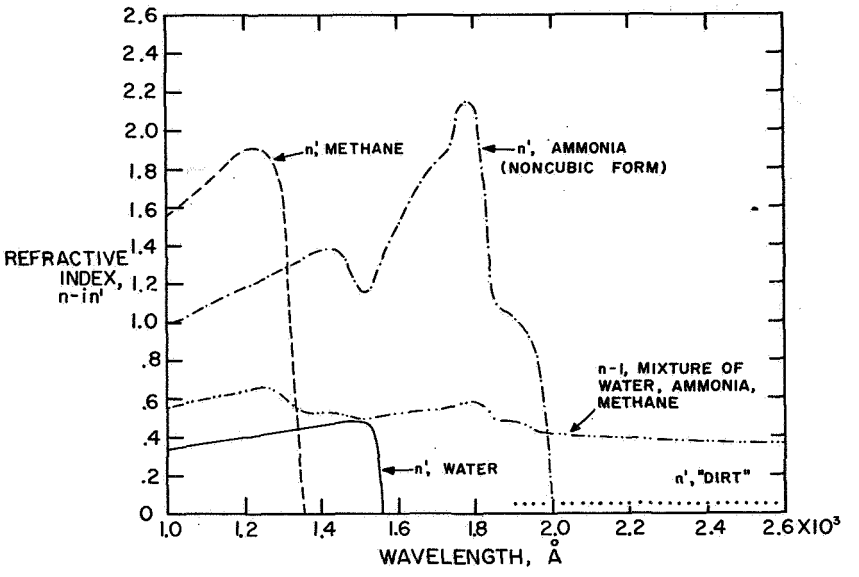

FIGURE 2.—Laboratory data on refractive index in the ultraviolet. Note distinct absorption edges for each material. Calculation of $n-1$ was made by weighting approximate expressions representing extrapolations of data in the visible. (From ref. 2.)

It can be seen in figure 2 that in each case n' rises sharply at the absorption edge, which occurs for water at 1570 Å, for ammonia at 1990 Å, and for methane at 1350 Å. Rapid changes of n (the real part) are anticipated in the neighborhood of these limits, but these have apparently not been measured and only estimates can be made. Estimates were made as explained in the appendix, where it is shown that for water (which dominates the situation, see fig. 1) one can obtain a better approximation than was used by application of the Kramers-Kronig dispersion relation. The values of $n-1$ in figure 1, without marked rapid changes, were used for the case of the mixture of water, ammonia, and methane; these values were typical of those used in the other cases. Hence, the spectral changes in the extinction found are due primarily to n' and not to n. The value of 0.05 was assumed for n' for values of the wavelength greater than 1.9.

An exponential distribution of particle radii obtained from reference 4 was used. Physical reasons are given in reference 4 for such a distribution, and van de Hulst has showed that this distribution gives analytic results for the equation

$$\overline{Q}(\lambda) \equiv \frac{1}{2\bar{a}^3}\int_0^\infty e^{-a/\bar{a}} a^2 Q(a/\lambda)\,da \tag{1}$$

in the asymptotic approximation $n-1,\ n' \to 0$; namely

$$\frac{1}{2}\bar{Q}=1-\frac{(1+\bar{\rho}\tan\beta)^2-\bar{\rho}^2}{[(1+\bar{\rho}\tan\beta)^2+\bar{\rho}^2]^2} \tag{2}$$

where Q is the extinction efficiency, $\bar{\rho}=\dfrac{4\pi\bar{a}(n-1)}{\lambda}$, and $\tan\beta=\dfrac{n'}{n-1}$. It may be shown that equation (1) gives exact results (agrees with Mie theory) in both the limits $\bar{\rho}=0$ and $\bar{\rho}=\infty$ for $\tan\beta > 0.05$. Equation (2) for a typical case, $\tan\beta=0.17$, was compared with the exact results of reference 5 averaged according to equation (1), and the maximum difference was 13 percent. Clearly in our cases larger errors are to be expected because $n-1$ and n' become large, but the simplicity of this procedure outweighs the modest errors incurred.

RESULTS

Calculations were carried out for the three mixtures for values of $\bar{a}$ of 0.01 μ, 0.03 μ, 0.1 μ, 0.3 μ, and 1.0 μ. It was found that the ground-based measurements of extinction summarized in reference 6 could best be fitted with 0.05 μ. This fit was good to 5 percent probable error, unexpectedly good for a one-parameter calculation. This should not be considered an indication that the actual particles have the assumed properties, but rather, that if the distribution and materials are those

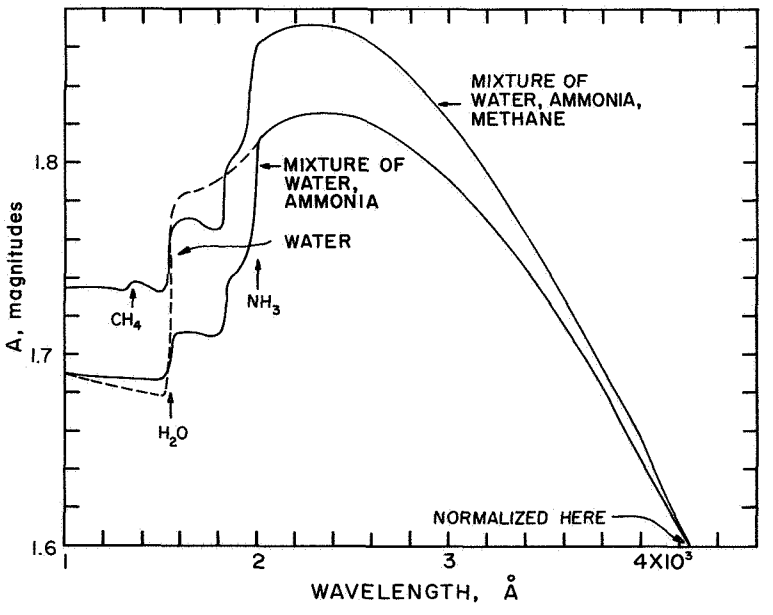

FIGURE 3.—Ultraviolet extinction in magnitudes normalized to 1.6 in the photographic for an exponential particle size distribution with $\bar{a}=1000$ Å.

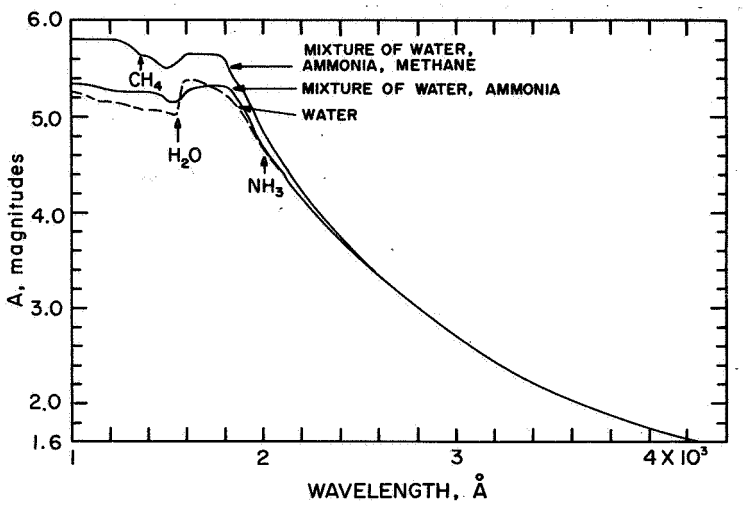

FIGURE 4.—Ultraviolet extinction in magnitudes normalized to 1.6 in the photographic for an exponential particle size distribution with $a = 300$ Å.

assumed, $\bar{a}$ cannot be very different from 0.05 μ. This value is considerably smaller than the mean of the Oort-van de Hulst distribution, 0.19 μ. (See ref. 3.) Such a change is obviously indicated by the large increases over van de Hulst's curve at 2200 Å and 2600 Å found in reference 6.

The results of interest are therefore those for 0.10 μ and 0.03 μ, which are shown in figures 3 and 4, normalized to 1.6 magnitudes at 4250 Å. It is seen that the 0.1-μ curves increase rather slowly from the photographic value in contradiction with the observation at 2200 Å and 2600 Å, as explained previously. The effect of interest is the decrease in extinction ahead of the three characteristic limits. This effect, amounting to 5 percent for water and less for the other components, is surprising at first. The explanation is to be found in the fact that at 1550 Å, for example, $\bar{\rho} \simeq 6$, so that the grains are larger than the wavelength. The curves on page 28 of reference 3 show that, for large particles of a certain size range, increasing the value of n' can decrease the total extinction. This effect is explained as due to a decrease in the amplitude of the rays transmitted by the grain, with the accompanying interference effects which lead to large scattering.

This effect persists with 0.03-μ grains, which more nearly match the observed extinction in the near ultraviolet. Here the effects are percentagewise of the same order, but numerically larger. For an unknown reason, the effect of ammonia is to flatten the otherwise rising curve, while water and methane show abrupt decreases as before.

A value for $\bar{a}$ of 0.01 μ was used to obtain the results shown in figure 5; however, large numbers of such particles are probably not present.

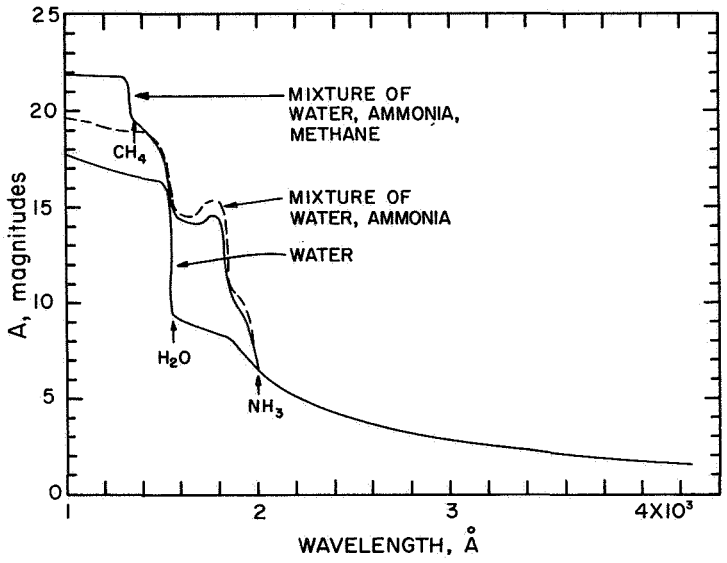

FIGURE 5.—Ultraviolet extinction in magnitudes normalized to 1.6 in the photographic for an exponential particle size distribution with $\bar{a} = 100$ Å.

For these small particles the true absorption is dominant, as predicted by van de Hulst, for $\bar{\rho} < 1$. The dramatic increases in extinction amount to 7, 9, and 2 magnitudes for water, ammonia, and methane, respectively.

CONCLUSIONS

In each case effects are seen which are characteristic of the three assumed components; whether or not these are detectable is unknown. At least one can say that if early-type stars with typical photographic extinctions can be seen at all in these wavelengths, then ice particles with $a = 0.01$ μ are quite rare, but this fact is already strongly indicated by the optical data. The abrupt flattening of the curves for $\bar{a} = 0.03$ μ may possibly become measurable as techniques improve (for such measurements, see the paper by Stecher in the present compilation), and the details, combined with improved versions of the calculation described here, should lead to quantitative estimates of abundances. Present estimates of $\bar{a}$ suggest that rocket observers should not anticipate being hindered by a drastic increase in extinction in the range from 1000 Å to 2000 Å, as suggested by the data in figure 1. Rather, because of van de Hulst's effect, the extrapolation of the curve of reference 6 may well lead to an overestimate of the extinction in this region.

APPENDIX

Evaluation of n From n' by Using Dispersion Relations

The linear absorption coefficient α, related to n by $n' = \lambda\alpha/4\pi$, where λ is the vacuum wavelength, has been measured in reference 2. The Kramers-Kronig dispersion relation can be written

$$\epsilon_1 - 1 = \frac{2}{\pi} P \int_{\nu_*=0}^{\infty} \frac{\nu_* \epsilon_2(\nu_*)\, d\nu_*}{\nu_*^2 - \nu^2} \tag{A1}$$

where the complex dielectric constant $\epsilon_1 - i\epsilon_2$ is the square of the complex refractive index $n - in'$. Substitution of $\epsilon_1 = n^2 - (n')^2$ and $\epsilon_2 = 2nn' = \lambda\alpha n/2\pi$ into equation (A1) yields

$$n^2 = (n')^2 + \left[1 + \frac{c}{\pi^2} P \int_{\nu_*=0}^{\infty} \frac{n(\nu_*)\alpha(\nu_*)\, d\nu_*}{\nu_*^2 - \nu^2}\right], \tag{A2}$$

which is a nontrivial integral equation for n if n' (and hence α) are given for all frequencies. The method of crude approximation on which values of n in figure 2 are based is simply to equate the expression in brackets to the observed value of n^2 down to the shortest wavelength for which it has been determined (which is longer than the absorption limit, so that $n' = 0$). Ahead of the absorption limit, n was approximated by

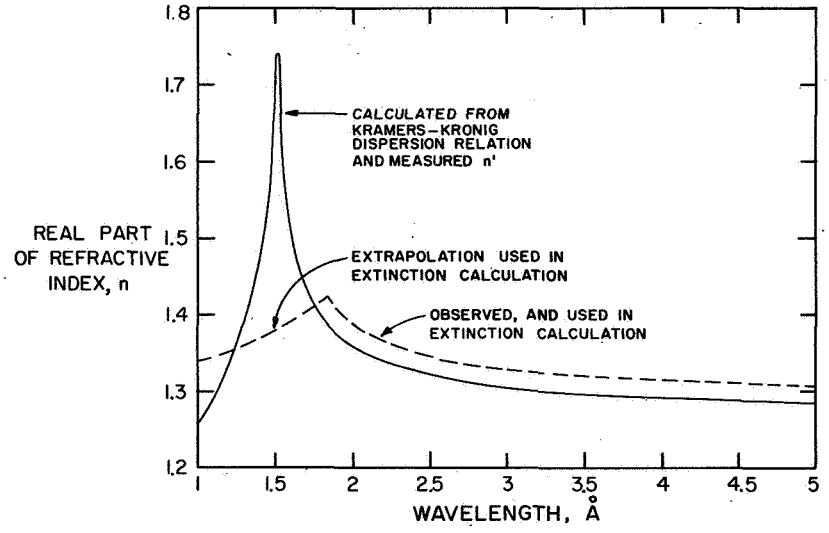

FIGURE 6.—Comparison of values of n for ice as observed in the laboratory and extrapolated for use in present paper (dashed line) with those calculated from observed values of n' (fig. 2) based on Kramers-Kronig dispersion relation. The agreement is complete above 1800 Å if a slight adjustment factor in α_0 is introduced, suggesting that the peak is probably real, and should be used in more accurate calculations.

n_0^2, the optical value, and this curve was extrapolated to meet the observed one. The results for pure water are represented by the dashed line in figure 6. Some increase at the absorption limit is introduced by the term $(n')^2$ in equation (A2).

A better approximation is obtained by evaluating the integral with some assumed value of n under the integral sign. A consistent first approximation if n' is small is evidently to take $n=1$ under the integral. It was found that α for water could be represented by

$$\alpha=\alpha_0 \qquad \nu>\nu_0$$

$$\alpha=\alpha_0 \exp\left[(\nu-\nu_0)/\Delta\nu\right] \qquad \nu<\nu_0$$

with $\alpha_0=4.0\times10^5/\text{cm}^1$, $\lambda_0=c\nu_0=1.57\times10^{-5}$ cm, and $\Delta\lambda=\lambda_0^2\Delta\nu/c=2.3\times10^{-7}$ cm. With such a representation, equation (A2) can be calculated analytically to obtain

$$n^2=(n')^2+1+\frac{\lambda_0\alpha_0}{2\pi^2}g(x,x_0) \tag{A3}$$

where $x=\nu/\Delta\nu$ and $x_0=\nu_0/\Delta\nu$. The dominant terms in the expansion of the function $g(x, x_0)$ for x close to x_0 are

$$g(x,x_0)=\frac{x_0}{x}\left[\ln\frac{x_0+x}{x_0-x}-\frac{1}{x+x_0}+e^{(x-x_0)}Ei(x_0-x)\right] \qquad x<x_0$$

$$g(x,x_0)=\frac{x_0}{x}\left[\ln\frac{x+x_0}{x-x_0}-\frac{1}{x+x_0}+e^{(x-x_0)}Ei(x_0-x)\right] \qquad x>x_0$$

where Ei is the exponential integral function. These functions have the common value

$$g(x,x_0)=\ln 2\gamma x_0-\frac{1}{2x_0}$$

where $\ln\gamma$ is Euler's constant at $x=x_0$, the absorption edge, as a result of the cancellation of the logarithmic singularity of the first term with that of the exponential integrals. Away from the absorption edge the initial terms alone are accurate to within inverse powers of $(x-x_0)$.

A plot of n calculated from equation (A3) is shown in figure 6. The large peak is absent in the cruder estimate. This peak seems quite reasonable when one reflects that the integral operator is in some ways similar to differentiation—for example, when applied to a symmetrical resonance peak representing α, it yields the antisymmetric resonant dispersion curve. Hence, the peak here is due to the rapid increase in α at the ab-

sorption edge, and its width in some sense is defined by $\Delta\nu$. It can be seen that there is a good correspondence with the shape of the refractive index observed in the laboratory, so that the first approximation to the solution of the integral may be fairly accurate. The difference between the curves disappears with a slight adjustment of the value of $\lambda_0\alpha_0$.

REFERENCES

1. DANIELSON, R. E.; WOOLF, N. J.; and GAUSTAD, J. E.: A Search for Interstellar Ice Absorption in the Infrared Spectrum of Mu Cephei. Astrophys. J., vol. 141, 1965, p. 116.

2. DRESSLER, K.; and SCHNEPP, O.: Absorption Spectra of Solid Methane, Ammonia, and Ice in the Vacuum Ultraviolet. J. Chem. Phys., vol. 33, 1960, p. 270.

3. VAN DE HULST, H. C.: The Solid Particles in Interstellar Space. Rech. Astron. Obs. Utrecht, vol. 11. pt. 2, 1949.

4. WICKRAMASINGHE, N. C.: Roy. Astron. Soc., Monthlv Notices, vol. 130, 1965, p. 221.

5. JOHNSON, J. C.; and TERRELL, J. R.: J. Opt. Soc. Am., vol. 45, 1955, p. 451.

6. BOGGESS, A.; and BORGMAN, J.: Interstellar Extinction in the Middle Ultraviolet. Astrophys. J., vol. 140, 1964, p. 1638.

DISCUSSION

Lind: Did you say that, for the best fit, the 300-Å particle size referred to dielectric?

Field: Yes, but I should qualify that remark. At that time, I did not have the infrared data. I don't know what would happen there. In the range between 2200 Å and 8400 Å the data fit to 5 percent. Therefore, I am saying that one can get a rough fit and that is really all that is needed.

Lind: You would need about 10 times larger particles for dielectric fit.

Field: Again, I think that we should be quite precise about the size distribution we are talking about. I am saying that an exponential size distribution with a mean size of 500 Å is actually the best fit.

Greenberg: I doubt that one could get a match. How do you support the 0.05 imaginary part of the refractive index in the visible? The imaginary part of the index of refraction is extremely critical for particle sizes as small as those you have considered.

Field: I quite agree. I don't mean to overemphasize the fit in the visible. We are trying to show here the sensitivity to the size and composition in the UV.

Greenberg: However, if you make a realistic size for dielectric particles to give the extinction in the visible, then the sizes will be such that any spectral characteristics in the ultraviolet will be completely washed out.

Field: That may be.

O'Dell: Krishna Swamy and I did calculations similar to yours using the wavelength dependence, but we used a value of 0.06 for the imaginary part. When we used the new ultraviolet data and all the infrared data of Johnson, we were able to fit the curve reasonably well out in the infrared by shoving the size parameter—mantle size—down to about 800 Å; we still got a reasonable fit in the visible.

Field: I would like to ask again, is one forced to ice, at least in mantles, by Stecher's UV observations? Dr. Wickramasinghe didn't think so.

Wickramasinghe: I did not have available Stecher's observations below 2000 Å. These would seem to force one to ice mantles.

Donn: How did you determine the instability of a species as a function of temperature?

Field: Evaporation rates exceed the accretion rate.

Donn: How did you get the accretion rate? Did you assume that all incident oxygen atoms combined with hydrogen to yield H_2O, and similarly for ammonia and methane?

Field: Yes; I simply assumed that each atom of C, N, and O that hits the grain, sticks.

Wickramasinghe: Do you assume a constant sticking coefficient for the growth and a size-independent destruction probability?

Field: It is exactly the same formulation that you gave. As for Dr. Donn's question, I think he was referring to the evaporation temperature which I gave in figure 1. The refractive index effect that Dr. Wickramasinghe and Dr. Stecher are talking about for graphite is a spectroscopic identification similar to the UV extinction effect.

Lind: For the Kramers-Kronig relationship, it seems that you get quite a large discrepancy from what we have. Was this for water?

Field: Ice.

Lind: Was this a plot of the real part of the index of refraction?

Field: Yes; since ice has a sharp absorption edge there must be a large value of n.

Lind: The data that we have don't seem to go down so wildly in the ultraviolet. Did you get less than 1 for the real part?

Field: No. The dispersion relation won't permit this.

Some Problems of Interstellar Grains

J. MAYO GREENBERG AND A. C. LIND
Rensselaer Polytechnic Institute
Troy, New York

RADIATION FORCES ON GRAINS

THE INTERACTIONS OF GRAINS WITH RADIATION show up either as modifications of the radiation field (scattering, extinction) by grains or as modifications of grains by the radiation. The principal effects on grains are to control their temperature and to exert forces (radiation pressure). This paper presents some radiation pressure calculations which may be pertinent to the problem of propulsion of grains outward from very hot, bright stars or more generally OB complexes. The radiation force is equal to the rate of transfer of momentum to the grain, which is equal, in turn, to the net rate of loss of momentum in the incident beam of electromagnetic radiation. It is readily shown that this force F is given by

$$cF = C_{abs} + (1 - <\cos\theta>)\, C_{sc} \tag{1}$$

where c is the velocity of light, C_{abs} is the absorption cross section, C_{sc} is the total scattering cross section. The average value of the cosine of the scattering angle is given by

$$<\cos\theta> = \frac{1}{4\pi}\int_0^{2\pi}\int_0^{\pi} \frac{C_{sc}(\theta,\phi)}{C_{sc}} \cos\theta \sin\theta \, d\theta \, d\phi \tag{2}$$

where $C_{sc}(\theta, \phi)$ is the differential scattering cross section.

The scattering cross section C_{sc} is a function of the size and the optical properties of the grain and also of the wavelength of the radiation impinging on the grain. In figure 1 are shown the complex indices which are considered to be representations for a "dirty ice" grain. In figure 2 is shown the radiation pressure (given as force per unit volume) acting on grains of three different sizes in the presence of black-body radiation fields of temperatures from 1° K to 100 000° K. The radiation pressure forces are also given in table I. In order to calculate the force at some

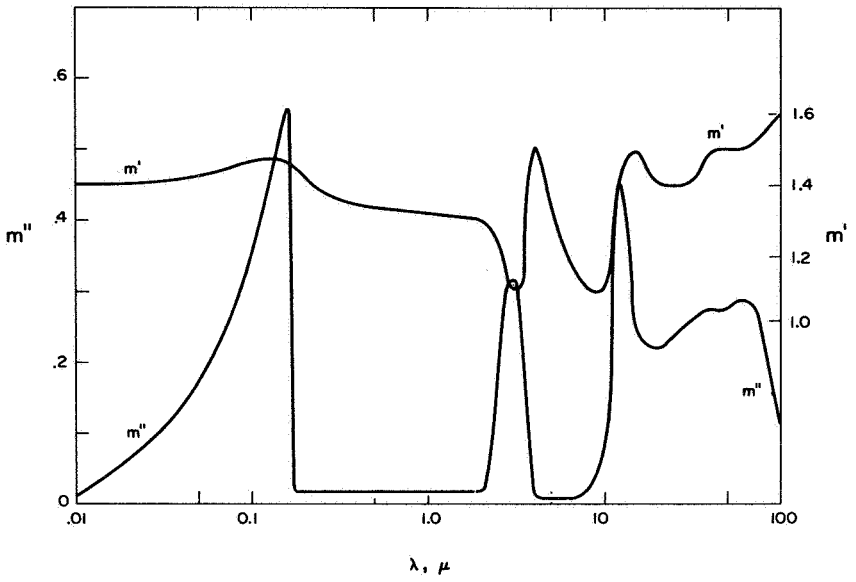

FIGURE 1.—Complex indices chosen as representative of ice grains. "Dirty ice" is arbitrarily given a value of $m''=0.02$ in the "visible" region to account for impurities. For dirty ice. $m=m'-m''i$.

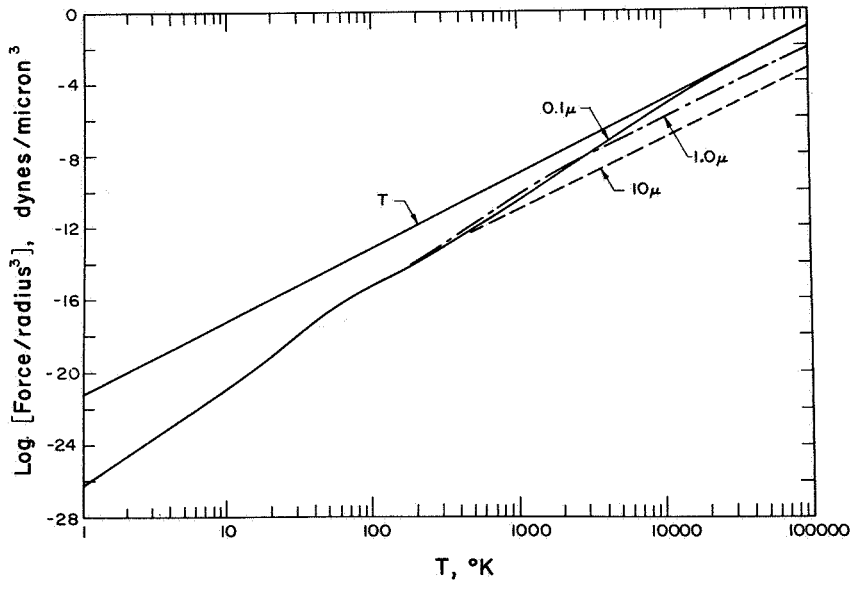

FIGURE 2.—Radiation forces on spherical dirty ice grains in the radiation fields of black bodies of various temperatures.

TABLE I.—*Radiation Pressure Forces*

Black-body temperature	Radiation force in dynes for sphere of radius—		
T, °K	0.1 μ	1 μ	10 μ
10	0.1415×10^{-23}	0.1415×10^{-20}	0.1521×10^{-17}
100	$.5197\times10^{-18}$	$.5360\times10^{-15}$	$.6872\times10^{-12}$
500	$.6478\times10^{-15}$	$.1074\times10^{-11}$	$.4834\times10^{-9}$
1000	$.2889\times10^{-13}$	$.4454\times10^{-10}$	$.7325\times10^{-8}$
1600	$.2262\times10^{-12}$	$.4162\times10^{-9}$	$.4545\times10^{-7}$
2500	$.1381\times10^{-11}$	$.2831\times10^{-8}$	$.2597\times10^{-6}$
3500	$.8030\times10^{-11}$	$.1146\times10^{-7}$	$.9696\times10^{-6}$
5000	$.7529\times10^{-10}$	$.4975\times10^{-7}$	$.3913\times10^{-5}$
7000	$.6163\times10^{-9}$	$.1923\times10^{-6}$	$.1462\times10^{-4}$
10 000	$.4587\times10^{-8}$	$.7731\times10^{-6}$	$.5944\times10^{-4}$
16 000	$.4509\times10^{-7}$	$.4651\times10^{-5}$	$.3805\times10^{-3}$
25 000	$.3104\times10^{-6}$	$.2566\times10^{-4}$	$.2236\times10^{-2}$
35 000	$.1226\times10^{-5}$	$.9444\times10^{-4}$	$.8536\times10^{-2}$
50 000	$.5054\times10^{-5}$	$.3806\times10^{-3}$	$.3541\times10^{-1}$
70 000	$.1878\times10^{-4}$	$.1430\times10^{-2}$	.1357
100 000	$.7449\times10^{-4}$	$.5859\times10^{-2}$	.5645

distance R from a star of radius r at temperature T, it is only necessary to multiply the values on the curves by a dilution factor $W=(r/R)^2$. One readily notes that in low temperature fields ($T<200°$) the radiation force per unit volume is almost the same for all the grains in the size range $0.1\ \mu \leq a \leq 10\ \mu$. For increasing stellar temperatures, the force per unit volume increases for the smaller grains relative to the larger ones until at about 20 000° K the force per unit area is roughly independent of the size so that the force per unit volume is inversely proportional to the size. For low temperatures, then, the ratio of radiation force to gravitational force is independent of the size, whereas in the neighborhood of sufficiently hot stars the ratio of radiation force to gravitational force is inversely proportional to the size.

Because the ratio of radiation force to gravitational force increases with size, the possibility exists for a differential ejection of particles of differing sizes, the larger ones remaining relatively closer to the stars. Compare, for example, the relative situation for ice grains of radii 0.1 μ and 1.0 μ in the neighborhood of a star whose temperature is 70 000° K. An 05 star is assumed whose size and mass are given by $\log (r/r_0)=1.3$ and $\log (m/m_0)=1.5$, where r_o and m_o are the radius and mass of the Sun taken as $r_o=6.96\times10^{10}$ cm and $m_o=1.99\times10^{33}$ g. For grain sizes $a \leq 1\ \mu$, the force ratio of radiation to gravity is $F_{rad}/F_{grav} \geq 10^5$, so that

the gravitational force may be neglected entirely in calculating the ejection of grains in the neighborhood of such a star. If it is assumed that the grain reaches a terminal speed v_t relatively soon, the terminal speed is then given by $F_{rad} = n_H A m_H v_t^2$, where n_H and m_H are the number density and mass of hydrogen atoms (or ions) and A is the cross-sectional area of the grain. As the grain recedes from the star, the radiation force decreases as the dilution factor $W = \left(\frac{r}{R}\right)^2$. The speed of ejection is then given by

$$v_t^2 = \frac{F_{rad}}{n_H A m_H} W \tag{3}$$

For $A = \pi a^2$, $n_H = 1/\text{cm}^3$, $m_H = 1.6 \times 10^{-24}$ g, the terminal velocity of the 0.1-μ grain is

$$\begin{aligned} v_t(0.1) &= \left[\frac{0.188 \times 10^{-4}}{(1 \times 3.14 \times 10^{-10})(1.6 \times 10^{-24})}\right]^{1/2} \left(\frac{r}{R}\right) \\ &= 1.94 \times 10^{14}\ (r/R)\ \text{cm/sec} \end{aligned} \tag{4}$$

The terminal velocity of a 1.0-μ particle is less by a factor of $(1.43/1.88)^{1/2} = 0.87$. Thus it appears that there is a separation effect. In solving equation (4), we write $v_t = \frac{dR}{dt}$ and obtain for the distance of ejection as a function of time

$$\begin{aligned} \frac{R^2 - r^2}{2r} &= (1.94 \times 10^{14})t \qquad a = 0.1\ \mu \\ &= (0.87 \times 1.94 \times 10^{14})t \qquad a = 1.0\ \mu \end{aligned}$$

The time scale for particle motion to a distance of 10 parsecs (roughly the order of size of the Orion nebulosity) is given by

$$\begin{aligned} t &= 0.25 \times 10^{-14} R^2/r \\ &= 5 \times 10^5 \text{ years} \end{aligned}$$

This is not an unreasonable estimate of the ages of the stars in Orion and it then appears possible for significant changes due to radiation pressure effects to occur in the size distribution of the grains.

EXTINCTION BY CORE MANTLE GRAINS

The suggestion in reference 1 tnat the graphite particles may be an important and perhaps dominant feature in the interstellar grains has led to the further possibility that these grains may form cores upon which dielectric mantles may grow. In figure 3 is shown a series of normalized extinction curves for various size distributions of dirty ice mantles on spherical graphite cores of radius 0.05 μ. The indices of

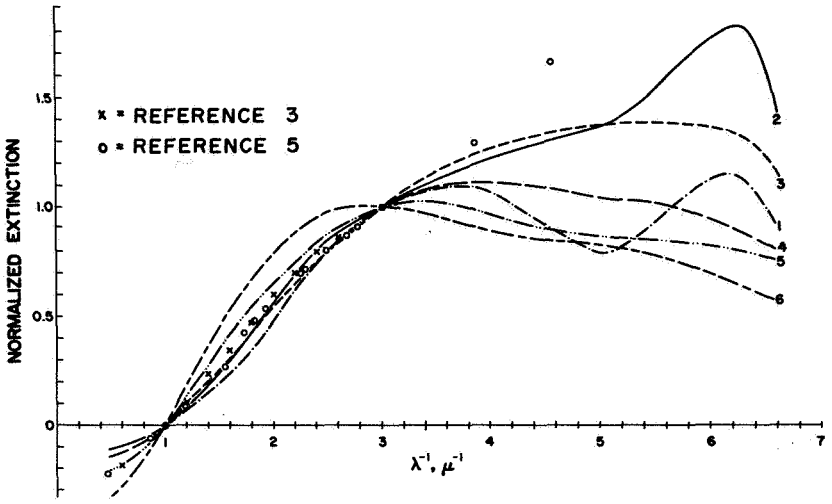

FIGURE 3.—Comparison of theoretical extinction curves for spherical core mantle grains (0.05-μ graphite core plus ice mantle) with observations of interstellar extinction. Mantle size distribution $n(a) = \exp\ [-5(a/a_i)^3]$; $a_i = 0.1\ \mu - 0.6\ \mu$, curves labeled 1 to 6, respectively.

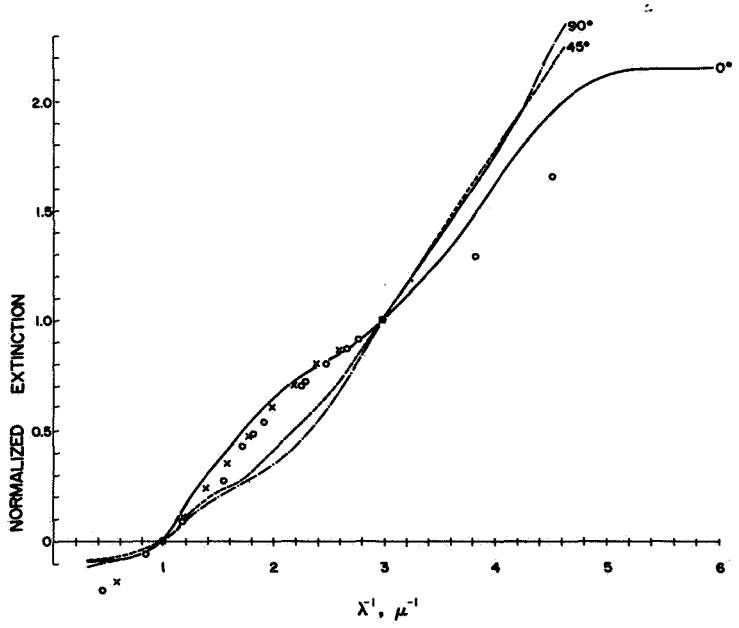

FIGURE 4.—Comparison of theoretical extinction curves for spinning dielectric ($m = 1.33$) cylinders of radius $a = 0.095\ \mu$. The angles 0°, 45°, 90° denote values of the angle between the plane of rotation of the cylinders and the line of sight.

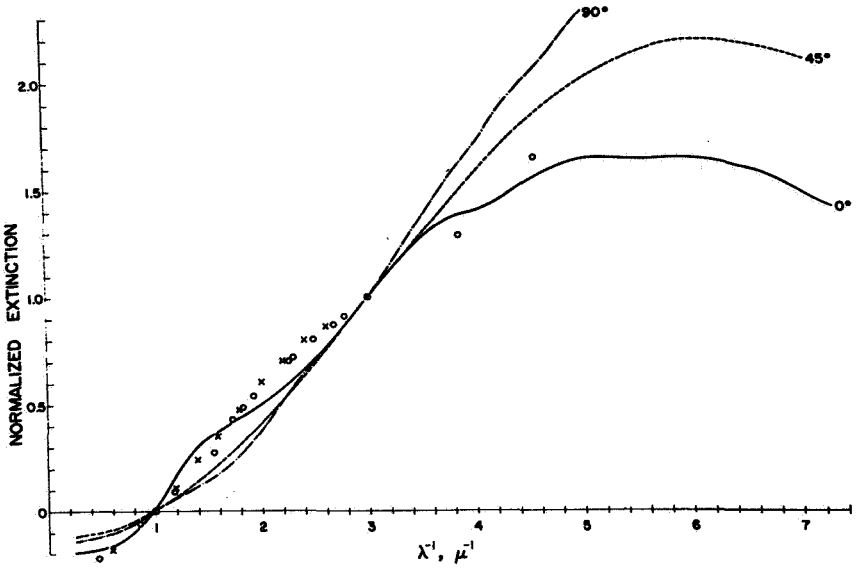

FIGURE 5.—Comparison of theoretical extinction curves for spinning dielectric ($m=1.33$) cylinders of radius $a=0.127\,\mu$. The angles 0°, 45°, and 90° denote values of the angle between the plane of rotation of the cylinders and the line of sight.

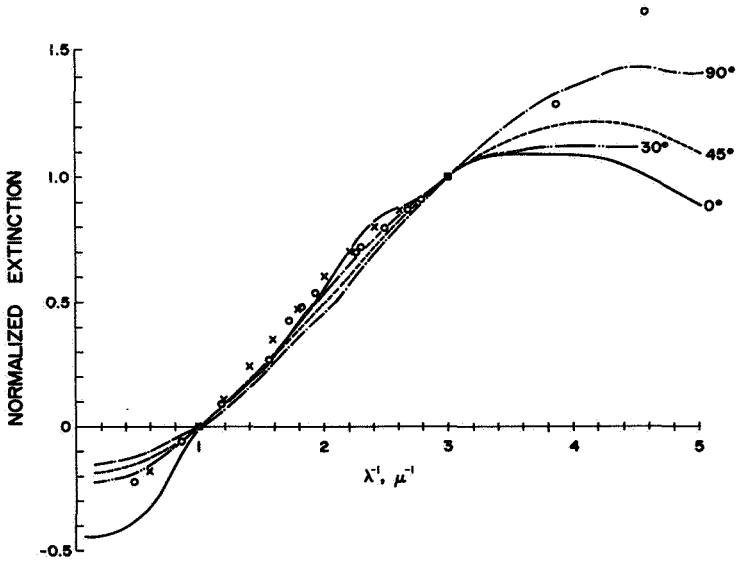

FIGURE 6.—Comparison of theoretical extinction curves for spinning dielectric ($m=1.33$) cylinders of radius $a=0.19\,\mu$. The angles 0°, 30°, 45°, and 90° denote values of the angle between the plane of rotation of the cylinders and the line of sight.

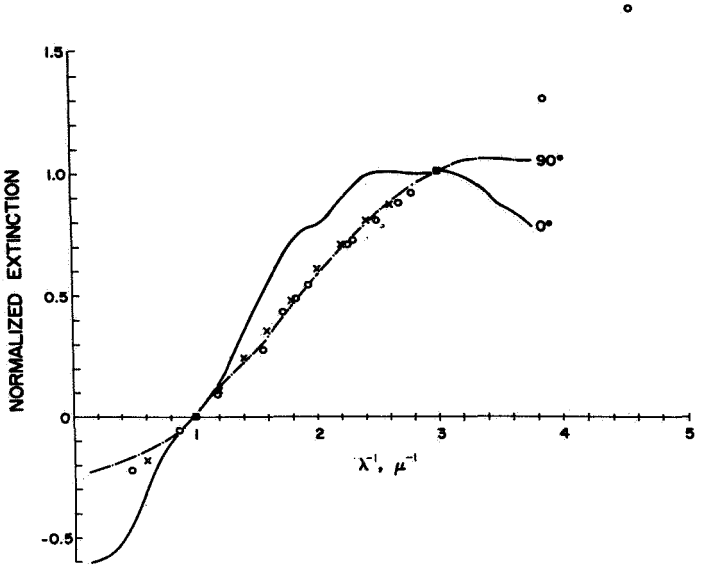

FIGURE 7.—Comparison of theoretical extinction curves for spinning dielectric ($m = 1.33$) cylinders of radius $a = 0.254\ \mu$. The angles 0° and 90° denote values of the angle between The plane of rotation of the cylinders and the line of sight.

refraction of the graphite are taken from reference 2. Comparison is made with the observed extinction for $\lambda^{-1} < 3\ \mu^{-1}$ in references 3 and 4 and for $\lambda^{-1} > 3\ \mu^{-1}$ in reference 5. The curve labeled as number 1 corresponds to a mantle size distribution which is almost negligible and therefore is essentially indistinguishable from the extinction which one obtains for the graphite core alone. It should be noted that only for a small (but not too small) mantle size can a reasonable match to the observed extinction in the ultraviolet as well as the visible be obtained. This effect was previously noted in reference 6 in calculations using a somewhat different form for the graphite refractive indices.

EXTINCTION BY INFINITE DIELECTRIC CYLINDERS

The calculations presented in the paper of this compilation by Greenberg and Shah are shown here in figures 4 to 7 as normalized extinction curves for a range of selected single sizes. As before, particles in perfect Davis-Greenstein spinning orientation about magnetic field directions making different angles with the normal to the line of sight are considered. Thus, 0° and 90° correspond to directions of the magnetic field B perpendicular to and along the line of sight, respectively. Comparison is made with the same observational points that are shown in figure 3. It appears that elongated particles in a size range between $a = 0.095\ \mu$

and $a=0.127\ \mu$ may provide a good overall fit to the average extinction in the ultraviolet as well as in the visible region.

REFERENCES

1. BOGGESS, A., III; and BORGMAN, J.: Interstellar Extinction in the Middle Ultraviolet. Astrophys. J., vol. 140, 1964, p. 1636.

2. GREENBERG, J. M.: The Optics of Interstellar Grains. Proceedings of the I.A.U. Symposium No. 24: Spectral Classification and Multicolor Photometry. (Saltsjobäden, Sweden), 1964.

3. HOYLE, F.; and WICKRAMASINGHE, N. C.: On Graphite Particles as Interstellar Grains. Roy. Astron. Soc., Monthly Notices, vol. 124, 1962, p. 417.

4. JOHNSON, H. L.; and BORGMAN, J.: The Law of Interstellar Extinction. Bull. Astron. Inst. Netherlands, vol. 17, 1963, p. 115.

5. WHITFORD, A. E.: The Law of Interstellar Reddening. Astron. J., vol. 63, 1958, p. 201.

6. WICKRAMASINGHE, N. C.; and GUILLAUME, C.: Interstellar Extinction by Graphite Grains. Nature, vol. 207, 1965, p. 366.

DISCUSSION

Wickramasinghe: Dr. Greenberg, I would like to refer to the curves you got for the graphite-core–ice-mantle case where you said you could not get a fit with the extinction curve by using the new graphite data. I have showed that one could get a very good fit by using a realistic size distribution; namely, an exponential size distribution of mantles around graphite cores of radii less than $0.6\ \mu$. The detailed fit depends upon the equilibrium size distribution.

Greenberg: The important difference between the mantles you used and those which we used lies in the choice of index of refraction. Your mantles have a pure real index of refraction, whereas our mantles have complex indices, as does ice in the ultraviolet. The use of complex indices has the effect of reducing the extinction in the ultraviolet and therefore, if the interstellar grain mantles are indeed icelike (have ultraviolet absorption like most dielectric substances), our calculations are more realistic. Furthermore, we have calculated extinction by various linear combinations of mantle size distributions ($n=\sum n_i e^{-5(a/a_i)^3}$) where size a_i defines a curve as shown in figure 3. These size distributions bear little resemblance to the Oort-van de Hulst distribution and, therefore, the theoretical extinction curves which we obtain for these distributions are quite general and they involve as many as seven parameters. In any case, none of these linear combinations can produce an extinction in the ultraviolet relative to the visible larger than that given by curve (2) in figure 3.

Wickramasinghe: For the mantle distribution obtained from my theory, I get perfect fit with the Cygnus curve all the way down from the infrared measurements of Johnson, through the curve of Nandy in

the visible including the knee, to ultraviolet points of Boggess and Borgman.

I would also like to question the fact that you can get a good fit with your ice cylinders. For a curve of extinction efficiency Q_{ext} as a function of $2\pi a$ times inverse wavelength for a single ice sphere, I could make the curve go up wherever I wanted by choosing a sufficiently small particle size. The only problem here is that if one arranged to match the *UV* points he would get a curve bowed down in the visible. If you demand a close fit with the λ^{-1} curve in the visible, you are essentially using a very small region in the curve of Q_{ext} as a function of $2\pi a/\lambda$. Once you pin this down in the visible by choosing a, you are forcing the extinction curve to turn down beyond $\lambda^{-1} \sim 3\mu^{-1}$.

Greenberg: I think the fits I got for the various individual sizes were not very good. But the qualitative fits were not as bad as you say. Actually the relatively small infinite cylinders did not fit that badly. It should be noted that the extinction by the smallest cylinders (see fig. 4) was not necessarily bowed down in the visible as would have been the case for spheres whose diameters were equal to the cylinder diameter.

Wickramasinghe: My claim is that you get the same thing for single spherical isotropic ice spheres. By choosing the particle size small enough, one could make the curve rise at 2200 Å and go through the *UV* point, but the curve no longer fits the observations in the visible.

Greenberg: That is not correct.

Wickramasinghe: What I am trying to say is that the ice cylinders do not give a situation essentially different from the case of the spherical particle. The moment you fit your λ^{-1} curve in the visible (the best determined part of the interstellar extinction curve) accurately, your curve immediately goes down in the ultraviolet.

Greenberg: That is incorrect. There is a noticeable difference between long and spherical particles of diameter $2d = 0.2\,\mu$. The extinction by the spherical particles of diameters of the order of $2a = 0.2\,\mu$ will not go up as high in the ultraviolet and still be reasonably matched to observations in the infrared.

Wickramasinghe: I don't agree.

Greenberg: The size distribution of the nonspherical particles, which appear to fit the extinction, has radii which are somewhat smaller than I would have anticipated on the basis of spheres. The major difference in the ultraviolet extinction would be a function of both the size as well as the orientation.

Nandy: If the variation in the ratio of the slope of the ultraviolet relative to the blue is not dependent on the orientation properties of the particles, is it conclusive that the particles are not dielectric?

Greenberg: I think it might be true. However, since the graphite is anisotropic in its scattering characteristics, it seems to me that the

graphite should also exhibit some differences in extinction. These differences are probably smaller because most of the extinction is characterized by the index of refraction; i.e., the absorption in the ultraviolet. For the dielectric particles, the extinction is characterized more by the particle shape. As I said before I would not expect the effect to extend as far into the ultraviolet for graphite as for dielectric particles.

Nandy: But there is yet another parameter: the coating of ice.

Wickramasinghe: For graphite, or graphite-core–ice-mantle grains, both the knee that Nandy gets and the ultraviolet observations emerge from physical properties of the graphite.

Greenberg: This is correct.

Wickramasinghe: I believe Stecher has obtained the computer output of the experimental data on the refractive index of graphite and it is quite noticeable that a change in the absorptive index takes place pretty close to $\lambda^{-1}=2.2\,\mu^{-1}$. This is the wavelength that Nandy gets for his kink.

Greenberg: I think that this deserves considerable attention. No theory that I know of on dielectric particles predicts any kink at $2.2\,\mu^{-1}$.

Field: One effect which I don't think has been accounted for in these radiation pressure calculations is the fact that these particles would tend to be coupled with the magnetic field. I have just calculated the gyrofrequency of the particles in the magnetic field for a charge of 1 electron. The value I obtained was 10^4 years. I also made some rough estimates of the charge that might be expected, and it would be on the order of 100 electrons, I believe, in an H II region. The result would be then that they gyrate every 100 years. The effect of radiation pressure, I think, would be to induce a drift perpendicular to B and to the radius vector, leading to a circulation of the particles rather than an outward expansion.

Greenberg: What fields do you use in the H II regions?

Field: I used 1 gamma as an example.

Greenberg: Is such a magnetic field in a H II region expected?

Field: I think you can argue that the magnetic field may be pushed out by expansion of the H II region if it is an old region; but young H II regions have not expanded and should contain whatever magnetic field was present before the ionization took place.

Greenberg: I would like a clarification on this. I had always thought that the H II regions were essentially free of even modest magnetic fields.

Hall: The stars in the directions of H II fields don't show any differences in polarization from that found for other stars.

Greenberg: That would seem to indicate the possibility of the same size magnetic fields.

Field: I think that the Oort-van de Hulst theory of clouds when they consider that the grains are essentially independent of the cloud during

the collision and then colliding with each other depends very critically on this question. If the grains are coupled to the magnetic field, and the field is coupled to the ions and atoms of the cloud, the grains would not be able to leave the cloud. Hence, the region of interpenetration of grains from various clouds would be much reduced and the rate of destruction might be reduced by a factor of 10 or 100.

Wickramasinghe: The sputtering could come in here, couldn't it?

Greenberg: We can always make and destroy grains. However, we certainly know they exist.

Diffuse Interstellar Lines and Chemical Characterization of Interstellar Dust

FRED M. JOHNSON
Electro-Optical Systems, Inc.
Pasadena, California

THE PROBLEM OF CHEMICAL IDENTIFICATION of the interstellar dust grains has vexed astronomers for over three decades. The earliest evidence for the mere presence of interstellar dust was deduced from the observation of stars (via star counts) in the Milky Way. The best presently available clues for possible chemical identification are spectroscope data, particularly the diffuse (hitherto unidentified) interstellar absorption lines. This paper is concerned primarily with a discussion of new theoretical interpretations of the spectroscopic data.

Much related information on the dust grains was obtained from observations of space reddening, its wavelength dependence, and from interstellar polarization. Furthermore, correlation of space reddening and the strength of some of the diffuse lines is important to the discussion of possible chemical identification of the dust.

The observed interstellar polarization requires asymmetrically shaped dust grains, and, according to the theory of Davis and Greenstein, they must be paramagnetic. References 1 to 24 contain much pertinent information on various aspects of the grain problem. An excellent introduction to the field is given in reference 1, and an extensive bibliography is found in reference 5. The chemical problems are discussed in reference 13; experiments on trapped radicals are described in reference 6; and a recent article (ref. 10) revives the graphite particle hypothesis. Theoretical discussions on the formation of dust particles and on other related topics on the interstellar medium are given in references 19 to 22. The fact that all identified interstellar molecular lines involve a carbon atom (OH excepted) makes it highly likely that grains could wholly or partly involve carbon.

Among the properties which these grains would have to satisfy are:

1. They are probably elongated dielectric particles (or semiconductors).

2. Their average size is about 10^{-5} cm.

3. Their density in space is between 10^{-25} and 10^{-26} g/cm^3.

4. The fact that they are paramagnetic follows from the fact that the polarization of starlight requires them to be oriented in the galactic magnetic field.

Of particular significance among the interstellar lines are the rather wide diffuse bands, mainly those at 4430 Å, 4760 Å, 4890 Å, and 6180 Å (ref. 14), and others recently discovered by G. H. Herbig. Table I lists the known theories on the identification of the diffuse lines. An abbreviated description of these theories and some remarks are included.

TABLE I.—*Suggestions for Identification of Interstellar Lines*

Author	Reference	Scheme	Remarks
A. Unsöld	17	Absorption of metallic particles of size λ	Theory cannot predict individual wavelengths of absorption lines
C. A. Whitney	25	Absorption of metallic particles of size λ	Some crude experiments to test Unsöld's theory
G. H. Herbig	26	Absorption bands arising from metastable ground state of H_2 molecule	Requires H_2 molecules in excited states; would account for 4430-Å band only
G. Herzberg	3	Predissociated bands of triatomic or polyatomic free radicals similar to HCO or transitions of O^-, C^-, N^-	No coincidences with interstellar lines so far
	27, 24		See reference 24
A. McKellar	28	Absorption lines in solid O_2	Would require matrix shifts—very suggestive for about three diffuse lines
J. R. Platt	29	Quantum effects in 10 Å to 100 Å size molecular-type particles	Particle-size dependent absorption wavelengths
F. M. Johnson	18	F-centers in alkali hydrides	Experimental width of F-center lines too wide at 4° K

TABLE I.—*Suggestions for Identification of Interstellar Lines*—Concluded

Author	Reference	Scheme	Remarks
E. E. Ferguson and H. P. Broida	30, 31	Molecular complex charge transfer Bands example	No coincidence found so far
P. Swings and M. Desirant	32		General discussion on absorption in spectra in solids at low temperatures
P. Swings and Y. Öhman	33	Suggest molecular crystals and amorphous metals	
F. M. Johnson	Present compilation	Hydrocarbons	Frequency analysis of all interstellar lines could be fitted to a simple pattern

MODELS FOR VIBRATIONAL ANALYSIS

A frequency analysis was made of the 18 interstellar diffuse bands provided by Dr. G. H. Herbig. It was found that these bands could be arranged in groups as shown in figure 1.

It should be noted that some of these energy differences are multiples of a mean value, an indication of the possibility for as yet undiscovered interstellar features. However, the absence of such missing lines does not necessarily invalidate this theory since variations of intensities of molecular lines are well known. (See ref. 34.)

Distinctive but previously unrecognized patterns corresponding to vibrational energy separations within electronic bands have been identified among the 18 diffuse interstellar lines. Each of the 18 lines falls into one of four groups. The first group contains two subgroups which occur in the vicinities of 4600 Å and 6100 Å, respectively, the former being the more diffuse. Both of these subgroups comprise a set of 3 lines with wavenumber separations of 556 cm^{-1} and 1568 cm^{-1}. The remaining 12 lines fall within a third group, also near 6100 Å, whose mean wavenumber separations can be sorted into 226 cm^{-1} or multiples thereof.

Since a vibrational analysis was thought to be suggestive of vibrational structure associated with complex molecules, the following models were considered: electronic-vibration transitions and inverse Raman effect. This latter phenomenon shows some interesting coinci-

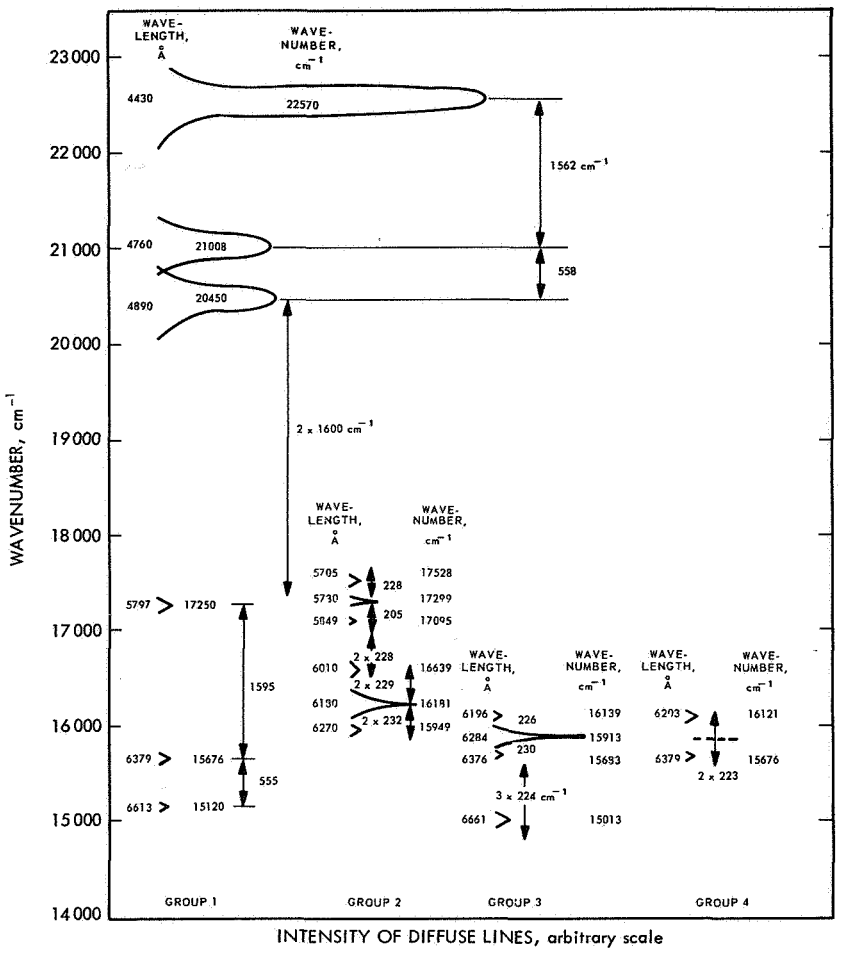

FIGURE 1.—Relative intensities and wavelengths of diffuse lines.

dences, and was, in fact, independently considered by B. P. Stoicheff; however, it is thought to be unlikely for several reasons discussed later.

Electronic-vibration transitions

If electronic-vibrational transitions are responsible for producing diffuse interstellar features, one requires transitions from the ground state to various excited states in these complex molecules or radicals. Examination of the literature of molecular spectroscopy reveals many hydrocarbons of the type $C_x-H_y-N_z$ having a large variety of vibrational frequencies close to those of interest. Some examples are C_2N_2 and diacetylene having vibrational frequencies of 226 and 231 wavenumbers, respectively, for the lowest electronic-vibrational states. Note that vibrational frequency in the excited states of the molecular

radicals is desired. It is possible that a variety of similar compounds embedded or associated with these grains may be involved. Thus one can explain the difference in the widths of the broad lines compared with the narrow lines of figure 1. A large selection of similar molecules would give a broader line, or the same set of molecules in different matrices might yield the diffuse lines (4430 Å, 4760 Å, and 4890 Å). Since the strongest absorption lines are the widest, it seems more likely that a larger selection of molecules is the more likely explanation for the width and stronger intensity. The symmetric line shape of the absorption lines might rule against this hypothesis, however. The fact that no single molecule fits the observed vibrational lines exactly indicates that perhaps a selection of similar molecular vibrations are superimposed to give these broad features.

One interstellar line (6379 A) is used in the figure twice. It could either belong to the 225 or 555 wavenumber system. The fact that energy differences corresponding to a mean value of 225 cm^{-1} can be established among the remaining 9 interstellar lines indicates that a molecular vibrational frequency corresponding to this value plays a dominant role in the production of these features. In order to produce these molecular vibrational electronic excited states, either free radicals or a much larger type of molecular complex would have to be postulated. This analysis clearly shows that experimental work is necessary in order to make a definitive identification of these features. One of the severe experimental difficulties in attempting to duplicate these astronomical stellar features in the laboratory lies in the fact that low-temperature absorption studies in the solid state reqüire substrates. These substrates can introduce "matrix"-shifts of as much as 100 Å. (See ref. 35.)

Inverse Raman effect

The theory of this phenomenon is described in references 36 to 39 and has been demonstrated experimentally, as discussed in reference 40. The probability of absorption of a frequency ν_0 and emission of ν_1 where $\nu_1 = \nu_0 \pm \nu_m$ for ν_m an arbitrary frequency is given by

$$\frac{16\pi^4}{h^4} \int \mu^2 \rho_0 \left(\rho_1 + \frac{8\pi h \nu_1^3}{c^3}\right) d\nu_0$$

where h is Planck's constant, c is the velocity of light, and μ is the matrix element for the two-photon process. The energy density ρ_1, at $\nu_0 \mp \nu_m$ is incident simultaneously with light at frequency ν_0 and density ρ_0.

Although order-of-magnitude calculations indicate that the probability of a two-quantum process is extremely small, a discussion and a corresponding frequency analysis based on this model is included. This model requires the simultaneous irradiation of the interstellar grains by

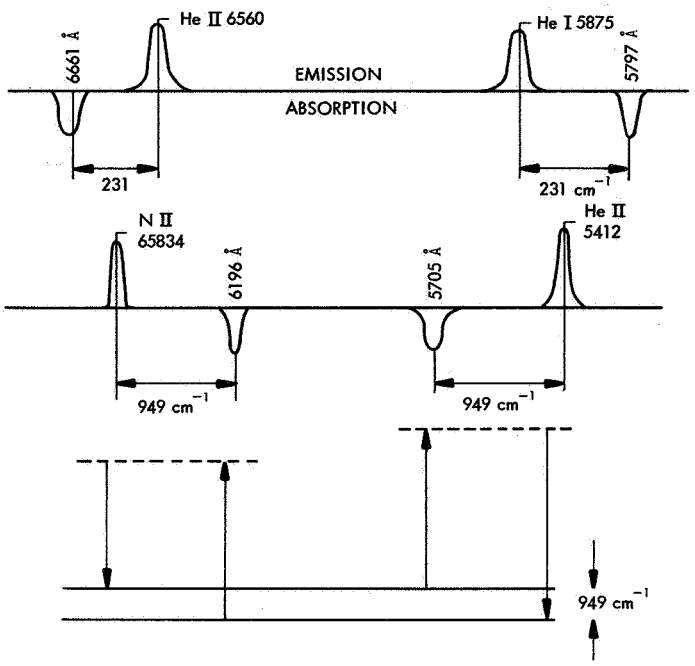

FIGURE 2.—Interstellar absorption and emission lines.

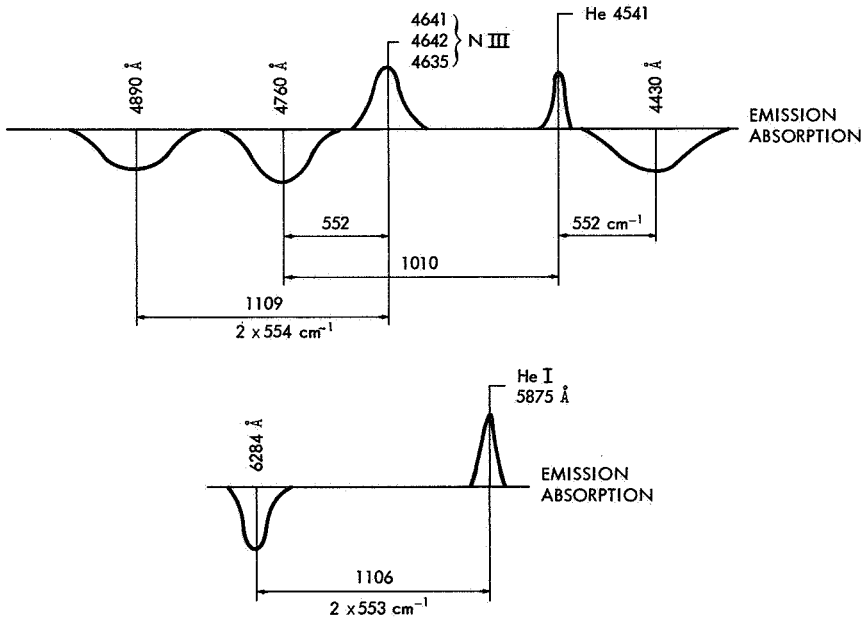

FIGURE 3.—Possible diffuse interstellar absorption lines.

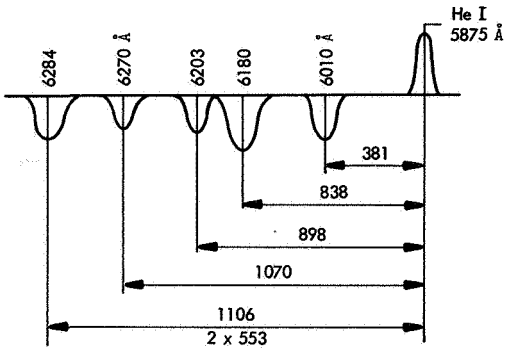

ALLENE	$CH_2 = C = CH_2$	838, 1071 cm^{-1}
CYCLOPENTENE C_5H_8	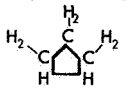	386, 896, 1104 cm^{-1}
CYCLOPROPANE C_3H_6	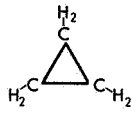	382, 1022, 1070, 1120 cm^{-1}
DIACETYLENE	$HC \equiv C - C \equiv CH$	231 ν_7, π_g, (ν_9)
CH_3CN	$C - C \equiv N$	380s ν_8 (e) BENDING VIBRATION

FIGURE 4.—Scheme for correlating "Stokes" absorption lines with an exciting source at 5875 Å.

emission lines ($\nu_0 \pm \nu_m$) as well as the usual stellar continuum. Both stellar as well as nebular emission lines were considered.

Because of the grain temperature (~ 4° K), all absorption transitions must arise from the ground state. Consequently, for both Stokes and anti-Stokes transitions to be observed, a pair of exciting sources are necessary.

Figures 2 and 3 show possible schemes satisfying these conditions. Figure 2 shows schematically the corresponding Raman transition through a virtual state. Figure 4 shows a possible scheme for correlating "Stokes" absorption lines with an exciting source at 5875 Å. With the exception of the 6284-Å line, all other absorption lines in figure 4 are inconsistent with the model unless corresponding anti-Stokes lines can be found. If this model were correct, it would be possible to identify these absorption features with well-known chemicals, such as allene, diacetylene, and a host of similar compounds. Table II lists some of these compounds with their pertinent vibrational frequencies. The width of

the diffuse lines could be accounted for on this model by two possible schemes: (a) a variety of similar chemical species; and (b) width of exciting source, in particular the blend of three exciting lines 4641 Å, 4642 Å, and 4635 Å comprising the N III source, which could account for the width of the wavelength 4430-Å, 4760-Å and 4890-Å diffuse lines.

Although more study is necessary to lend credence to the inverse Raman model, it is included here for completeness, particularly in view of the "pair coincidences" of a number of diffuse interstellar lines of figures 2, 3, and 4.

TABLE II.—*Vibrational Frequencies*

Compound	Vibrational frequencies, cm^{-1}
C_2H_3N	380
C_3H_8 propane	375
C_4H_8 dimethylethene	378
$C_2H_8N_2$ dimethylhydrazine	949
C_3H_6N dimethylcyanamid	526, 899, 1105
$C_3H_5N_2$	1010, 829
C_3H_5N	384, 545, 220, 1003, 835, 2245
C_2N_2	506, 250, 2336, 2150

CONCLUSION

Preliminary results of a vibrational analysis of the diffuse interstellar lines is strongly suggestive of electronic-vibrational transitions in complex hydrocarbon molecules and/or radicals associated with the interstellar grain. Since none of the laboratory spectra so far fit the astronomical data, one is probably dealing with either very complex hydrocarbon molecules or simpler molecules in electronic states not ordinarily achieved under normal laboratory conditions, such as those embedded in specific matrices. Since it has been difficult to fit the optical astronomical absorption data, it is hoped that, as an intermediate step, the vibrational data might provide clues to the chemical identification.

REFERENCES

1. GREENSTEIN, J. L.: Interstellar Matter. Astrophysics (J. A. Hynek, ed.), McGraw-Hill Book Co., Inc., 1951.

2. DUFAY, J.: Galactic Nebulae and Interstellar Matter. Hutchinson, London, 1957.

3. HERZBERG, G.: Laboratory Investigations of the Spectra of Interstellar and Cometary Molecules. Mem. Liège, vol. 15, 1955, p. 291.

4. DONN, B.: Survey of Theoretical and Experimental Research on Interstellar Grains. Lowell Obs. Bull., vol. 4, 1960, p. 273.

5. DONN, B.: Trapped Radicals in Astrophysics. (A. M. Bass and H. P. Broida, eds.), Academic Press, 1960, pp. 347–362.

6. ANON.: Formation and Trapping of Free Radicals. (A. M. Bass and H. P. Broida, eds.), Academic Press, 1960.

7. HERBIG, G. J.: Some Spectroscopic Problems of the Interstellar Medium. J. Quant. Spectr. Rad. Transfer, vol. 3, 1963, p. 529.

8. BASS, A. M.; and BROIDA, H. P.: Absorption Spectra of Solids Condensed at Low Temperatures from Electric Discharges. Mol. Spectros., vol. 2, 1958, p. 42.

9. PLATT, J. R.; and DONN, B.: Astron. J., vol. 61, 1956, p.11.

10. HOYLE, F.; and WICKRAMASINGHE, N. C.: On Graphite Particles as Interstellar Grains. Roy. Astron. Soc., Monthly Notices, vol. 124, 1962, p. 417.

11. WICKRAMASINGHE, N. C.; and GUILLAUME, C.: Interstellar Extinction by Graphite Grains. Nature, vol. 207, 1965, p. 366.

12. VAN DE HULST, H. C.: Light Scattering by Small Particles. John Wiley & Sons, Inc., 1957.

13. DONN, B.: Some Chemical Problems of Interstellar Grains. Mem. Liège, vol. 15, 1954, p. 571.

14. MERRILL, P. W.: Space Chemistry. Ann Arbor University Press, 1963.

15. PIKELNER, S.: Soviet Science of Interstellar Space. Philosophical Library, New York, 1963.

16. DAVIS, L.; and GREENSTEIN, J. L.: Polarization of Starlight by Aligned Dust Grains. Astrophys. J., vol. 114, 1951, p. 206.

17. UNSÖLD, A.: On the Interpretation of the Interstellar Absorption Bands. Z. Astrophys., vol. 56, 1963, p. 221.

18. JOHNSON, F. M.: Color Centers in Alkali Hydrides. Columbia University, Radiation Laboratory Progress Report, 1955, p. 30.

19. KAHN, F. D.: On the Formation of Interstellar Dust. Roy. Astron. Soc., Monthly Notices, vol. 112, 1952, p. 518.

20. SPITZER, L., JR.: Behavior of Matter in Space. Astrophys. J., vol. 120, 1954, p. 1.

21. BATES, D. R.; and SPITZER, L., JR.: The Density of Molecules in Interstellar Space. Astrophys. J., vol. 113, 1951, p. 441.

22. SPITZER, L., JR.; and TUKEY, J. W.: A Theory of Interstellar Polarization. Astrophys. J., vol. 114, 1951, p. 187.

23. GREENBERG, J. M.: Interstellar Grains. Am. Rev. of Astron. and Astrophys., vol. 1, 1963, p. 267.

24. HERZBERG, G.: Molecular Spectroscopy and Astrophysical Problems. J. Opt. Soc. Am., vol. 55, 1965, p. 229.

25. WHITNEY, C. A.: Exptl. Smithsonian Inst. Rept. No. 163, 1964.

26. HERBIG, G. H.: The Diffuse Interstellar Bands. I. A Possible Identification of λ4430. Astrophys. J., vol. 137, 1963, p. 200.

27. HERZBERG, G.: Publ. Roy. Obs. Edinburgh, vol. 4, 1964, p. 67.

28. MCKELLAR, A.: Astron. J., vol. 60, 1955, p. 170.

29. PLATT, J. R.: On the Optical Properties of Interstellar Dust. Astrophys. J., vol. 123, 1956, p. 486.

30. FERGUSON, ELDON E.; and BROIDA, H. P.: Charge-Transfer Absorption Spectra of NO in Kr and CH_3OH Solutions. J. Chem. Phys., vol. 40, 1964, p. 3715.

31. FERGUSON, E. E.; and BROIDA, H. P.: A Possible Mechanism for Light Absorption by Interstellar Grains, Astrophys. J., vol. 141, 1965, p. 807.

32. SWINGS, P.; and DESIRANT, M.: Ciel et Terre—No. 5, 1939, p. 160.

33. SWINGS, P.; and OHMAN, Y.: The Observatory, vol. 62, 1939, p. 150.

34. HERZBERG, G.: Spectra of Diatomic Molecules. Van Nostrand, 1950.

35. WELTNER, W., JR.; WALSH, P. N.; and ANGELL, C. L.: Spectroscopy of Carbon Vapor Condensed in Rare-Gas Matrices at 4° and 20° K. J. Chem. Phys., vol. 40, 1964, p. 5.
36. KRAMERS, H. A.; and HEISENBERG, W.: Z. Physik., vol. 9, 1931, p. 273.
37. GOPPERT-MAYER. M.: Ann. Physik., vol. 9, 1931, p. 273.
38. BREIT, G.: Rev. Mod. Phys., vol. 4, 1932, p. 504.
39. PLACZEK, G.: In Handbuch der Radiologie. (E. Marx, ed), vol. 6, pt. 2 Akademische Verlagsgesellschaft, Leipzig, Germany, 1934, p. 205.

DISCUSSION

O'Dell: Have you tried to evaluate this process quantitatively? For instance, you used the N III recombination lines which are extremely weak. You also used He II lines, which aren't at all common in H II regions.

Johnson: I know that these are very weak features, but I forgot to mention that the inverse Raman effect has been experimentally proved by someone in Canada.

O'Dell: The reason I mention this is that there are more common ions which just don't happen to fall in the region of the visible spectrum, and this very attractive mechanism may be just as well excited in the case of He I by 10 830. This is a line we do not consider in the spectrum, yet it is extremely intense in the H II regions and there are other ultraviolet lines. I wonder if perhaps you could present an even stronger argument if you include lines that you would expect to observe rather than just those that are?

Johnson: This is a good point. If these are indeed vibrational frequencies, you should get some of the higher overtones that would then take you into the UV; so perhaps one should look into the UV region.

Wickramasinghe: What is the number density or mass density that you require to produce the observed strengths of the interstellar lines?

Johnson: For mechanism two, I feel confident that there is enough strength to account for the interstellar lines because the *f*-values for unpaired electrons are quite high for these transitions.

Stecher: Do you have any estimate of the cross section? If you take diatomic molecules, such as H_2, the Raman scattering has a very small cross section, about 1 percent that of Rayleigh scattering.

Johnson: What I am doing is extrapolating the experimental results. There is a very small probability that the inverse Raman effect will occur. In fact, no one had seen it with incoherent light until the advent of lasers. It needed this high-intensity laser flash, plus a Stokes-shifted Raman line to give a continuum occurring at the same time. I tried to get the inverse Raman effect by using a flash lamp and a laser lamp and it was very difficult to do experimentally because the two pulses must occur at the same time or ordinarily just blackening of the plate results.

However, I am doing a lot of coherent Raman scattering work with lasers and I have recently been able to get the inverse Raman effect.

Donn: I think that the set of alternatives proposed here is a very exciting and stimulating argument for looking at the chemical theory of interstellar matter. It is a very constructive hypothesis, for it suggests various things that may be involved. One point of interest is that the basis of Wickramasinghe's suggestions for grains, various molecules may form and be ejected from these red giant stars. In fact, as calculations that have been made by Bauer and by Tsuji show, the atmospheres for these red giant stars contain many species of molecules of the kind suggested by Johnson. If this mechanism of mass exchange takes place through these cool stars, we may be feeding many such molecules into interstellar space, as Tsuji has already pointed out. This suggests that we may be able to tie together several features of interstellar matter.

With regard to the Raman scattering, I think that the coincidences are interesting, but because of the small cross sections for Raman scattering and the larger cross section for Rayleigh scattering, it would seem that if enough material were in space to give the Raman scattering for these lines, Rayleigh scattering would then give a significant contribution to interstellar extinction.

Greenberg: How many molecules would be required per unit of volume?

Johnson: I can only give you preliminary estimates. At the moment it doesn't look optimistic, but I don't have good numbers for the intensities of these emission features.

Dressler: In answer to Dr. Greenberg's question, I think I have given the relevant numbers in my paper. For instance, in the 4430-Å band the number of absorbing molecules times the f-value is on the order of $10^{-8}/\text{cm}^3$. When you compare that with a classical type of grain density, you get something like 10^{-5} absorbing molecules per bulk molecule of the grain. If these molecules are assumed to be in the grains and 10^{-3} is assumed as the f-value for that type of transition in the visible, it suffices to have a concentration of about 1 percent of the absorbing type of molecule in the grain. In other words, it is not necessary to have grains existing exclusively of these absorbing molecules.

Nandy: Your mechanism requires the presence of an emission line. If that emission has to be produced by the star, then 4430 Å should be present in the spectra of only those stars which show emission lines. Have you checked that?

Johnson: I have not done this. However, there are much more fundamental difficulties with the inverse Raman type than these astronomical ones; namely, you always need an emission line and you also have to start off with an anti-Stokes line. For some of the ones I showed

there are none of these anti-Stokes emission features, so it can be ruled out on that basis alone. But maybe I don't see the whole picture. Is it not correct that some observations have been made on the polarization of the 4430-Å feature?

Wampler: We now have a theory that we can check rather easily and observations can be obtained rather quickly. I am curious as to why you have only 24 lines; why don't you have a thousand lines in the spectrum? I would think there would be an enormous number of different types of simple molecules, and each of these would have two or three lines and very quickly the entire spectrum would be filled up.

Johnson: Maybe it is a question of strength. I picked out the ones which were strongest.

W. E. Thompson: It should be pointed out that when you come to the stage of attempting to identify carriers of these features, you need to consider the vibrational frequencies of the electronically excited molecules, not the ground state molecules. I expect that most of the molecular vibrational frequencies you have quoted were obtained by infrared or Raman measurements, and hence apply to the ground electronic state. They will be different in the excited state.

Johnson: That's a good point. These are for the excited state.

Walker: The inverse Raman effect is also an efficient scatterer of the appropriate emission line itself. Thus for the helium emission lines, for example, it is quite possible that we wouldn't detect an emission line of appreciable intensity. But the more serious criticism is that there is no absorption band associated with the Balmer series.

Johnson: But I threw out the Balmer series. I looked at Hα, Hβ, Hγ, etc., and I threw them out because I didn't see any pairing. I needed two emission lines; so I used Hα in conjunction with all the other emission lines and I could not get any sets. Maybe this is the wrong criterion to use. On the other hand, Hα is pretty far in the red and some emission lines farther in the blue region are desirable.

Field: In your second hypothesis you can predict whether the energy absorbed by the molecule will be accommodated to the solid or whether it will be immediately reemitted at the same wavelength, thus producing a scattering which might be observed.

Johnson: These features that you pointed out I think are worth investigating in detail.

Classical Grains and Platt Particles: Structural Characteristics and Interaction With Galactic Radiation

J. A. McMILLAN
Argonne National Laboratory
Argonne, Illinois

DURING THE LAST 20 YEARS much work has been done, both theoretical and experimental, that has improved the understanding of the nature and characteristics of interstellar grains; most of it, however, has not been primarily involved in this particular field. Unfortunately, the problem is extremely complex. As recently pointed out (ref. 1), an analysis of the nature and growth of interstellar grains calls for consideration of: (1) nucleation of condensing vapors; (2) mechanisms of crystal growth; (3) chemical reactions at low temperature including surface reactions of free radicals; and (4) radiation chemistry of solids. Simultaneous analysis of all these factors seems to be, at the present time, a hopeless endeavor. With the exception of radiation effects, separate analyses of each one have extensively been made. So far, however, it seems that combined effects cannot be overlooked. Partial aspects of the problem are discussed in this paper. The treatment of radiation is essentially exploratory, and its relative success ought not to blind us to the uncertainty of the data and to the speculative character of some of the assumptions.

CHEMICAL PROCESSES

Chemical reactions in interstellar grains must be intimately related to the mechanisms of growth. In the simplified assumption that growth takes place by incorporating with the grain all hitting atoms heavier than hydrogen (with the exception of the rare gases) plus the hydrogen atoms needed to saturate the lowest weight molecules, it is necessary to account for two factors; namely: (1) the evolution of heat accompanying chemical reactions; and (2) the possible existence of activation bar-

riers. The evolution of heat would warm up a local region favoring partial vaporization and structural rearrangement. The existence of activation barriers would deny the initial statement that all encounters must lead to chemical combination.

According to the simple picture given in the previous paragraph, chemical reactions would essentially be addition reactions between radicals, i.e., $OH + H \rightarrow H_2O$, $CH + H \rightarrow CH_2$, $N + H \rightarrow NH$, and so on. Eventual recombination of hydrogen atoms, adsorbed and diffusing on the grain surface, should yield molecular hydrogen that would soon evaporate, releasing to the grain a fraction of the recombination energy. (See ref. 2.) All these reactions should proceed, in the gaseous state, with little or no activation energy at all. Radicals attached to the grain, however, should behave differently, and activation energies of as much as 1 kcal/mole could reasonably be expected. Under such circumstances, the rate of growth could be reduced by a large factor. Subtraction reactions of the type $CH_4 + H \rightarrow CH_3 + H_2$, that could lead to polymerization and further cross-linking, would be much less probable since they should have larger activation energies. Mechanisms of polymerization and cross-linking could occur, however, as a consequence of reactions among radicals other than hydrogen. Since most heavy atoms, with the exception of the rare gases, have rather low ionization potentials, increasing consideration has lately been given to reactions involving ionic species. Whether or not their larger cross section for chemical reactions could compete with the overwhelming abundance of hydrogen has not yet been proved. In one way or another, it is clear that the simplified theory of growth is unsubstantial, and that more sophisticated mechanisms must be sought to account for the growth and nature of interstellar grains.

Radicals trapped in a classical grain seem to be improbable. Hydrogen atoms would not only attach to the grain but also diffuse through it with ease, pairing unpaired electrons with very small activation energy. A Platt particle, on the other hand, could indeed have unfilled electron bands since the hydrogen atoms would not enter the big, unsaturated molecule but probably react at the surface, if at all. With the recent discovery of the chemistry of rare gases, one is tempted to introduce them in the pattern of growth. Their potential role is discussed in reference 3. Such reactions would seem to be very improbable with the light elements helium and neon, whose abundance is significant, although their bearing in ionic reactions could be important. (See ref. 3.) Reactions with the heavier ones, whose abundance is small, are probably unimportant. The field, however, is open. It should be noted that consideration of the interaction of the grain with galactic radiation is imperative.

STRUCTURAL CHARACTERISTICS OF CLASSICAL GRAINS

An important question about classical grains is the extent to which their molecules are arranged in a regular pattern resembling the long-range order of crystalline material. Recent experiments presented in references 4 and 5 have provided values for the activation barriers of structural transformations that might occur in a classical grain. If one considers a grain of ice, in order to simplify the treatment one may ask, in view of its low temperature, whether it would be amorphous or crystalline. Low-temperature, low-pressure condensation of water molecules leads to an amorphous state of aggregation that undergoes the following experiences during warmup: (1) a glass transformation at about 140° K; (2) crystallization in the space group $F\bar{4}3m$ at about 150° K; and (3) recrystallization in the space group $P6_3/mmc$ at about 185° K. Table I, taken from reference 4, displays the values of the activation barriers of each transformation.

The fundamental difference between these experiments and the process of accretion in a classical grain of ice is that, whereas in the laboratory water molecules are collected and thus the energy corresponding to formation of van der Waals and hydrogen bonds and eventually the excess thermal energy is released, in space this process must be accompanied by the release of heat due to chemical reactions. If one avoids the primordial question of how the first atoms stuck together, one may start with a small grain (nucleus) that will grow by accretion. Formation of chemical bonds upon attachment of an additional atom (H or O) would warm up the grain above the crystallization temperature unless it were large enough to absorb the energy released by chemical bond formation without a significant temperature rise. In this latter case, it would be necessary to study the structural implications of local warmup.

In order to estimate the limiting size above which only local warmup

TABLE I.—*Activation Thermodynamic Functions for Different Low-Temperature, Structural Transformations of Water Substance*
[*From ref. 4*]

Transformation	Free energy, kcal/mole	Enthalpy, kcal/mole	Entropy, eu	Temperature, °K
Glass to supercooled liquid	8.8	.....	.....	ca. 140
Supercooled liquid to $F\bar{4}3m$	9.5	14.4	33	ca. 150
F43m to $P6_3/mmc$	[a] 12.9	7.4	[a] −30	ca. 185

[a] Fictitious values that probably include a small coefficient of transmission for activation, indicating dislocation-controlled growth.

could play a significant role, synthesis of a water molecule at the grain surface is assumed to occur with an energy release of 9 electron volts. The problem is further simplified by assuming that the saturated grain first fixes an oxygen atom, and then two hydrogen atoms (that might have been diffusing on the surface), each one releasing about 4.5 eV. If it is assumed that the initial temperature of the grain is 20° K and that if its temperature is raised by 100° K crystallization will occur at a measurable rate, the critical size comes close to 200 water molecules. Such a core should be crystalline and most likely hexagonal since the rise in temperature must have been larger while the grain was smaller.

It should be noted that the energy released by crystallization in the space group $F\bar{4}3m$ increases the temperature to a value very close to that at which recrystallization occurs in the space group $P6_3/mmc$. Further deposition should be considered for local heating and the seeding effect of the grain. In this case it seems that one has to deal with a competitive process between the half-life of the activated complexes leading to long-range order and the dissipation of heat into the bulk of the grain. It is not known whether dislocations would play a significant role in this type of mechanism since local heating could destroy local order in a region where the chemical attachment takes place. Since the energy released by a single chemical event is enough to warm up a number of molecules able to nucleate collectively, if this effect occurs faster than the dissipation of thermal energy to the bulk of the grain, one imagines the hypothetical grain as hexagonal and polycrystalline.

An alternative that would give utmost importance to the existence of dislocations would be to assume that the surface of the grain is saturated with diffusing hydrogen atoms, and that oxygen atoms are preferentially trapped at or near a dislocation. Chemical combination would take place mainly at the dislocation. If the heat only produced a transitory, reversible process of disorder in the surroundings of the dislocation, one should expect preferential growth of whiskers and platelets. Water molecules formed far from the dislocation could still diffuse toward it and incorporate in the lattice. In the case of crystallization of hydrazine monohydrate, the activation energy for self-diffusion drops has been observed to two-thirds in the molecular layers close to the growing crystal. This result supports the idea of having much smaller activation energies for surface diffusion in a vacuum.

These conclusions cannot be extrapolated without reserve to a classical grain of complex composition, but they nevertheless support the idea of a classical grain with the longest range order compatible with its chemical composition. As in the case of chemical reactions, introduction of galactic radiation completely changes the general pattern since the energies involved in this type of interaction are of the order of 30 eV. It is once more obvious that separate treatment of the different factors

affecting the growth and nature of interstellar grains may be hopelessly misleading.

INTERACTION WITH GALACTIC RADIATION

Although numerous speculations have been made regarding mechanisms of growth and size-determining factors, not until recently has degradation of grains by galactic radiation been quantitatively considered. (See ref. 6.) A tentative survival equation is derived by taking into account (1) the rate of growth; (2) the radiation dose rate; (3) the specific dose needed for destruction; and (4) the energy released by a single excitation process. No consideration is given to stopping mechanisms other than inelastic collisions.

In the simple theory of growth, the mass $m(t)$ of a grain at age t is

$$m(t) = kt^3 \tag{1}$$

where k is the tridimensional growth-rate constant. The constant k is related to the rate of growth k_0 (mass per unit area per unit time) by $k \cong 4k_0^3$. The surface of the grain has been considered proportional to $m^{2/3}$. An elongated, tridimensional grain accounting for polarization phenomena would still follow the rate law expressed by equation (1) with an uncertainty factor of order unity affecting the value of k.

The total dose of irradiation at age t is

$$W = \int_0^t D'm(t)\,\mathrm{d}t \tag{2}$$

where D' is the dose rate per unit mass. In order to simplify the treatment, the following three assumptions are made:

(1) The parameters k and D' have remained constant through the ages.

(2) Cosmic particles lose energy to the grain in discrete bursts of average value $\bar{W}_m$. In dealing with a single grain, setting equation (2) equal to W_m permits evaluation of the probable age at which the single event of interaction will take place.

(3) Complete vaporization of a grain occurs upon single absorption of a specific dose D_0.

The condition of survival may then be expressed by the inequality

$$W_m < D_0 m(t) \tag{3}$$

The probable age at which such an absorption will take place is given by

$$W_m = \int_0^t D'm(t)\mathrm{d}t \tag{4}$$

There will be, in general, a distribution around the root t of equation (4) accounting for those grains that will absorb W_m at earlier and later ages, as well as a distribution of values around W_m. Introduction of equation (1) into equation (4) and integration results in

$$W_m = \frac{1}{4} k D' t^4 \tag{5}$$

in view of the first assumption. Elimination of t by an appropriate combination of equations (1), (3), and (5) finally yields the equation of survival

$$64 k D_0^4 / (W_m D'^3) > 1 \tag{6}$$

Survival is therefore favored by large values of k and D_0, as well as by small values of W_m and D'. If the value of W_m is not essentially affected in dealing with very small grains—and this may be a weak point of this argument—one could expect a critical size below which interaction with radiation would lead to destruction. If this value is reached before absorption of the burst of energy W_m, the grain will have a significant chance of surviving; otherwise, it will vaporize. The next step is then to evaluate this size.

Since survival is favored by large values of k, it is assumed that growth takes place by incorporating with the grain all hitting atoms heavier than hydrogen (except the rare gases) and the hydrogen atoms needed to saturate the lowest weight molecules. Such an oversimplified theory of growth provides an absolute maximum for the growth-rate constant in H I regions of average density:

$$k = 6 \times 10^{-23} \text{ g/megayear}^3 \tag{7}$$

by adopting a simplified spherical grain and accepted values for the abundance of the elements and the temperature of the gas in H I regions, i.e., $k_0 \simeq 2.5 \times 10^{-8}$ g/cm^2-Myr. (See ref. 3.) The shape of the grain has no significant bearing on the treatment that follows, provided that it grows tridimensionally. A separate treatment is needed for platelets and whiskers in view of their exponential rate of growth.

The specific energy required for complete vaporization is evaluated in reference 7 as

$$D_0 = 6 \times 10^{21} \text{ eV/g} \tag{8}$$

A lower value is proposed in reference 6:

$$D_0 = 10^{21} \text{ eV/g} \tag{9}$$

with an uncertainty factor of order unity. Since the highest value of D_0

imposes the least stringent condition for survival, the result of reference 7 will be used.

Estimates of W_m vary from 30 eV (ref. 6) to as much as 100 eV (ref. 8). This energy is transferred as excitation of a small cluster of molecules and rapidly decays to either thermal motion or chemical dissociation, or both. For a metal, this energy is stored in the form of interstitials and vacancies. (See ref. 9.) The weak point of this treatment is that electronic excitation of a very small grain may result in ionization of the grain by loosing an electron that would carry out a large fraction of W_m. In the treatment that follows, this possibility is disregarded.

An estimate tending to favor survival is, therefore,

$$W_m = 30 \text{ eV} \tag{10}$$

By replacing the figures for the parameters in equation (6), one obtains the value of the maximum specific dose rate compatible with survival:

$$D'_M = 10^{21} \text{ eV/g-megayear} \tag{11}$$

Since the present estimate of the specific dose rate is 0.6 to 2.2 millirad/hr (ref. 10), i.e.,

$$D' = 3.3 \times 10^{20} \text{ to } 1.2 \times 10^{21} \text{ eV/g-Myr} \tag{12}$$

survival is improbable since the actual value of the growth-rate constant k is likely to be smaller, by orders of magnitude, than the maximum value derived from the simple theory of growth. The H I regions of high density, however, could eventually favor survival because of the weight of k_0 in the value of k, where $k = 4k_0^3$. The value of D_0 could not be seriously in error. Moreover, as has been pointed out in reference 6, it might be smaller, as indicated in equation (9), since destruction of a grain could be accomplished by its splitting into atoms, molecules, and smaller grains. Subject to the restrictions imposed by the indetermination of W_m in the case of very small grains, such an argument would strongly favor destruction in view of the weight of the term D_0^4 in the survival equation.

The maximum mass of a classical grain must then be given by

$$W_m/D_0 = m(t) \tag{13}$$

Replacing the values for the constants, one arrives at

$$m(t) = 5 \times 10^{-21} \text{ g} \tag{14}$$

which is too low to account for the optical properties of a classical

grain. The mass of a classical grain of three linear dimensions of order 0.5 micron and densities of about 1 g/cm^3 would be about 10^{-14} to 10^{-13} g, depending on the shape. Even whiskers could not weigh less than 10^{-18} g.

Whiskers must be treated separately, as follows: Assume a prism of square cross section a^2 and length z, which grows along the z-axis, at one end. The growth-rate equation is then

$$m_1(t) = \mu_1 \exp(k_1 t) \tag{15}$$

where μ_1 is the mass of the initial nucleus. The constants k_1 and k are related by

$$k = 4k_0^3 \tag{16}$$

$$k_1 = 4k_0/a \tag{17}$$

where k_0 is the rate of accretion in g/cm^2-Myr, the density of the grain having been assumed to be 1 g/cm^3. Equations (15) and (16) are easily derived by considering the volume and surface of a spherical grain, $\frac{4}{3}\pi r^3$ and $4\pi r^2$, and the volume and surface area of a whisker, za^2 and $4az + 2a^2 \cong 4az$, respectively. In the case of whiskers, it is supposed that atoms are adsorbed, diffuse, and eventually react, and that the products diffuse until they are trapped by the dislocation at one end.

The total radiation dose at age t for a whisker is

$$D = \mu_1 \int_0^t D' \exp(k_1 t)\mathrm{d}t = (\mu_1/k_1) D' \exp(k_1 t) \tag{18}$$

The survival equation for whiskers results from considering, again, equations (3) and (4):

$$k_1 D_0/D' > 1 \tag{19}$$

or, introducing equation (17):

$$4k_0 D_0/aD' > 1 \tag{20}$$

Survival is therefore favored by small values of a. Since equations (15) to (20) are valid only for small values of a (because the term $2a^2$ was neglected in the grain surface) the value

$$a = 10^{-7} \text{ cm} \tag{21}$$

is assumed. By using $k_0 = 2.5 \times 10^{-8}$ g/cm^2-Myr and the value of D_0

given by equation (8), one arrives at the maximum dose rate compatible with whisker survival

$$D'_w = 3 \times 10^{21} \text{ eV/g-Myr} \tag{22}$$

which is essentially in agreement with the value derived for tridimensional grains (eq. (11)). The maximum mass of a whisker would again be given by equations (13) and (14); i.e., three orders of magnitude smaller than the mass of a whisker of $a = 10^{-7}$ cm and $z = 5 \times 10^{-5}$ cm and density close to unity. However, the chance of survival of thicker whiskers may be higher, although it seems that the chance of survival could hardly counterbalance the significantly lower, actual values of the rate of growth. A similar treatment of platelets leads to comparable results.

The point made in a preceding paragraph about having an electron expelled from the grain, carrying out a large fraction of the energy burst W_m, may be considered again in the case of a whisker. The probability of such a loss would seem, in this case, to be independent of size, because both surface and mass grow at the same rate for a constant cross section. One may then assume, in order to estimate the importance of such a loss, that interaction with the outer layer (about 10^{-8} cm wide) would lead to the loss of an energetic electron, while interaction inside that layer would transfer the energy W_m to the grain. In the assumption of a whisker of square cross section of edge $a = 10^{-7}$ cm, the ratio of the volume of the layer to the total volume of the grain is about 0.4. In order to account for the loss of energy by the expelled energetic electrons, one may multiply D' by the probability of bulk transfer 0.6 and use this value in the survival equation. Although introduction of this factor slightly favors survival, the results remain practically unchanged since the rate of growth is likely to be much smaller.

One may conclude that, in view of the present estimates of the intensity of the galactic radiation—assumed to be uniform throughout space—and the abundance of elements, classical grains of the proper size are unlikely to exist (perhaps with the exception of the very high density H I regions), unless one accepts the idea of reference 11 that a solid grain can result from evaporation of a larger grain.

In the case of a Platt particle, the value of D_0 should be at least 10 times larger since it would be necessary, in order to destroy the grain, to break chemical bonds. By adopting the minimum value of the galactic specific dose rate of equation (12), one may estimate the minimum value of the growth-rate constant of equation (1) above which a tridimensional Platt particle could survive. The result is

$$k_P = 7 \times 10^{-30} \text{ g/Myr}^3 \tag{23}$$

271-992 O-67—17

or 10^7 times smaller than the maximum value provided by the simple theory of growth. This leads to a value of k_0 that is $10^{7/3}$ smaller than its maximum value. The age of a Platt particle, estimated with this value of k_P by neglecting effects that could tend to decrease its size by partial decomposition, would then be of the order of 1 gigayear. Should growth of a Platt particle be interpreted as an increase of the molecular weight by chemical attachment of gaseous matter, it would be reasonable to expect an average activation energy. In the absence of steric factors (entropy of activation close to zero), an average activation energy $E^* = 1.28$ kcal/mole (about 0.05 eV per impinging atom, equivalent to a kinetic temperature of 640° K) could account for the factor $10^{-7/3}$ in k_0, since the term $\exp(-E^*/rT)$ would have that value at $T = 100°$ K, the temperature of interstellar gas in H I regions. One may then conclude that if there is an average activation energy for growth of a Platt particle, it must be less than 1.3 kcal/mole.

FINAL REMARKS

The least compromising conclusion is, perhaps, that the assumption of a single class of grains may be oversimplifying, if not naïve. There are, however, certain speculative conclusions that may be advanced, subject to a revision of the present knowledge:

1. Classical grains are likely to be in a high degree of structural order, and grow by dislocation-controlled mechanisms leading to platelets and whiskers.

2. Classical grains are unlikely to have trapped radicals, although they may have a steady surface concentration of hydrogen atoms continuously recombining to produce hydrogen molecules that would evaporate. This latter process could provide enough energy for partial evaporation, enriching the grain in heavier elements. Whether or not this mechanism could account for the present size as estimated from optical properties seems difficult to decide.

3. If interaction with galactic radiation does not destroy classical grains at an early age, it could induce polymerization and cross-linking, as well as partial vaporization. Whether or not such a process could lead to Platt particles is still a matter of speculation.

4. Platt particles seem to be more probable, however, if the arguments on interaction with galactic radiation presented in this paper are essentially correct. One is then tempted to imagine a Platt particle as an unsaturated molecule, perhaps as old as the universe itself, in dynamic equilibrium with radiation—that would tend to destroy it—and the interstellar gas—that would tend to restore it.

5. There are at least two other possibilities that should be studied; namely: (1) further classical growth around a Platt particle; and (2)

growth around galactic debris expulsed from H II regions. This latter possibility would permit the investigator to avoid the puzzling mechanism that gave birth to the nuclei.

REFERENCES

1. DONN, B.: The Physics and Chemistry of Interstellar Grains. Am. Astr. Soc. Meeting (Lexington, Kentucky), Mar. 1965.

2. LEBEDINSKY, A. I.: Akademiia Nauk SSSR, Doklady, vol. 92, 1953, p. 507.

3. DONN, B.: Survey of Theoretical and Experimental Research on Interstellar Grains. Lowell Obs. Bull., vol. 4, 1960, p. 273.

4. MCMILLAN, J. A.; and LOS, S. C.: Nature, vol. 206, 1965, p. 806.

5. MCMILLAN, J. A.; and LOS, S. C.: Hydrazine-Water System II. Nonequilibrium Phase Transformations. J. Chem. Phys., vol. 42, 1965, p. 829.

6. KIMURA, H.: J. Astron. Soc. Japan, vol. 14, 1963, p. 374.

7. OORT, J. H.; and VAN DE HULST, H. C.: Gas and Smoke in Interstellar Space. Bull. Astron. Inst. Netherlands, vol. 10, 1946, p. 187.

8. SIEGEL, S.: Model for OH Radical Stabilization in Ice at 77° K under γ Irradiation. J. Chem. Phys., vol. 39, 1963, p. 390.

9. SEITZ, F.: The Effects of Irradiation on Metals. Rev. Mod. Phys., vol. 34, 1962, p. 656.

10. EVANS, D. E.; PITTS, D. E.; and KRAUS, G. L.: Venus and Mars Nominal Natural Environment for Advanced Manned Planetary Mission Programs. NASA SP–3016, 1965.

11. CERNUSCHI, F.: The Physics of Cosmic Grains. Astrophys. J., vol. 105, 1947, p. 241.

Formation of Molecular Hydrogen in Interstellar Space[1]

H. F. P. KNAAP, C. J. N. VAN DEN MEIJDENBERG,
J. J. M. BEENAKKER, and H. C. VAN DE HULST
Leiden University
Leiden, The Netherlands

ALTHOUGH SEVERAL ATTEMPTS at observing the interstellar hydrogen molecules in the ultraviolet or infrared are in preparation (ref. 1), these molecules are still undetected. They may form the most abundant unobserved constituent of the interstellar gas. The strongest indirect argument for the presence of these molecules lies in the fact that the density of atomic hydrogen observed by the 21-cm line goes down in some dark clouds, where the dust density and, presumably, the total gas density goes up by a large factor.

Inasmuch as the density in the interstellar clouds is of the order of 10 atoms/cm^3 and the temperature is only of the order of 100° K, any formation of molecules by atom-atom collisions is too slow to be of importance. The most eligible process for H_2 formation is recombination on the surface of an interstellar dust grain. Rate estimates of this process have been made in various degrees of detail, as reported in references 2 to 4. The case in which the atoms are bound to the grain surface by van der Waals forces, that is, by physical adsorption, is examined in these references. The binding at the surface then must be of such a type that two atoms can reach each other by surface mobility within the residence time on the grain surface, or before evaporation. In reference 4 it is pointed out that a large surface mobility, independent of temperature, exists as a consequence of quantum-mechanical barrier penetration (tunneling). A conversion time shorter than 10^8 years is found. However, some aspects of the problem are overlooked, and thus this conclusion may be wrong. Results presented herein show that physical adsorption of atoms on grains of the type proposed in reference 2 does not provide efficient conversion into hydrogen mole-

[1] The contents of this paper were published previously in the Bull. of the Astron. Inst. of the Netherlands, vol. 18, 1966, pp. 256-258.

cules within the age of the galaxy. The possibility of other, more efficient, models based on chemical absorption remains open.

RECOMBINATION BY PHYSICAL ADSORPTION

A Lennard-Jones interaction potential is assumed as follows:

$$\phi(r) = -4\epsilon\left[\left(\frac{\sigma}{r}\right)^6 - \left(\frac{\sigma}{r}\right)^{12}\right] \tag{1}$$

where ϵ and σ are constants and r is the distance between an H atom and any molecule of the grain surface. In view of the composition of the grains as proposed by van de Hulst, the quantity ϵ/k, where k is Boltzmann's constant, will have values between 60° K and 100° K, the latter value corresponding to the interaction with H_2O. By summing up the pair interactions the total potential energy of a single H atom can be calculated as a function of the position of the H atom with respect to the solid lattice. The minimum potential energy is then found to be $\phi_{min} = -6\epsilon$. (See ref. 5.) Classically the adsorption energy would be equal to $|\phi_{min}|$. Here the first deviation from the treatment of reference 4 occurs. According to quantum mechanics theory, the zero-point energy for a light particle restricted in space is appreciable. As a result, the adsorption energy for the H atom is significantly smaller than $|\phi_{min}|$. Under the conditions mentioned previously, the adsorption energy of an H atom at the grain surface is reduced from its classical value of 6ϵ to below 2.5ϵ. (See refs. 6 to 8.) A similar situation arises for the analogous problem of the heat of evaporation of a three-dimensional solid. Here the classical value for the heat of evaporation is 8.7ϵ. For light molecules, as, for example, H_2 and He, the heat of evaporation is reduced to 2.5ϵ and 0.7ϵ, respectively.

The following notation and numbers are assumed:

q_a adsorption energy, 2.5ϵ
ν_0 vibration frequency perpendicular to surface, 10^{12}/sec to 10^{13}/sec
T temperature of grain, arbitrary
S surface area of one grain, 10^{-8} cm^2
N number density of H atoms in cloud, 10/cm^3
T_g temperature of gas of H atoms, 100° K
V average velocity of H atoms at this temperature, 1.45×10^5 cm/sec
α sticking coefficient, 1/3
τ average residence time of an atom on a grain, $\frac{1}{\nu_0} \exp\left(\frac{q_a}{kT}\right)$ (2)

The justification for the numbers chosen is as follows: The sticking coefficient is experimentally found to be between 0.1 and 1.0 (refs. 9 and 10). The gas density is that often adopted for an average cloud. The average density near the galactic plane is much smaller, about

0.5/cm^3. The reason for employing the larger value is that the mean free path of the atoms between gas-kinetic collisions is small. An atom once present in a cloud of this density would move by diffusion not farther than 1 parsec in 10^9 years, so that it is released from the cloud only if the cloud itself expands or dissolves, which may occur in 10^7 or 10^8 years. Hence it seems appropriate to maintain the high density estimate during the entire time considered.

The gas temperature is chosen between the usually adopted 130° K and the lower values which may occur in dense clouds. The surface area of a grain follows from the best single-diameter fit to the extinction curve, which gives a diameter of 0.6 μ. Refinement by a distribution of grain sizes (refs. 2 and 3) gives at most a correction by a factor 2 in the conversion rate. The characteristic frequency ν_0 depends on the precise structure of the surface and can in any model be derived from the shape of the potential well.

A necessary condition for recombination is that during the time an H atom spends at the surface a second one arrives. This requires

$$\tau > (\alpha NVS)^{-1}$$

or

$$T < T_{max}$$

where

$$T_{max} = \frac{q_a}{k}\left(\ln \frac{\nu_0}{\alpha NVS}\right)^{-1} = 4.5° \text{ K to } 7.5° \text{ K} \tag{3}$$

A change by a factor of 100 in any of the quantities under the logarithm introduces a change of about 10 percent in T_{max}. The remaining uncertainty is fully in q_a. For temperatures above T_{max}, the probability of finding two atoms on the same grain is approximately

$$\frac{\alpha VNS}{\nu_0} \exp\left(\frac{q_a}{kT}\right) \approx 10^{-15} \exp\left(\frac{q_a}{kT}\right) \tag{4}$$

Already for $T = 1.1\ T_{max}$ the number of grains with two atoms is reduced by a factor 50 and the consequent average recombination time prolonged to 10^9 years. It may therefore be concluded that at the grain temperatures usually assumed, that is, 10° K to 20° K, the recombination mechanism based on physical adsorption of H atoms on the grain surface is completely ineffective.

The reason that this result deviates from the conclusion reached in reference 4 is twofold: (1) the effect of zero-point energy on q_a was not accounted for in reference 4, and thus q_a is reduced by a factor 2.4; and (2) it was implicitly assumed in reference 4 that an H atom by surface mobility could go on scanning an infinite area for the possible presence of other H atoms, whereas, in fact, the scanning area is limited to the surface of one grain.

FINAL REMARKS

The situation in the physical adsorption model is more favorable for deuterium atoms than for H atoms. Because the zero-point energy is smaller for the heavier D atoms than for H atoms, the adsorption energy for D atoms is larger.

Hence, D atoms will be adsorbed for longer times. From equation (3) is found a value of 10° K for T_{max} for HD formation; this value is larger than the value of T_{max} for H_2 formation. Therefore, if the grain temperatures were low enough for the process to work at all, selective disappearance of atomic D with respect to atomic H would occur and thus preferential formation of HD would result.

Although, at the actual grain temperature, physical adsorption provides an insufficient basis for the recombination of H atoms, a recombination process based on more complicated models is not ruled out. For example, a combination of physical and chemical adsorption might work quite well. Consider a grain with a number of sites on the surface where an H atom is chemically more or less permanently trapped; then the grain is virtually always occupied with H atoms. A physically adsorbed atom can reach a chemically adsorbed atom by surface migration before evaporation. As pointed out in reference 4, the surface mobility of a physically adsorbed atom is quite large because of quantum-mechanical tunneling. The proposed type of traps on the grain might result from radiation.

REFERENCES

1. VARSAVSKY, C. M.: Review Paper at COSPAR Symposium. (Mar del Plata), May 1965.

2. VAN DE HULST, H. C.: The Solid Particles in Interstellar Space. Rech. Astron. Obs. Utrecht, vol. 11, pt. 2, 1948.

3. MCCREA, W. H.; and MCNALLY, D.: The Formation of Population I Stars, Part II, The Formation of Molecular Hydrogen in Interstellar Matter. Roy. Astron. Soc., Monthly Notices, vol. 121, 1960, p. 238.

4. GOULD, R. J.; and SALPETER, E. E.: The Interstellar Abundance of the Hydrogen Molecule I. Basic Processes. Astrophys. J., vol. 138, 1963, p. 393.

5. STEELE, W. A.; and ROSS, M.: General Theory of Monolayer Physical Adsorption on Solids. J. Chem. Phys., vol. 35, 1961, p. 850.

6. DE BOER, J.; and BLAISSE, B. S.: Quantum Theory of Condensed Permanent Gases II. The Solid State and the Melting Line. Physica, vol. 14, 1948, p. 149.

7. LUNBECK, R. J.: Thesis, Amsterdam, 1951.

8. ROSS, M.; and STEELE, W. A.: Monolayer Adsorption of Helium on Argon. J. Chem. Phys., vol. 35, 1961, pp. 862–882.

9. HUNT, A. L.; TAYLOR, C. E.; and OMOHUNDRO, J. E.: Advances in Cryogenic Engineering, vol. 8, 1962, p. 101.

10. BRACKMANN, R. T.; and FITE, W. L.: Condensation of Atomic and Molecular Hydrogen at Low Temperatures. J. Chem. Phys., vol. 34, 1961, p. 1572.

DISCUSSION

Harteck: Are these theoretical or experimental results?

Knaap: Theoretical.

Harteck: For interstellar grains of a metal oxide, the absorption may be less for a water layer, or for oxygen, nitrogen, or carbon; but hydrogen atoms still should not act like a noble gas with mass 1.

Knaap: That is true. The absorption depends on whether the substrate is H_2 or water. It might be that H atoms are chemically trapped with sufficient mobility to reach each other on the surface.

Harteck: How do you suppose there would be a layer of hydrogen molecules on the surface? At 7° K the hydrogen would have evaporated.

Knaap: This is not necessarily true, because there is a balance between incoming H atoms and evaporating H_2 molecules. H atoms hit the surface, H_2 is produced, and subsequently H_2 molecules have a chance of evaporating ($\sim \exp(-q_a/kT)$). Hence, the chance of having a layer of hydrogen molecules depends on the amount coming in, the formation rate of molecules, and the number of molecules evaporating.

Harteck: But suppose I had solid hydrogen. The temperature still cannot be 6° K or 7° K.

Knaap: Certainly it would evaporate, if no new molecules were condensed or formed on the surface. That would even be true at a much lower temperature of, for example, 2° K, if one would wait long enough.

Harteck: The heat of evaporation of hydrogen is 204 calories; the heat of fusion is almost 84 calories. You have almost the heat of sublimation, or 304 calories. So you can see at 1° K or 2° K it never evaporates. There is a critical temperature for the density of hydrogen atoms in interstellar space where they cannot remain. I cannot remember the number but I think it is 5° K or 6° K. But at 2° K evaporation would never occur.

Knaap: The interaction energy of the H atom with the solid is obtained by placing the H atom above a crystal. For a number of positions of the H atom the distances to the atoms or molecules of the crystal are calculated. By summing the energies of all binary interactions the total interaction energy is obtained. This has been done with a computer for several positions of the H atom, and -6ϵ was found to be approximately the minimum potential energy of the H atom.

Donn: I think the possibility of experimentally studying these problems using molecular beam techniques is worth mentioning. It has been found that a very low hydrogen recombination probability exists except near 20° K, and that the anomalously large values there may have been caused by the condensation of water vapor to produce an ice coating. I think such experiments, carefully designed to study astrophysical problems, could furnish important data.

Knaap: Unfortunately, no direct experimental results are available. The experiments of Brackmann and Fite are not conclusive as to the absorption rate of H atoms.

Interstellar Dust and the H_2 Molecule

K. H. SCHMIDT
Jena Observatory
Jena, Germany

NEARLY 20 YEARS AGO van de Hulst stated that the formation of molecular hydrogen occurs on the surfaces of the interstellar grains. (See ref. 1.) In the last years several authors discussed the problem of the interstellar abundance of the H_2 molecule. (See refs. 2 to 9.) They all found that the percentage of the molecular hydrogen in the interstellar gas probably is much larger than had been thought in the past and that the essential mechanism of H_2 formation is the formation on the particle surfaces. Therefore, the formation rate of interstellar H_2 is a function of the area of the grain surface per unit volume, which is dependent on the average radius of the grains $\bar{a}$, on the number of dust particles per unit volume $N(\bar{a})$, and on the distribution function of the particle radii. The formation rate is determined by the density of the atomic hydrogen n_H and the temperature of the interstellar gas T_{gas}. Finally, the formation rate of H_2 depends on the probability π that an impinging hydrogen atom on a grain joins with another hydrogen atom to form a molecule. The formation rate of H_2 may be written as

$$\frac{dn_{H_2}}{dt} \approx n_H^2 \bar{a}^2 N(\bar{a}) k T_{gas}^{1/2} \pi \tag{1}$$

Here k is a factor characterizing the distribution function of the particle radii. It is seen from equation (1) that the formation rate of H_2 is very sensitive to the average radius of the grains. In other words, the abundance of interstellar H_2 will be different for classical and Platt particles. This is valid since $N(\bar{a})$ for the two types of dust particles is nearly of the same order. In figure 1, the dependence of the portion of the interstellar H_2 on the whole hydrogen density in interstellar space is shown for classical grains and Platt particles. The computations were made for different values of the probability π and a temperature of the interstellar gas of 100° K. Also shown is the abundance if the formation occurs in reactions of hydrogen with the H^- ion proposed in reference 10 and in reactions between hydrogen and the CH radical discussed in reference 2. For each formation type it was assumed that the dissociation of the

hydrogen molecules takes place only in an interstellar cloud passing a hot star, as proposed in reference 6. It is further assumed that the formation of H_2 occurs in the same manner on the surfaces of Platt particles as on classical grains. From this figure it follows that the H_2 abundance will be very low at normal densities of the interstellar gas if the Platt particles are responsible for the observed extinction and polarization. Otherwise, for classical grains and a value of π that is not too small, the abundance of the molecular hydrogen will be between about 10 and 90 percent at a density of some 10 hydrogen atoms cm^3 in an interstellar cloud.

Therefore, it is possible to decide the type of grains that are realized in nature from observations concerning the abundance of the interstellar hydrogen molecule. Unfortunately, direct observations of the H_2 molecule are not possible from the Earth because the absorption lines of the molecule lie in the ultraviolet and its emission lines lie in the far infrared. Thus, until observations are made from rockets or orbiting telescopes, indirect methods of determining the abundance of the interstellar H_2 must be found. One possibility follows from dynamic considerations. The discrepancy between the density observed in the Sun's vicinity and the density following from the force perpendicular to the galactic plane is examined in reference 4. The difference between these two values of the density is assumed to belong to the interstellar hydrogen molecule. A similar consideration was made in references 7 and 8, in which the K force was determined in small distances from the galactic plane by the density distribution perpendicular to the galactic plane and the velocity distribution of the interstellar gas. It was found from this and the observed density of the stars and the interstellar matter that an abundance ratio of molecular to atomic hydrogen as high

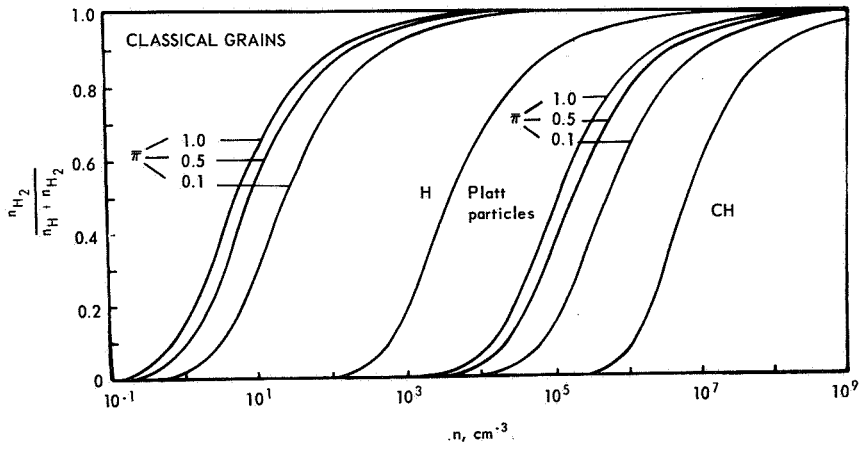

FIGURE 1.—Relative number density of hydrogen molecule in interstellar space for classical grains and Platt particles. $T = 100°$ K.

as 4 or 5 is quite conceivable. The K force was determined in reference 11 by using the density distribution perpendicular to the galactic plane and the distribution of radial velocities of the interstellar gas and cepheids. The obtained K force is valid only for small distances from the galactic plane up to about 100 parsecs. Therefore, for the normal to the galactic plane $z > 100$ pc the result was fitted with the two K forces determined in references 12 and 13. The dependences of K with z obtained in this manner are called models I and II, respectively. By the aid of Poisson's equation and Maartin Schmidt's model of the galaxy, the density distribution was obtained perpendicular to the galactic plane. The uncertainties in Schmidt's model do not very strongly affect the distribution up to a value of z of about 400 pc. Figure 2 shows the dependence of the resulting density distribution on z for the K force (model I). The comparison between this curve and the density distribution curves of the observed stars and interstellar matter clearly shows an invisible component which is strongly concentrated to the galactic plane. Mainly this concentration leads to the supposition that the invisible matter is identical with interstellar H_2.

Now we shall examine whether or not the density distribution from the k force is compatible with an H_2 abundance following from a formation of the molecules on the surfaces of classical grains. The equilibrium density of H_2 between formation and dissociation near hot stars for classical particles is

$$n_{H_2} = 1.14 \times 10^{-2} \pi T_{gas}^{1/2} n_{HI}^{5/2}. \tag{2}$$

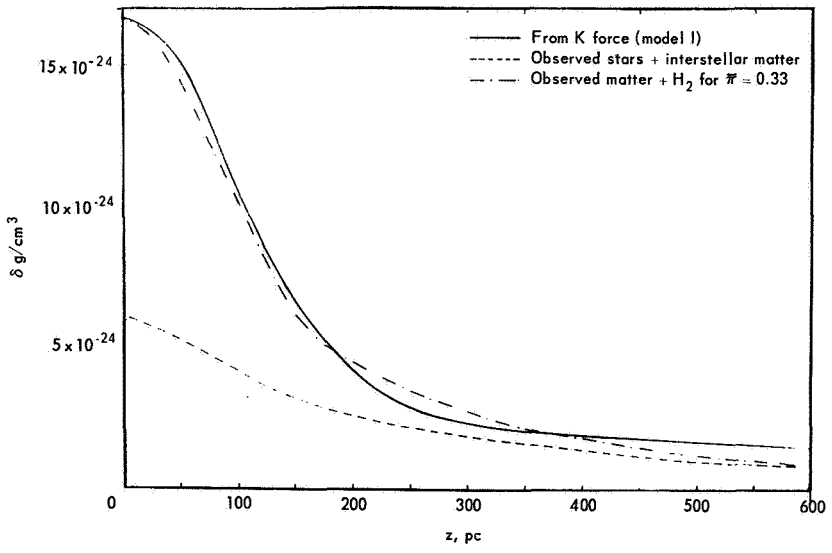

FIGURE 2.—Density distributions as function of z.

In order to get this equation, the relation between the density of dust and atomic hydrogen as stated in reference 14 was used:

$$\delta_{dust} \sim \delta_{HI}^{3/2}. \tag{3}$$

Furthermore, the result found in reference 8 concerning the independency of the density ratio between molecular and atomic hydrogen on the distance from the galactic plane was applied. In order to get the H_2 density from equation (2), the density of the atomic hydrogen as a function of the distance from the galactic plane must be known. The interstellar matter is therefore assumed to be concentrated in clouds according to the model of reference 15. Therein the average radius is $\bar{r}=1.7$ pc, the distribution function of cloud radii is given by

$$\delta(r) = \frac{1}{\bar{r}}\, e^{-r/\bar{r}} \tag{4}$$

and the density inside a cloud is determined by the condition

$$r n_{HI} = 46 \text{ pc/cm}^3 \tag{5}$$

The observed hydrogen density perpendicular to the galactic plane from the 21-cm observations should be proportional to the number of clouds per unit volume. By the aid of these assumptions, the density of H_2 perpendicular to the plane was computed for a temperature $T_{gas}=100°$ K and for different values of the probability π. Then these density distributions of H_2 were added to the density distribution of the observed stars and interstellar matter and compared with the distribution following from the K force. There is a satisfactory agreement between the two curves for the probability $\pi=0.33$ at least up to 400 pc. From this it is concluded that the percentage of the interstellar molecular hydrogen is very large, about 80 percent. Clearly this value is not very certain and a value of 30 percent is also possible.

As has been seen from figure 1, this large content of H_2 is only possible if the formation of the molecules occurs on the surfaces of classical grains. It must therefore be concluded that mainly classical grains are responsible for the observed phenomena of the interstellar dust.

This conclusion is supported by the value of π. Values in the range 0.10 to 0.25 for the case of metal surfaces were found experimentally in reference 16. These values are for room temperatures. Some recent experimental work is reported in reference 17, in which a thermal beam ($T=80°$ K) of partially dissociated hydrogen was directed at a cooled copper surface; the reflection probability of the atomic hydrogen was measured as the temperature of the solid surface was lowered from 80° K to 3° K. They found that recombination occurred very efficiently when the temperature of the solid surface was between 10° K and 20° K. The agreement with our $\pi=0.33$ is satisfactory.

REFERENCES

1. VAN DE HULST, H. C.: The Solid Particles in Interstellar Space. Rech. Astron. Obs. Utrecht, vol. 11, pt. 2, 1949.

2. TAKAYANAGI, K.; and NISHIMURA, S.: Possibility of Observing the 28μ Radiation from the Interstellar Hydrogen Molecules. Contr. Dept. Astron. Tokyo, no. 18, 1961.

3. ZWICKY, F.: The Molecular-Hydrogen Content of the Universe. Astron. Soc. Pacific, Pub., vol. 71, 1959, p. 468.

4. GOLD, T.: The Problem of the Abundance of the Hydrogen Molecule. Comm. Coll. Internat. Astrophys. Liège, vol. 10, 1961, p. 476.

5. MCCREA, W. H.; and MCNALLY, D.: The Formation of Population I Stars. Part II. The Formation of Molecular Hydrogen in Interstellar Matter. Roy. Astron. Soc., Monthly Notices, vol. 121, 1960, p. 238.

6. GOULD, R. J.: Interstellar Abundance of the Hydrogen Molecule. Astron. J., vol. 67, 1962, p. 115.

7. GOULD, R. J.; and SALPETER, E. E.: The Interstellar Abundance of the Hydrogen Molecule I. Basic Processes. Astrophys. J., vol. 138, 1963, p. 393.

8. GOULD, R. J.; GOLD, T.; and SALPETER, E. E.: The Interstellar Abundance of the Hydrogen Molecule II. Galactic Abundance and Distribution. Astrophys. J., vol. 138, 1963, p. 408.

9. LAMBRECHT, H.; and SCHMIDT, K. H.: Zur Häufigkeit des Interstellaren H_2-Moleküls. Astron. Nachricht, vol. 288, 1964, p. 11.

10. MCDOWELL, M. R. C.: On the Formation of H_2 in H I Regions. Observatory, vol. 81, 1961, pp. 240–243.

11. DORSCHNER, J.; GÜRTLER, J.; and SCHMIDT, K. H.: Zur Beschleunigung Senkrecht zur Galaktischen Ebene und zur Häufigkeit des Interstellaren H_2-Moleküls. Astron. Nachricht, vol. 288, 1965, p. 149.

12. YASUDA, H.: The Kinematics of High Velocity Stars and a Galactic Force, K_z, at a Larger Distance from the Galactic Plane. Ann. Tokyo Astron. Obs., ser. 2, vol. 7, 1961, p. 47.

13. OORT, J. H.: Note on the Determination of K_z and on the Mass Density Near the Sun. Bull. Astron. Inst. Netherlands, vol. 15, 1960, p. 45.

14. LAMBRECHT, H.; and SCHMIDT, K. H.: Über die Relative Häufigkeit Einiger Komponenten des Interstellaren Mediums. Mitt. Univ. Sternwarte Jena, no. 40, 1959.

15. BLAAUW, A.: Interstellar Gas and Young Stars Near the Sun. The Distribution and Motion of Interstellar Matter in Galaxies (L. Woltjer, ed.), W. A. Benjamin, Inc. (New York), 1962.

16. WOOD, B. J.; and WISE, H.: Diffusion and Heterogeneous Reaction II. Catalytic Activity of Solids for Hydrogen-Atom Recombination. J. Chem. Phys., vol. 29, 1958, p. 1416.

17. BRACKMANN, R. T.; and FITE, W. L.: Condensation of Atomic and Molecular Hydrogen at Low Temperatures. J. Chem. Phys., vol. 34, 1961, p. 1572.

DISCUSSION

Donn: Great care must be used in extrapolating the results of Brackmann and Fite to the interstellar problem. Although they found an anomalously high recombination coefficient between 15° K and 20° K, the conditions in their vacuum system and in interstellar space are most likely not equivalent.

I think it is also of interest to consider the formation of hydrogen molecules by a process other than surface recombination. If there are complex

molecules in space, as a result of ejection from cool stars, atomic hydrogen may abstract a hydrogen atom from these hydrogen-rich molecules and form molecular hydrogen.

Ultraviolet Photochemistry of Some Frozen Gases

WARREN E. THOMPSON
Case Institute of Technology
Cleveland, Ohio

THERE SEEMS TO BE AGREEMENT that laboratory studies are necessary in the pursuit of a better understanding of the interstellar medium. Herein is described some experiments performed on the effects of far ultraviolet radiation on molecules containing the astronomically abundant atoms H, O, C, and N. In particular, the attempts that have been made to prepare, isolate, and identify various free radicals and other reactive species, some of which may play a role in the processes occurring in the interstellar medium, are discussed.

CARBON TRIOXIDE

In one of the studies, a frozen film of pure carbon dioxide at 77° K was irradiated with the light from a low pressure xenon discharge lamp equipped with a LiF window. This lamp is activated by radio-frequency radiation, and the emitted light is rich in the 1470-Å resonance line of xenon. A comparison of the infrared absorption spectrum of the CO_2 film before and after irradiation showed that several new bands appeared as a result of the irradiation. One of these, at 2139 cm^{-1}, is attributed to CO, presumably produced along with an oxygen atom in the primary photolysis step:

$$CO_2 \xrightarrow{h\nu} CO + O$$

where h is Planck's constant and ν is frequency. The other new features, at 2045 cm^{-1}, 1880 cm^{-1}, 1073 cm^{-1}, and 972 cm^{-1}, could not be assigned to known molecules. This was evidence that some unknown molecular species was being produced in the solid CO_2. Further infrared spectroscopic studies supported the conclusion that the species contains just one carbon atom and very likely three oxygen atoms. This conclusion was reached as a result of performing photolytic studies on carbon dioxide enriched in C^{13} and in O^{18}. For example, when a solid film of carbon dioxide consisting of 56 percent $C^{13}O_2$ and 44 per-

271-92 O-67—18

cent $C^{12}O_2$ was irradiated, the resulting infrared spectrum showed that three of the previously mentioned bands had lower frequency counterparts of about the same intensity. The fourth band, at 1073 cm^{-1}, was relatively twice as intense as before, indicating that it was composed of two unresolved bands. From these results it was concluded that the new molecule possesses just one carbon atom. The molecules containing C^{12} gave rise to the set of higher frequency bands, and those with C^{13}, to the lower frequency set. If more than one carbon atom were present in the molecule, the resulting larger number of possible isotopic species would have yielded a more complex spectrum. In a similar way it was concluded from experiments utilizing CO_2 enriched to varying degrees in O^{18} that there are three oxygen atoms present in the molecule.

One can write various structures for this carbon trioxide molecule, and at the present time attempts are being made to determine which one is correct. This determination involves finding all the infrared-active fundamentals, considering their frequencies, and measuring the frequency shifts upon isotopic substitution. For CO_3, this work is still in progress.

The visible-ultraviolet spectrum of CO_3 is of interest to astronomers. Unfortunately, attempts to record this spectrum have been unsuccessful to date. The molecule is easily decomposed photolytically by light in both the near and far ultraviolet.

PHOTOLYSIS OF CARBON SUBOXIDE

In a second study, carbon suboxide, C_3O_2, was embedded in a solid argon matrix at 4° K in the ratio of one part C_3O_2 to 700 parts argon. The deposit was then irradiated by using the previously mentioned xenon discharge lamp. The purpose of this experiment was (if possible) to produce and isolate the CCO radical:

$$OCCCO \xrightarrow{h\nu} CCO + CO$$

Several new infrared absorption features appeared, including three near 381 cm^{-1}, 1074 cm^{-1}, and 1978 cm^{-1}. In addition, the strong absorption band of CO at 2140 cm^{-1} was observed. At the same time that we were doing these experiments, M. E. Jacox and D. E. Milligan were carrying out studies on the photolysis of cyanogen azide, N_3CN. They found that in the presence of CO, photolysis of N_3CN leads to the same three bands that we observed. Further work by Jacox and Milligan that involved isotopic substitution with C^{13}, N^{15}, and O^{18} showed that the absorption features indeed arise from the linear molecule CCO, and that in their study it had been produced by the reaction of carbon atoms with CO. One interesting feature of this molecule is its reactivity with carbon monoxide, even at temperatures as low as

4° K, to form carbon suboxide, C_3O_2. Apparently there is very little or no activation energy required for this reaction.

Jacox and Milligan, in a study of the 7000 Å to 2500 Å spectral region, found that CCO shows a broad absorption near 5000 Å.

NCN

If carbon suboxide is embedded in a matrix of solid nitrogen rather than solid argon, and the deposit is irradiated as before, one again obtains the spectroscopic features characteristic of CCO, and some new bands as well. The new bands were puzzling at first because they apparently arise as a result of reaction with the N_2 matrix, and N_2 was thought to be essentially inert at 4° K. Two of these new bands, at 423 cm^{-1} and 1478 cm^{-1}, agree in wave number with spectroscopic features arising from the photolysis of N_3CN, studied in detail as reported in reference 1. These features were shown by them to arise from the molecular species NCN. This is strong evidence that in our experiment carbon atoms, produced by the photolysis of CCO, reacted with N_2 by insertion to form NCN. It is possible that other infrared absorption features observed in this experiment arise from CNN, formed by terminal addition of carbon to N_2.

CARBON ATOM REACTIONS

In the foregoing discussion evidence has been presented that indicates that photolytically produced carbon atoms react with both CO and N_2. It seemed of interest to see whether carbon atoms produced in this way would react with other simple molecules, such as H_2, NO, and HCl. When a deposit of C_3O_2, H_2, and Ar is irradiated with ultraviolet light, as described previously, several new infrared absorption bands appear in the spectrum. Most easily identified are methane (CH_4) and ketene (CH_2CO). The replacement of hydrogen in the matrix by deuterium leads to the formation of CD_4 and CD_2CO; and when a mixture of H_2 and D_2 is used, CH_2CO, CD_2CO, CH_4, CD_4, and CH_2D_2 are produced. These products suggest that methylene (CH_2 or its deuterium counterpart) is produced by the reaction of carbon atoms with H_2:

$$C + H_2 \rightarrow CH_2$$

The methylene thus produced then reacts with a nearby molecule of H_2 or CO (the latter also being produced in the photolysis of C_3O_2 and CCO):

$$CH_2 + H_2 \rightarrow CH_4$$
$$CH_2 + D_2 \rightarrow CH_2D_2$$
$$CH_2 + CO \rightarrow CH_2CO$$

Experiments designed to trap methylene before it could react further were unsuccessful. Methylene is known to be very reactive, and in these experiments it was generated in the vicinity of molecules of CO and H_2, for which it apparently has great affinity.

It would be incorrect to conclude from these experiments that the carbon atoms reacting with CO, N_2, and H_2 have electronic and kinetic energies corresponding to 4° K, the temperature of the matrix. Depending on the energy of the photon responsible for the process, the liberated carbon atom may be in any of several electronic states. Furthermore, it will in general be produced with excess kinetic energy, and may well react with some environmental molecule before losing this energy by nonreactive collisions. Further studies are needed to determine the required activation energies for these reactions.

ULTRAVIOLET-VISIBLE SPECTRA AND MATRIX EFFECTS

With our own experimental apparatus it has not generally been possible to record the ultraviolet-visible spectra of the product of photolysis. Such spectra are, of course, of importance to astronomers, and fortunately, there are workers in this field who are presently equipped to record such spectra. One point that should be mentioned is that the appearance and frequency of a spectral feature arising from an embedded molecule often depend on the composition and physical condition of the surrounding matrix.

SUMMARY

Various low-temperature experiments in which chemical reactions are induced in various pure and mixed frozen gases by vacuum ultraviolet irradiation have been discussed. Experimental evidence for the formation of CO_3, CCO, NCN, and HCH has been presented, and the usefulness of infrared spectroscopy in identifying such species and in determining their structures has been illustrated. These studies have demonstrated the reactivity of photolytically produced carbon atoms toward CO, N_2, and H_2. There is a need for further ultraviolet-visible studies, including studies with matrices appropriate to the astronomical problem.

REFERENCES

1. MILLIGAN, D. E.; JACOX, M. E.; COMEFORD, J. J.; and MANN, D. E.: Infrared Spectrum of the Free Radical NCN. J. Chem. Phys., vol. 43, 1965, pp. 756–757.

The following papers contain additional studies on this subject:

2. JACOX, M. E.; MILLIGAN, D. E.; MOLL, N. G.; and THOMPSON, W. E.: Matrix-Isolation Infrared Spectrum of the Free Radical CCO. J. Chem. Phys., vol. 43, 1965, pp. 3734–3746.

3. MILLIGAN, D. D.; JACOX, M. E.; and BASS, A. M.; Matrix Isolation Study of the Photolysis of Cyanogen Oxide. The Infrared and Ultraviolet Spectra of the Free Radical NCN. J. Chem. Phys., vol. 43, 1965, p. 3149.

4. MOLL, N. G.; and THOMPSON, W. E.: Reactions of Carbon Atoms with N_2, H_2 and D_2 at 4.2° K. J. Chem. Phys., vol. 44, 1966, p. 2684.

5. MOLL, N. G.; CLUTTER, D. R.; and THOMPSON, W. E.: Carbon Trioxide: Its Production, Infrared Spectrum, and Structure Studied in a Matrix of Solid CO_2. J. Chem. Phys., vol. 45, 1966, pp. 4469–4481.

DISCUSSION

Harteck: Did you say that the C_2O radical was stable, or did it decompose when it was warm, or was it very fast reacting?

W. E. Thompson: It reacts very fast with carbon monoxide. Over a period of minutes it disappears from the spectrum. It reacts quickly with CO to form carbon suboxide at 4° K.

Harteck: But this is very difficult to do and isn't very likely.

W. E. Thompson: You can photolyze C_2O away eventually to get carbon atoms, and carbon monoxide.

Harteck: Yes, I know. I am just saying that at a low temperature C_2O is stable.

W. E. Thompson: If you warm up the matrix to a sufficiently high temperature so that diffusion can occur, then it will react.

Harteck: Then it is gone.

W. E. Thompson: Not quantitatively gone; the bands decrease, perhaps to 20 percent of their original intensity.

Harteck: Do you really think these reactions will occur at 0°?

W. E. Thompson: I wouldn't be surprised if C_2O reacted with CO within 2° of absolute zero. What I am surprised about is our evidence that carbon atoms react with N_2 to form NCN. If this is correct, then the carbon atom inserts between the two nitrogen atoms, which are bound by a triple bond. My only evidence for this is the agreement with Milligan's results on the NCN radical. We get the same band. Remember that the carbon atoms might be quite hot. These carbon atoms are not at 4° K when they are formed. Therefore, considerable activation energy may be necessary, and it may be provided by the photolytic process. In the photolysis of the C_2O you may get a hot C atom which can then hit a nitrogen molecule.

Harteck: I don't know all the details, but it is known that if you make C atoms photochemically, they enter the molecules.

W. E. Thompson: Yes, I am aware of that.

Harteck: And so they may enter the nitrogen.

W. E. Thompson: To enter a triple bond is quite a feat.

Harteck: That is why I asked you; but the whole of the reaction is exothermic.

W. E. Thompson: I'm glad to hear you say that. We have made the same calculation. I was worried more about the activation energy that was required.

U.S. GOVERNMENT PRINTING OFFICE : 1967 OL—271-992

"The aeronautical and space activities of the United States shall be conducted so as to contribute . . . to the expansion of human knowledge of phenomena in the atmosphere and space. The Administration shall provide for the widest practicable and appropriate dissemination of information concerning its activities and the results thereof."

—NATIONAL AERONAUTICS AND SPACE ACT OF 1958

NASA SCIENTIFIC AND TECHNICAL PUBLICATIONS

TECHNICAL REPORTS: Scientific and technical information considered important, complete, and a lasting contribution to existing knowledge.

TECHNICAL NOTES: Information less broad in scope but nevertheless of importance as a contribution to existing knowledge.

TECHNICAL MEMORANDUMS: Information receiving limited distribution because of preliminary data, security classification, or other reasons.

CONTRACTOR REPORTS: Scientific and technical information generated under a NASA contract or grant and considered an important contribution to existing knowledge.

TECHNICAL TRANSLATIONS: Information published in a foreign language considered to merit NASA distribution in English.

SPECIAL PUBLICATIONS: Information derived from or of value to NASA activities. Publications include conference proceedings, monographs, data compilations, handbooks, sourcebooks, and special bibliographies.

TECHNOLOGY UTILIZATION PUBLICATIONS: Information on technology used by NASA that may be of particular interest in commercial and other non-aerospace applications. Publications include Tech Briefs, Technology Utilization Reports and Notes, and Technology Surveys.

Details on the availability of these publications may be obtained from:

SCIENTIFIC AND TECHNICAL INFORMATION DIVISION

NATIONAL AERONAUTICS AND SPACE ADMINISTRATION

Washington, D.C. 20546